HOST NUCLEAR RECEPTOR ACTIVATION IN THE COLON: CONSEQUENCES FOR INFLAMMATORY BOWEL DISEASES AND COLORECTAL CARCINOGENESIS

A Dissertation

by

JENNIFER AGNES ALPHA DELUCA

Submitted to the Office of Graduate and Professional Studies of
Texas A&M University
in partial fulfillment of the requirements for the degree of

DOCTOR OF PHILOSOPHY

Chair of Committee,	Clinton D. Allred
Committee Members,	Robert S. Chapkin
	Arul Jayaraman
	Bradley R. Weeks
Head of Department,	David W. Threadgill

December 2020

Major Subject: Nutrition

ABSTRACT

Inflammatory Bowel Diseases (IBDs) and Colorectal Cancers (CRC) are a complex collection of diseases with limited and invasive treatment options. Therefore, prevention is key but effective methods of doing so are elusive. While it is increasingly accepted that host genetics, the gut microbiota, and environmental exposures including diet can impact disease development and progression, exact mechanisms are still being investigated and results are sometimes conflicting. Host nuclear receptor (NR) activation, including that of the estrogen receptors (ER) and the aryl hydrocarbon receptor (AhR), has been linked to both exacerbation and prevention of these diseases.

One ER ligand present in the diet, bisphenol-A (BPA), has been shown to exert estrogenic activity, but the mechanisms by which it may exacerbate IBDs are unclear. Therefore, the ability of BPA to exacerbate colitis and alter microbial derived metabolites (MDMs) was investigated in mice. BPA not only worsened disease activity, but exposure also slowed recovery, increased inflammation, and reduced levels of several metabolites associated with decreased inflammation. Furthermore, this activity was attributed to the ability of BPA to reduce cell number similarly to 17β-Estradiol *in vitro*.

Diets high in saturated fat (HFD) have been linked to increased risk for IBDs and CRC, and AhR activation by colonic metabolites has been associated with preventing both diseases. However, the interaction of HFD and AhR in intestinal epithelial cells (IECs) has yet to be established. Therefore, a chemically-induced CRC mouse model lacking AhR in IECs ($Ahr^{\Delta IEC}$) and fed a HFD was employed to investigate this

interaction, and though colon mass incidence was not increased compared to low fat diet (LFD) fed control animals, colon mass multiplicity as well as β-catenin intensity and nuclear localization all increased.

To investigate the impact of the dysbiotic feces observed in *Ahr*$^{\Delta IEC}$ mice, a fecal transplant model was used. Wild-type mice were treated with antibiotics, then dosed with *Ahr*$^{\Delta IEC}$ donor feces depleted in *Akkermansia muciniphila*. *A. muciniphila* was then gavaged in an attempt to rescue decreased gut barrier integrity associated with *Ahr*$^{\Delta IEC}$ donors and fecal transplant recipients. While *A. muciniphila* was not significantly increased in any group that received it compared to respective vehicle controls, antibiotic treated animals without fecal transplant had a significant increase in the relative abundance of *A. muciniphila* that corresponded with improved gut barrier integrity and an increase in MDMs that act as AhR ligands.

These results demonstrate the complex interactions and varied effects of environmental exposures through diet, the gut microbiome and MDMs, and host NR activation in the colon on the development and progression of IBDs and CRC. Findings such as these will allow the advancement of therapeutics in the prevention of these diseases.

DEDICATION

To ESB, MEB, GHKD, and LBD.

Thank you for being the best examples, each in your own way.

Words cannot express the lasting impact your love has had on me

and my ability to achieve my goals and dreams.

With all my love, thank you.

ACKNOWLEDGEMENTS

First, I would like to thank my committee chair, Dr. Clinton Allred, for his mentorship, guidance, and advice regarding my scientific and professional development, as well as life in general. I am incredibly grateful to have been provided this opportunity to grow as a scientist and person, and I sincerely thank you for all of your contributions to my personal and professional growth.

I would also like to acknowledge and thank my committee members, Dr. Robert Chapkin, Dr. Arul Jayaraman, and Dr. Bradley Weeks for giving their own time, equipment, and scientific expertise during the course of my studies.

I want to extend my heartfelt appreciation to all members of the Allred Lab, who helped make my time as a graduate student so positive. Kim, I cannot thank you enough for the endless ways you supported me during my time in the lab. Thank you for all the technical knowledge you shared, as well as your support as a friend. To my lab mates, Erika, Jordan, Christina, Gyhye, and all the other graduate and undergraduate students that have passed through our lab during my time there, I am so grateful for the positive atmosphere you all brought to our lab home. Thank you for your friendship and always being willing to help, trouble-shoot, and laugh together when nothing else worked.

To my colleagues in labs across campus, I sincerely thank you for all the ways that you helped and supported me throughout my degree. This includes all of Dr. Chapkin's and Dr. Jayaraman's lab members, as well as several faculty members whose help and advice was crucial to the completion of my projects including Dr. Martha Hensel, Dr. Ivan Ivanov, and Dr. Stephen Safe. I'd also like to thank the faculty, staff,

and trainees in the Departments of Nutrition and Food Science for their mentoring, support, and friendship during my time in graduate school.

To my family and friends, I am so grateful for the emotional, mental, and financial support you provided while I earned my degree: from the endless stream of words of encouragement to just listening to me vent, from sending food to sharing perspective to keep me motivated to finish what I started. Mom, thank you for teaching me by example to be a strong woman and for always answering the phone. Dad, thank you for showing me how to stand tall under any circumstance. James, thank you for igniting a love of science in me at a very young age. And a big thank you to Aunt Alice, the Floyd family, all of our extended families, new and old friends both near and far, and Maribel as each of you contributed in vital ways you may not even realize. It takes a village, and I could not have achieved all that I did without each and every one of you. Thank you for being understanding of all the missed events and adjusting your lives to connect with Austin and me as much as possible during this time.

And finally, but most importantly, under no circumstances could I have accomplished this goal without the unconditional love and support I received from my wonderful husband, Austin. I'm not sure one of us working on a Ph.D. and the other in vet school was the best idea we've ever had, but, not only did we make it, we crushed it. I am overcome with gratitude for all the ways you held me up throughout this process. Thank you for snarky cookie cakes, washing countless dishes, and always letting me be me. I love you.

CONTRIBUTORS AND FUNDING SOURCES

Contributors

This work was supervised by a dissertation committee consisting of Dr. Clinton D. Allred and Dr. Robert S. Chapkin of the Department of Nutrition and Dr. Arul Jayaraman of the Artie McFerrin Department of Chemical Engineering and Dr. Bradley R. Weeks of the Department of Veterinary Pathobiology.

The quantification of metabolites from aromatic amino acids presented in Chapter 2 was conducted by Rani Menon and Rebekah Riordan of the Artie McFerrin Department of Chemical Engineering and was published in 2018. The animal model verification in Chapter 3 was conducted and provided by Evelyn Callaway of the Artie McFerrin Department of Chemical Engineering and was published in 2020. The colon mass type data analyzed for Chapter 3 was provided by veterinary pathologist Dr. Martha Hensel of the Department of Veterinary Pathobiology and were published in 2020. In Chapter 4, the *Akkermansia muciniphila* culture and bacterial qPCR for Chapter 4 was provided and fecal samples for the intestinal microbiome, short chain fatty acid, and untargeted metabolomics assays were prepared by Evelyn Callaway of the Artie McFerrin Department of Chemical Engineering. 16S rRNA data and untargeted metabolomics data in Chapter 4 was analyzed by Fang Yang of the Artie McFerrin Department of Chemical Engineering.

All other work conducted for this dissertation was completed by the author.

Funding Sources

Graduate study was partially supported by the Willie Mae Harris Fellowship from Texas A&M University.

Research reported in Chapter 2 was supported by the Center for Translational Environmental Health Research of the National Institute of Environmental Health Sciences of the National Institutes of Health under Grant Number 1P30ES23512-01 and The National Cancer Institute of the National Institutes of Health under Grant Number 1RO1-CA-20267. Research reported in Chapters 3 and 4 was supported by the National Cancer Institute of the National Institutes of Health under Grant Numbers RO1-CA-202697 and R35-CA-197707, the National Institute of Environmental Health Sciences of the National Institutes of Health under Grant Number RO1-ES-025713, the Cancer Prevention and Research Institute of Texas under Grant Number RP160589, and funds from the Allen Endowed Chair in Nutrition & Chronic Disease Prevention and Syd Kyle Chair. Contents of this dissertation are solely the responsibility of the author and do not necessarily represent the official views of any funding sources.

TABLE OF CONTENTS

Page

LIST OF FIGURES

Page

LIST OF TABLES

Page

CHAPTER I

INTRODUCTION AND LITERATURE REVIEW

Colon Overview

Anatomy and Physiology of the Large Intestine

The colon, also known as the large intestine, is the last main organ of the digestive tract. The colon is responsible for absorbing water, electrolytes, and vitamins from previously undigested food material.[1] The colon also propels all ultimately indigestible food material, forming and excreting wastes through the rectum as feces.[1] Finally, the colon is a reservoir for commensal microbes that symbiotically aid their hosts by harvesting energy from indigestible food material, producing vitamins and other compounds vital to host health, developing and maintaining the host immune system, and protecting against pathogenic infection.[2]

In order to conduct these functions, the colon is composed of 4 layers from the central lumen outward: the mucosa, submucosa, muscular layer, and serosa.[1] The muscular layer is composed of two layers of smooth muscle that aid motility: the inner, circular layer and the outer, longitudinal layer covered by serosa.[1] The mucosa is primarily composed of simple columnar epithelial cells that line invaginations called crypts anchored to the submucosa.[1] Stem cells at the base of each crypt give rise to all daughter cell types present in each crypt, including enterocytes, goblet cells, enteroendocrine cells, Paneth cells, and microfold cells.[3] The epithelial cells of colonic crypts are lined with two mucus layers, the outer, loose layer containing bacteria and the inner, dense, sterile layer, both of which are produced by goblet cells in the crypts.[3] Mucin 2 (MUC2) is a gel-

forming mucin protein that primarily makes up these mucus layers and prevents microbes and their products from easily accessing colonocytes.[4] Transmembrane mucin proteins including Mucin 1 (MUC1) form a glycocalyx on epithelial cells, preventing pathogenic infection of these cells.[4] Along with these mucus layers, the junctional complexes between epithelial cells prevent arbitrary movement of hydrophilic compounds and microbes from the lumen of the colon into the lamina propria and ultimately the body.[3] These tight junction protein complexes consist of several proteins including transmembrane claudins, occludins, and intracellular zonula-occludens proteins.[4] If components of these structures are lacking or imbalanced, luminal contents including bacteria, their products, and other inflammatory molecules can enter the submucosa, increasing inflammation in the gut.[4] These complex structures aid in maintaining gut barrier integrity in an effort to preserve homeostasis and prevent negative health consequences.

Pathologies of the Large Intestine

Inflammatory Bowel Diseases

Inflammatory bowel diseases (IBDs) are a collection of gastrointestinal disorders marked by dysregulation of gut immune responses resulting in chronic inflammation, thought to develop due to an interaction between genetic, environmental, and microbial factors.[5] The two most common types of IBDs, Crohn's disease (CD) and Ulcerative Colitis (UC) differ in their pathophysiology, patterns of incidence, and risk factors.[6,7] UC occurs in the large intestine, with inflammatory lesions often beginning at the rectum and extending continuously towards the proximal colon.[1,8] In contrast, CD can occur at

any location in the gastrointestinal tract, potentially in skip lesions, but most commonly impacts the regions surrounding the ileocecal junction.[1,8] Historically, IBDs were considered diseases of the Western world, but globally, the incidence of IBDs increases as countries become more industrialized.[9]

In light of this fact, a growing body of data suggests environmental exposures, including diet, estrogen-containing medication usage, altered gut microbiome, and toxins or pollutants, significantly influence IBD development and relapse.[6,7,10,11] Biological sex also impacts risk for developing IBDs. Women are at increased risk for developing autoimmune diseases of any type, however epidemiological evidence for a link between endogenous estrogens or estrogenic compounds and IBDs is conflicting and complex.[11–14] For example, fluctuations in IBD symptoms are reported during female patients' menstrual cycles, oral contraceptive pills have been shown to increase risk of both UC and CD, and hormone replacement therapy is associated with an increased risk for developing UC but not CD.[12,13,15]

Colorectal Cancer

Colorectal cancers (CRC), another collection of gastrointestinal diseases, are a group of malignancies affecting the colon and rectum. CRC is the third most common cancer in the United States, and is the leading cause of cancer death.[16] In recent years, CRC incidence and mortality have decreased in those over 65, but these rates are increasing among those younger than fifty, a concerning trend as routine screenings are not recommended for this group.[16] About 20%-30% of CRC cases have a familial basis while the remaining incidence is believed to be due to sporadic carcinogenesis.[17] Patients

with IBDs have an increased relative risk of developing CRC, referred to as colitis-associated cancer (CAC), of greater than 2, as inflammation is a well-established cancer promoter.[18,19] Though differences exist in the pathophysiology of different types of CRC, both non-inflammatory CRC and CAC follow a similar multi-step tumorigenesis progression, share common genetic and signaling pathways, and associate with gut microbiota dysregulation.[19] As CRC progresses from adenoma to carcinoma, successive mutations contribute to the malignancy of the cells, including the loss of function of tumor suppressor genes and the gain of function of oncogenes or genes that promote malignant transformation.[20] Mutations in several such genes are frequently associated with CRC, including adenomatous polyposis coli (APC), tumor protein 53 (TP53), and Ki-ras2 Kirsten rat sarcoma viral oncogene homolog (KRAS), which are implicated in 85%, 35-55%, and 35-45% of CRCs, respectively.[20] Dysregulation of signaling pathways associated with these mutated genes, including the Wnt pathway, the RAS/MAPK pathway, and others contribute to the progression of CRC.

Therefore, risk factors that are associated with the initiation of these mutations and promotion of cell growth are implicated in colorectal carcinogenesis and progression. Due to the challenges associated with detection, treatment, and survival of CRC, prevention is an important method for reducing CRC burden. Environmental risk factors, particularly modifiable dietary and lifestyle factors, are implicated in 50-60% of CRC cases in the United States.[21] Obesity, lack of physical activity, decreased intake of dietary fiber, and increased intake of red and processed meat are all associated with an increased risk of CRC.[21] Though a dysbiotic gut microbiome is well associated with

CRC, it is still unknown whether dysbiosis is a cause or consequence of CRC.[21] However, the ability of the gut microbiome to interact with environmental factors to impact host physiology is becoming increasingly well established, including their ability to produce unique metabolites that can impact signaling in host receptors, including nuclear receptors.[21,22]

Nuclear Receptors Overview

Nuclear Receptor Structure and Signaling

Nuclear receptors (NR) are a superfamily of similarly structured ligand-activated transcription factors that regulate diverse cellular functions.[23] NRs typically translocate into the nucleus upon ligand binding to regulate gene expression, but non-canonical, rapid cytoplasmic signaling functions of these receptors have been the focus of increased research in recent years.[24] Classical NRs are genetically similar, share a common molecular structure and signaling pathways, and include steroid receptors such as estrogen receptors (ERs).[24] Though the aryl hydrocarbon receptor (AhR) has not historically been considered a classical nuclear receptor based on its molecular structure, it shares many features with classical NRs, including heterodimerization upon activation, translocation to the nucleus, and ligand-activated transcriptional activity.[25] The signaling pathways of both ER and AhR have been associated with alterations in gut physiology that impact risk of IBD and CRC development.

Estrogen Receptor

Estrogens and their Discovery

The three main endogenous forms of estrogens in females are estrone (E_1), estradiol (E_2 or 17β-estradiol), and estriol (E_3).[26] Each is produced from androgens via the enzyme aromatase, and the primary estrogen at various life cycle stages in females varies.[26] E_2 is the predominant and most potent form during reproductive years, while E_1 is the main form produced postmenopausally, and E_3 is produced in large quantities by the placenta during pregnancy.[26]

Though the existence of steroid sex hormones was hypothesized for centuries, E_1 was first isolated from the urine of pregnant women in the 1920s.[27] E_2 and E_3 were purified in subsequent decades.[27] Estrogenic compounds for pharmaceutical use quickly became available, instigating hormone replacement therapy to treat hot flashes, dysmenorrhea, and eventually osteoporosis.[27] Radio-labeled estradiol was used by Elwood Jensen and his students to discover the first estrogen receptor (ER), ultimately named estrogen receptor α (ERα), in 1958.[26] A second subtype of the receptor, named estrogen receptor ß (ERß), was discovered by Jan-Ake Gustafsson's group in 1996.[28]

Since the discovery of naturally-occurring, endogenous estrogens and their receptors, many compounds that exhibit estrogenic activity have been discovered. These include synthetic, dietary, and environmental compounds that have been shown to have diverse structures and various health effects dependent upon the target tissue and ER subtype.[29]

Estrogen Receptor Subtypes

ERs are nuclear hormone receptors that exist in two subtypes, ERα and ERß.[30] Upon ligand-binding, ERs dimerize, translocate to the nucleus, and bind to estrogen-response elements in the DNA to regulate transcription.[31] Other mechanisms of ER signaling have been discovered, including ligand-independent activation, membrane-initiated actions, and regulation of mitochondrial function.[26] Additionally, more recently, a membrane bound receptor capable of binding estrogenic compounds has been discovered and named G protein-coupled estrogen receptor-1 (GPER-1).[27]

Though encoded by two different genes, ERα and ERß are structurally similar.[30] However, tissue distribution differences exist between subtypes, with ERα or ERβ predominating in specific tissues.[30] ER signaling can be pro- or anti-inflammatory depending on dose, target tissue, ER subtype ratio, and timing of exposure relative to disease course.[32] Furthermore, in cell lines, E_2 can stimulate proliferation via ERα while inhibiting proliferation via ERß.[33] This indicates that the predominant isoform of ER present in a given tissue will dictate the outcome of E_2 signaling in that tissue.[33]

Role in Colon Physiology and Pathologies

ERß is the main form of ER expressed in the colon.[31] ERß signaling is associated with anti-inflammatory effects in the colon, and ERß knockout mice develop worsened colitis compared to wild-type controls.[34] Intestinal barrier integrity is compromised in colitis, resulting in increased bacterial adhesion and invasion.[35] ERβ signaling, which is associated with decreased colonic permeability, appears to be protective against colitis.[36] Estrogenic compounds play a role in both innate and adaptive immune responses,

partially explaining the gender differences observed in autoimmune diseases, including IBDs.[37] In addition, CRC progression has been associated with a shift from high to low ERβ:ERα ratio.[34,38] Furthermore, worsened CRC tumor grade and stage, poor tumor differentiation, and decreased patient survival were all associated with a greater reduction of ERβ.[31] Furthermore, women are at decreased risk of developing CRC compared to men, and hormone replacement therapy reduces CRC risk in postmenopausal women.[37] These data indicate that ERβ signaling is important for normal gut physiology and protection against IBD and CRC.

Aryl Hydrocarbon Receptor

Discovery, Signaling, and Role in Colon Physiology

AhR is a ligand-activated transcription factor of the Per-Arnt-Sim (PAS) superfamily.[39] Without ligand, AhR is found in a complex that sequesters it in the cytoplasm.[39] Upon ligand-binding, the AhR complex translocates to the nucleus, where AhR dissociates from the complex and heterodimerizes with the aryl hydrocarbon receptor nuclear translocator (ARNT).[25,39] This complex can then bind dioxin response elements of DNA and result in transcription of AhR target genes.[25,39] The best known of these genes are the cytochrome p450 enzymes including CYP1A1, CYP1A2, CYP1B1, which function as xenobiotic metabolism enzymes.[25,39]

AhR was discovered in the 1970s and was originally thought to primarily be involved in the biotransformation and toxic effects of environmental toxins, including 2,3,7,8-Tetrachlorodibenzo-p-dioxin (TCDD) and polycyclic aromatic hydrocarbons (PAHs).[40] However, more recently, additional roles for AhR signaling have been

discovered, including regulation of the immune system, proteasomal degradation, and chemoprevention.[39,41,42] The environmental toxin TCDD and its effects on AhR signaling have been widely studied as it is one of the most potent agonists of AhR.[25] Though AhR has long been considered an orphan receptor with no high-affinity endogenous ligands, recent studies have identified dietary bioactive substances such as flavonoids, carotenoids, and tryptophan metabolites including indoles that can bind AhR and result in transcription of AhR responsive genes.[25,41,42] These dietary and microbially-derived ligands are considered less toxic and result in relatively short-term activation of AhR signaling and appear to elicit beneficial physiological effects.[41]

However, these effects are tissue, ligand, and allele form specific. Several different alleles of murine AhR exist, including the Ahr^{b1} and Ahr^{d} allele variants, the latter of which has a lower ligand binding affinity than the former.[43] This finding highlights the importance of using the appropriate animal model to study human health and disease, as humans possess an allelic variant that more closely resembles the Ahr^{d} allele rather than the Ahr^{b1} allele that naturally occurs in C57BL/6 mice that are frequently used for translational studies.[44] Therefore, a "humanized" strain of C57BL/6 mice that possess the Ahr^{d} allele should be used in such experiments, including those investigating pathologies of the colon.[44]

Role in Colon Pathologies

Mounting evidence suggests that appropriate AhR activation alleviates IBD symptoms and reduces CRC development. For example, AhR activation has been shown to reduce inflammation associated with IBDs. With pretreatment of TCDD, symptoms of

dextran sulfate sodium (DSS)-induced colitis were reduced.[45] TCDD treatment reduced symptoms and inflammatory markers associated with 2,4,6-trinitrobenzene sulfonic acid (TNBS) in wild-type (WT) but not AhR null animals.[46] This reduction in inflammation unsurprisingly translates to a reduction in CAC. In one study, AhR activation by the dietary ligand indole-3-carbinol (I3C) reduced colon tumorigenesis in a CAC model.[47] Furthermore, AhR appears to be protective against CRC in other models of carcinogenesis. Activation of AhR by dietary ligands including indole-3-acetic acid (IAA) and I3C resulted in decreased cecal and small intestine tumors in $Apc^{Min/+}$ animals but not in $Apc^{Min/+}$ mice also lacking AhR.[48] While supplemented dietary molecules appear to directly activate AhR to reduce CRC, recent studies that examine the impacts of the gut microbiome in producing AhR ligands that reduce colon carcinogenesis are also promising. In a recent study, dietary tryptophan supplementation improved DSS-induced colitis in mice, and this beneficial effect was dependent upon AhR.[49] This implies that dietary compounds and metabolites positively impact AhR signaling to reduce CRC and IBD.

Gut Microbiome Overview

Major Bacterial Phyla and General Ecology

The mammalian GI tract retains a complex ecosystem of microbes that includes organisms of the Archaea, Bacteria, and Eukarya domains.[50] There are trillions of microbes in the human body, with hundreds to thousands of bacterial species in the human intestine alone.[50] The dominant bacterial phyla that inhabit the lower GI tract include Bacteroidetes, Firmicutes, Actinobacteria, Proteobacteria, and

Verrucomicrobia.[50] Bacterial diversity and load generally increases along the length of the GI tract, as pH increases and antimicrobial compounds and oxygen decrease.[50] This highlights an example of symbiotic evolution between bacteria and host, as an increased prevalence of these bacteria in more proximal regions of the digestive tract could lead to competition between the host and microbes for nutrients.[50] However, as the colon is the most highly bacterially populated region of the GI tract, the anatomy and physiology of this system allows microbes access to indigestible material that can be harnessed for fuel by the bacteria and ultimately result in the production of by-products that benefit the host.

Role in Gut Physiology

In a eubiotic environment, these gut bacteria are largely non-pathogenic, aiding the host in nutrient and xenobiotic metabolism, preventing colonization of pathogenic organisms, and maintaining a functioning immune system and gut barrier integrity.[51]

The Metabolome and Host Responses

The gut microbiota is considered a living organ of its own, evolved to maintain a symbiotic relationship with the host under appropriate conditions. The microbiome harvests nutrients from the host's dietary components, shed host cells, and other microbes.[51] Metabolism of a wide variety of substrates results in an extensive array of metabolites that can be garnered by the host as energetic, nutritive, or other bioactive compounds that can have a variety of impacts. These metabolites can include short chain fatty acids (SCFAs), metabolites derived from aromatic amino acids (MDAs), and vitamins or xenobiotics, drugs, and even carcinogens.[21,51]

Short Chain Fatty Acids

Gut bacteria mainly use dietary carbohydrates in the form of fibers that are indigestible by the host for fuel.[51] Fermentation of these complex carbohydrates results in the production of saturated fatty acids with fewer than six carbon atoms called short chain fatty acids (SCFAs), including the straight-chain SCFAs acetic acid, butyric acid, propionic acid, and valeric acid.[52,53] These straight-chain SCFAs represent 90-95% of SCFAs produced in the colon. Additional branched-chain SCFAs including isobutyric acid and isovaleric acid are also produced from the metabolism of branched-chain amino acids such as valine, leucine, and isoleucine, but these compounds typically contribute approximately 5% of total SCFAs in the GI system.[52,53] SCFAs can modulate host metabolism, both in the colon, where butyrate is used as the main energy source of colonocytes, and more globally, where butyrate, propionate, and acetate all appear protective against diet-induced obesity and result in reduced food intake and butyrate also reduces insulin resistance.[52] In the colon, SCFAs decrease the pH of the lumen, inhibiting pathogenic growth and resulting in an increase in the absorption of some nutrients.[52] Furthermore, SCFAs can stimulate mucin production and expression of various tight junction proteins, resulting in improved gut barrier integrity.[52] SCFAs have also been shown to have immunomodulatory effects, resulting in the differentiation, function, and epigenetic regulation of T-regulatory cells.[51,52] These mechanisms have implications for colon pathologies, as reductions in fecal butyrate concentrations are correlated to both IBDs and CRC.[52] In addition to mechanisms involved in gut barrier integrity and immunomodulation in the colon, SCFAs can induce apoptosis, inhibit

tumor cell progression, and inhibit histone deacetylation, all beneficial mechanisms in preventing CRC.[51,52] In fact, the chemopreventive properties of a diet high in fiber and low in saturated fat and red meat have been linked to increased butyrate production, as SCFAs are derived from host dietary compounds.[21,52]

Microbial Metabolites Derived from Aromatic Amino Acids

Another source of substrates for microbes that contributes to the gut metabolome are aromatic amino acids, including phenylalanine, tryptophan, and tyrosine. Though these are essential amino acids for humans, microbes can synthesize them through the shikimate pathway and their byproducts include important bioactive compounds such as kynurenines, indoles, and serotonin.[54] Kynurenic acid (KA), a tryptophan degradation product, can antagonize excitatory amino acid receptors, preventing overstimulation of neurons by neurotransmitters.[54] However, both KA abundance and depletion have been implicated in neurological conditions.[55] Furthermore, a high kynurenine to tryptophan ratio has been implicated in irritable bowel syndrome, inflammatory conditions, and some cancers.[56] Indole and its metabolites, produced from tryptophan by enteric bacteria, have been demonstrated as AhR ligands that have been implicated in improving host gut barrier integrity and immunomodulation.[55,57] Furthermore, 95% of serotonin production from tryptophan occurs in the GI tract of mammals, and changes in serotonin signaling in the gut have been implicated in IBDs, irritable bowel syndrome, constipation and diarrhea.[56,58] Tryptamine, which is also a tryptophan byproduct, regulates the excitatory versus inhibitory balance of serotonin.[56] Clearly, the modulation

of tryptophan and its metabolites in the gut by both the host and microbes is important in prevention of a variety of GI and other host diseases.

Other Metabolites

The microbiome is also involved in the production of other important metabolites, including vitamins and polyphenols essential to host health, xenobiotics, drugs, and even carcinogens. Vitamin K and some types of vitamin B are synthesized by the host's microbiome.[51,59] Additionally, bacteria can metabolize polyphenols, making them more bioavailable and bioactive than the parent compounds, and this metabolism can vary from host to host based on the composition of their microbiome.[60] For example, some humans can produce equol, an estrogenic compound derived from isoflavones, while others cannot.[60]

In the case of xenobiotics, drugs, and carcinogens, the host and microbes may have competing interests in their metabolism of these compounds. While the goal of metabolism of these compounds in humans is often excretion via the addition of polar functional groups and conjugation to more polar compounds via Phase I and Phase II enzymes, respectively, gut microbes modify these compounds in different ways through their normal metabolic activities, resulting in altered toxicities, lifetimes, and pharmacokinetic properties in the host.[61] In a relevant example, azoxymethane (AOM), a procarcinogen, used to initiate CRC in rats and mice is metabolized to methylazoxymethanol (MAM), the active carcinogen, via cytochrome p450 2E1 and then MAM-glucuronide (MAM-G) via uridine diphosphate-glucuronosyltransferase (UGTs) in the host liver for excretion.[62] However, gut bacteria reactivate MAM-G to

MAM via removal of the glucuronide via microbial β–glucuronidase in the colon where MAM can form DNA adducts and initiate CRC.[62,63] Other carcinogens including polycyclic aromatic hydrocarbons are also hypothesized to be metabolized via similar pathways.[62] Therefore, the composition and functional capacity, of the gut microbiome as well as the means to modulate them, is vitally important to understand the role of these organisms in the development of disease in the host.

Competition Against Pathogens and Immunomodulation

Resistance to pathogens may be mediated by nutrient limitations, the production of antimicrobial compounds, and adherence of commensals to the mucosa to prevent pathogens from accessing colonocytes.[50] Additionally, the host immune system has co-evolved with gut microbes to allow tolerance of beneficial species while discouraging colonization by pathogens.[51] Several hypotheses exist for the mechanism by which commensal species and the host communicate to allow persistence of beneficial bacteria while preventing the overgrowth of harmful bacteria. For example, the production of polysaccharide A (PSA) by commensal bacteria signals for anti-inflammatory cytokine production by the host, and the binding of immunoglobulin A secreted by the host (sIGA) to gut bacteria aids in reducing inflammatory signaling.[50] A fine balance of these processes allows for tolerance of beneficial bacteria and exclusion of pathogens. Furthermore, *Akkermansia muciniphila*, a bacteria that resides in the mucus layer near host epithelial cells, directly interacts with the host immune system to induce the production of antigen-specific immunoglobulin G1 (IgG1) antibodies during

homeostasis, indicating additional methods by which the gut microbiome modulates the host immune system to allow commensal colonization while excluding pathogens.[64]

Gut Barrier Integrity

Increasing evidence demonstrates that the gut microbiota is important for maintaining gut barrier homeostasis. Several bacterial species are linked with increased tight junction protein expression, including *Bifidobacterium infantis*, *Bifidobacterium bifidum*, *Lactobacilllus rhamnosus*, and *Faecalibacterium prausnitzii*.[65] SCFA-producing bacteria have also been associated with increased mucin production and goblet cell differentiation, including *Bacteroides thetaiotaomicron*, *Faecalibacterium prausnitzii*, and *Akkermansia muciniphila*.[65] In fact, *A. muciniphila* has been shown to induce anti-inflammatory host responses and bolster gut barrier integrity. In contrast, other mucin degrading bacteria such as *Ruminococcus gnavus* and *Ruminococcus torques* are implicated in loss of the mucin layer of IBD patients, allowing bacteria access to the epithelial surface to exacerbate inflammation.[65] Careful modulation of the gut bacteria clearly has a role in preventing diseases of the large intestine, including IBDs and CRC, therefore understanding how the microbiome can be altered has an important role in the prevention of these diseases.

Modulation of Gut Microbiome by Host Environment

Many factors can influence the composition of the gut microbiome, potentially resulting in the unbalance referred to as dysbiosis that can impact not only gut health but also overall host health.[51] These factors include host age, diet, antibiotic use, and genetics.[51,66] More recently, methods to modulate the microbiome in an attempt to

prevent or treat dysbiosis have gained interest, including the use of probiotics, prebiotics, and fecal microbiota transplant.[51,66]

Increasing evidence suggests that the gut microbiome is mainly modulated by host environment. In one study, significant similarity was shown between unrelated hosts that cohabitate.[67] In one analysis of a twin study that examined the heritability of the gut microbiome, overall heritability is between 1.9 and 8.1%.[67] Diet patterns can directly alter the gut metabolome by altering the compounds available for metabolism as well as indirectly by causing shifts in the gut microbiome that participate in that metabolism.[68] Bioactive compounds introduced via the diet are capable of modulating gut physiology by acting as ligands for receptors.[69] Ligand-dependent activation of these receptors results in signaling that alters gene expression to modulate IBD and CRC risk. In addition to directly acting as ligands, many dietary compounds are metabolized by the gut microbiota to produce bioactive compounds that can additionally act as ligands.[68] These ligands can be relevant in many host physiological processes including immune responses.[70] Understanding how diet modulates the gut microbiome and therefore the metabolome is important for immune modulation and prevention of gastrointestinal diseases including IBD and CRC.

Role in Colon Pathologies

Alterations in the Gut Microbiome

The major bacterial phyla of the GI tract contain species of bacteria that are generally considered both beneficial and harmful for health, and their ratios appear to be vitally important in some disease states. For example, historically, the pathogenic

bacterial species *Helicobacter pylori* has been directly implicated in gastric cancer, and gut microbiome diversity is often decreased in human CRC patients.[21,71] More recently, the concept of dysbiosis or an imbalance in the gut microbiota or its functions has been associated with a variety of host diseases, including IBDs and CRC.[72] Specific species or strains of bacteria can disrupt the microbiome and promote inflammation or carcinogenesis, increasing the risk of IBD and CRC development.[21] For example, pathogenic infection with microbes such as *Salmonella enterica* can induce inflammation and activate β-catenin signaling and *Citrobacter rodentium* drives colonocyte proliferation and reduces barrier function.[21] However, pathogenic bacterial species are not the only microbes implicated in IBD and CRC risk. *Fusobacterium nucleatum*, long considered a commensal oral microbe, is enriched in CRC patients, activates oncogenic Wnt signaling, and alters the function of immune cells.[73] *Fusobacterium* spp. are also increased in UC patients compared to healthy controls, and its ability to invade the mucosa worsens IBD severity.[74] The impacts of these bacteria can even extend beyond cancer initiation or promotion. *F. nucleatum* has also been shown to lead to the resistance of CRC cells to the chemotherapeutic drug oxaliplatin in preclinical models.[73]

Alterations in the Gut Metabolome

The functional properties of the gut microbiome can also be linked to these pathologies. For example, several genera involved in SCFA production including *Bifidobacterium*, *Lactobacillus*, *Rosburia*, *Lachnospira*, and others are present in lower relative abundances in CRC patients.[21,51,52] In another example, bacteria can also

modulate the flux of tryptophan metabolism through the enzyme indoleamine 2,3-dioxygenase 1 (IDO1).[56] *Bifidobacterium infantis* can decrease the kynurenine-to-tryptophan ratio by reducing IDO1 activity, resulting in decreased risk of irritable bowel syndrome and inflammatory diseases.[56] Additionally, red meat, which has been linked to increased risk of CRC, is particularly high in choline and carnitine that can be converted to trimethylamine N-oxide (TMAO) which has been linked to CRC development.[21] Correspondingly, several species associated with higher TMAO production are enriched in CRC patients, including *Klebsiella oxytoca* and *Escherichia coli*.[21] Similarly, hydrogen sulfide (H_2S), produced from red and processed meat, has been linked to both IBD and CRC, and sulfur-reducing species of the genera *Fusobacterium* and *Bilophila* have been found to be enriched in these patients.[21]

Future Directions and Implications

As the important role of the gut microbiota in colon health and disease development is increasingly elucidated, several methods have been proposed to mediate the microbiome to prevent IBD and CRC development. Everything from probiotic supplements, selective antibiotics, fecal microbiota transplant, and vaccines have been proposed to reduce the risk of the development of these colon pathologies, prevent their progression, and decrease the toxicity associated with their treatments.[73]

Despite all that is known of the gut microbiome, most of the bacterial species discovered in the GI tract are uncultivated and therefore unidentified microorganisms.[75] Despite the discovery of mechanisms that may directly connect the gut microbiome to IBD and CRC risk, there is still limited evidence for the appropriate balance of bacterial

species for optimal gut health.[21] Furthermore, the dysbiosis associated with IBDs and CRC could be either a cause or consequence of these disease states.[21] Additionally, the collection of bacteria that may lead to disease in one individual may not negatively impact another host.[72] These insights highlight the importance of further investigation of this ecosystem that is vital to human health.

Overall Objective

The main objective of this dissertation is to determine the effects of exogenous, endogenous, or microbially-derived ligands on nuclear receptor signaling in colonic epithelial cells and how this signaling impacts inflammation and carcinogenesis in the colon.

CHAPTER II

BISPHENOL-A ALTERS MICROBIOTA METABOLITES DERIVED FROM AROMATIC AMINO ACIDS AND WORSENS DISEASE ACTIVITY DURING COLITIS*

Introduction

Inflammatory Bowel Disease (IBD) is a complex collection of gastrointestinal disorders. IBD incidence is on the rise, a concerning trend, as treatment is lifelong and often requires surgery, and colitis associated inflammation is a risk factor for developing colon cancer.[6,7,10] Increased prevalence of these diseases has been observed in North American and European nations for decades, but as developing nations become more industrialized, IBD prevalence increases in these countries.[6,10] A growing body of data suggests environmental exposures significantly influence IBD development and relapse.[6,7,10] The two most common IBDs, Crohn's Disease (CD) and Ulcerative Colitis (UC), differ in their pathophysiology, patterns of incidence, and environmental risk factors, complicating the elucidation of the role of the environment in IBD.[6] Proposed environmental risk factors for IBD include diet, smoking, infections and pharmaceutical usage, altered gut microbiome, estrogen-containing medication usage, and toxins or pollutants.[6,10,11]

Both endogenous estrogens as well as pharmaceutical estrogens in oral contraceptive pills and hormone replacement therapy are potential risk factors for IBD development and relapse.[6,10,11] Therefore, it is plausible that environmental exposure to xenoestrogens (XEs) could increase the risk of IBD. One such XE, bisphenol A (BPA) is used in the production of polymers including those that compose polycarbonate plastics, epoxy resins, and thermal paper.[76] A major source of human exposure to BPA is in the diet, particularly through canned foods.[76,77] Epoxy resins line metal food and beverage containers, and polycarbonate plastics are also used in a variety of food related containers.[77] Worldwide, over 3.8 million tons of BPA are produced annually, and because BPA is used in a wide variety of consumer and industrial applications, it is pervasive in the environment and human tissues.[77,78] For example, in the United States, BPA was detected in the urine of 92.6% of tested individuals over the age of 6.[79] One review found BPA levels in human serum between 0.2 and 20 ng/mL, and these levels are above those BPA concentrations known to cause adverse effects *in vitro*.[78] Exposure to the compound has been linked with obesity, reproductive issues, metabolic disorders, hormone dependent tumors, and other health effects.[78,80] The Environmental Protection Agency has established guidelines for acceptable levels of BPA exposure in humans.[81] The No Observed Adverse Effect Level (NOAEL) is 5 mg/kg-bw/day, the Lowest Observed Adverse Effect Level (LOAEL) is 50 mg/kg-bw/day, and the reference dose is 50 µg/kg-bw/day.[81] This reference dose is an estimate of the daily exposure level that is unlikely to cause deleterious effects in humans over the course of the lifespan. However,

several studies have shown negative effects of this or lower doses, and a lower reference dose of 16 µg/kg-bw/day has been proposed.[82–84]

BPA is considered an endocrine disruptor capable of binding estrogen receptor α and β (ERα and ERβ, respectively), as well as G-protein coupled receptor 30 (GPR30), and other non-classical estrogen-related receptors, which may provide a mechanistic explanation for these adverse effects.[85] More specifically, BPA mimics 17β-estradiol (E_2) when binding to ERα, but acts as an antagonist when binding ERβ.[85] This is particularly relevant in the colon, where ERβ is the primary ER and is considered to mediate the protective effects of estrogen in inflammation-associated and sporadic colon cancer.[38,86] It is has been previously shown that BPA is linked to changes in gut barrier function, inflammation, and altered gut microbiome.[82,87,88] Previous studies have linked changes in gut microbiome and the levels of metabolites present in the feces with colonic inflammation and IBD development.[89] Reduced levels of tryptophan (Trp) and several microbiota metabolites derived from aromatic amino acids (MDAs) including serotonin have been associated with IBD and with increased severity of symptoms in human patients and animal models.[90] Therefore, compounds that alter the gut microbiome and, as a result, the metabolome of the colon, could impact IBD development and symptom severity.

The purpose of this study was to determine the effects of BPA exposure on colonic inflammation and the intestinal metabolome both in the absence of and during dextran sulfate sodium (DSS)-induced colitis. Previous studies have shown that BPA does not alter disease severity or is mildly protective against 2,4,6-trinitrobenzene

sulfonic acid (TNBS)-induced colitis.[82,91] However, previous studies in our laboratory and others have demonstrated differential effects of E_2 signaling on varying models of colitis, particularly a worsening of disease severity during DSS-induced colitis.[92–94] In the work presented here, we hypothesized that BPA exacerbates DSS-induced colitis and reduces Trp and MDAs in the colon. Furthermore, we hypothesized that BPA would act similarly to E_2 *in vitro* in non-transformed mouse colonocytes.

Materials and Methods

Animal Model

Wild type C57BL/6 mice were obtained from Charles River Laboratories. The mice were housed at the Laboratory Animal Resources and Research facility at Texas A&M University. All procedures were performed under a protocol approved by the Institutional Animal Care and Use Committee at Texas A&M University. 10-week-old female C57BL/6 mice were randomly divided into four groups that received either no treatment (n=12), BPA alone (n=10), DSS alone (n=12), or BPA and DSS (n=12). The experimental timeline is shown in Figure II.1. Animals were allowed to acclimatize for one week prior to the start of the study. To limit the effects of variations in endogenous estrogen production, animals were ovariectomized as described previously.[86] Mice were transferred to a pelleted, purified, phytoestrogen-free diet (Baker Amino Acid Diet 5CC7, Test Diet) at the time of surgery and allowed food and reverse osmosis and UVUF treated water (Nanopure Diamond, Barnstead) ad libitum. Diet composition is provided in Figure A.1 of Appendix A. Mice were housed in polyethylene cages and provided drinking water in polyethylene bottles.

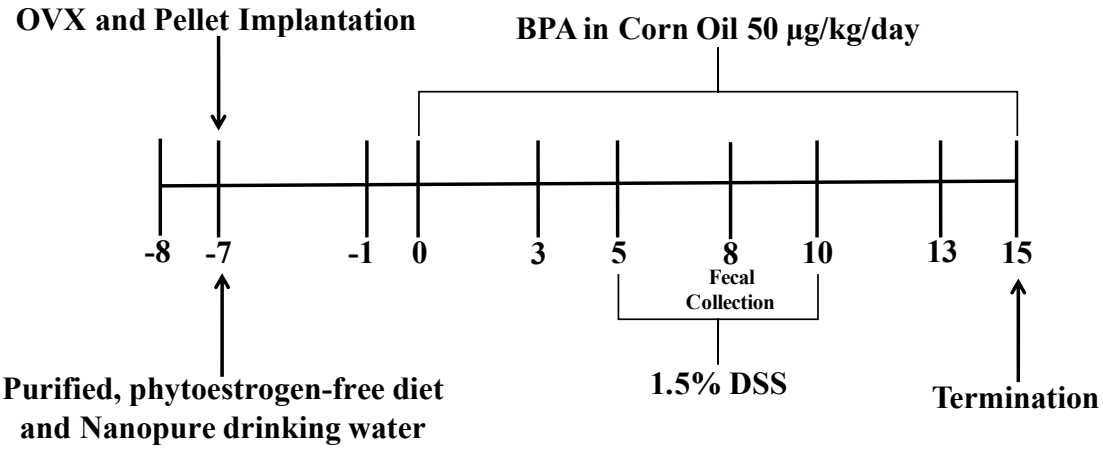

Figure II.1 Experimental Design.

Beginning one week after ovariectomy, animals were gavaged with 50 µg/kg-bw/day BPA (Sigma Aldrich) dissolved in corn oil or vehicle control for fifteen days at the same time each morning. BPA was first dissolved in ethanol for a final ethanol concentration in treatment and controls groups of 0.01%. BPA was dissolved in corn oil at a concentration of 6.25 µg/mL. This concentration allowed gavage of 1.25 µg BPA per 200 µL corn oil for a 25 g mouse such that the maximum gavage volume of 1% body weight was not exceeded. The same calculations were used to dose vehicle controls with corn oil. Treatments were prepared fresh daily.

Induction of Colitis

1.5% DSS (MP Biomedicals; 36-50 kDa) was provided *ad libitum* in drinking water from days five through ten of BPA treatment. DSS was replaced every 48 hours. Animals in control groups received normal drinking water. Body weight, fecal consistency score, and macroscopic fecal blood scores were obtained daily on all animals. Disease activity index (DAI), providing an average measure of body weight loss, fecal consistency score, and macroscopic rectal bleeding scores were adapted from

previous work.[95,96] Briefly, body weight loss percentage from start of study was scored as 0: weight gain or 0-1% loss, 1: 1-5% loss, 2: 5-10% loss, 3: 10-15% loss, 4: >15% loss compared to study day -1. Fecal consistency was scored as 0: normal stool, 1: soft but formed pellet, 2: very soft pellet, 3: diarrhea (no pellet), or 4: dysenteric diarrhea (blood in diarrhea). Rectal bleeding was scored as 0: no bleeding, 2: presence of visible blood in stool (red/dark pellet), 4: gross macroscopic bleeding (blood around anus). Body weight as well as fecal consistency, rectal bleeding, and disease activity scores are only reported through day 12. After this point, the loss of animals influenced these data points such that they were not interpretable.

Fecal and Tissue Collection

Animals were singly housed for up to two hours, and feces were collected prior to BPA treatment (day -1), and on days 3, 8, and 13 of BPA treatment, and at termination. For targeted metabolomics, day 8 samples were chosen because this time point would best allow for determining the effects of BPA on the gut metabolome during DSS-induced inflammation. Fecal pellets were flash frozen and stored at -80°C until analysis.

Animals were terminated on study day 15, five days following cessation of DSS. Final treatments of BPA or vehicle control were gavaged two hours before termination. Blood was collected via cardiac puncture, and plasma was stored at -20°C. Colons were resected, flushed with PBS, and opened longitudinally. Half of each colon was Swiss rolled, fixed in 4% paraformaldehyde (JT Baker) for 4 hours, and then sectioned for pathological analysis. 4 µm, non-serial sections from fixed colons were H&E stained and

scored for severity of acute colonic inflammation and injury by a blinded, board-certified pathologist (B. Weeks). Degree of inflammation was scored as 0: no unexpected inflammation, 1: minimal to very mild inflammation, 2: mild to moderate inflammation, or 3: moderate to severe inflammation. Degree of tissue injury was scored as 0: no unexpected injury, 1: minimal to very mild injury, 2: mild to moderate injury, or 3: moderate to severe injury. Nodularity or aggregation of inflammation was scored as 0: diffuse inflammation, 1: minimal to very mild nodular inflammation 2: moderately nodular inflammation, or 3: very nodular inflammation.

Cytokine Analysis

Cytokine analysis was performed as described previously.[92] The other longitudinal half of the colons were snap frozen in liquid nitrogen at termination and stored at -80°C until analysis. Briefly, the middle third of these sections of colon were homogenized in 333 µL Tissue Protein Extraction Reagent (Thermo Scientific). Homogenate was centrifuged at 10,000 g for 5 minutes before 100µL aliquots of supernatant were stored at -20°C until analysis. Following protein concentration measurement using the DC Protein Assay (Bio-Rad), all samples were diluted to 2 mg/mL. The Milliplex Map Mouse Cytokine/Chemokine Magnetic Bead Panel Immunology Multiplex Assay (Millipore, MCYTMAG-70K-PX32) was used per the manufacturer's instructions with provided internal quality controls. The plate was analyzed on a BioPlex 200 (Bio-Rad).

Quantification of Metabolites from Aromatic Amino Acids

Fecal samples for targeted metabolomics were processed and run at Integrated Metabolomics Analysis Core at Texas A&M University. Nine metabolites derived from aromatic amino acids were quantified from fecal samples.[97] Fecal samples were homogenized in methanol/chloroform and metabolites were extracted as previously described with minor modifications.[98] Briefly, metabolites were sequentially extracted twice using 1 ml of cold methanol and 0.5 ml of chloroform using a homogenizer (Omni International). The polar phase was separated and concentrated using a vacufuge (Eppendorf, Hauppauge, NY). The concentrated pellet was re-suspended in methanol/water (1:1 v/v) and metabolites of interest were quantified using a Synergi Fusion-RP 4µ 80Å 150 x 2.0 mm column (Phenomenex) on a triple Quadrupole Mass Spectrometer (TSQ Quantiva™) coupled to liquid chromatography (Agilent). The solvents used were Water + 0.1% Formic Acid and Methanol, 0.1% Formic Acid. Pure standards were run for 10 known concentrations (ranging from 0.009 µg/ml to 10 µg/ml) for each metabolite and metabolite concentrations in the samples were determined from the integration of the standard curves.

Assessment of BPA in Non-Transformed Mouse Colonocytes

To assess the estrogenic activity of BPA in non-transformed mouse colonocyte cells, Young Adult Mouse Colonocyte (YAMC) bleo/neo cells, provided by Dr. Hartmut Land (University of Rochester Medical Center), were grown at the permissive condition of 33°C in RPMI 1640 media (Sigma Aldrich) with 10% fetal bovine serum (FBS, Hyclone), 1% gentamycin (GIBCO), and 0.1% insulin, transferrin, and selenious acid

(ITS, BD Biosciences) as well as 0.5 μL Interferon- γ (IFN-γ) per 10 mL media on rat collagen-coated cell-culture dishes. For experiments, cells were transferred to media containing charcoal dextran–stripped FBS to remove estrogenic compounds 48 h before plating. FBS was charcoal dextran-stripped as previously described.[99] Cells were seeded at a concentration of 7.5 x 10^4 cells/well in rat collagen-coated 6-well plates (Grenier Bio-One) at the non-permissive temperature of 39°C without IFN-γ. Twenty-four h after plating, cells were treated with vehicle (0.1% DMSO), 1 nM E_2, and 1mM-1 nM BPA at 10-fold dose increments. This experiment was repeated with the same conditions, using vehicle (0.2% DMSO), 1 nM E_2, and 10 nM BPA with and without 1 μM ICI 182, 780 (ICI, Tocris Bioscience). Three wells per treatment per experiment were used, and three replicate experiments were conducted. Seventy-two hours after treatment, cells were trypsinized and cell number was quantified. Dose response experiments were quantified using a Cellometer Auto 1000 (Nexcelom Bioscience) according to the manufacturer's protocol. Twenty μL of 1mL total media containing trypsizined cells was loaded into the cell counting chamber, and each sample was counted in triplicate. The ICI experiments were quantified using a Countess II Automated Cell Counter (Invitrogen) according to the manufacturer's protocol. Ten μL of 0.5 mL total media containing trypsinized cells was combined with 10 μL Trypan blue before 10 μL of mixture was loaded into the cell counting chamber, and each sample was counted in triplicate.

Apoptosis of YAMCs treated with BPA was then assessed. Cells were seeded with the same conditions as the cell number assay, but treatments consisted of vehicle (0.1% DMSO), 1 nM E_2, 10 nM BPA, and 1 nM BPA. Cells were trypsinized and

washed twice with PBS. Caspase-3 activity was estimated by fluorescence using the manufacturer's protocol for the EnzChek Caspase-3 Assay Kit #2, Z-DEVD-R110 substrate (Molecular Probes). Fifty μL of 1X cell lysis buffer was used to lyse cells on ice for 30 mins before buffer was collected and centrifuged at 5000 rpm for 5 min. Fifty μL of supernatant of each sample was transferred to a 96-well, flat bottom, black plate (BD Bioscience). Fifty μL of 2X substrate was added to each well, and plates were incubated in the dark at room temperature for 30 min. A TECAN infinite M200 plate reader was used to measure florescence at wavelengths 496 (excitation)/520 (emission) at 3 separate 15 minute intervals.

Statistical Analysis

Data was analyzed using JMP 13.0.0 software. Outliers were removed, one-way ANOVA was used to determine significant ($p < 0.05$) differences between groups, and, once found significant, student's t test was used to compare means between specific groups. To determine if survival times were significantly different ($p < 0.05$) between groups, the log-rank test was performed. Non-parametric, categorical inflammation, injury, and nodularity score data was transformed to achieve normality by assigning an average rank within each sub-group as previously reported.[100] One-tailed student's t test assuming unequal variances was then used to determine significance ($p < 0.05$). Metabolome data was normalized to per gram of the starting material and analyzed using KaleidaGraph. Outliers were removed following Grubb's test and scatterplot analysis, then data was normalized and analyzed using a one-tailed t test.

Results

Disease Activity

In the presence of DSS, BPA co-treatment resulted in earlier and increased mortality compared to control animals (Figure II.2). Log-rank test indicated significant differences between survival among all groups ($p < 0.001$), and DSS and BPA co-treatment resulted in significantly worsened mortality compared to DSS alone ($p=0.0084$). DSS alone did not result in significantly increased mortality compared to vehicle control ($p=0.1483$). DSS and BPA combination resulted in 67% mortality, with most deaths between 5 and 7 days after initiation of DSS. DSS alone resulted in 17% mortality, with most deaths occurring between 7 and 9 days after the start of DSS. No control or BPA alone treated animals died during the course of the study.

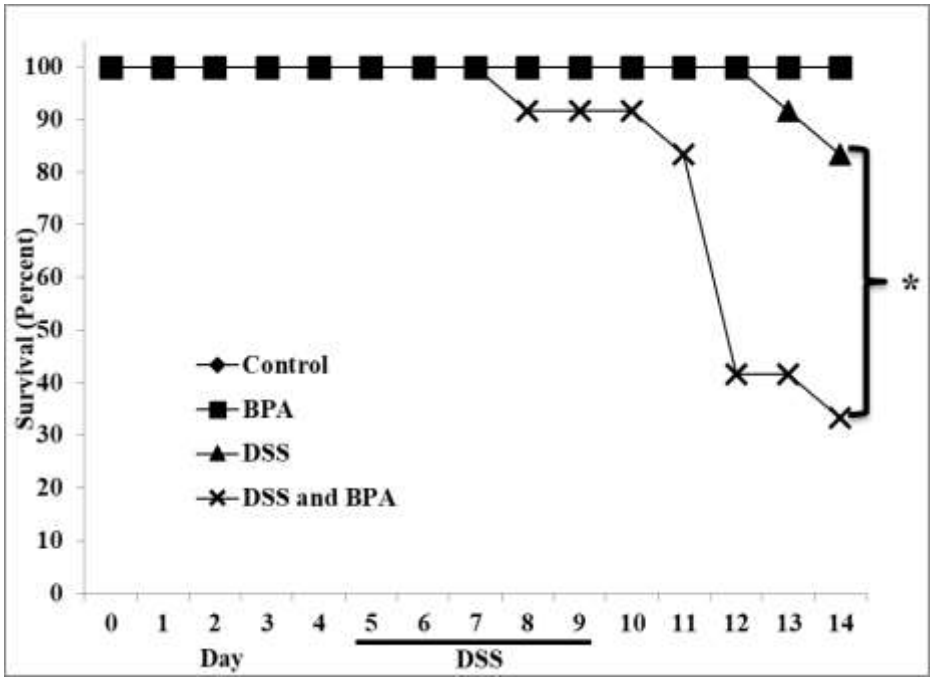

Figure II.2 Survival Curve. Animals alive at start of day, expressed as percent of total group size at start of experiment. n=10 to 12 per group at the start of the study and declined over time as shown. Log-rank $p < 0.0001$. * indicates significant difference; $p < 0.05$.

Average group body weight did not differ significantly at start of study. By day eleven, six days after initiation of DSS treatment, DSS groups had significantly lower body weight than non-DSS groups, but BPA exposure did not significantly reduce body weight compared to controls in either DSS or non-DSS treated mice (Figure II.3A). As expected, DSS worsened fecal consistency scores beginning 24 hours after initial exposure. This difference was significant regardless of BPA exposure. After cessation of DSS, DSS alone animals showed improved fecal consistency scores, however, animals co-treated with BPA exhibited significantly worsened scores during the recovery period on days 10-12 (Figure II.3B). DSS worsened rectal bleeding scores within three days of DSS initiation. BPA exposure significantly worsened macroscopic rectal bleeding beginning four days after initial DSS exposure and throughout the remainder of the study (Figure II.3C).

A.

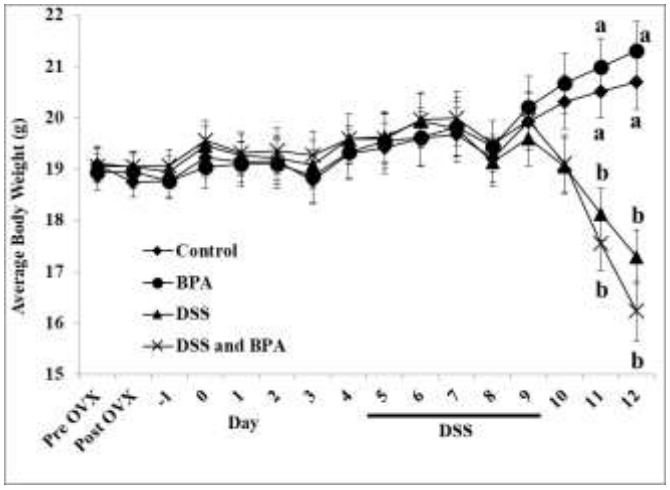

B.

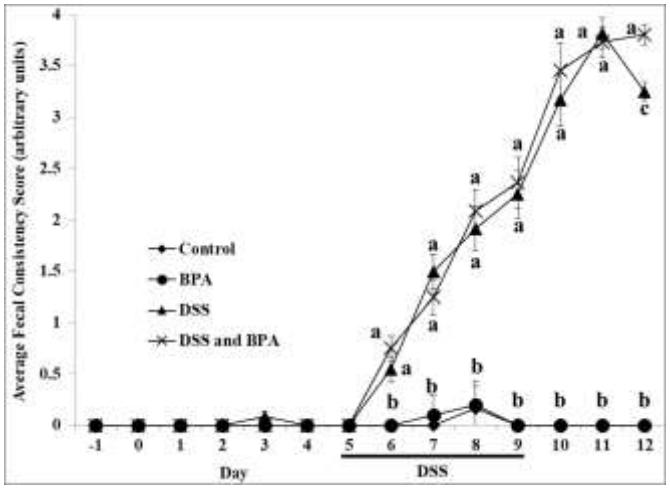

Figure II.3 Measures of Disease Activity. Scoring system adapted from Murthy, et al. *Dig Dis Sci* 1993 and Singh, et al. *Immunity* 2014. n=10 to 12 per group at the start of the study; n declined over time as shown in the survival curve. Mean +/- SEM. Points without a common letter differ on the given day; $p < 0.05$. A. Average Body Weight. B. Average Fecal Score. Scoring System: 0 = Normal Stool, 1 = Soft but Formed Pellet, 2 = Very Soft Pellet, 3 = Diarrhea (No Pellet), 4 = Dysenteric Diarrhea (Blood in Diarrhea). C. Average Rectal Bleeding Score. Scoring System: 0 = No visible blood, 2: presence of visible blood in stool (red/dark pellet), 4: gross macroscopic bleeding (blood around anus). D. Disease Activity Index. Average of body weight loss, fecal consistency, and rectal bleeding scores.

C.

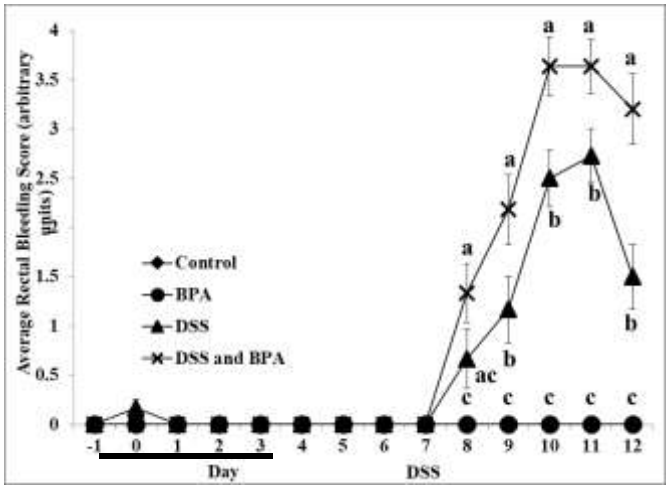

D.

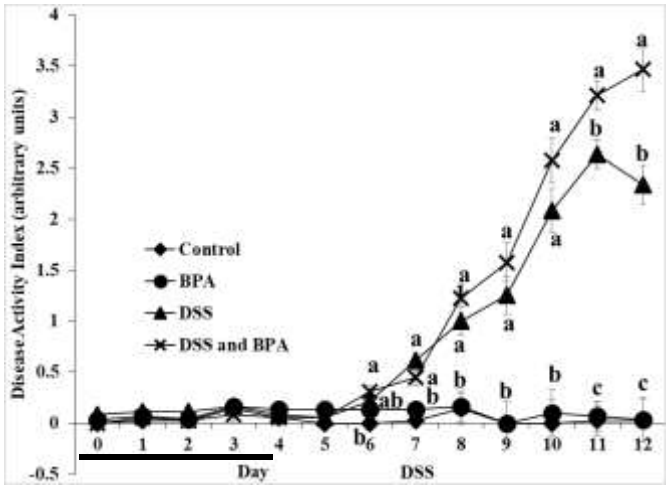

Figure II.3 Continued.

DAI was significantly worsened in both DSS treated groups within 48 hours of initiation of DSS (Figure II.3D). Following cessation of DSS, the DSS group showed score improvement more quickly than the DSS and BPA group. By day 11 of the study, BPA exposure resulted in a significantly worse DAI when compared to the DSS controls. BPA treatment did not significantly alter DAI in groups not treated with DSS. DSS treatment shortened colon length regardless of BPA treatment, and DSS alone significantly increased colon weight/length (Figure II.4A-C).

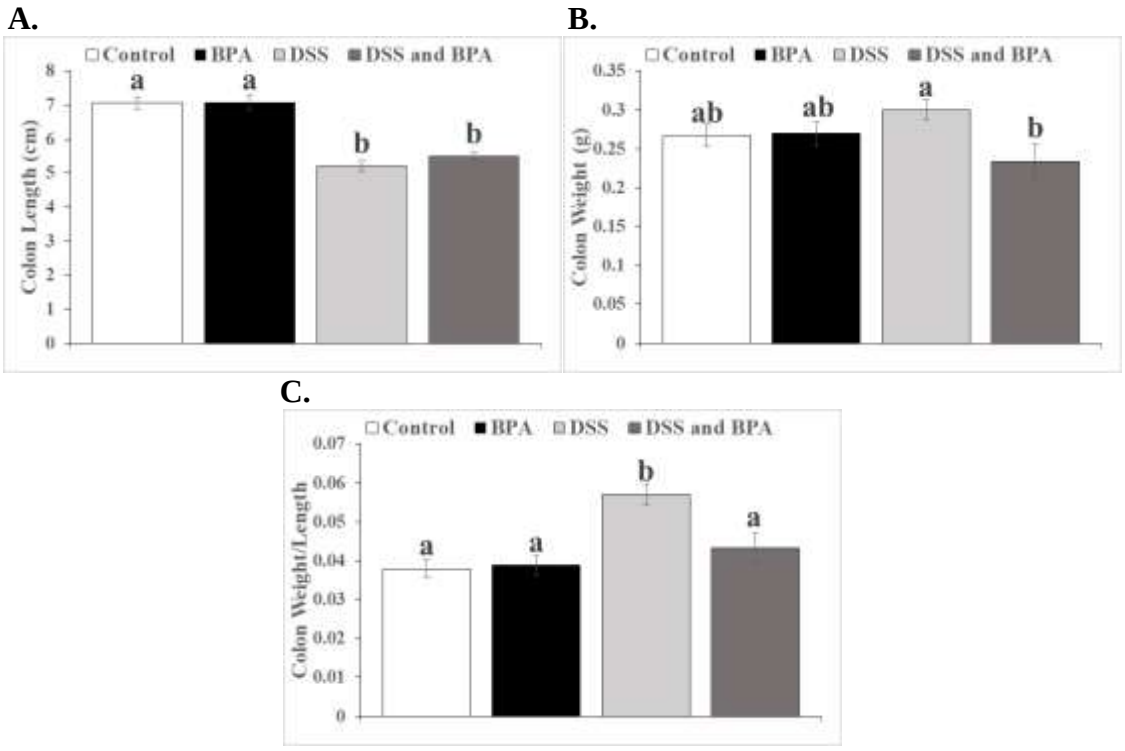

Figure II.4 Colon Length and Weight. A. Colon length. B. Colon weight. C. Colon weight/length. Mean +/- SEM. Bars without a common letter differ; p < 0.05.

Histological Scores

Pathologist scoring of tissues from each group showed an increase in inflammation in the middle portion of the colon in BPA dosed animals regardless of DSS. This increase was not significant in BPA treated animals compared to controls (Figure II.5A). However, inflammation score was significantly increased in the middle colon region in mice exposed to BPA and DSS when compared to DSS treated controls ($p=0.04$; Figure II.5B). Injury was also scored in these tissues, and, as expected, DSS significantly increased both inflammation and injury scores. BPA did not significantly alter injury score in the presence or absence of DSS (data not shown). Nodularity was assessed in DSS treatment groups to assess pattern of inflammation. Nodularity score was also significantly increased in the middle colon region in BPA and DSS co-treated

animals compared to DSS controls (p=0.02; Figure II.5C). Representative images of increased inflammation in the middle portion of the colon, colon ulceration and erosion, as well as nodular and diffuse inflammation are shown in Figure II.5D-H.

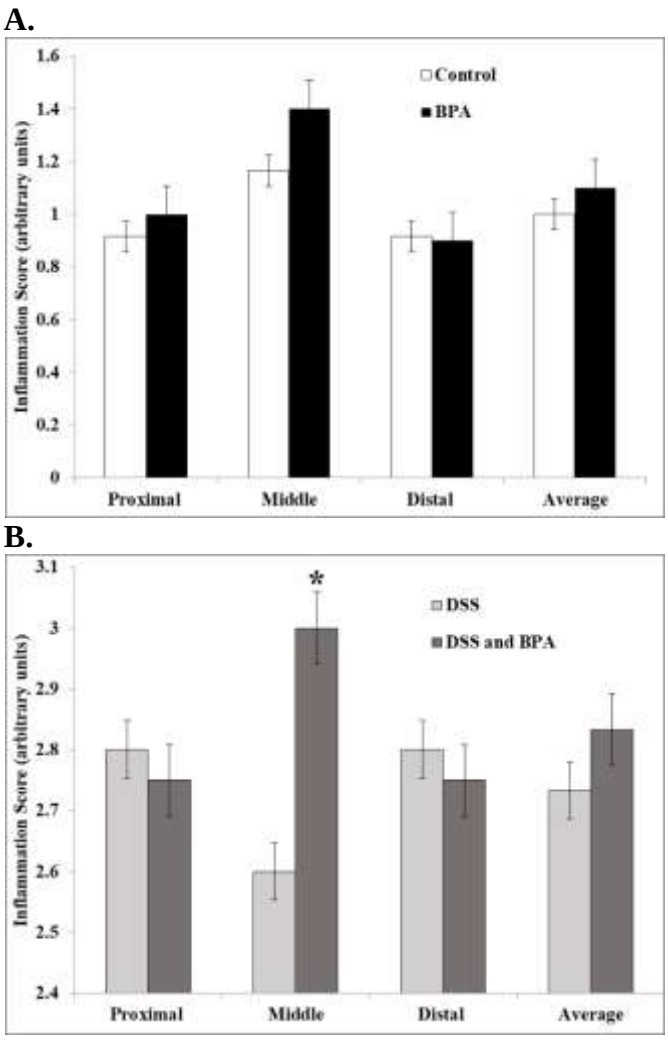

Figure II.5 Colon Inflammation and Nodularity. A. BPA and colonic inflammation in the absence of DSS. B. BPA and colonic inflammation in the presence of DSS. C. Nodularity in the presence of DSS. Mean +/- SEM. * indicates significant difference compared to control; p < 0.05. D. Representative image of increased inflammation in middle portion of colon. Inflamed portion of the middle colon is indicated by black arrows. E. Representative image of ulceration in the colon. Ulcer is indicated by the black arrow. F. Representative image of erosion of the colon. Erosion is indicated by the black arrow. G. Representative image of nodular inflammation. Nodular inflammation is indicated by the black arrow. H. Representative image of diffuse inflammation. Diffuse inflammation is indicated by the black arrows.

C.

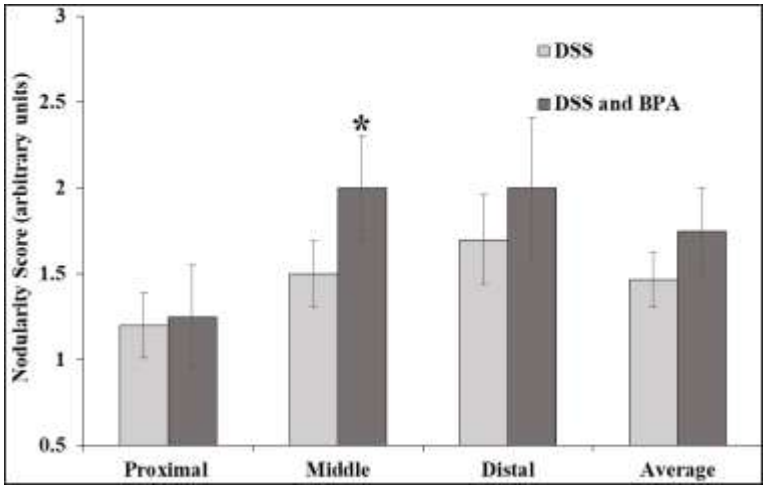

D.

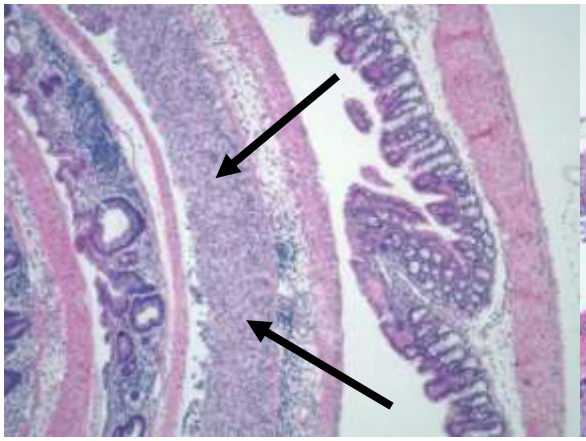

E.

F.

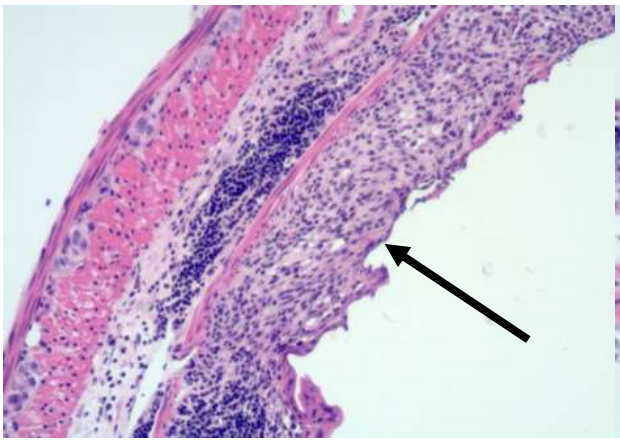

G.

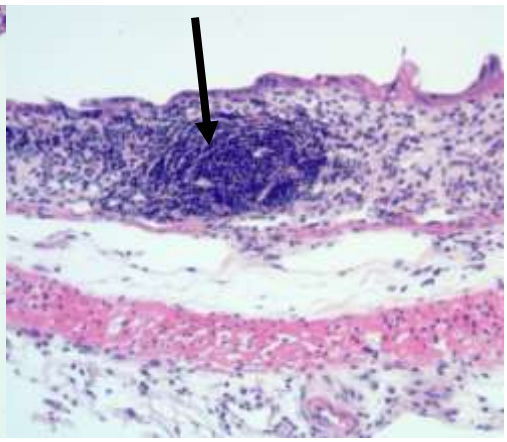

Figure II.5 Continued.

H.

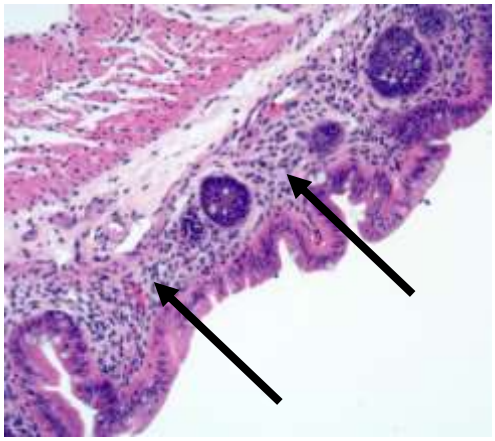

Figure II.5 Continued.

Cytokine Measurements

Cytokine protein levels were determined using multiplex magnetic bead assays. Cytokine expression is often used to assess inflammation in DSS models.[101,102] In the present study, cytokines were measured in the middle portion of the colon as significant differences in histological inflammation score were observed in this region. As expected, DSS treatment led to an increase in cytokines (e.g. TNF- α and IL-1β) that have been previously reported to be elevated in DSS treated mice compared to controls (data not shown).[101–103] This supports the pathological analysis that DSS induced tissue inflammation in this portion of the colon. However, we chose to focus on cytokines that were changed between the DSS alone and DSS and BPA treated mice to explore how BPA may be exacerbating the effects of DSS. DSS and BPA co-treatment significantly increased expression of IL-1α, IL-12p(70), IL-13, and IL-31 compared to all other treatment groups (Figure II.6A-D). VEGF expression was significantly decreased by DSS and BPA treatment compared to control (Figure II.6E).

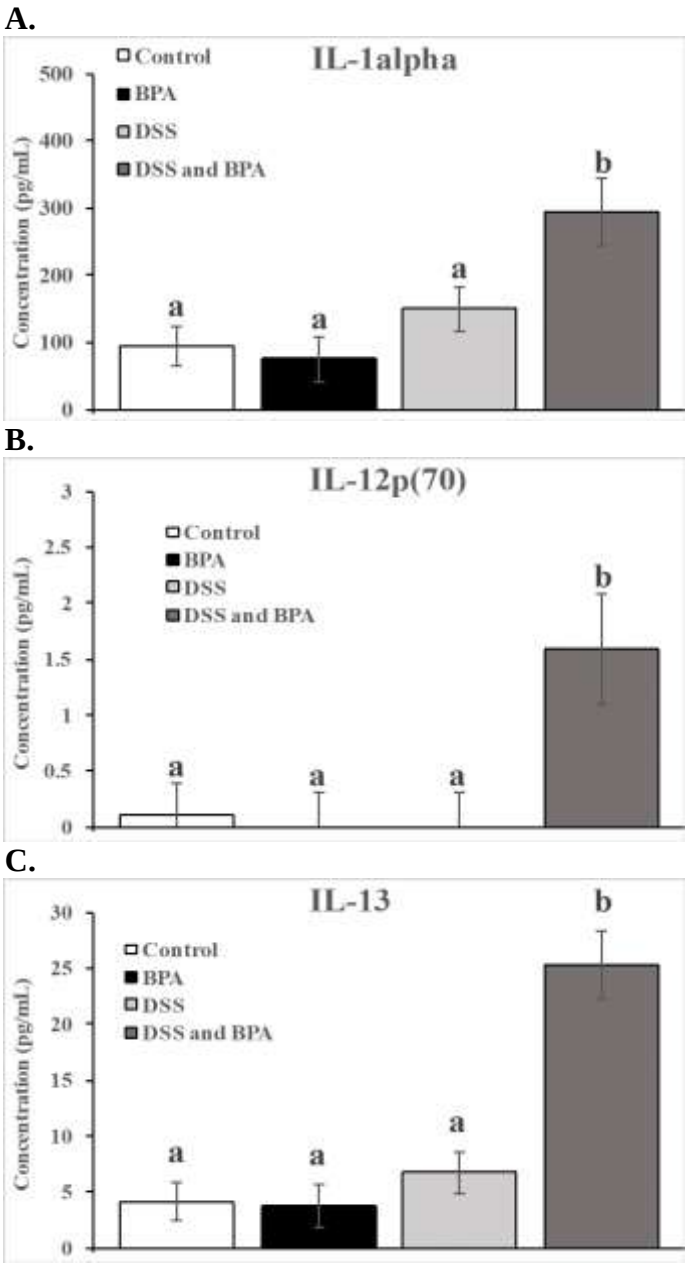

Figure II.6 Concentration of Cytokines in Middle Portion of Colon. A. IL-1α. B. IL-12p(70). C. IL-13. D. IL-31. E. VEGF. Mean +/- SEM. Bars without a common letter differ; $p < 0.05$.

D.

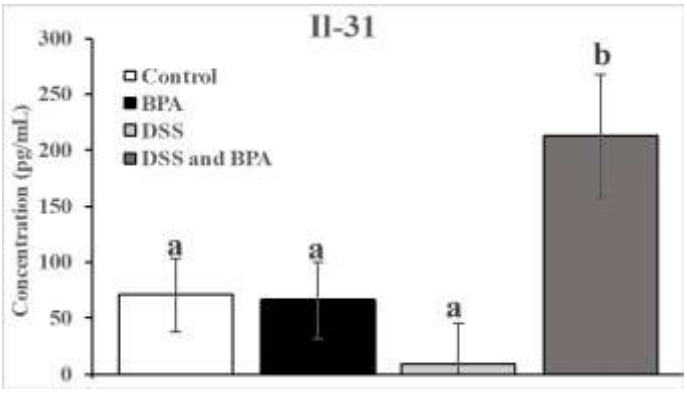

E.

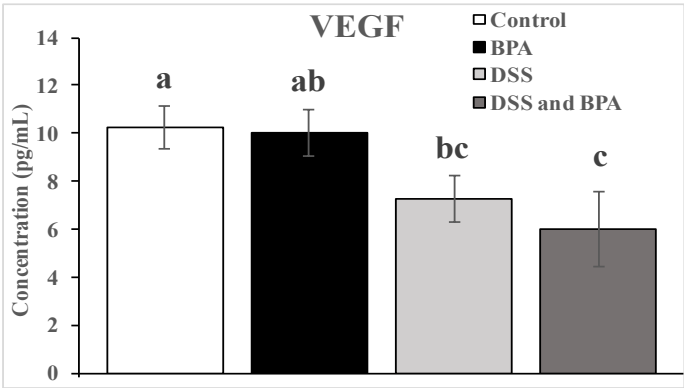

Figure II.6 Continued.

Targeted Metabolomics

The concentration of 9 MDAs in fecal pellets collected on day 8 of BPA treatment was analyzed. 5-hydroxy indole 3-acetic acid (HIAA), serotonin, and Trp concentrations were significantly decreased in the presence of BPA compared to vehicle control without DSS treatment ($p<0.05$; Figure II.7A-I). HIAA concentration decreased 66% ($p=0.0004$, Figure II.7B), serotonin concentration decreased 35% ($p=0.003$, Figure II.7F), and Trp concentration in feces decreased 52% ($p=0.006$; Figure II.7I), in BPA treated animals compared to vehicle treated controls. No significant changes were found in other MDAs measured, including 3-indole acetic acid (Figure II.7A), anthranilic acid

(Figure II.7C), indole 3-acetamide (Figure II.7D), indole 3-carboxaldehyde (Figure II.7E), shikimic acid (Figure II.7G), and tryptamine (Figure II.7H).

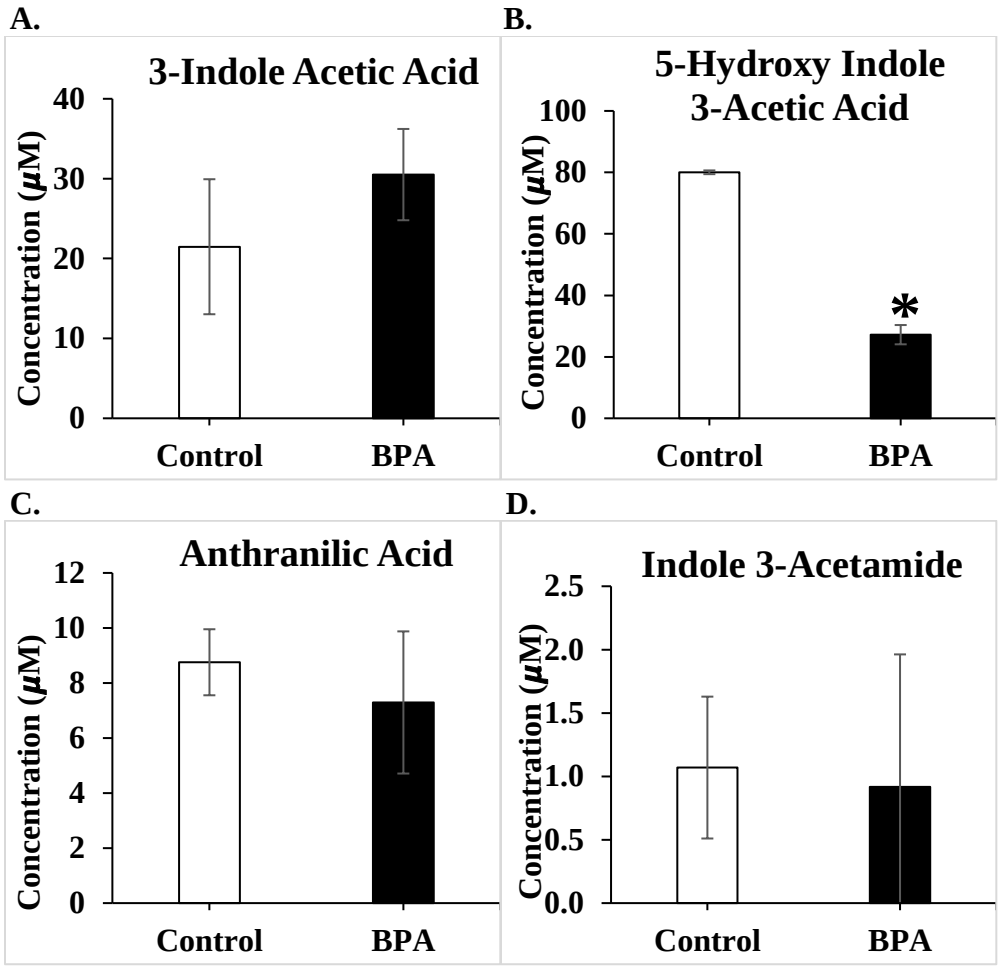

Figure II.7 Concentration of Specific Metabolites in Feces on Day 8 in Control Compared to BPA Treated Animals in the Absence of DSS Treatment. A. 3-Indole Acetic Acid. B. 5-hydroxy Indole 3-Acetic Acid. C. Anthranilic Acid. D. Indole 3-Acetamide. E. Indole 3-Carboxaldehyde. F. Serotonin. G. Shikimic Acid. H. Tryptamine. I. Tryptophan. Mean +/- SEM. * indicates significant difference compared to control; $p < 0.05$.

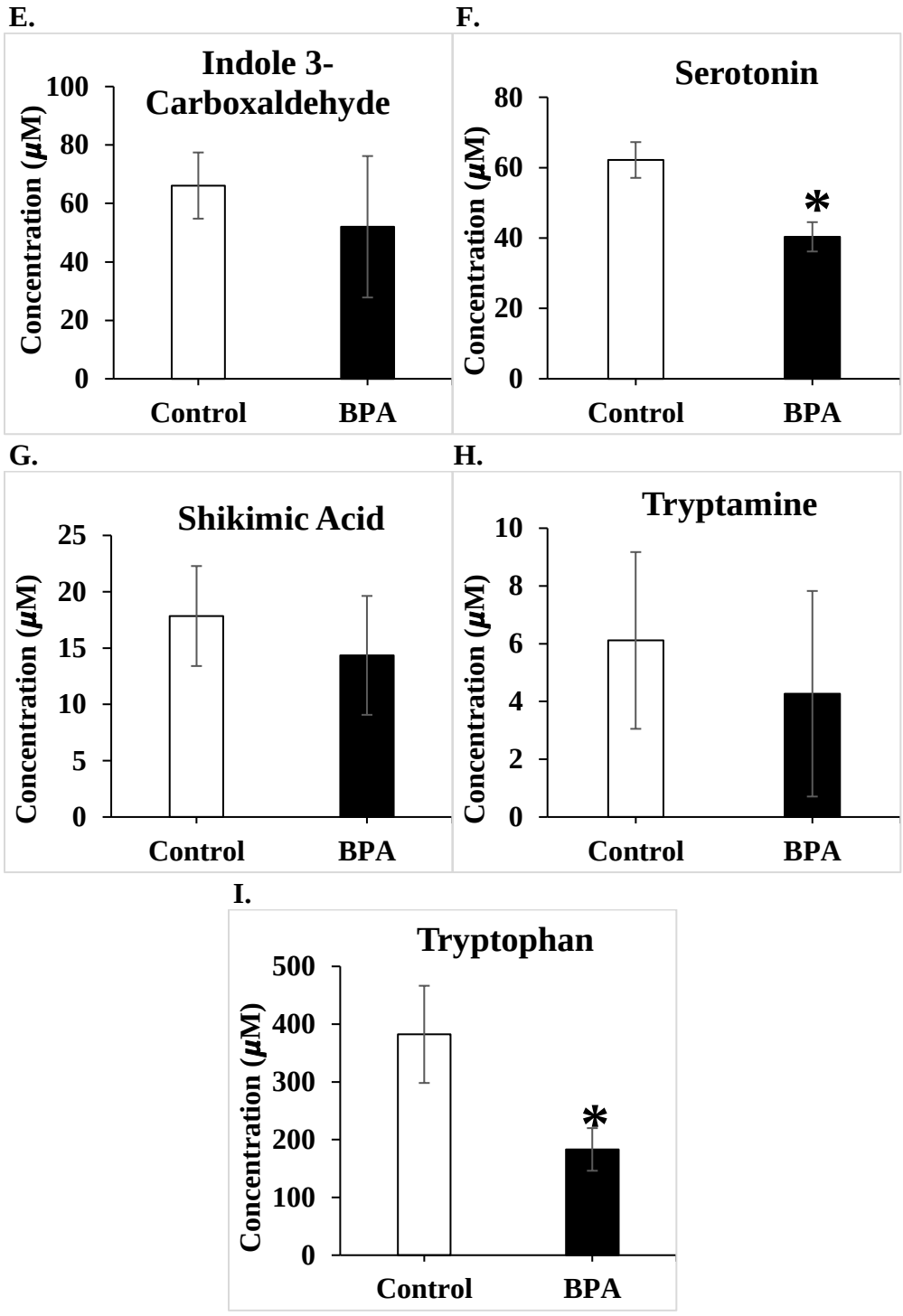

Figure II.7 Continued.

A heat map shows the changes in the concentrations of the quantified metabolites with or without BPA treatment in the absence of DSS (Figure II.8).

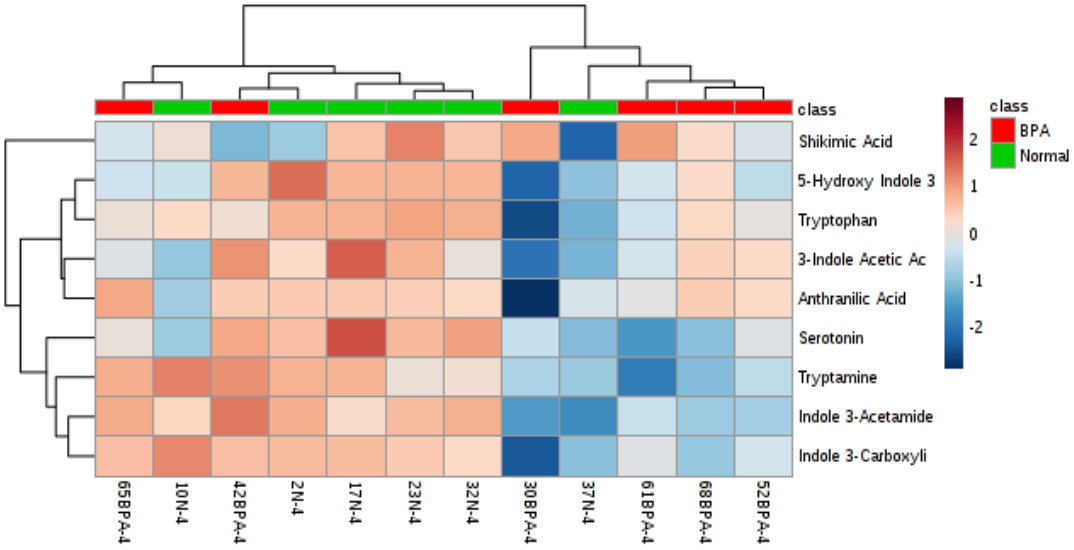

Figure II.8 Changes in Concentrations of Trp Metabolites with or without BPA Treatment in the Absence of DSS.

Trp, tryptamine, HIAA, indole 3-carboxaldehyde, and shikimic acid significantly decreased in the presence of BPA and DSS co-treatment compared to DSS alone ($p<0.05$; Figure II.9A-I). Metabolite concentration were decreased in feces of DSS and BPA treated mice compared with DSS and vehicle control mice as follows: HIAA by 77% ($p=0.02$, Figure II.9B), indole 3-carboxaldehyde by 87% ($p=0.007$, Figure II.9E), shikimic acid by 32% ($p=0.03$, Figure II.9G), tryptamine by 73% ($p=0.003$, Figure II.9H), and Trp by 26% ($p=0.001$, Figure II.9I). Other metabolites measured, including 3-indole acetic acid (Figure II.9A), anthranilic acid (Figure II.9C), indole-3-acetamide (Figure II.9D), and serotonin (Figure II.9F), did not significantly change.

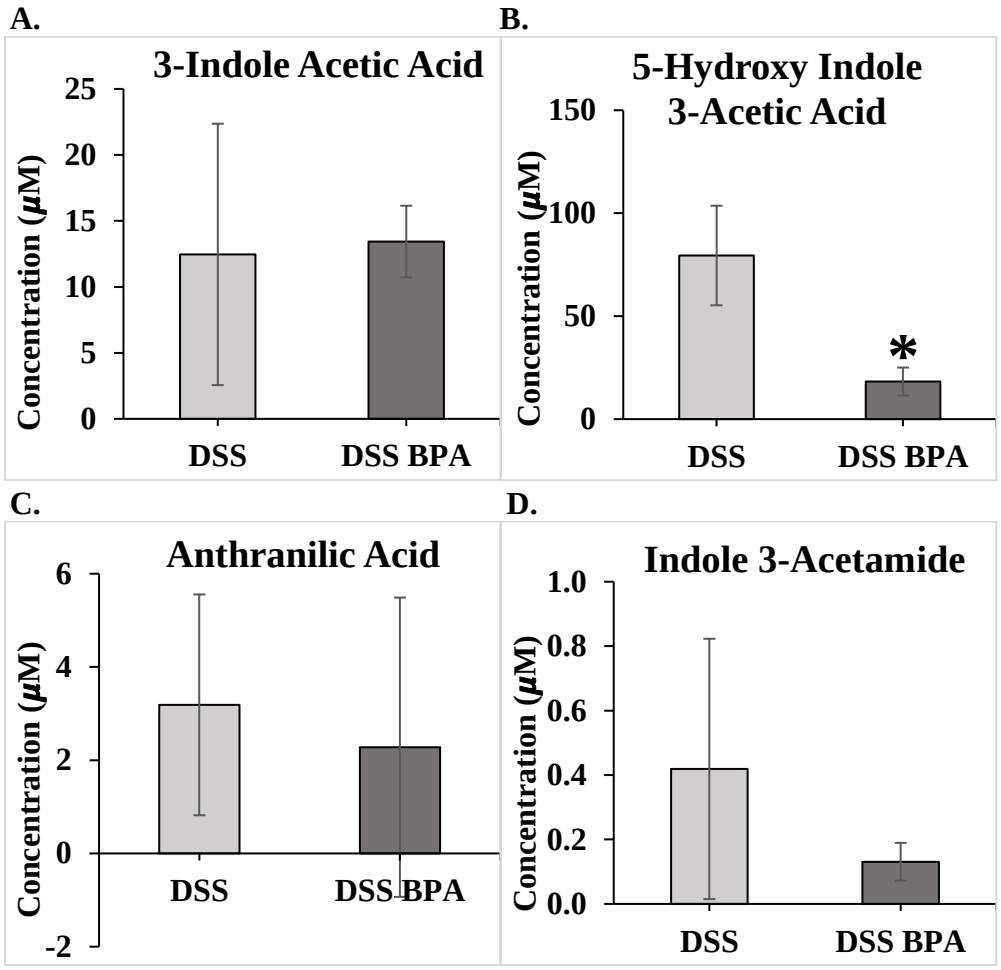

Figure II.9 Concentration of Specific Metabolites in Feces on Day 8 in Control Compared to BPA Treated Animals Co-Treated with DSS. A. 3-Indole Acetic Acid. B. 5-hydroxy Indole 3-Acetic Acid. C. Anthranilic Acid. D. Indole 3-Acetamide. E. Indole 3-Carboxaldehyde. F. Serotonin. G. Shikimic Acid. H. Tryptamine. I. Tryptophan. Mean +/- SEM. * indicates significant difference compared to DSS alone; $p < 0.05$.

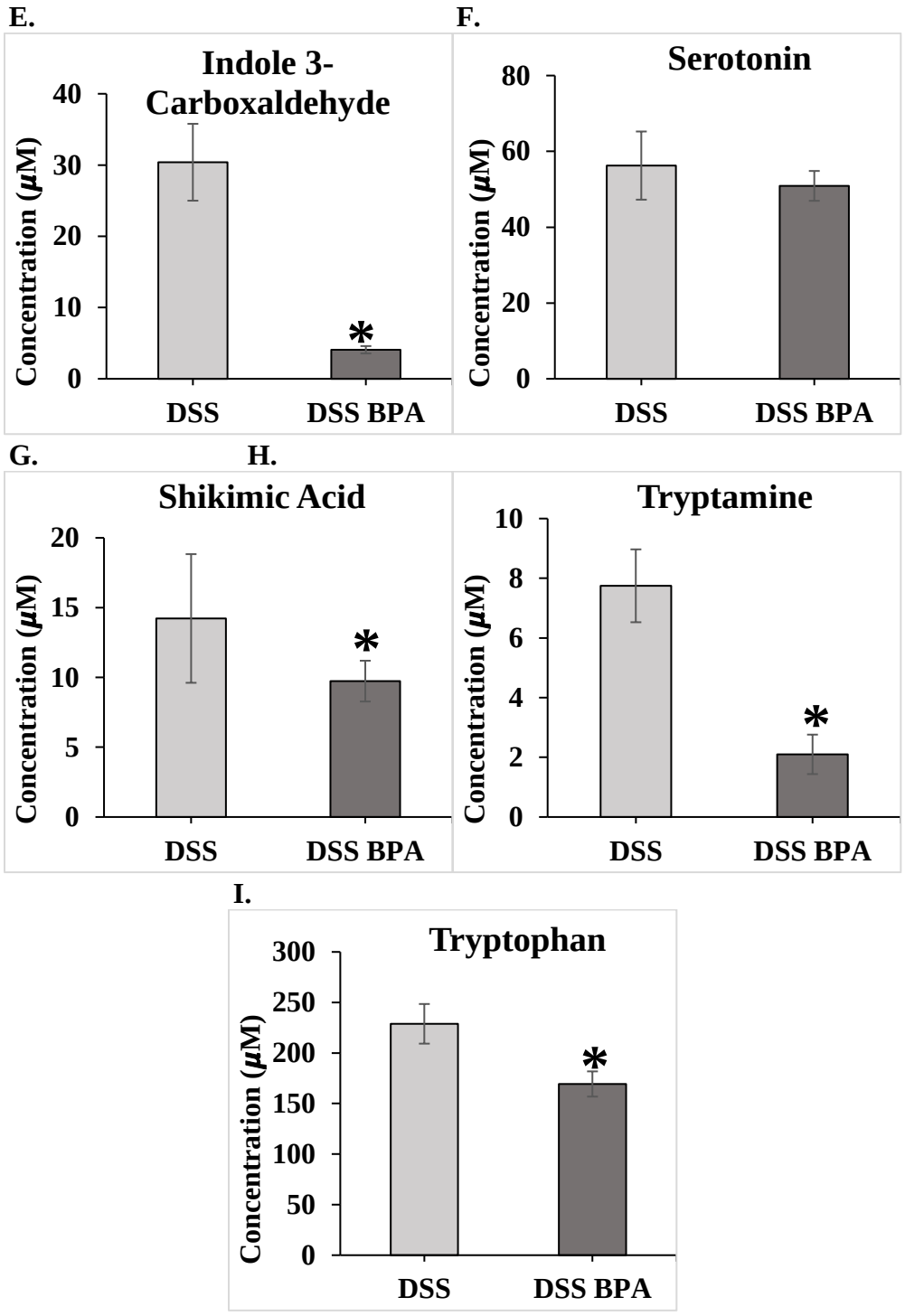

Figure II.9 Continued.

A heat map shows changes in concentrations of the same metabolites with or without BPA treatment in the presence of DSS (Supplementary Figure II.10).

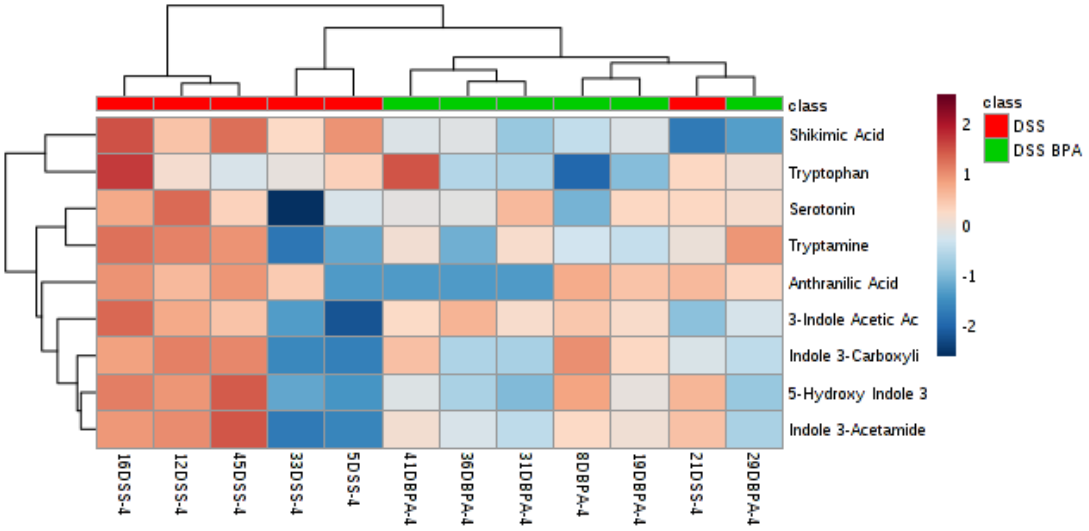

Figure II.10 Changes in Concentrations of Trp Metabolites with or without BPA Treatment in the Presence of DSS.

BPA treatment appears to alter MDAs in the feces more predictably during DSS treatment compared to the absence of DSS treatment, as evidenced by clustering on the heat map of BPA vs control treated animals in the DSS treated groups.

Assessment of BPA in Young Adult Mouse Colonocytes

The impact of BPA treatment was assessed in non-transformed YAMC cells. Percentage of cell number compared to vehicle treated control was quantified, and E_2 significantly reduced cell number to about 80% of control as previously reported (Figure II.11, ANOVA $p<0.0001$, n=9 wells/treatment). Ten μM and 10 nM BPA treatment also significantly reduced cell number by a similar amount (Figure II.11, ANOVA $p<0.0001$, n=9 wells/treatment).

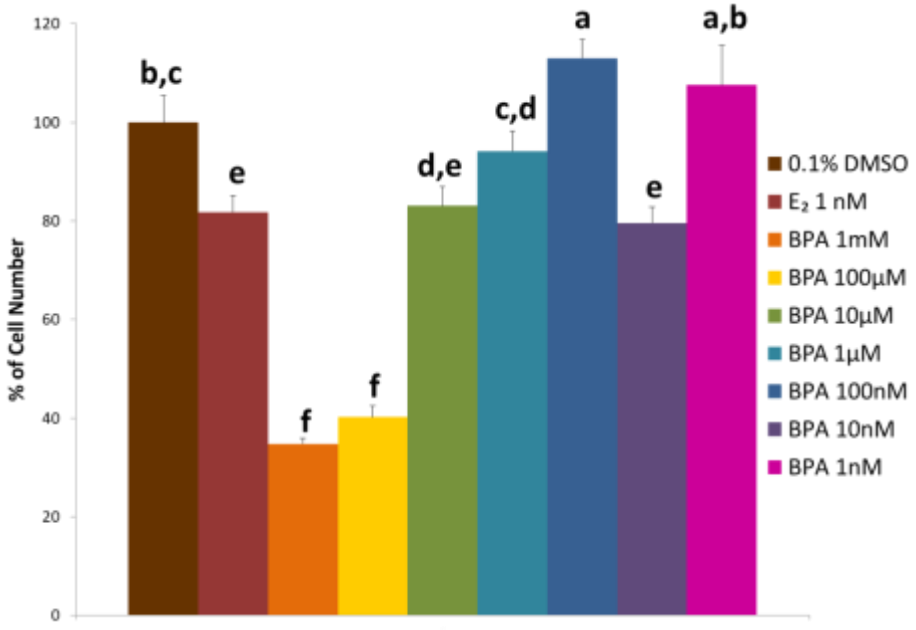

Figure II.11 Relative Young Adult Mouse Colonocyte Cell Number in BPA Treated Cells Compared to Vehicle Treated Cells. Data are expressed as percentage of cell numbers of the vehicle treated control group. ANOVA p<0.0001. Mean (*n* = 9) +/- SEM from triplicate experiments. Bars without a common letter differ; *p* < 0.05.

Percentage of cell number compared to vehicle treated control was quantified, and E_2 significantly reduced cell number to about 70% of control again, and this reduction was reversed by co-treatment with ICI (Figure II.12, ANOVA p=0.0419, n=9 wells/treatment). Ten nM BPA treatment also significantly reduced cell number by a similar amount compared to control, and this reduction was similarly reversed by co-treatment with ICI (Figure II.12, ANOVA p=0.0419, n=9 wells/treatment).

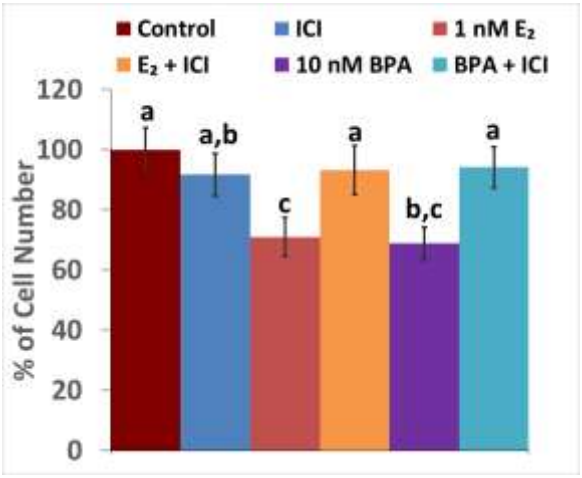

Figure II.12 Relative Young Adult Mouse Colonocyte Cell Number in BPA Treated Cells with and without ICI Compared to Vehicle Treated Cells. Data are expressed as percentage of cell numbers of the vehicle treated control group. ANOVA p=0.0419. Mean (*n* = 9) +/- SEM from triplicate experiments. Bars without a common letter differ; $p < 0.05$.

To investigate one of the possible causes of change in cell number, apoptosis was measured in BPA treated YAMCs, but BPA treatment at neither 10 nM nor 1 nM did not significantly change apoptotic activity in YAMCs at any time point compared to control (Figure II.13, n=9 wells/treatment). In contrast, 1 nM E_2 treatment increased apoptosis compared to vehicle and BPA treated cells, but this increase was not significant at any time point (Figure II.13, n=9 wells/treatment).

A.

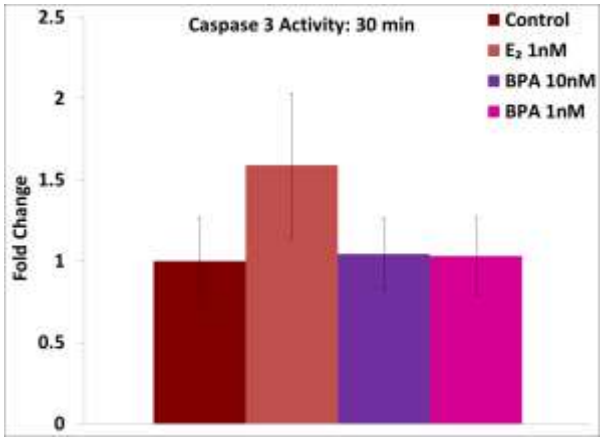

B.

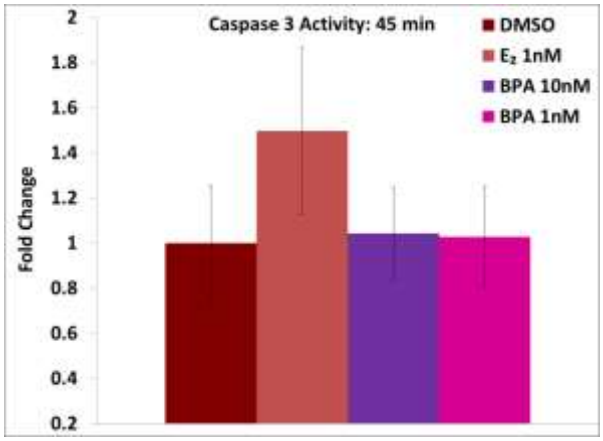

C.

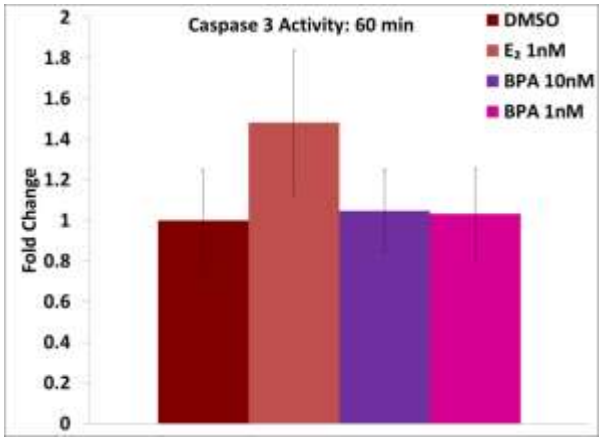

Figure II.13 Apoptosis in Young Adult Mouse Colonocytes Treated with BPA. Data are expressed as fold change of cell numbers of the vehicle treated control group. Mean (*n* = 9) +/- SEM from triplicate experiments. Bars without a common letter differ; *p* < 0.05.

Discussion

BPA exposure during DSS-induced colitis worsens measures of disease severity. Survival is one method by which degree of colitis can be assessed, and DSS and BPA co-treated animals showed decreased survival compared to DSS alone controls. In addition to survival, severity of experimental colitis is often assessed using a scoring system that accounts for body weight loss, fecal consistency, and rectal bleeding.[95,104] These measures were assessed daily in all mice, and, as expected, DSS treatment worsened all disease activity scores, regardless of BPA treatment. Recovery of the scores in animals following cessation of DSS is also used to measure the effects of treatments during experimental colitis. Interestingly, DSS and BPA co-treatment inhibited recovery of animals compared to DSS alone controls following cessation of DSS.

Previous experiments have linked BPA and inflammation. This correlation is most well established between BPA and the low-grade chronic inflammation associated with obesity. For example, several human studies have shown a positive correlation between serum or urinary BPA levels and increased levels of inflammatory markers such as malondialdehyde, 8-hydroxydeoxyguanosine, C-reactive protein, interleukin-6 (IL-6), and tumor necrosis factor-α (TNFα) in serum.[105,106] *In vitro and in vivo* experiments have also demonstrated that BPA exposure results in increases in inflammatory markers in serum (leptin and resistin) and white adipose tissue (IL-6, TNFα, interferon-γ (IFN-γ), and inducible nitric oxide synthase 2) as well as in adipose tissue or differentiated adipocytes (IL-6 and IFN-γ).[107,108]

Our results demonstrate that BPA exposure at 50 µg/kg/day can exacerbate acute colonic inflammation in the DSS model. This dose is the BPA reference dose set by the Environmental Protection Agency.[81] While this dose is in the upper end of what is estimated for human exposures to BPA, it results in circulating BPA concentrations in C57BL/6 mice within the range of that observed in humans.[109] The effects of BPA on gut physiology have been investigated in other models. Perinatal exposure to BPA has been shown to decrease gut permeability at relatively low oral doses and in an ERβ dependent manner, altering gut physiology similar to E_2.[82] The same group found that BPA treatment protected against measures of TNBS induced colitis. These conflicting results are mirrored in similar experiments using E_2; E_2 treatment seems to protect against DNBS or TNBS induced colitis while exacerbating DSS induced colitis.[92,93] While the effects of estrogenic signaling in intestinal inflammation are clearly complex, these varying results are likely due to the mechanism by which colitis is induced in each model.[93] For example, Roy and colleagues used 2,4-dinitrobenzene sulfonic acid (DNBS) for colitis induction while directly exposing animals to 50 µg of BPA/kg/day as in our model.[91] Similarly to TNBS, this chemical acts as a haptenating agent to induce colitis via increased immune activation in the colon that more closely mimics the symptoms of CD.[110] DSS chemically damages colonic epithelial cells, leading to inflammation that more closely resembles UC.[110] The differing mechanisms of action of these chemicals likely explain the varied results of the Roy and colleagues study compared to the present study.

Intestinal epithelial cell damage, increased gut permeability, and the resultant migration of colonic bacteria and lipopolysaccharides (LPS) have been implicated in the mechanisms of DSS induced colitis.[93,111] As noted by Verdú and colleagues (2002), E_2 has been shown to increase macrophage sensitivity to LPS, providing a possible mechanism by which other estrogenic compounds such as BPA could exacerbate DSS induced colitis.[112,113] BPA exposure in utero has also been shown to alter innate immune responses without affecting adaptive immune responses, possibly explaining the different responses of animals treated with DSS or TNBS.[109] E_2 has been shown to sensitize immune cells, and coupled with damage caused by DSS, innate immune cells are likely exposed to increased levels of bacteria and their products in BPA and DSS co-treated animals compared to vehicle controls, resulting in a worsening of systemic symptoms.[114]

To further understand the effects of BPA on inflammation during acute colitis, inflammatory markers were measured. While there is limited information in the literature on cytokine expression following BPA and DSS exposure *in vivo*, BPA's effects on cytokine expression has been examined *in vitro*. BPA significantly increased expression of TNF-α and IL-6 in THP-1 macrophages *in vitro*, and these changes were attenuated by treatment with an ERα and ERß antagonist, ICI 182,780.[115] E_2 has also been shown to induce pro-inflammatory cytokine expression in the DSS model. 0.5 mg E_2/pellet and 5% DSS co-treated C57BL/6 mice showed a significant increase in TNF-α compared to DSS alone.[93] In the present study, TNF-α was significantly increased during DSS treatment, regardless of BPA treatment (data not shown). Significant increases in

TNF-α in the DSS and BPA group compared to DSS alone may not have been observed as only the middle portion of the colon was analyzed. At least one report has shown that cytokine expression differs regionally in the colon following acute DSS colitis.[101] Several cytokines that were significantly altered by DSS and BPA treatment have been connected to inflammatory responses in the colon, including IL-31, IL-13, and VEGF. IL-31 treatment resulted in STAT, ERK, and Akt phosphorylation in HCT116 and SW480 colon cells *in vitro*.[116] IL-13 has been shown to be increased in UC patients, and this cytokine induces apoptosis in epithelial cells and reduces the ability of epithelial cells to migrate into wounds during repair.[117] Increased VEGF levels are commonly found in IBD patients and animal models of colitis, and this increase accompanies an increase in pro-inflammatory cytokines in inflamed tissue.[118] However, one study showed that inhibition of VEGF prior to acute DSS colitis resulted in worsened inflammation on day 19 post-DSS, and the authors suggest that VEGF inhibition may impact recovery following an acute bout of colitis.[119] Therefore, it is possible that the significant reduction in VEGF expression in DSS and BPA treatment has an impact on delayed recovery observed in the DAI scores of this group compared to mice treated with DSS alone.

Another possible mechanism by which BPA could exacerbate intestinal inflammation could be microbial dysbiosis and a resultant shift in MDAs present in the intestinal lumen. Dietary exposure to BPA resulted in a decrease in gut microbial diversity, similarly to animals fed a high fat diet, as well as an increase in *Proteobacteria* which is associated with intestinal inflammation.[88] Evidence exists that this association

may persist in later generations as gut microbial dysbiosis caused by BPA exposure has also been shown to persist in offspring unexposed to BPA.[120] Our results indicate that BPA treatment can reduce Trp and MDAs in mouse feces compared to vehicle controls. We have previously used Trp and the metabolites measured to describe phenotypic changes in the intestinal microbiota.[97] Trp is the precursor for serotonin synthesis, and HIAA is the metabolic product of serotonin. Our results suggest that BPA affects the metabolism of the essential amino acid Trp itself. This is important since many MDAs like indole are anti-inflammatory and are beneficial to the host, and exposure to BPA might downregulate the metabolism of Trp.[121] Low levels of Trp and MDAs have been associated with increased autoimmune disease activity, including IBD.[122,123] Human patients with confirmed IBD had decreased levels of Trp in serum compared to controls.[122] Patients with active CD or UC also had reduced Trp serum levels compared to those whose disease was in remission.[122] In a mouse model, increased levels of Trp result in increases in the lactobacilli population in the gut, causing increased indole-3-aldehyde production which contributes to interleukin-22 production and anti-inflammatory effects.[123]

One specific metabolite, serotonin, is significantly reduced in BPA alone treated animals compared to vehicle controls. While serotonin is also decreased in DSS and BPA treated animals compared to DSS alone controls, this decrease is not significant. Human patients with UC have reduced levels of serotonin in gut mucosa, likely due to alterations in serotonin synthesis, signaling, and reuptake.[90] Reduced serotonin reuptake has been suggested to exacerbate colonic inflammation and the symptoms of IBD

including diarrhea.[90] Conversely, a study by Ghia and colleagues did not find that mice globally lacking tryptophan hydroxylase 1 had decreased levels of serotonin in the GI tract, but that these mice had decreased colitis severity.[124] While this conflicts with our results, tryptophan hydroxylase 1 deficiency could result in increased levels of metabolites produced via other pathways including the kynurenine pathway by indoleamine 2,3-dioxygenase-1 (IDO-1) which is upregulated during colonic inflammation.[122,125] For example, tryptophan depletion following host IDO-1 activation reduced microbial proliferation and increased production of the MDA indole-3-alydehyde in IDO-1 knockout mice infected with *Candida albicans*.[123] These mechanisms cannot be separated in the model used by Ghia and colleagues. In the present study, though concentrations of serotonin were similar between the control and DSS alone groups, a variety of reasons can be implicated, including the sample source (feces rather than mucosa), mouse strain, sex, age, and time of sample collection after initial DSS exposure.

Additional MDAs were significantly reduced with BPA treatment. HIAA, a metabolite of serotonin, was also significantly depleted in BPA treated animals regardless of DSS treatment. Reduction in HIAA level could result from inhibition of the enzymes that converts serotonin to HIAA, monamino-oxidases, or serotonin uptake.[126] The reduction in HIAA without a similar reduction in serotonin in the BPA and DSS treated animals could indicate impairment of serotonin reuptake and metabolism.[126] Additional metabolites were found to have decreased concentrations in BPA treated mice compared to controls in the presence of DSS treatment. These metabolites include

tryptamine, indole-3-acetate, and shikimic acid. Tryptamine and indole-3-acetate have both been previously shown to reduce production of pro-inflammatory cytokines in LPS stimulated murine macrophages *in vitro*.[127] Shikimic acid has been previously shown to reduce measures of disease activity in acetic acid induced colitis.[128] Regardless of DSS treatment, BPA appears to significantly alter MDAs in ways that negatively impact gut physiology.

Concentration differences in MDAs between DSS treated groups and controls could be the result of microbial dysbiosis caused by DSS treatment. Alterations in gut microbiome by DSS is well reported.[114] However, Trp and several MDAs are decreased in BPA treated animals that were not exposed to DSS. This indicates that BPA is capable of altering Trp concentrations irrespective of microbiome changes resulting from DSS treatment. Though BPA treatment increased inflammation score in non-DSS treated animals, this increase was not significant. However, significant changes in measured metabolites show that BPA alters MDAs in the colon and may therefore affect intestinal epithelial cell physiology in uninflamed states as well.

Finally, to assess the impact of BPA in non-transformed Young Adult Mouse Colonocytes (YAMCs), the effects of BPA doses ranging from 1 mM to 1nM on cell number relative to vehicle treated control were measured. Compared to vehicle treated controls, 1nM E_2 significantly reduces cell number by about 20%, as previously reported.[129] Similarly to E_2, BPA also significantly reduces cell number compared to vehicle treated cells at 10 μM and 10 nM, a concentration found in human tissues.[130] Furthermore, this reduction in cell number was mediated through the binding of BPA to

ERs, as the reduction in YAMC number treated with 10 nM BPA was reversed with co-treatment by ICI, an estrogen receptor antagonist.

The measured reduction in cell number could be the result of increased apoptosis or decreased proliferation, either or both of which could explain the inhibition of recovery following DSS treatment in BPA treated mice compared to DSS treatment alone. Therefore, apoptosis was assessed, but no significant differences were observed at any time point between either 10 nM or 1 nM BPA treatment and vehicle control. BPA's effects on YAMC proliferation should be separately assessed in future experiments.

Additionally, the dose response assay revealed a non-monotonic dose response of YAMCs to BPA. This pattern has been previously reported for BPA and other compounds and implies that the effects of BPA would be most pronounced at relatively low or high doses.[131] The implications of this finding indicate that previous estimates of safe doses of BPA may not be accurate, a hypothesis that is gaining traction and is echoed in recent analyses of BPA and its metabolites in human tissues.[131,132] Additional research is needed to determine if "low" doses of BPA are truly safe for all segments of the population.

Findings of this chapter are summarized in Figure II.14. In the present study, BPA treatment reduced fecal Trp content, along with that of MDAs including serotonin and its metabolite HIAA, indicating a mechanism by which BPA treatment worsens DSS-induced colitis disease activity and affects recovery after DSS treatment has been halted. The present study is the first to show that BPA treatment alone can alter MDAs in the colon in a way that has been linked with increased colonic inflammation and IBD.

Further studies are necessary to determine the mechanisms by which BPA lowers levels of Trp and MDAs in the colon.

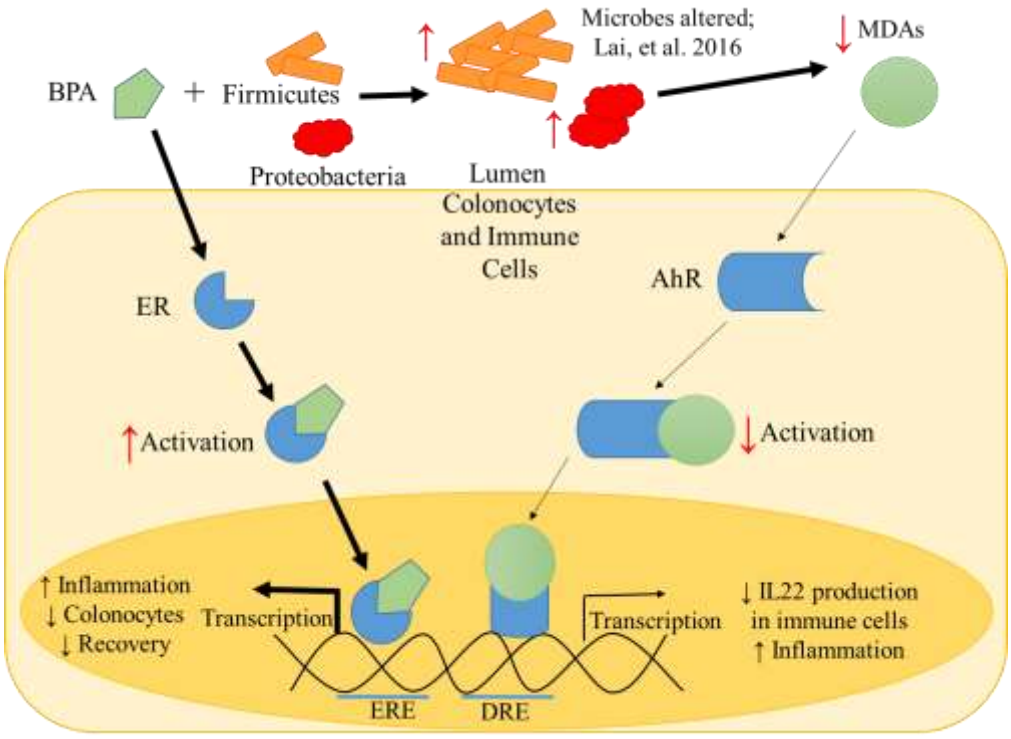

Figure II.14 Effects of Bisphenol-A on Colonic Inflammation, Colitis Recovery, and Microbial Metabolites Derived from Aromatic Amino Acids. AhR, Aryl Hydrocarbon Receptor; BPA, Bisphenol-A; DRE, Dioxin Response Element; ER, Estrogen Receptor; ERE, Estrogen Response Element; MDAs, Microbial Metabolites Derived from Aromatic Amino Acids.

CHAPTER III

EFFECTS OF HIGH-FAT DIET AND INTESTINAL ARYL HYDROCARBON RECEPTOR DELETION ON COLON CARCINOGENESIS*

Introduction

Colorectal cancer (CRC) has been identified as the third most diagnosed type of cancer and the third leading cause of cancer-related death in the United States of America.[133] Although various screening tests and treatments (chemotherapy, surgery, radiation, and various drugs targeting biological signaling molecules) are available, some are not effective for patients with advanced stages.[134] CRC development is characterized by a long, multi-stage progression of mutations in which normal epithelium acquires and accumulates gene mutations that dysregulate the normal growth and function of intestinal epithelial cells (IECs) until the formation of adenocarcinomas and metastasis occurs. Hence, early identification of premalignant lesions is crucial for the diagnosis and the development of prevention strategies.[135,136]

Epidemiological data suggest that while about 5% of cancer incidence has a genetic component, 95% is linked to the environment.[137] Environmental elements include lifestyle factors such as tobacco and alcohol use, diet, physical activity, exposure to radiation, infections, or toxins.[137] Researchers have suggested that the diet is linked to

---

* Reprinted with permission from sections of "Effects of high-fat diet and intestinal aryl hydrocarbon receptor deletion on colon carcinogenesis" by Garcia-Villatoro, E.L. [1], DeLuca, J.A.A. [1], Callaway, E.S., Allred, K.F., Davidson, L.A., Hensel, M.E., Menon, R., Ivanov, I., Safe, S.H., Jayaraman, A., Chapkin, R.S., and Allred, C.D., 2020. The American Journal of Physiology Gastrointestinal and Liver Physiology, 318(3), G451-G463, Copyright 2020 by The American Physiological Society.
[1]Equally contributing co-first authors. Reprint permission has been granted by the co-first authors.

approximately one third of cancer mortality in the US.[138] Diets low in dietary fiber and high in saturated fat have been associated with a higher risk of developing CRC.[137] Specifically, an increased inflammatory response, loss of tumor suppression capacity, and increased stemness of progenitor cells have been suggested as mechanisms linking a diet high in fat (High Fat Diet, HFD) to increased tumorigenesis in the colon.[139–142] Moreover, chronic HFD consumption not only facilitates proliferation and survival of tumor cells but also promotes genetic instability leading to increased colon cancer incidence.[143]

Dietary components and their metabolites are able to bind specific nuclear receptors in the host that can induce the expression of genes that maintain normal intestinal epithelial cell functions such as growth and apoptosis. Particularly, it has been shown that the aryl hydrocarbon receptor (AhR) is sensitive to environmental cues in the large intestine. AhR is a ligand-activated nuclear receptor of the Per-Arnt-Sim (PAS) superfamily that shares similarities with other nuclear receptors[39] Upon ligand activation, cytosolic AhR translocates to the nucleus and binds to the AhR nuclear translocator (ARNT). There they interact with the dioxin response elements (DREs) on the promoter regions of genes targeted by AhR including drug-metabolizing enzymes such as cytochrome P450 (CYP) enzymes such as CYP1A1, CYP1A2, and CYP1B1, consequently activating their transcription.[144,145] The AhR has been considered an orphan receptor with no high-affinity endogenous ligands; however, recent studies have identified dietary, microbial, and host-derived compounds that can bind AhR and elicit a variety of beneficial physiological effects.[25,41,42] In the large intestine, these effects

include regulation of mucosal inflammation, tissue regeneration, regulation of the immune system, and proteasomal degradation.[39,41,42,134,144–146] Specifically, AhR activation by exogenous ligands has been associated with increased E3 ubiquitin ligase activity that participates in the degradation of transcription factors that promote cell proliferation such as β-catenin.[48,147]

The role of AhR in cancer pathologies is complex and only beginning to be elucidated. AhR's impact on cancer appears to be cell type and disease stage dependent. Overexpression of AhR has been associated with several gastrointestinal cancers at advanced stages. For example, AhR expression was increased in gastric cancer tissues and cell lines compared to premalignant lesions.[148] Additionally, constitutively active AhR has been shown to induce stomach tumors in a mouse model.[149] In the colon, immunohistochemical staining and immunoblot analysis have reported a significant increase of AhR expression and protein levels, respectively, in colon tumor tissue compared to their adjacent non-tumor tissue in clinical samples.[145] Contrarily, increasing experimental evidence suggests that AhR activation may also be protective against colonic inflammation and carcinogenesis in both sporadic and colitis-associated models of CRC.[46–48,150] Although it has been recently described that intestinal epithelial cell-specific AhR deletion enhances inflammation-induced tumorigenesis,[147] the effect of diet composition, particularly the fat content of the diet, on development of CRC in the context of AhR activity in colonocytes has yet to be elucidated. Furthermore, the stage of the CRC continuum at which AhR elicits its protective effects remains unknown. Hence, in the present study we investigated the effects of the loss of AhR activity in

intestinal epithelial cells (IEC) at different stages of colorectal cancer development in the context of both high- and low-fat diets. Taken together, our data support that AhR activity in IECs can be an essential player at early stages of CRC development, while further progression to colorectal cancer seems more dependent upon both saturated fat consumption during the peri-initiation period and loss of AhR activity in IECs.

Materials and Methods

Animal Model and Validation

Constitutive, intestinal-epithelial cell specific AhR knockout C57BL/6 mice ($AhR^{f/f}$ x VillinCre, $Ahr^{\Delta IEC}$) and wildtype littermates ($AhR^{f/f}$, WT) were employed as the animal model for this study as previously described by Biljes and Walisser.[151,152] This model expresses the lower affinity AhR^{d} allele, similar to humans.[153,154] For genotyping analysis, DNA was extracted from tails using DNeasy Blood and Tissue Kit (Qiagen; 69506). PCR was performed using the following primers: Cre recombinase (F: 5'-CAA GCC TGG CTC GAC GGC C-3', R: 5'-CGC GAA CAT CTT CAG GTT CT-3'), $AhR^{flox/flox}$ (F: 5'-GGT ACA AGT GCA CAT GCC TGC-3', R: 5'-CAG TGG GAA TAA GGC AAG AGT GA-3'). To assess successful deletion of AhR in the colonic crypts in the $Ahr^{\Delta IEC}$ mice (n=4), protein levels of AhR were measured using isolated colonic crypts via Western blot using rabbit anti-mouse AhR (Enzo Life Sciences, Cat# BML-SA210, 1:2000 dilution).[155]

Colon Mass Formation Study, Diets, and Tissue Collection

Litters were weaned to 4% Teklad Rodent Diet (Envigo, 8604), henceforth referred to as chow, before being enrolled in the study. Diet composition is provided in

Figure A.4 of Appendix A. Starting at week six, mice received a low-fat diet (LFD) containing 10% kcal from fat as the control diet (Research Diets, D12450B), and a high-fat diet (HFD), providing 60% kcal from fat as the experimental diet (Research Diets, D12492). Diet compositions are provided for LFD and HFD in Figures A.2 and A.3 of Appendix A, respectively. Following 3 weeks on the experimental diets, sporadic colorectal cancer was chemically-induced with AOM for six consecutive weeks. To account for differences in body composition, animals weighing less than 40 g received AOM injections of 10 mg/kg body weight, while those weighing 40 g or more received AOM at 7.5 mg/kg body weight. To assess the impact of HFD during the peri-initiation period, HFD groups were switched to LFD (HtLFD) thirteen weeks after the final AOM injection and were terminated 47 weeks after the last injection of AOM. All procedures were performed under a protocol approved by the Institutional Animal Care and Use Committee at Texas A&M University. Body weight was assessed weekly upon enrollment. Experimental design is provided in Figure III.1.

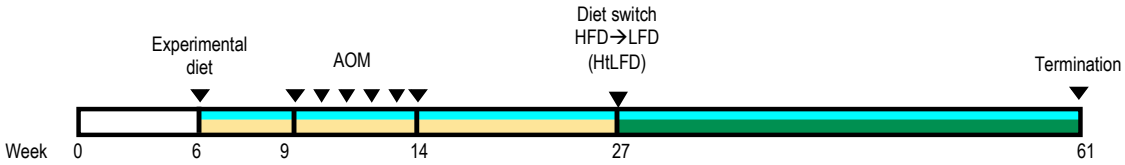

Figure III.1 Experimental Design.

Two hours prior to termination, select animals were intraperitoneally injected with 50 mg/kg body weight 5-Ethynyl-2'-deoxyuridine (EdU; A10044, Life Technologies), as a proliferation marker. Blood was collected via cardiac puncture. The colons were immediately resected, opened longitudinally, flushed with sterile PBS, and fecal pellets were collected. Macroscopically visible colon masses were mapped,

measured with calipers, excised, and fixed in 4% PFA for 4 hours before being dehydrated through several washes of 50% and 70% ethanol. Tissues were stored at 4˚C in 70% ethanol until they were processed, embedded, and sectioned for histological analyses.

Histological Analysis of Colon Masses

Colon masses were sectioned, H&E stained and diagnosed by a board-certified pathologist blinded to treatment groups. Masses and surrounding tissues were thoroughly assessed. All diagnoses including those resulting from epithelial, lymphoid, or stromal cell aberrations were considered for mass diagnosis. Pathological descriptions of colon mass diagnoses are provided in supplemental materials (Table III.1). Colon mass incidence was quantified as any occurrence of a given pathological diagnosis within one animal. Colon mass multiplicity was quantified as the number of times a given pathological diagnosis occurs within one animal. Colon mass surface area was calculated by multiplying the caliper measured length of the mass by the width using Microsoft Excel for Mac, version 16.16.10. Mean incidence, multiplicity, and surface area were then calculated per group using Microsoft Excel for Mac, version 16.16.10.

Hyperproliferative Epithelial Cell Diagnoses (Included in Analyses)	
Mucosal Hyperplasia	Mucosal epithelium is multifocally thickened by piling layers of cells.
Mucosal Dysplasia	Multifocally, the mucosal epithelium has foci of dysplasia characterized by increased nuclear to cytoplasmic ratio and loss of basal polarity.
Polyp	Arising from the mucosa is an exophytic, pedunculated nodule composed of hyperplastic mucosal epithelial cells.
Adenoma	Arising from the colonic mucosa is an exophytic, partially encapsulated, well demarcated nodules of neoplastic epithelial cells arranged in tubules and nests of a fibrovascular stroma. Neoplastic cells do not extend beyond the muscularis mucosa.
Adenocarcinoma	Arising from the colonic mucosa is an infiltrative, poorly demarcated, moderately cellular neoplasm on an exuberante fibrous stroma (desmoplasia). Neoplastics cells form small tubules and nests that transmurally infiltrate the colon wall and extend through the mesentery and invade the pancreas. Neoplastic cells are within lymphatics and small vessels (intravascular invasion).
Other Diagnoses (Excluded from Analyses)	
Lymphoid Hyperplasia	Submucosal lymphoid tissue is prominent and elevates the overlying mucosa.

Table III.1 Examples of Descriptions of Colon Mass Diagnoses Provided by the Veterinary Pathologist.

Immuno-histo-fluorescence Staining

PFA-fixed/paraffin-embedded colon sections (5 µm) were deparaffinized, rehydrated and stained with antibodies using standard immunofluorescence (IF). Detection of proliferative activity was measured using the Click-iT EdU Alexa Fluor 488 Imaging Kit (Invitrogen, C10637) as per manufacturer's indications. β-catenin was subsequently co-stained via immunohistochemistry as described previously.[156] Briefly, mouse monoclonal β-catenin antibody (610154, BD Transduction, San Jose, CA, USA; dilution 1:500) was used in conjunction with donkey, anti-mouse secondary antibody

conjugated to Alexa Fluor 647 (A-31571, Life Technologies; dilution 1:200). ProLong Gold AntiFade with DAPI (P36931, Life Technologies) was used to stain the nucleus. A negative control section was stained on each slide by excluding primary antibody. Slides were imaged at 40X magnification using an all-in-one fluorescent microscope (Keyence BZ-X700).

Slide Scoring of Cell Proliferation & β-Catenin Intensity and Localization

Sections of masses diagnosed with IEC hyperproliferation were analyzed for proliferation as well as β-catenin expression and nuclear localization were assessed. At least 5 fields of view from within each mass were captured for analysis. Quantification of proliferative cells, β-catenin staining density, and β-catenin nuclear localization were performed using Fiji ImageJ software, version 2.0.0-rc-69/1.52 (imagej.net). Up to 500 nuclei per mass (100 per a minimum of 5 fields of view) were identified without the 488-channel activated. Actively proliferating cells within those 500 were then quantified with the 488-channel activated. The percentage of proliferating cells per mass was determined by dividing the number of proliferating cells by the 500 selected nuclei within the mass and multiplying by 100 using Microsoft Excel for Mac, version 16.16.10. For β-catenin analysis, up to 100 proliferating (EdU positive) cells per mass (20 per a minimum of 5 fields of view) were selected for measuring β-catenin staining density (whole cell, C) and nuclear localization measurements (nuclei, N). β-catenin nuclear localization measurements were performed as previously described.[156] Briefly, nuclear to cytoplasmic β-catenin ratio was quantified in 100 cells (C) and nuclei (N) per

colon mass from 5 fields of view per mass. Nuclear localization was calculated as N/(C-N) using Microsoft Excel for Mac, version 16.16.10.

Statistical Analysis

All statistical analyses and figures were generated in GraphPad Prism version 8.1.2 for macOS, Graph Pad Software (La Jolla CA, www.graphpad.com). Means were compared using parametric or non-parametric methods according to compliance of normality (Shapiro-Wilk test). Outliers based on ROUT (Q=1.0%) were excluded. Parametric methods included unpaired t test for comparing two means or one-way ANOVA followed by Tukey's multiple comparisons test for comparing three or more means. Two-way ANOVA was used to test interaction effects between variables. Non-parametric methods include the Mann-Whitney U (MW) test for comparing two means or the Kruskal-Wallis (KW) test followed by Dunn's multiple comparisons test for comparing three or more means. One-tailed p-values are reported in all analyses due to directionality of the hypothesis. All values listed are group means and error bars are presented as SEM. Differences among groups were considered statistically significant when the p-value was ≤ 0.05. Within figures, * indicates $p \leq 0.05$, ** indicates $p \leq 0.01$, *** indicates $p \leq 0.001$, and the absence of * indicates p-values >0.05.

Results

Animal Model and Validation

Data supporting the AhR silencing phenotype in IECs ($Ahr^{\Delta IEC}$) are shown in Figure III.2. This data is consistent with silencing of genes in other genetic knockout mouse models.[157,158]

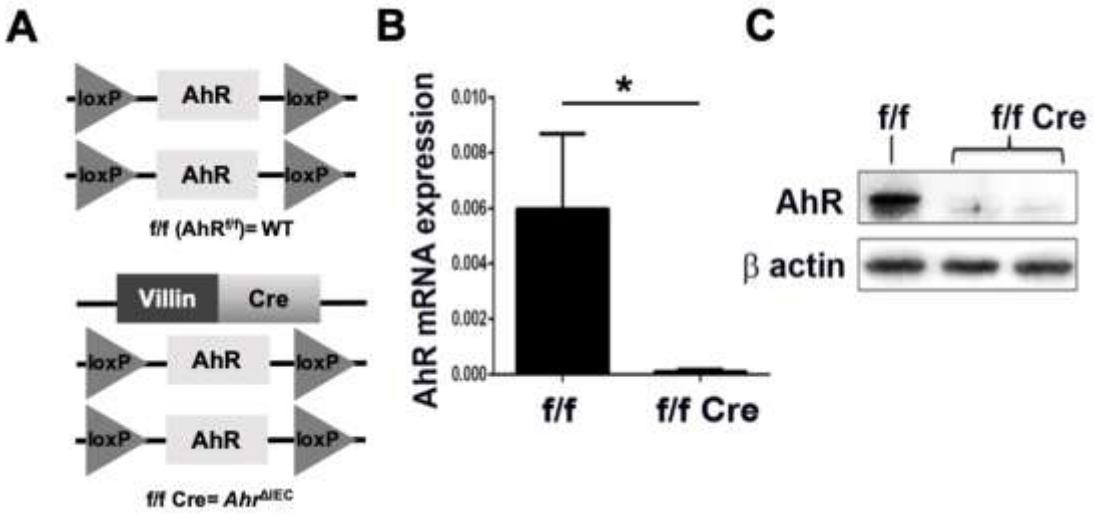

Figure III.2 Model Verification in the *Ahr*$^{\Delta IEC}$ Mice. A: Schematic representation of Cre-lox intestinal-specific knockout (*Ahr*$^{\Delta IEC}$) and controls (AhR$^{f/f}$) used in the study. B: AhR mRNA expression normalized to 18s rRNA. AhRf/f (f/f, WT) vs Ahr$^{f/f}$ x VillinCre (f/f Cre, *Ahr*$^{\Delta IEC}$) from isolated colonic crypts (n= 6). C: Representative Western blot analysis of AhR protein expression. β-actin was used as a loading control. *p<0.05 vs. control (WT). Values are means ± SEM. * indicates p ≤ 0.05, ** indicates p ≤ 0.01, * indicates p ≤ 0.001, and the absence of * indicates p-values >0.05.**

Body Weight

No significant differences were observed in body weight with respect to genotype or diet at any time point in the mass formation cohort (Figure III.3A-C).

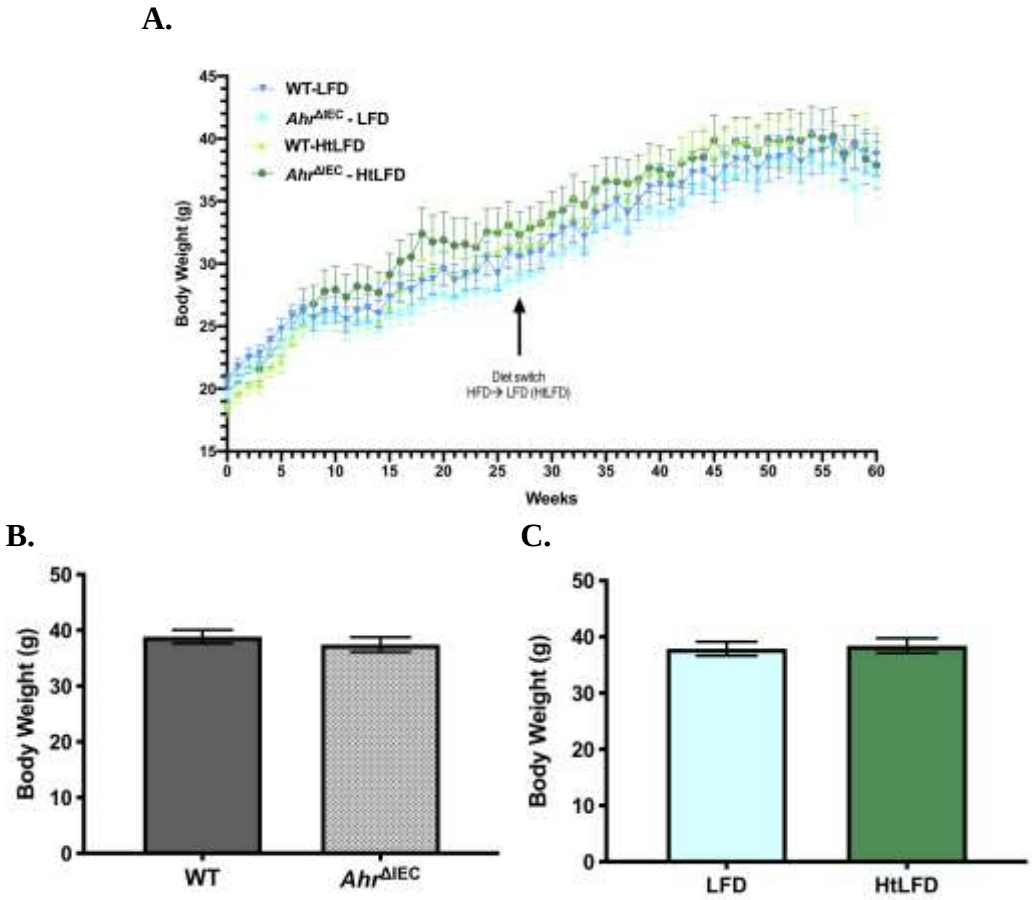

Figure III.3 Effect of Diet and Genotype on Body Weight. A. Weekly body weight (grams) is not significantly different between groups (LFD-WT, LFD-*Ahr*$^{\Delta IEC}$, HtLFD-WT, HtLFD-*Ahr*$^{\Delta IEC}$) when compared within a given time point (ANOVA p≥0.05). B-C. At termination (week 61), no differences in body weight are observed between genotype (p=0.2156) or diet (p=0.3808). Values are means ± SEM. * indicates p ≤ 0.05, ** indicates p ≤ 0.01, * indicates p ≤ 0.001, and the absence of * indicates p-values >0.05.**

Colon Mass Incidence, Multiplicity, and Surface Area

To assess the impact of *Ahr*$^{\Delta IEC}$ on the stages of CRC development and the impact of HFD exposure solely during the peri-initiation period, HFD fed animals were switched to a LFD (HtLFD) thirteen weeks following the final AOM injection (Figure III.I). 47 weeks after the last AOM injection, macroscopic masses in the colon were collected and then assessed by a board-certified veterinary pathologist blinded to

treatment groups. Since the focus of this study was the response of IECs to the loss of AhR and CRC development, analyses were confined to masses exhibiting a hyperproliferative phenotype (e.g., mucosal hyperplasia, mucosal dysplasia, polyp, adenoma, adenocarcinoma), while other diagnoses were excluded from these analyses (e.g., lymphoid hyperplasia, fibrosis, colitis, and edema) (described in Table III.1). *Ahr*$^{\Delta IEC}$ animals did not differ with respect to colon mass incidence compared to controls (p=0.5000) (Figure III.4A), nor did HtLFD exhibit altered colon mass incidence compared to mice exclusively fed a LFD (p=0.2172) (Figure III.4B). While not statistically significant, the interaction of diet and genotype tended to increase colon mass incidence (statistical interaction, p=0.0709) (Figure III.4C). Loss of AhR in IECs did not impact colon mass multiplicity compared to WT mice (p=0.4624) (Figure III.4D), however, exposure to HFD during the peri-initiation period did significantly increase colon mass multiplicity compared to LFD fed animals independent of genotype (p=0.0170) (Figure III.4E). Specifically, this observation is primarily the result of the more than two-fold increase in multiplicity in the HtLFD-*Ahr*$^{\Delta IEC}$ animals compared to the LFD-*Ahr*$^{\Delta IEC}$ mice (p=0.0172) (Figure III.4F). Although this suggests a biologically relevant interaction between diet and genotype, these variables cooperatively were not statistically significant (statistical interaction, p=0.0658). There was also a trend toward reduced colonic mass surface area in *Ahr*$^{\Delta IEC}$ mice compared to control animals (p=0.0724) (Figure III.4G). HtLFD did not alter colonic mass surface area compared to the LFD control (p=0.5222) (Figure III.4H). While both LFD-*Ahr*$^{\Delta IEC}$ and HtLFD-

Ahr$^{\Delta IEC}$ groups had a reduced colon mass surface area compared to their respective WT controls, this effect was not significant (ANOVA p=0.1974) (Figure III.4I).

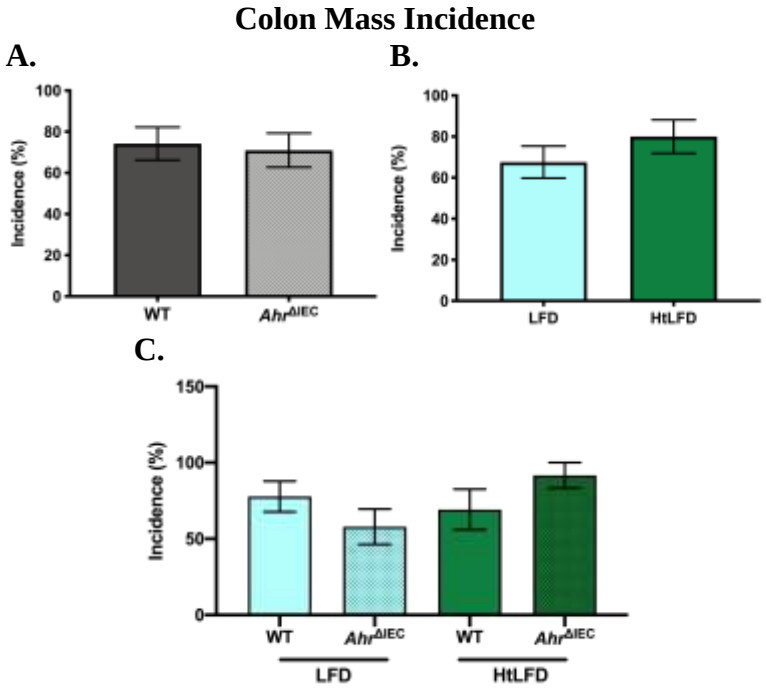

Figure III.4 Effect of Diet and Genotype on Incidence (Percentage of Animals with Masses) of Colon Masses Diagnosed with Enhanced IEC Growth. A. Colon mass incidence compared by genotype; p=0.5000 (MW). B. Colon mass incidence compared by diet; p=0.2172 (MW). C. Colon mass incidence compared by genotype and diet; p=0.2123 (KW). No interaction between diet and genotype (p=0.0709). Effect of diet and genotype on multiplicity (number of masses per animal) of colon masses diagnosed with enhanced IEC growth. D. Colon mass multiplicity compared by genotype; p=0.4624 (MW). E. Colon mass multiplicity compared by diet; p=0.0170 (MW). F. Colon mass multiplicity compared by genotype and diet; p=0.0306 (KW). No interaction between diet and genotype (p=0.0658). Effect of diet and genotype on surface area of colon masses diagnosed with enhanced IEC growth. G. Colon mass surface area compared by genotype; p=0.0724 (MW). H. Colon mass surface area compared by diet; p=0.5222 (MW). I. Colon mass surface area compared by genotype and diet; p=0.1974 (KW). No interaction between diet and genotype (p=0.6271). Values are means ± SEM. * indicates p ≤ 0.05, ** indicates p ≤ 0.01, * indicates p ≤ 0.001, and the absence of * indicates p-values >0.05.**

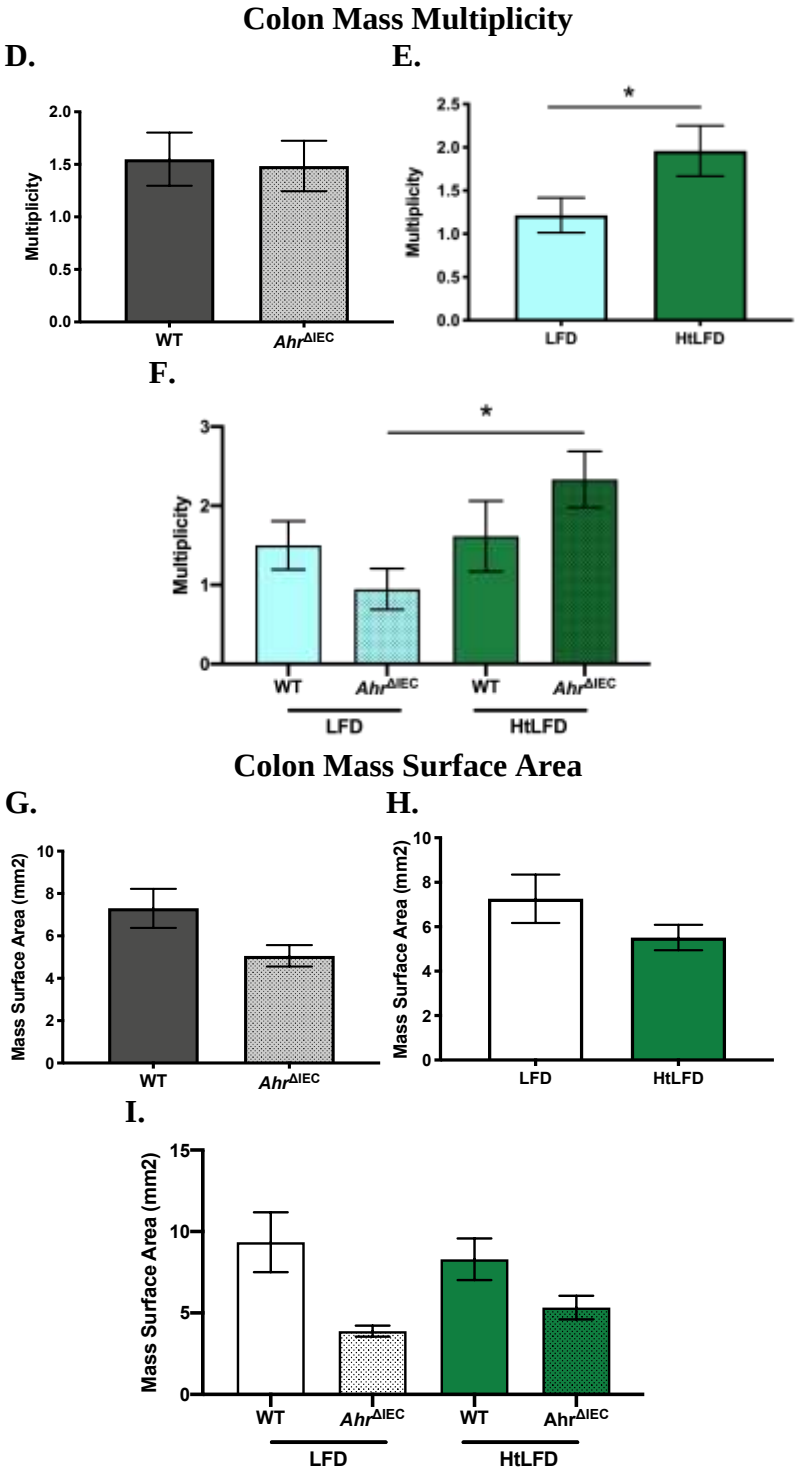

Figure III.4 Continued.

β-Catenin Intensity and Nuclear Localization in Proliferating Cells in Colon Masses

Although the effects of AhR on cellular proliferation and β-catenin signaling have been investigated in both mouse colonic organoids and a genetic model of CRC,[48,147] the consequences of *Ahr*$^{\Delta IEC}$ within colon masses from a sporadic model of CRC have yet to be elucidated. Therefore, the percentage of proliferative cells was quantified in hyperproliferative colon masses in an AOM-induced model of sporadic CRC to determine the impact of *Ahr*$^{\Delta IEC}$ and HFD. Representative images of EdU positive proliferative cells are shown in Figure III.5.

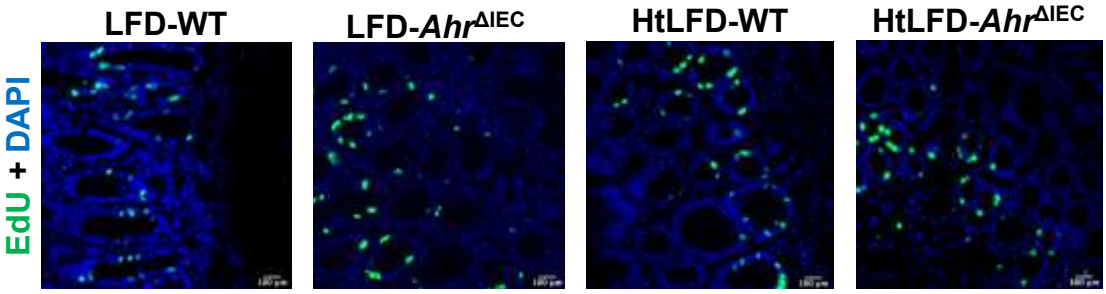

Figure III.5 Representative Images of Immunofluorescence Stained Proliferative Cells (EdU in Green) and Nuclei (DAPI in Blue) within Colon Masses of both WT and *Ahr*$^{\Delta IEC}$ Mice. Objective 40x.

Loss of AhR did not significantly impact the percentage of proliferative cells in colon masses compared to controls (p=0.0958) (Figure III.6A). Similarly, fat content of the diet did not alter the percentage of proliferative cells in colon masses (p=0.2689) (Figure III.6B). When considering diet and genotype together, *AhR*$^{\Delta IEC}$ and exposure to HFD independently tended to increase proliferation in colon masses compared to WT (Figure III.6C). However, a significant reduction in proliferative cells was observed in HtLFD-*AhR*$^{\Delta IEC}$ colon masses compared to HtLFD-WT masses (p=0.0473) (Figure

III.6C). Interestingly, a statistically significant interaction effect between diet and genotype on proliferation within colon masses (p=0.0229) was observed.

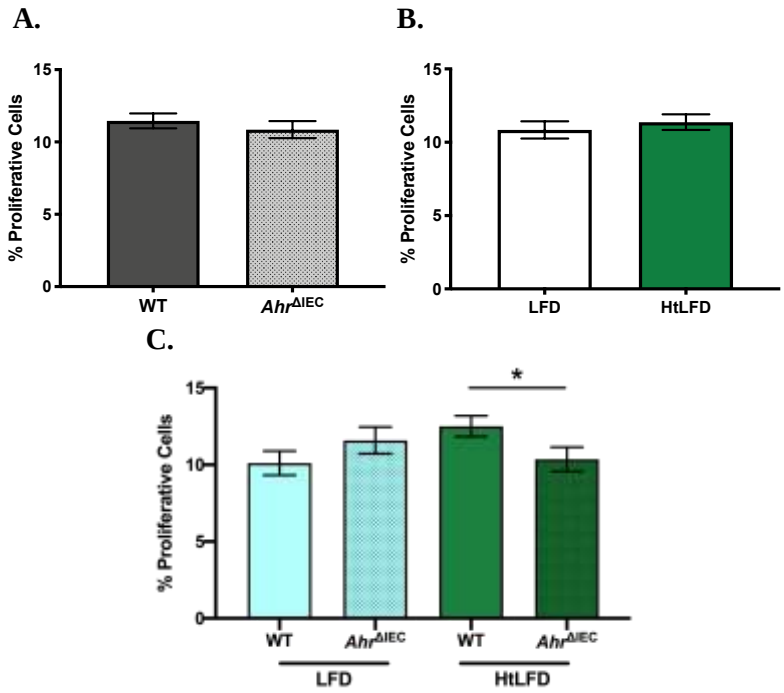

Figure III.6 Effect of Diet and Genotype on Cell Proliferation within Colon Masses Diagnosed with Enhanced IEC Growth. Proliferation in 500 cells per colon mass was quantified from 5 fields of view per mass. A: Proliferation within colon masses compared by genotype; p=0.0958 (MW). B: Proliferation within colon masses compared by diet; p=0.2689 (MW). C: Proliferation within colon masses compared by genotype and diet; p=0.0351 (KW). An interaction was observed between diet and genotype (p=0.0229).

To remove any potential bias of differences in β-catenin expression in proliferating versus quiescent cells, β-catenin staining intensity and nuclear localization were only quantified in proliferating cells (EdU^+). Representative images of β-catenin staining alone, overlaid with DAPI, and with regions of interest (ROIs) are shown in Figure III.7.

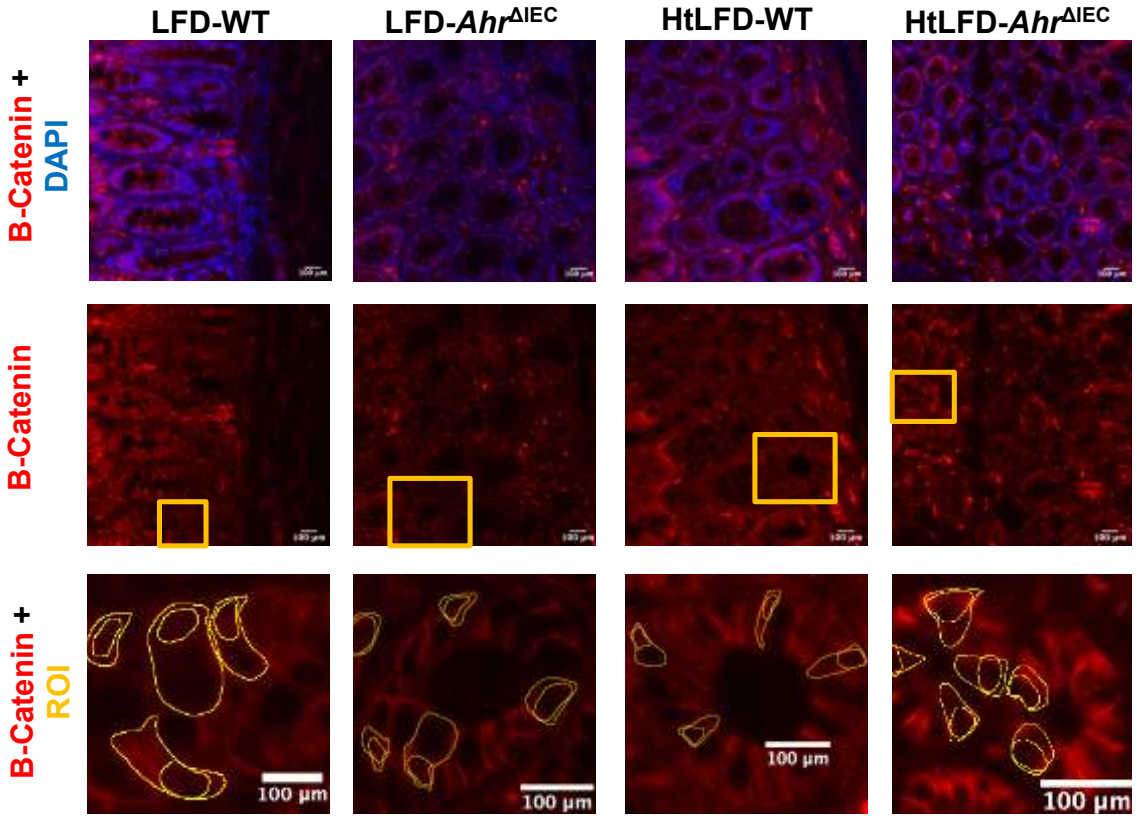

Figure III.7 Representative Images of Immunofluorescence Stained β-Catenin (in Red) and Nuclei (DAPI in Blue) within Colon Masses of both LFD and HtLFD Fed WT and *Ahr*$^{\Delta IEC}$ Mice. Magnified images (yellow box) contain representative regions of interest (ROIs) outlined in yellow that were used to calculate β-catenin intensity and nuclear localization. Objective 40x (Scale bar=100 µm).

Expression of β-catenin in actively proliferating cells in colon masses was significantly increased with the loss of AhR in IECs (p=0.0005) (Figure III.8A), and when comparing HtLFD fed mice compared to those consistently fed LFD ($p < 0.0001$) (Figure III.8B). Loss of AhR in IECs significantly increased the expression of β-catenin in LFD fed animals (p=0.0001), while this expression was not altered in *Ahr*$^{\Delta IEC}$ cells in HtLFD fed animals ($p > 0.9999$) compared to WT cells (Figure III.8C). Furthermore, an interaction effect between diet and genotype was observed with respect to β-catenin

intensity (p=0.0003). Nuclear localization of β-catenin was quantified as the percentage of β-catenin stain localized to the DAPI stained nucleus versus stain in the total cell. Nuclear localization of the transcription factor β-catenin was significantly increased in actively proliferating cells in colon masses lacking AhR compared to those with active AhR (p=0.0174) (Figure III.8D). HtLFD also increased nuclear localization of β-catenin compared to LFD control (p=0.0207) (Figure III.8E). HtLFD-*Ahr*$^{\Delta IEC}$ cells exhibited a significantly increased nuclear localization of β-catenin compared to LFD-WT cells (p=0.0171) (Figure III.8F). However, no interaction effect between diet and genotype on nuclear localization of β-catenin was observed (p=0.5862).

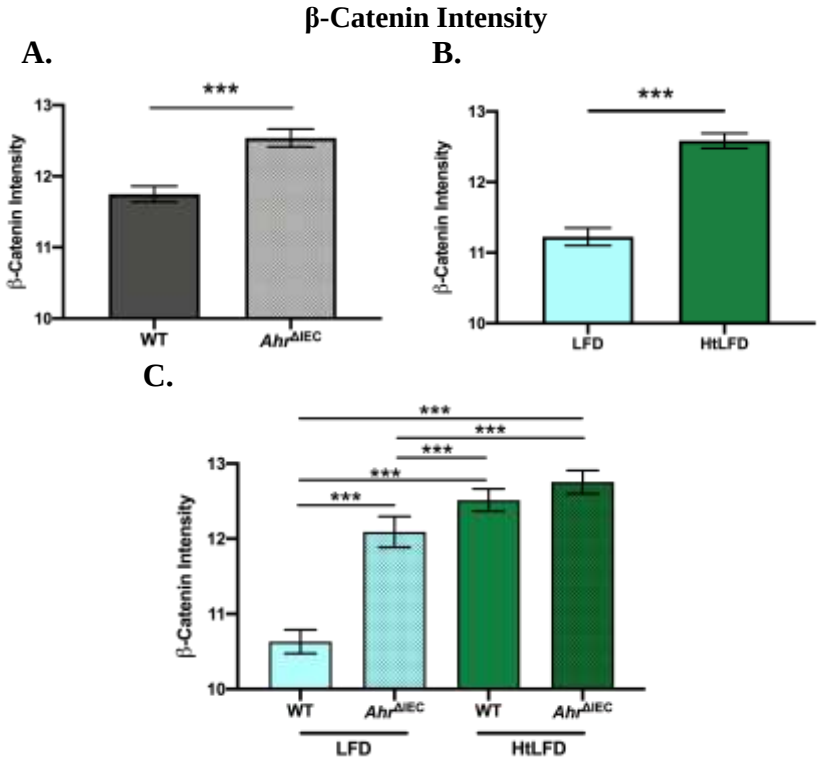

Figure III.8 Effect of Diet and Genotype on β-Catenin Intensity within Actively Proliferating Cells in Colon Masses. Fluorescent intensity was quantified in 100 cells per colon mass from 5 fields of view per mass. D: β-Catenin intensity within colon masses compared by genotype; p=0.0005 (MW). E: β-Catenin intensity within colon masses compared by diet; p<0.0001 (MW). F: β-Catenin intensity within colon masses compared by genotype and diet; p<0.0001 (KW). An interaction was observed between diet and genotype (p=0.0003). Effect of diet and genotype on β-Catenin nuclear localization within actively proliferating cells in colon masses. Fluorescent intensity was quantified in 100 cells (C) and nuclei (N) per colon mass from 5 fields of view per mass. Nuclear localization was calculated as N/(C-N). G: β-Catenin nuclear localization within colon masses compared by genotype; p=0.0174 (MW). H: β-Catenin nuclear localization within colon masses compared by diet; p=0.0207 (MW). I: β-Catenin nuclear localization within colon masses compared by genotype and diet; p=0.02501 (KW). No interaction was observed between diet and genotype (p=0.5862). Values are means ± SEM. * indicates p ≤ 0.05, ** indicates p ≤ 0.01, * indicates p ≤ 0.001, and the absence of * indicates p-values >0.05.**

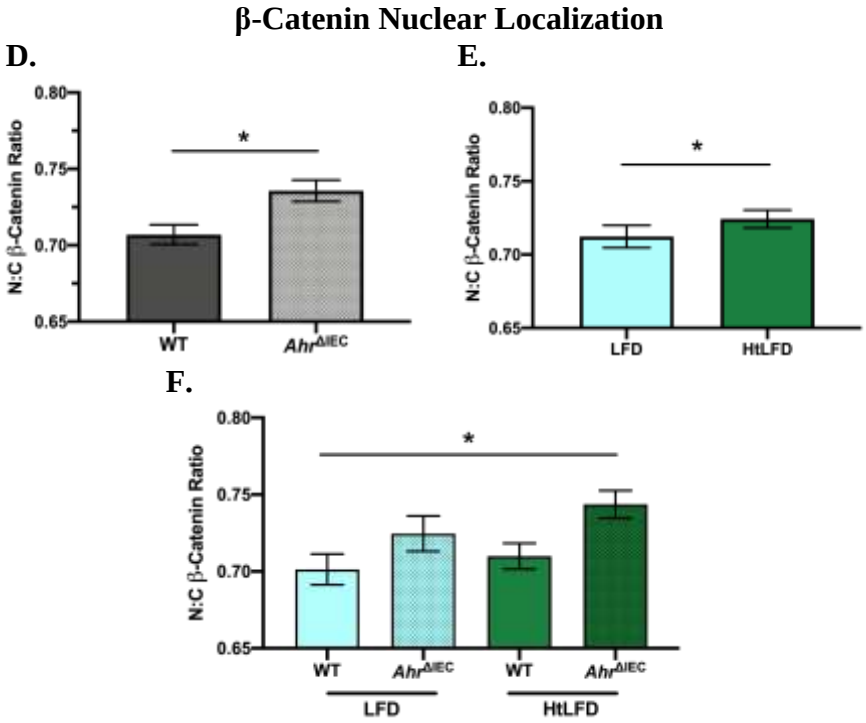

Figure III.8 Continued.

Discussion

AhR plays a significant role not only in regulating detoxification pathways, but also in a myriad of cellular processes, such as cell cycle, immune surveillance, epithelial barrier function, cell proliferation and tumorigenesis.[47,144,159] Moreover, activation of AhR by a varied group of endogenous and dietary ligands has been described to exert beneficial effects in the colon.[144] In recent years, an inverse association between expression of AhR and colon carcinogenesis has been reported using AhR-deficient mice (AhR null), which exhibited an increased rate of spontaneous colon-cecal tumors and increased colitis-associated colon tumor formation.[46–48,150] Since the use of a global AhR null model limits the ability to understand the significance of its expression within specific cell types, we utilized the IEC-specific, AhR knockout mouse model (*Ahr*$^{\Delta IEC}$)

in order to further investigate the role of AhR in IEC-related biology. Although it has been recently described that intestinal epithelial cell-specific AhR deletion enhances inflammation-induced tumorigenesis,[147] no information is yet available identifying how consumption of saturated fat can affect the different stages of sporadic CRC formation in the context of AhR activity in colonocytes. Given that colon tumor development is a multistage process, it is important to determine the specific stages in which AhR may provide its beneficial effects. To that end, this is the first study that has explored the contribution of AhR activity in IEC at different stages of the sporadic CRC formation continuum in the presence of HFD.

Previous studies have shown that exposure to HFD before and/or during AOM-induced CRC initiation is sufficient to significantly increase colon masses including polyps and tumors in WT animals regardless of body weight loss or maintenance following a dietary switch.[160,161] Therefore, we chose to investigate the effects of HFD feeding before, during, and for thirteen weeks following AOM exposure on colon carcinogenesis in the context of AhR activity in IECs. Loss of AhR in IECs was not sufficient to increase the incidence of colon masses, representing mucosal hyperplasia, mucosal dysplasia, polyp, adenoma, and adenocarcinoma. While this finding appears to conflict with previous studies that observed a marked increase in tumors in *Ahr*$^{\Delta IEC}$ compared to WT mice,[147] colon mass multiplicity was significantly increased in our *Ahr*$^{\Delta IEC}$ model when animals were exposed to HFD. In our model, HFD exposure during this peri-initiation period did not significantly increase colon mass incidence but was sufficient to increase colon mass multiplicity in *Ahr*$^{\Delta IEC}$ animals. Notably, HtLFD-

Ahr$^{\Delta IEC}$ animals had a nearly two-fold increase in colon mass multiplicity compared to LFD-*Ahr*$^{\Delta IEC}$ mice. Considering the similarity of the averages of colon mass multiplicity between the HtLFD-WT and LFD-WT groups, these results imply a biologically relevant interaction effect between diet and genotype on mass multiplicity (p=0.0658). This suggests that an increase in colon mass multiplicity in *Ahr*$^{\Delta IEC}$ mice is dependent upon fat content of the diet, even if exposure to HFD is transient. In addition, similar to previous reports,[162] *Ahr*$^{\Delta IEC}$ mice tended to have smaller colon masses as measured by reduced surface area. Colon tumor size has been negatively associated with survival in human patients, possibly due to a variety of factors, including the biology of the tumor itself or the microenvironment.[163] As such, this difference in colon mass size between *Ahr*$^{\Delta IEC}$ and WT animals could be relevant, but future experiments are necessary to test the mechanisms by which loss of AhR results in smaller colon masses.

The Wnt-β-catenin pathway is often mutated in CRC, and increased expression and nuclear translocation of β-catenin can result in increased colonocyte proliferation through the expression of *c-Myc* and *Cyclin D1*.[164,165] Hyperproliferative colon mass sections were co-stained for the proliferation marker EdU and β-catenin to assess the impact of the loss of AhR in IECs on β-catenin expression and nuclear localization in actively proliferating cells. In the colon mass formation cohort, proliferation was not significantly increased by *Ahr*$^{\Delta IEC}$ or HFD possibly because quantification was performed in hyperproliferative colon masses. In fact, proliferation was significantly reduced in HtLFD-*AhR*$^{\Delta IEC}$ compared to HFD-WT colon masses, yet the mechanism for

this disparity remains unclear. Although cellular proliferation was not significantly increased by *Ahr*$^{\Delta IEC}$ or HFD within colon masses, β-catenin intensity and nuclear localization were increased by both *Ahr*$^{\Delta IEC}$ and HFD. Furthermore, the effect of genotype on β-catenin expression was significantly dependent on the diet. As increased stabilization and nuclear localization of β-catenin is known to be associated with metastasis in a variety of cancers and models,[166–169] these results potentially indicate a mechanism by which *Ahr*$^{\Delta IEC}$ colon masses could exhibit increased metastatic potential, despite similar rates of incidence and proliferation compared to WT masses.

Since an increase of colonic polyps, ACFs, and tumors after chemically-induced CRC have been reported in HFD-induced obesity studies,[170,171] an increased inflammatory response has been implicated as a driving mechanism of this phenotype.[140,172] However, it is interesting to note that the consumption of a diet high in saturated fats did not affect body weight throughout this study. While resistance to body weight gain despite high fat feeding has been previously reported,[173] it has recently been shown that increased intestinal inflammation and loss of tumor suppression capacity are able to promote colon carcinogenesis in the presence of high fat diet without an increase in weight gain.[139–141,174,175] These results are consistent with our findings that HFD did significantly increase the multiplicity of colon masses or β-catenin intensity and nuclear localization within colonic masses. Overall, we have obtained comprehensive results demonstrating that the content of saturated fat in the diet, even if fed only during the peri-initiation period, as well as AhR activity in IECs, is implicated in an increase in the multiplicity of colon masses. Additionally, HFD diet has been reported to not only

promote a pro-carcinogenic gene signature but also to induce functional changes in the intestinal microbiota that could further exacerbate colon carcinogenesis via a reduction in AhR ligand availability.[176,177]

Findings of this chapter are summarized in Figure III.9. Although loss of AhR activity in IECs did not significantly increase colon mass incidence or cell proliferation within masses, nuclear β-catenin levels were elevated. These effects were further promoted in animals fed a HFD during the peri-initiation period. Though the cessation of HFD feeding in this study may have stunted the development of colon tumors in *Ahr*$^{\Delta IEC}$ animals, these data support recommendations that a diet high in saturated fat should be avoided to reduce the risk of CRC. Finally, it is likely that AhR activity in cells other that IECs or the effects of an altered gut microbiome could potentially have contributed to the prevention of colon mass formation in this model. Hence, future studies should focus on investigating the contribution of the gut microbial profile observed in LFD-fed *Ahr*$^{\Delta IEC}$ mice.

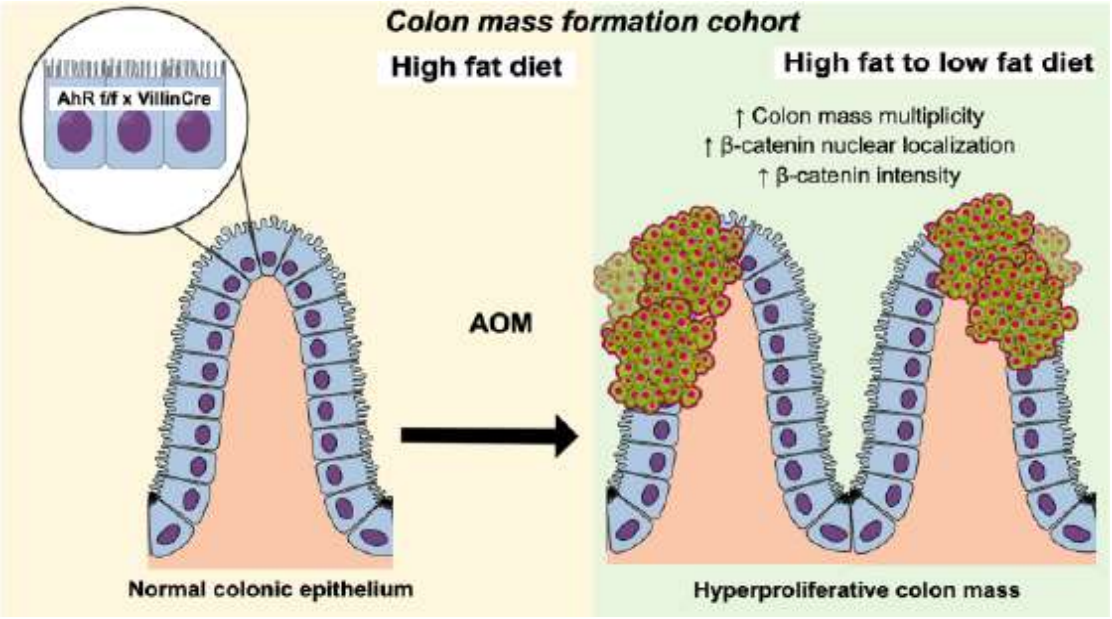

Figure III.9 Impacts of the Loss of the Aryl Hydrocarbon Receptor and High Fat Diet during the Peri-Initiation Period on Colorectal Carcinogenesis. AhR f/f, Aryl Hydrocarbon Receptor Flox/Flox; AOM, Azoxymethane; VillinCre, Villin 1 Promoter Directing Expression of Cre Recombinase.

CHAPTER IV

FECAL TRANSPLANT FROM ANIMALS LACKING INTESTINAL EPITHELIAL CELL ARYL HYDROCARBON RECEPTOR RESULTS IN WORSENED GUT BARRIER INTEGRITY

Introduction

The gut microbiome plays an important role in gut inflammation and colorectal cancer (CRC) development. Alterations in the gut microbial community or dysbiosis have been well documented in humans and animals with altered gut homeostasis, inflammation, and CRC.[178,179] Additionally, germ-free rodents develop fewer chemically-induced colorectal tumors than conventional animals.[179] Despite this evidence that the gut microbiome impacts CRC, it is still unclear whether microbial dysbiosis is a cause or consequence of CRC.[179] In an attempt to clarify the mechanisms that link the gut microbiome and host gut health, germ-free, antibiotic-treated, or transplantation models have been increasingly employed.[180–182] As the gut metabolome is affected by both the host and certain gut microbes, an antibiotic-treated, fecal transplantation model would be useful to determine the contribution of certain microbial profiles to the gut metabolome and host inflammation and therefore CRC development. One such study used transplantation of fecal samples from human CRC patients to germ-free and antibiotic treated mice injected with the colon-specific carcinogen, azoxymethane (AOM).[182] The fecal transplants from CRC patients increased colonocyte proliferation, expression of inflammatory cytokines and oncogenic genes, and immune cell infiltration.[182]

Furthermore, fecal transplants from animals deficient in genes considered protective to gut health have also been shown to be sufficient to cause detrimental changes in gene expression that result in increased susceptibility to colitis.[183] Similarly, germ-free animals transplanted with feces from Aryl Hydrocarbon Receptor global knock-out (AHRKO) animals develop increased inflammatory gene expression.[184] These experiments demonstrate the ability of gut microbial dysbiosis associated with host genetic changes to promote inflammation. However, the ability of the gut microbiome in feces from mice lacking AhR in intestinal epithelial cells ($Ahr^{\Delta IEC}$) to promote such gut inflammation has not been demonstrated. Our collaborative group has previously shown that $Ahr^{\Delta IEC}$ animals have an increase in premalignant colon lesions called aberrant crypt foci (ACF).[185] As discovered by Menon, R., et al., in addition to other changes in the gut microbiome, this increase in ACF was particularly observed in low-fat diet (LFD) fed $Ahr^{\Delta IEC}$ females that also exhibited a marked decrease in the genus *Akkermansia* (Figure IV.1A).[186] The only currently identified and culturable species of this genus to inhabit mammalian gastrointestinal tracts, *Akkermansia muciniphila*, is abundant and typically found in healthy human and mouse gastrointestinal tracts.[187,188] While a decrease in *A. muciniphila* is associated with negative health outcomes, including Inflammatory Bowel Diseases (IBDs),[188] results from studies investigating the levels of *A. muciniphila* in animals and humans with CRC is conflicting. In APC mutant mice, the early presence of *A. muciniphila* was associated with a decrease in mean tumor number.[189] However, in a small study, *A. muciniphila* was 4 times higher in the stool of CRC patients compared to controls.[190] Due to these conflicting results, the effects of *A. muciniphila* on gut barrier

integrity and inflammation should be further assessed. Additionally, our collaborative group led by Dr. Rani Menon has shown that beneficial microbial metabolites, including short chain fatty acids (SCFA) such as butyric acid and propionic acid (Figures IV.1B-F), as well as those derived from aromatic amino acids such as tryptophan metabolites (Figures IV.1G-J), were reduced in LFD fed *Ahr*$^{\Delta IEC}$ mice compared to wild type LFD fed controls.[186] *A. muciniphila* has been previously shown to favorably influence gut barrier integrity and inflammation via increased SCFA and mucin production, goblet cell number, and anti-inflammatory Interleukin-22 (IL-22) production.[191–193] Furthermore, *A. muciniphila* may activate the AhR by production of microbial metabolites derived from aromatic amino acids (MDAs) as well as potentially providing tryptophan as a substrate for other microbes through production of tryptophan from chorismate through the shikimate pathway according to the Kyoto Encyclopedia of Genes and Genomes (KEGG) database.[194]

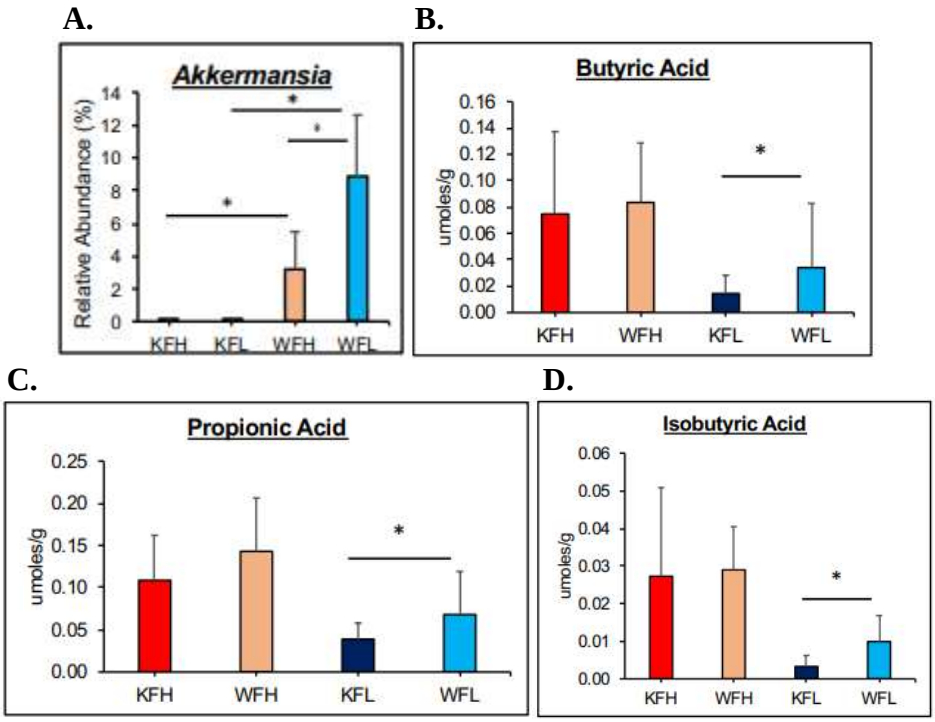

Figure IV.1 Relevant Supporting Data of *Akkermansia*, Short Chain Fatty Acids, and Putatively Identified Microbial Metabolites Derived from Aromatic Amino Acids from Unpublished Manuscript by Menon, R., et al. A. Relative Abundance of *Akkermansia*. B. Concentration of Butyric Acid in feces. C. Concentration of in Propionic Acid feces. D. Concentration of Isobutyric Acid in feces. E. Concentration of Isovaleric Acid in feces. F. Concentration of Valeric Acid in feces. G. Peak Intensity of 1H-Indole-3-acetamine. H. Peak Intensity of 5-Hydroxyindoleacetic acid. I. Peak Intensity of 3-Methyldioxyindole. J. Peak Intensity of 1H-Indole-3-carboxyaldehyde. * indicates statistical significance at $p < 0.05$ using the Wilcoxon rank-sum test. Mean +/- SEM. KFH, Aryl Hydrocarbon Receptor Intestinal Epithelial Cell Specific Knock Out High Fat Diet Female; KFL, Aryl Hydrocarbon Receptor Intestinal Epithelial Cell Specific Knock Out Low Fat Diet Female; WFH, Wild Type High Fat Diet Female; WFL, Wild Type Low Fat Diet Female.

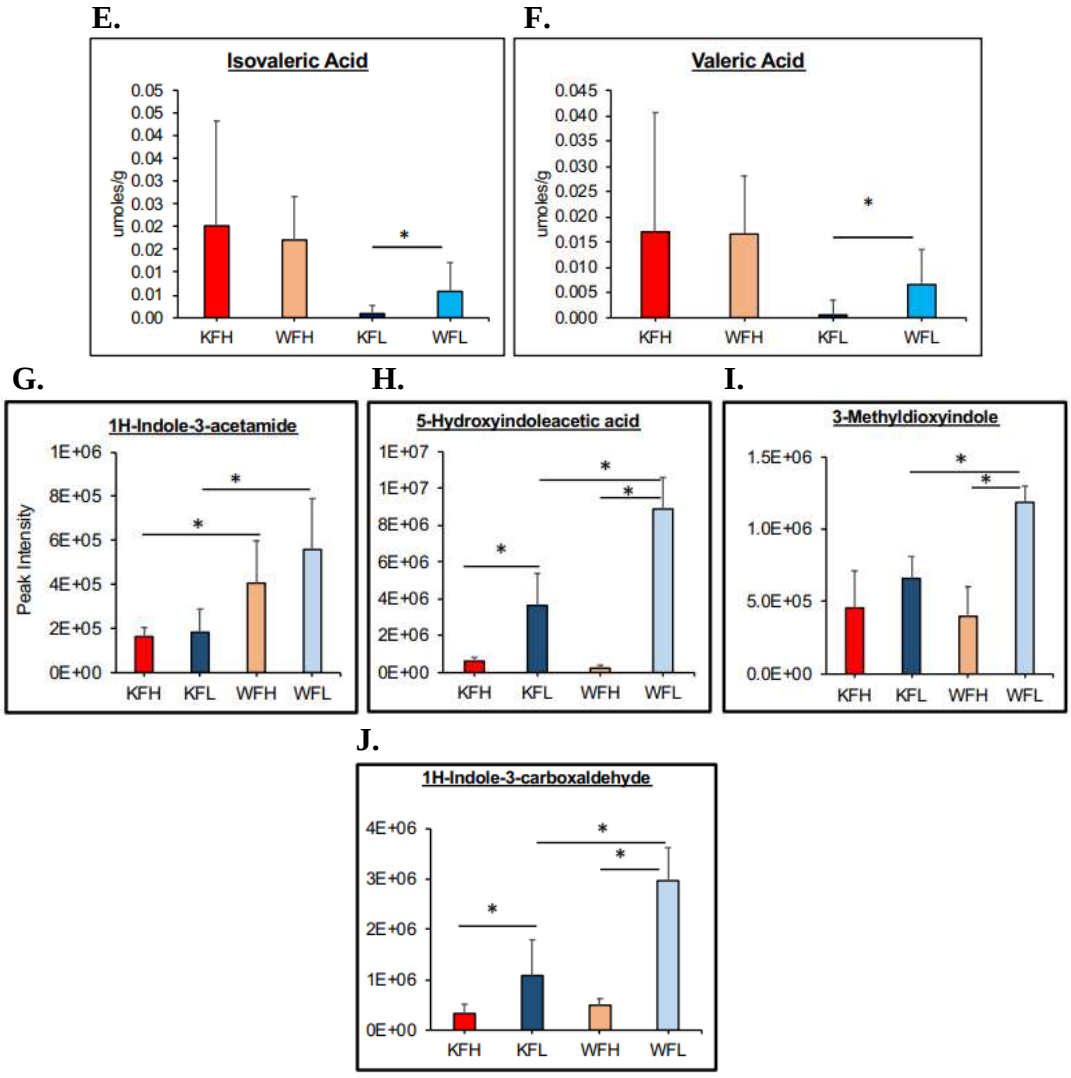

Figure IV.1 Continued.

The effects of the gut microbiota from *Ahr*$^{\Delta IEC}$ female mice fed a LFD on host gut barrier integrity and inflammation has not yet been examined in a fecal transplantation model in wild-type, conventionally raised female animals fed the same diet. This study aims to determine the impact of antibiotic reduction and fecal transplant of the dysbiotic gut microbiome from *Ahr*$^{\Delta IEC}$ mice depleted in *A. muciniphila* into wild-type, conventionally raised mice on host gut barrier integrity, inflammation, and the colonic

metabolome. Additionally, we hypothesized that negative gut barrier and inflammation changes associated with fecal transplant from *Ahr*$^{\Delta IEC}$ mice could be rescued with subsequent administration of *A. muciniphila*.

Materials and Methods

Animal Model and Experimental Timeline

All mice were housed at the Laboratory Animal Resources and Research facility at Texas A&M University. All procedures were performed under a protocol approved by the Institutional Animal Care and Use Committee at Texas A&M University. Wild type, C57BL/6J female recipient mice were ordered from Jackson Labs Barrier AX8. Animals were age-matched to 8 weeks old +/- 3 days. Animals were sorted into polycarbonate micro isolator cages and allowed to acclimate for 6 days before being placed on low-fat diet (LFD) containing 10% kcal from fat (Research Diets, D12450B). Diet composition is provided in Figure A.2 of Appendix A. The experimental timeline is displayed in Figure IV.2.

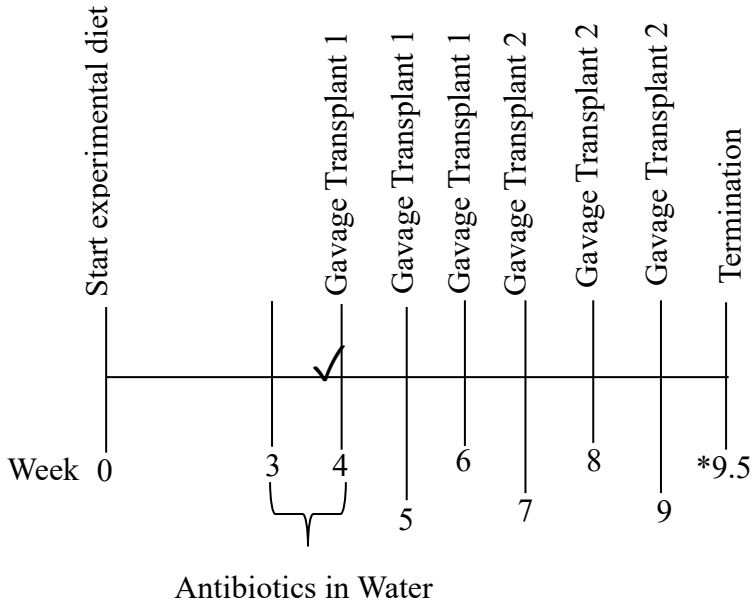

Figure IV.2 Experimental Design. * indicates a full fecal collection in which a minimum of 10 fresh fecal pellets per animal were collected over 2 days for gut microbiome and metabolome analyses. ✓ indicates a smaller fecal collection in which a minimum of 2 fresh fecal pellets per animal were collected on a single day to measure gut microbiome depletion via qPCR. Respective treatments for each transplant are provided in Table IV.1.

Antibiotic Treatment

Following three weeks of LFD feeding, animals were switched to irradiated LFD (Research Diets, D12450Bi) and sterile cages with sterile bedding and nesting material. Diet composition is provided in Figure A.2 of Appendix A. Simultaneously, antibiotic cocktail was administered in red, sterile water bottles to deplete the intestinal microbiota. The antibiotic cocktail was prepared as previously described.[195,196] Briefly, 2 g streptomycin (RPI, S62000), 0.5 g gentamycin (RPI, G38000), 0.125 g ciprofloxacin (Sigma, 17850), and 1 g bacitracin (Sigma, 11702) were added in order to sterile water in a sterile red bottle. Each antibiotic was allowed to dissolve completely before the

subsequent reagent was added, and the solution was protected from light and stirred for at least 3 hours before being administered fresh to mice. Fresh antibiotics were prepared and administered 3 days later, and, on day 6 of antibiotic treatment, a fresh fecal pellet was collected from individual animals placed in an empty sterile cage to assess intestinal microbiota depletion via quantitative PCR (qPCR) for total bacteria and *Akkermansia*. The sequences for each DNA oligo primer are as follows: *Akkermansia* (Forward: CAGCACGTGAAGGTGGGGAC, Reverse: CCTTGCGGTTGGCTTCAGAT).

Akkermansia muciniphila and Fecal Transplant Preparation and Gavage

After 7 total days of antibiotic treatment and confirmation of intestinal microbiota depletion, fresh sterile water was replaced for 24 hours before treatments were gavaged once per week for six weeks as outlined in Table IV.1.

A. muciniphila gavage was adapted from Plovier, et al.[197] Frozen glycerol stocks of *A. muciniphila* (ATCC, BAA-835) were thawed and seeded under anaerobic conditions into fresh, sterile brain heart infusion broth (BHI) 5 days before each gavage so bacteria was in log phase growth at gavage. On the day of gavage, optical density was measured and cultures were diluted to provide $1.33x10^6$ CFU/μL/kg body weight in 150 μL gavage. Procedures were completed under strict anaerobic conditions until gavage.

Fecal transplant was performed as described previously with minor modifications.[182] Briefly, fresh fecal pellets were collected from individual donor mice placed in clean, sterile microisolator cages. Using sterile forceps, feces from the appropriate group of donors was pooled and transferred to sterile BHI in glass test tubes with butyl rubber stoppers. Once tightly stoppered, tubes were returned to an anaerobic

jar, a gas pack was added, and the sealed jar was returned to an anaerobic chamber. Inside the anaerobic chamber, feces were weighed and slurried in fresh anaerobic media at 1 g feces per 5 mL BHI.

Vehicle gavage consisted of the same sterile BHI used to culture *A. muciniphila* and slurry fecal transplant. Butyl rubber stoppered tubes were returned to the anaerobic jar for transport to recipient animals where 150 μL of the appropriate mixture was gavaged to each recipient mouse as outlined in Table IV.1.

Treatment Group Label	**Antibiotics (In Water)**	**Transplant 1 (Once Weekly Gavage, Weeks 1-3)**	**Transplant 2 (Once Weekly Gavage, Weeks 4-6)**	**n**
-/-/-	-	Vehicle	Vehicle	10
ABX/-/-	+	Vehicle	Vehicle	10
-/Akk/Akk	-	*A. muciniphila*	*A. muciniphila*	10
ABX/Akk/Akk	+	*A. muciniphila*	*A. muciniphila*	10
ABX/Fec/Fec	+	Feces from $Ahr^{\Delta IEC}$	Feces from $Ahr^{\Delta IEC}$	10
ABX/Fec/Akk	+	Feces from $Ahr^{\Delta IEC}$	*A. muciniphila*	10

Table IV.1 Experimental Treatment Groups. -, vehicle; ABX, antibiotics; Akk, *Akkermansia muciniphila*; Fec, fecal transplant.

Donor Mice

Donor mice used for fecal transplant were female, constitutive, intestinal-epithelial cell specific AhR knockout C57BL/6 mice ($AhR^{f/f}$ x VillinCre, $Ahr^{\Delta IEC}$). Two groups of donor mice were used to more closely age match them at the time of fecal transplant of each cohort of experimental animals. One group of donor mice (n=4) was used for the first cohort of 20 experimental animals, while a second group of donors (n=3) was used for the second and third cohorts of 40 experimental animals. Age-matched $Ahr^{\Delta IEC}$ females were weaned to 4% Teklad Rodent Diet (Envigo, 8604),

henceforth referred to as chow diet, at 3 weeks old. Diet composition for chow diet is provided in Figure A.4 of Appendix A. Animals were switched to LFD at approximately 11 weeks of age +/- 2 days before being enrolled in the study. Each group of donors was on LFD for at least 3 weeks and depletion of *Akkermansia* was confirmed via qPCR before their feces was used for fecal transplant. The sequences for each DNA oligo primer are as follows: Total Bacteria (Forward: ACTACGTGCCAGCAGCC, Reverse: GGACTACCAGGGTATCTAATCC), *Akkermansia* (Forward: CAGCACGTGAAGGTGGGGAC, Reverse: CCTTGCGGTTGGCTTCAGAT).

Fecal and Tissue Collection

For two days prior to termination, fresh fecal pellets were collected from each animal placed in a sterilized, individual cage for no more than two hours. Feces were collected using sterilized forceps and placed in sterilized cryotubes before being flash frozen. A minimum of five fecal pellets were collected per animal each day before all collected pellets were combined prior to analyses.

Animals were terminated via ketamine/xylazine overdose, and blood was collected via cardiac puncture. The colon was immediately resected, and the most proximal and distal sections containing a fecal pellet were excised and cassetted immediately in ice cold Carnoy's fixative (60% absolute ethanol, 10% glacial acetic acid, and 30% chloroform) with the fecal pellets intact to preserve the mucus layers as previously described with minor modifications.[198,199] Briefly, following two hours of fixation, sections were washed twice for twenty minutes each with ice cold 100% ethanol before being stored in fresh, ice cold 100% ethanol. The remaining colon pieces

were then flushed with sterile PBS, fecal pellets were collected and flash frozen, and the most proximal 1 cm section was excised, opened longitudinally, and scraped with nuclease free tools before scraped tissue was stored in RNA Lysis Buffer (Zymo, R1060) at -80°C for later analyses. All remaining, flushed colon sections were opened longitudinally and stored for various later analyses, including flash frozen or fixed in 4% PFA for 4 hours before being dehydrated through several washes of 50% and 70% ethanol. Fixed colon sections were stored at 4°C in either 100% ethanol (Carnoy's fixed) or 70% ethanol (PFA fixed) until they were processed, embedded, and sectioned for histological analyses.

FITC-Dextran Gavage

Mice were fasted overnight prior to Fluorescein Isothiocyanate (FITC)-Dextran gavage. Four hours before termination, mice were gavaged with 600 mg/kg body weight of 80 mg/mL FITC-Dextran (Sigma, FD4) in sterile PBS as previously described with minor modification.[200,201] Briefly, FITC-Dextran was prepared the night before, and stored protected from light at 4°C until gavaged. Following cardiac puncture, blood was allowed to clot for 45 minutes at room temperature in the dark before being spun at 1,500 g for 10 minutes at 4°C. Samples were stored in the dark on ice until 60 μL of serum could be diluted with an equal volume of PBS. 60 μL of diluted serum was added to a 96-well plate in duplicate before the plate was read on a fluorometer with excitation 485 nm and emission 528 nm (20 nm band width). A single animal per termination did not receive FITC-Dextran to serve as a background control. A serial dilution of FITC-Dextran was also used to calculate the standard curve.

Histological Preparation and Staining of Colon Tissue

Carnoy's fixed colon sections were consistently stored at 4˚C for 120 hours before they were processed as previously described with minor modifications.[198] Briefly, samples were immersed in 3 one hour changes of xylene, then immersed in 2 changes of molten paraffin wax for 1.5 hours each. Following processing, sections were embedded in paraffin and cut to 5 μm thickness. Sections were stained with Alcian Blue and Nuclear Fast Red (Abcam, ab150662) according to manufacturer's protocol. Images were captured via an Aperio CS2 slide scanner at 40x.

Slide Scoring of Mucus Layer Thickness and Goblet Cell Percentage

Thickness of the inner mucus layer was assessed in Carnoy's fixed, distal colon sections that contained an intact fecal pellet. In 3 sections each of Alcian Blue, Nuclear Fast Red stained distal colon with intact luminal contents, 20 measurements were taken perpendicular to the colonic epithelium at random locations of at least 100 μm of intact inner mucus layer. Measurements were performed using Aperio ImageScope software v.12.3.3.5048.

Goblet cells were quantified in the same Alcian Blue, Nuclear Fast Red stained tissues. Total numbers of epithelial cells and goblet cells in 10 well-oriented crypts per each of the 3 tissue sections in distal colon. The percentage of goblet cells was then calculated as the total number of Alcian Blue positive cells per 100 Nuclear Fast Red stained nuclei. Cell counts were performed using ImageJ 2.0.0-rc-69/1.52p; Java 1.8.0_172 [64-bit].

Gene Expression Analyses from Colon Mucosal Scrapings

RNA was isolated from colon mucosal scrapings stored at -80˚C in RNA Lysis Buffer using the Quick-RNA MiniPrep Kit (Zymo, R1055) according to the manufacturer's instructions, including DNase treatment. Isolated RNA samples were cleaned and concentrated as necessary using the RNA Clean & Concentrator kit (Zymo, R1017). Following Nanodrop quantification, and confirmation of purity using 260/280 and 260/230 ratios above 2 and 1.8 respectively, cDNA was then synthesized using 500 ng of total RNA via the Transcriptor First Strand cDNA Synthesis kit (Roche, 04897030001) according to the manufacturer's protocol. cDNA was stored at -20˚C until real time quantitative PCR (RT-qPCR) was conducted.

RT-qPCR for Claudin-2 (*Cldn-2*), Interleukin-6 (*Il-6*), Interleukin-22 (*Il-22*), Lipocalin-2 (*Lcn2*), Mucin 2 (*Muc-2*), Occludin (*Ocln*), and Tight Junction Protein 1 (*Tjp1*) or Zonula Occludens-1 (*Zo-1*) was conducted using LightCycler 480 Sybr Green I Master (Roche, 04887352001) and DNA oligo primers (Sigma) , while RT-qPCR for Interleukin-22 (*Il-22*) and Mucin 1 (*Muc-1*) was conducted using (Roche, 04707494001) and Taqman probes (ThermoFisher). Each PCR was conducted in triplicate with 20 μL reaction volume. The sequences for each DNA oligo primer are as follows: *Cldn-2* (Forward: GAA AGG ACG GCT CCG TTT TCT A, Reverse: ACA GTG TCT CTG GCA AGC TG), *Il-6* (Forward: CTG CAA GAG ACT TCC ATC CAG TT, Reverse: AAG TAG GGA AGG CCG TGG TT), *Il-22* (Forward: ACA TCG TCA ACC GCA CCT TT, Reverse: CAG CCT TCT GAC ATT CTT CTG GAT), *Lcn2* (Forward: AAG GCA GCT TTA CGA TGT ACA GC, Reverse: CTT GCA CAT TGT AGC TGT GTA

CC), *Muc-2* (Forward: CTG ACC AAG AGC GAA CAC AA, Reverse: CAT GAC TGG AAG CAA CTG GA), *Ocln* (Forward: TTT TGT GGG ATA AGG AAC ACA, Reverse: ATA GTC AGA TGG GGG TGG AG), *Tjp-1/Zo-1* (Forward: GAT CCC TGT AAG TCA CCC AGA, Reverse: CTC CCT GCT TGC ACT CCT ATC), and 18S rRNA (Forward: TCA AGA ACG AAA GTC GGA GGT T, Reverse: GGA CAT CTA AGG GCA TCA CAG). Predeveloped Taqman assays were used for the following genes: *Muc-1* (ThermoFisher, Mm00449604_m1), and 18S rRNA (ThermoFisher, Mm03928990_g1). Sybr Green I/HRM Dye (Ex. 465-Em.510) RT-qPCR program was performed on a LightCycler 480II (Roche) for all RT-qPCR using Sybr Green assays. Mono Color Hydrolysis Probe/UPL Probe for FAM dyes (Ex. 465-Em.510) rt-PCR program was performed on a LightCycler 480II (Roche) for all RT-qPCR using Taqman assays. Expression levels of all genes were normalized to the appropriate 18S rRNA control, and the delta Ct (ddCt) method was used to calculate fold change in relation to the relevant control group.

Preparation of Feces for Metabolomic and Microbiome Analyses

Fecal pellets were maintained at -80˚C until processing. All fecal pellets were collected for two days prior to termination and were combined and lyophilized in a Labconco FreeZone 4.5 Liter Benchtop Freeze Dry System for 12 hours before being homogenized using a 5 mm 440C stainless steel bead (GBSS 196-2500-10, OPS Diagnostics) and a Precellys 24 tissue homogenizer (Bertin) at 5000 rpm for 20 seconds twice. Powdered feces were then weighed out as appropriate for each assay as follows:

25 mg for SCFA measurements, 20-25 mg for untargeted metabolites measurements, and 3-5 mg powdered feces for 16S rRNA analysis.

Measurement of Short Chain Fatty Acids in Feces

Concentrations of 6 SCFAs (acetic, butyric, isobutyric, isovaleric, propionic, and valeric acids) were quantified using Gas Chromatography-Mass Spectrometry (GC-MS) as previously described with minor modifications.[202] The 25 mg of powdered feces used for SCFA measurements was placed on ice for 10 min before 600 μL of cold 30 mM hydrochloric acid with 0.25 mM d7 Butyric acid was added as an internal standard. A bead was added, and the sample was vortexed briefly before being immediately returned to ice. The sample was homogenized using a bead beater for 30 seconds. After ensuring complete homogenization, samples were centrifuged at 13,000 x g for 10 min at 4°C. 300 μL of supernatant was transferred to a fresh, pre-cooled 1.5 mL Eppendorf tube, and 300 μL of cold GC grade ethyl acetate was added (Millipore). After vortexing for 10 seconds, samples were placed on ice to incubate for 5 min before being centrifuged again at 13,000 x g for 1 min at 4°C. The upper layer was then transferred to an autosampler vial with insert and capped immediately.

GC-MS was then conducted at the Integrated Metabolomics Analysis Core (IMAC) at Texas A&M University using a triple quadruple TSQ 8000 EVO Gas Chromatography – Mass Spectrometer (Thermo Scientific); a 30 m x 0.25 mm x 0.25 μm ZB-Wax plus column (Phenomenex) was used to perform chromatographic separation. Full scan mode was used to acquire the MS data and retention times in the m/z range of 40 to 500 for individual SCFAs. Target compounds were quantified in the

Selected Ion Monitoring (SIM) mode using the product ions. Injector temperature was maintained at 230°C, while the MS transfer line and ion source were both maintained at 240°C. Helium carrier gas flow was 1 mL/min. 1 μL of extracted sample was injected with a split ratio of 20:1, and samples were kept on the autosampler at room temperature before injection. Ionization was conducted in the electron impact (EI) mode at 70 eV. TraceFinder v 3.3 software (Thermo Scientific) was used to acquire and analyze samples. Pure standards were used to generate standard curves of 0 μM to 3000 μM for each SCFA. The weight of powdered, dry feces used for extraction and internal standard d7 Butyric acid of each sample was used to normalize the concentration of each SCFA.

Untargeted Metabolite Detection in Feces

Untargeted metabolomics was carried out using liquid chromatography-mass spectrometry (LC-MS) at the Integrated Metabolomics Analysis Core (IMAC) at Texas A&M University as previously described with minor modifications.[97,98,203,204] Metabolites were extracted from 20-25 mg of powdered feces by adding it to pre-cooled tubes, adding 400 μL ice-cold methanol and 200 μL of ice-cold chloroform, and shaking the parafilm sealed tube on the tissue homogenizer (Precellys 24, Bertin) at 5500 rpm for 20 seconds. After removing parafilm, samples were centrifuged at 1000 x g for 10 min at 4°C. Supernatant was transferred to a fresh tube, and the sample was homogenized and centrifuged again before supernatants were combined in fresh tube. 600 μL of ice-cold, sterile Milli Q water was added to the combined supernatants before samples were vortexed for 30 seconds, then centrifuged at 3000 x g for 5 min at 4°C. The upper phase was transferred to a Spin-X 0.22 μm filter (Costar, 8619) in a 2 mL tube. The filter and

tube containing the upper phase was centrifuged at 3000 x g for 1 min at 4°C. After transferring the filtrate to a 15 mL conical tube, 500 µL of ice-cold, sterile Milli Q water was added to each sample and mixed. Samples were lyophilized before storage at -80°C. Before samples were run, they were resuspended in 100 µL of 50% Omnisolv LCMS grade Methanol (VWR, EM-MX0486-1) and 50% Omnisolv LCMS grade water (VWR, EM-WX0004-1).

A Q-Exactive Plus orbitrap mass spectrometer (Thermo Scientific) coupled to an UltiMate 3000 binary pump UPLC (Thermo Scientific) was used to perform untargeted liquid chromatography high-resolution accurate mass spectrometry (LC-HRAM). Source and capillary temperatures were maintained at 350°F, and the spray voltage was set to 3.5 kV (Pos). Samples were maintained at 4°C before injection, and a 10 µL injection volume was used. Full MS spectra were obtained, followed by data-dependent MS-MS (ddMS2) spectra at 35,000 resolution (200 m/z). A scan range of 50-750 m/z and a stepped normalized collision energy corresponding to 5, 11, 17 eV was used. A Synergi Fusion 4 µm, 150 mm x 2 mm reverse phase column (Phenomenex) at 30°C using a solvent gradient method was used to achieve chromatographic separation. Solvent A was water with 0.1% formic acid, while Solvent B was methanol with 0.1% formic acid. The gradient method used was 0-5 min (10% B to 40% B), 5-7 min (40% B to 95% B), 7-9 min (95% B), 9-9.1 min (95% B to 10% B), 9.1-13 min (10% B), and the flow rate was 0.4 mL min^{-1}. Sample acquisition was performed using Xcalibur software (Thermo Scientific).

Raw LC-MS data files were processed by Compound Discoverer v 3.0 software (Thermo Fisher Scientific). The processing workflow provided with the application Untargeted Metabolomics with Statistics Detect Unknowns with ID Using Online Databases and mzLogic was used for spectra alignment, compound detection, grouping, compound identification, and pathway analysis. Raw data was normalized to the amount of fecal material used for extraction of each sample. Initial analysis focused on putative AhR ligands derived from aromatic amino acids. After reviewing the chromatograms, mass spectrum, and mzCloud match for each compound in the list of putative AhR ligands, five compounds were annotated with any reasonable confidence.

16S rRNA Analysis of Fecal Microbiome

DNA was isolated from 3-5 mg powdered feces using DNeasy PowerSoil kit (Qiagen) and then quantified on a Nanodrop. Samples were then sent on dry ice to the Microbial Analysis, Resources, and Services (MARS) core facility at the University of Connecticut for bacterial 16S rRNA sequencing of the V4 region on the MiSeq platform (Illumina) as previously described.[205] Data was analyzed using Mothur and Phyloseq. Briefly, chimeras in the raw sequences were removed using the uchime program in Mothur then aligned and classified using the SILVA database. Alpha diversity analysis was conducted in MicrobiomeAnalyst (www.microbiomeanalyst.ca). Beta diversity analysis and taxonomic composition analysis was conducted using Phyloseq.

Statistical Analysis

All statistical analyses and figures were generated in GraphPad Prism version 8.1.2 for macOS, Graph Pad Software (La Jolla CA, www.graphpad.com). Where

appropriate, means were compared using parametric or non-parametric methods according to compliance of normality (Shapiro-Wilk test). Where appropriate, outliers based on ROUT (Q=1.0%) were excluded. Parametric methods included unpaired t test for comparing two means or one-way ANOVA followed by Tukey's multiple comparisons test for comparing three or more means. Non-parametric methods include the Mann-Whitney U (MW) test for comparing two means or the Kruskal-Wallis (KW) test followed by Dunn's multiple comparisons test for comparing three or more means. Two-tailed p-values are reported in all analyses, unless otherwise noted due to directionality of the hypothesis. All values listed are group means and error bars are presented as SEM. Differences among groups were considered statistically significant when the p-value was ≤ 0.05. Within figures, * indicates $p \leq 0.05$, ** indicates $p \leq 0.01$, *** indicates $p \leq 0.001$, **** indicates $p \leq 0.0001$, and the absence of * indicates p-values >0.05 or bars without a common letter differ significantly.

Results

Body Weight

Average body weight of any experimental groups was not significantly different on any given week of the experiment but did increase as was expected over time (Figure IV.3; ANOVA p=0.8065, n=10 animals/group). Neither antibiotic treatment, fecal transplant, nor *A. muciniphila* gavage significantly impacted body weight.

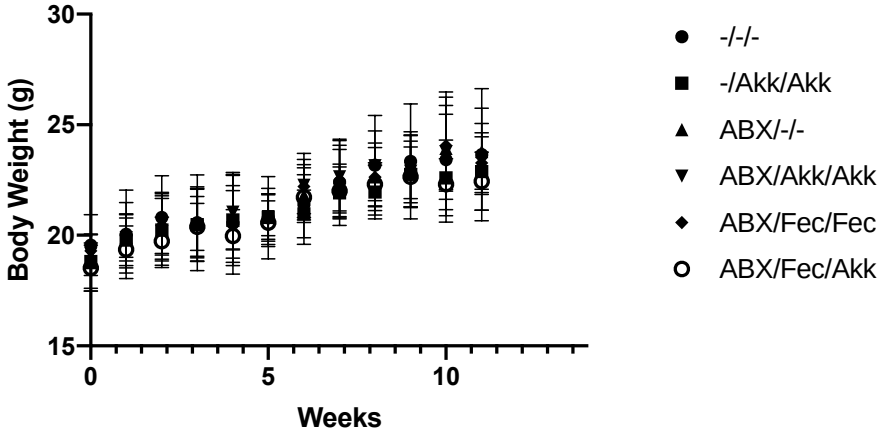

Figure IV.3 Average Weekly Body Weight. Weekly body weight of experimental mice (ANOVA p=0.8065). n=10 animals/group. Mean +/- SEM. -, vehicle; ABX, antibiotics; Akk, *Akkermansia muciniphila*; Fec, fecal transplant.

Depletion of Akkermansia muciniphila in Feces of Donor Mice

qPCR was used to confirm depletion of *A. muciniphila* in $Ahr^{\Delta IEC}$ female mice on LFD for at least 3 weeks before fecal transplant was performed. Donors were significantly depleted in *A. muciniphila* compared to wild type controls fed a chow diet (Figure IV.4, MW p=0.0008, n=2, 7 animals/group, genes run in triplicate).

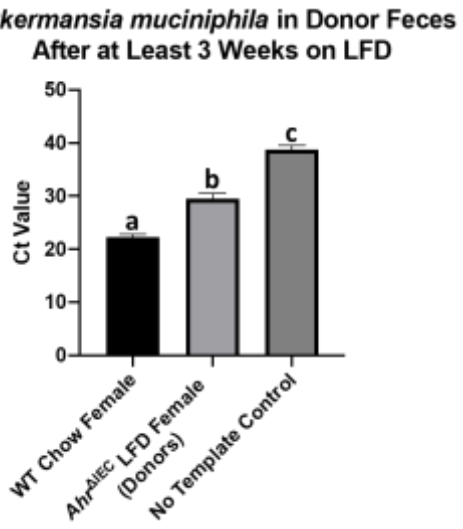

Figure IV.4 Depletion of *Akkermansia muciniphila* in Feces of Donor Animals on LFD for at Least Three Weeks (ANOVA p<0.0001, n=2, 7 animals, genes run in triplicate). Values are means ± SEM. Bars without a common letter differ significantly. ABX, antibiotics; LFD, low fat diet; WT, wild type.

Intestinal Microbiota Depletion and Akkermansia muciniphila Colonization

qPCR was also used to confirm depletion of total bacteria and *A. muciniphila* in the feces of experimental animals after receiving antibiotics in the water for 6 days compared to animals that received sterile water vehicle for 6 days. Total bacteria was depleted in animals receiving antibiotics compared to animals that did not receive antibiotics and were on either chow or LFD (Figure IV.5A, ANOVA p<0.0001, n=3, 20, 40, 3 animals/group, genes run in duplicate). Specifically, *A. muciniphila* was also depleted in animals receiving antibiotics compared to animals that received antibiotic-free vehicle on either chow or LFD (Figure IV.5B, ANOVA p<0.0001, n=3, 20, 40 animals/group, genes run in duplicate).

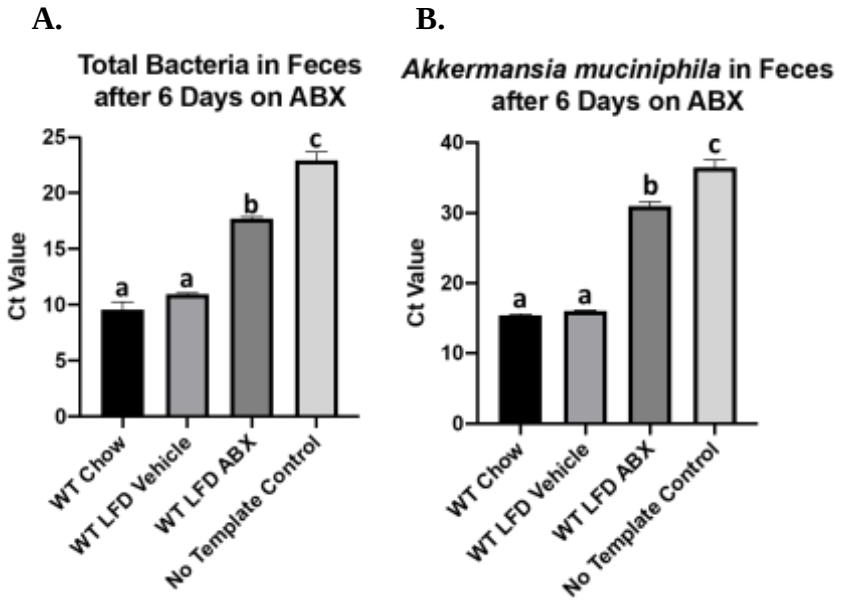

Figure IV.5 Depletion of Bacteria in Feces of Experimental Animals on ABX for 6 Days. A. Total bacterial depletion in feces following ABX treatment for 6 days (KW $p<0.0001$, n=3, 20, 40 animals, genes run in duplicate). B. *Akkermansia muciniphila* depletion in feces following ABX treatment for 6 days (ANOVA $p<0.0001$, n=3, 20, 40 animals, genes run in duplicate). Values are means ± SEM. Bars without a common letter differ significantly. ABX, antibiotics; LFD, low fat diet; WT, wild type.

16S rRNA Analysis of the Intestinal Microbiota

At the termination of the study, 16S rRNA analysis was used to characterize the intestinal bacterial profiles of the feces of the experimental groups as well as the donor mice. To assess the diversity within a group, two different alpha diversity indices were calculated: Shannon (Figure IV.6A, ANOVA $p<0.0001$, n=7-10 animals/group) and Fisher (Figure IV.6B, ANOVA $p<0.0001$, n=7-10 animals/group). In both indices, antibiotic treatment followed by vehicle transplant or *A. muciniphila* gavage significantly reduced alpha diversity compared to all other groups, including those that did not receive antibiotics, those that received fecal transplant with or without *A. muciniphila* gavage, and those mice that served as donors. According to the Fisher

diversity index, fecal transplant alone also significantly increased alpha diversity compared to the group that did not receive antibiotics but did receive *A. muciniphila* gavage, while all other groups were not different (Figure IV.6B).

Beta diversity, a measure of the variation in the microbiome between experimental groups, was assessed using Bray-Curtis dissimilarity in Principle Coordinates Analysis (Figure IV.6C). The vehicle group clustered similarly to the group that did not receive antibiotics, but did receive *A. muciniphila* gavage. The groups that received fecal transplant clustered with the donor mice, regardless of *A. muciniphila* treatment. Animals that received antibiotics alone also clustered similarly to the group that only received *A. muciniphila* after antibiotic treatment.

The relative abundance of major phyla was compared across groups (Figure IV.6D). Verrucomicrobia was depleted in groups that received fecal transplant and donors, regardless of *A. muciniphila* treatment. While Verrucomicrobia is present in both groups that did not receive antibiotics, regardless of *A. muciniphila* gavage, the relative abundance of Verrucomicrobia was markedly increased in both the group that received antibiotics alone and the group that received *A. muciniphila* following antibiotic treatment. This increase corresponded to a decrease in the phyla Firmicutes and Bacteroidetes compared to all other treatment groups and donors.

Finally, the relative abundance of the genus *Akkermansia* was compared across groups (Figure IV.6E). *Akkermansia* was present at expected levels of an average of between 2 and 5% relative abundance[187,206,207] in both groups that did not receive antibiotics, irrespective of *A. muciniphila* gavage. *Akkermansia* was significantly

increased in both groups that received antibiotics, regardless of *A. muciniphila* gavage, compared to the groups that did not receive antibiotics. Additionally, *Akkermansia* was significantly depleted in the fecal transplant and donor groups with or without *A. muciniphila* treatment compared to the group that received vehicle alone.

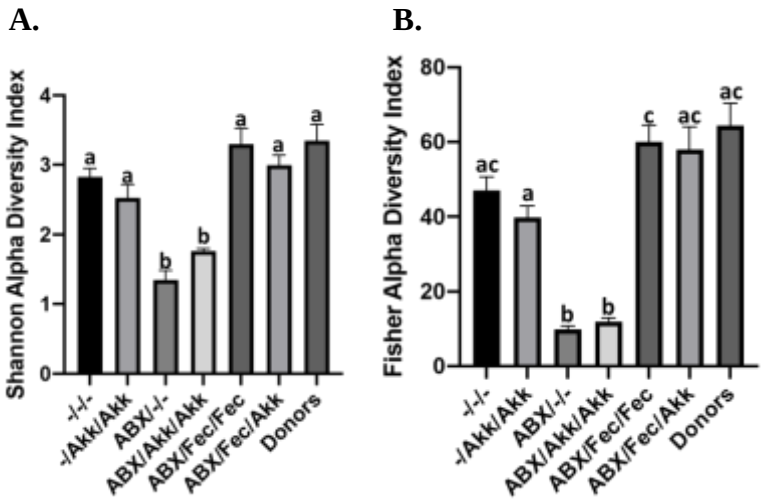

Figure IV.6 16S rRNA Analysis of the Intestinal Microbiota. A. Alpha diversity represented by Shannon Index for each group (ANOVA p<0.0001). B. Alpha diversity represented by Fisher's Alpha for each group (ANOVA p<0.0001). C. Beta diversity represented by Bray-Curtis dissimilarity-based non-metrical multidimensional scaling analysis. D. Relative abundances of major gastrointestinal bacterial phyla for each group. n=7-10 animals/group. E. Relative abundance of *Akkermansia* genus for each group. n=7-10 animals/group. Values are means +/- SEM. Bars without a common letter differ significantly. -, vehicle; ABX, antibiotics; Akk, *Akkermansia muciniphila*; Fec, fecal transplant.

C.

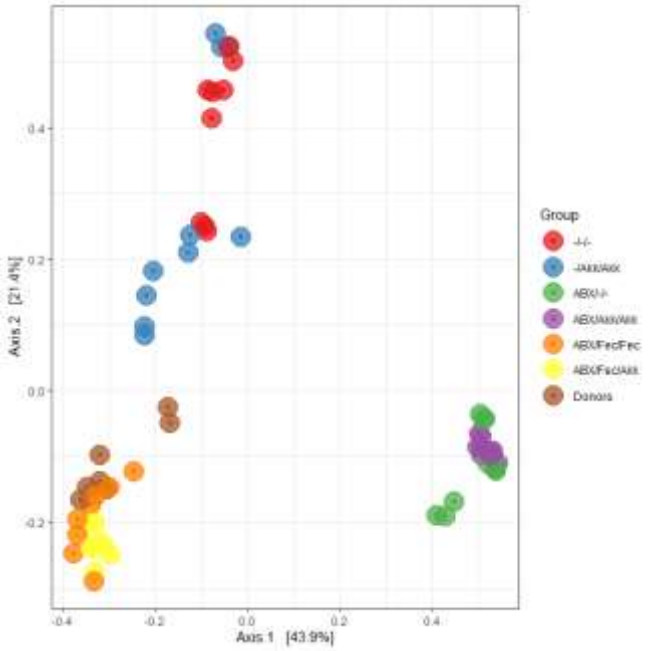

D.

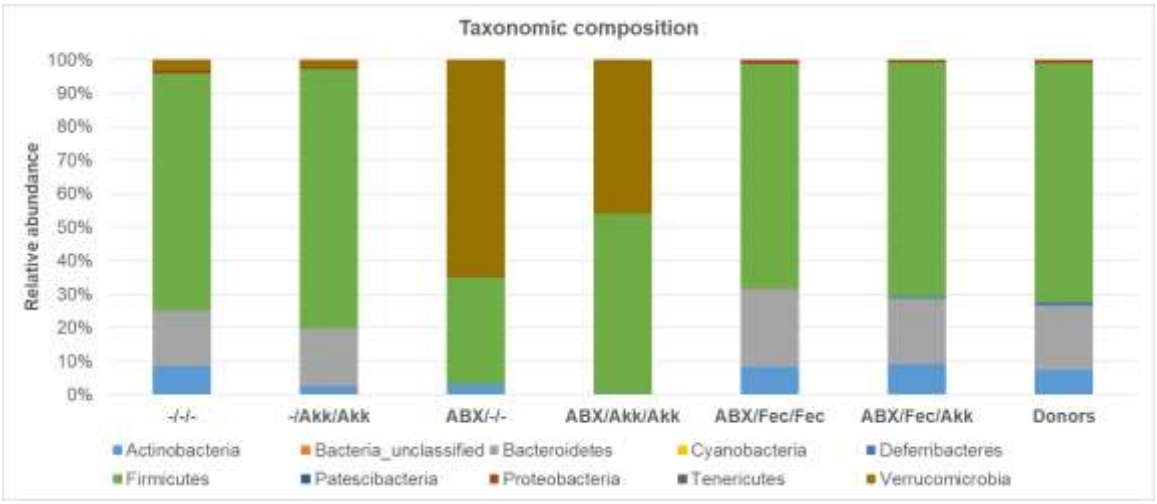

Figure IV.6 Continued.

E.

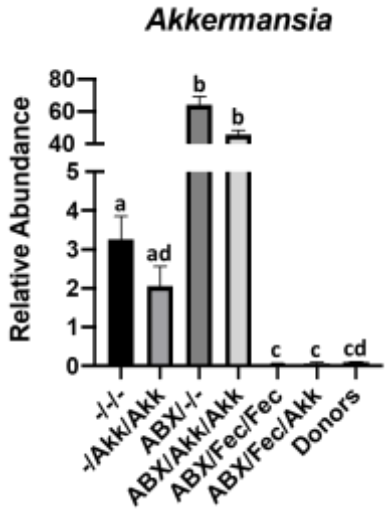

Figure IV.6 Continued.

Gut Permeability

To assess gut permeability, FITC-Dextran was gavaged 4 hours prior to termination. Compared to antibiotic treated controls, animals that received fecal transplant had significantly higher FITC-Dextran concentration in the serum and therefore gut permeability, regardless of *A. muciniphila* treatment (Figure IV.7A, ANOVA $p=0.0016$, n=5, 6, or 7 animals/group). Though antibiotic treatment reduced FITC-Dextran concentration compared to vehicle treated controls, this was not significant (Figure IV.7A). Overall, fecal transplant significantly increased FITC-Dextran concentration compared to animals that did not receive fecal transplant (Figure IV.7B). Donors also had significantly increased FITC-Dextran concentration and therefore worsened gut permeability compared to animals that did not receive fecal transplant (Figure IV.7B, KW $p<0.0001$, n=25, 13, 9 animals). Data is presented from first and third cohorts only due to error in second cohort's fluorescence data.

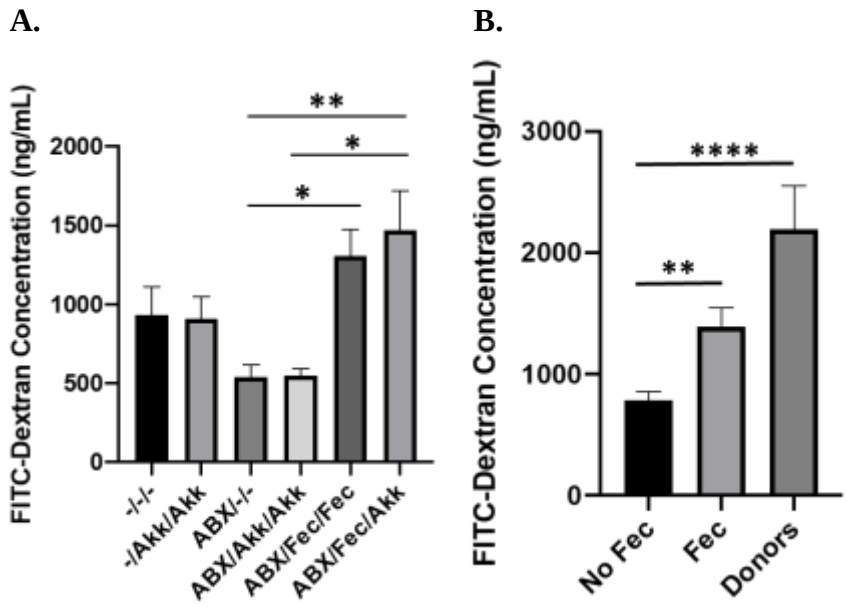

Figure IV.7 Fluorescein Isothiocyanate (FITC)-Dextran Concentration in Serum. A. Average serum FITC-Dextran concentration of experimental groups (ANOVA p=0.0016). n=5, 6, or 7 animals per group from first and third cohorts only. B. Average serum FITC-Dextran concentration of animals with or without fecal transplant and donor animals (KW p<0.0001). n=25, 13, 9 animals. Values are means ± SEM. * indicates p ≤ 0.05, ** indicates p ≤ 0.01, * indicates p ≤ 0.001, **** indicates p≤ 0.0001, and the absence of * indicates p-values >0.05. -, vehicle; ABX, antibiotics; Akk, *Akkermansia muciniphila*; Fec, fecal transplant. No Fec consists of groups -/-/-, -/Akk/Akk, ABX/-/-, and ABX/Akk/Akk, while Fec consists of ABX/Fec/Fec and ABX/Fec/Akk groups.**

Mucus Layer Thickness

The thickness of the intact mucus layer was assessed in Carnoy's fixed, Alcian Blue/Nuclear Fast Red stained distal colon sections at a 90 degree angle to the mucosa (Figure IV.8A). Compared to vehicle controls, *A. muciniphila* treatment alone significantly increased mucus layer thickness (Figure IV.8B). Conversely, antibiotic treatment with or without *A. muciniphila* gavage significantly decreased mucus layer thickness (Figure IV.8B). Interestingly, fecal transplant significantly increased mucus layer thickness compared to vehicle or antibiotic treated controls, regardless of *A.*

muciniphila treatment (Figure IV.8B). Upon closer examination, *A. muciniphila* gavage after fecal transplant did significantly increase mucus layer thickness compared to fecal transplant alone (Figure IV.8C, MW=0.0272, one-tailed, n=585, 480 measurements from 8-10 animals/group).

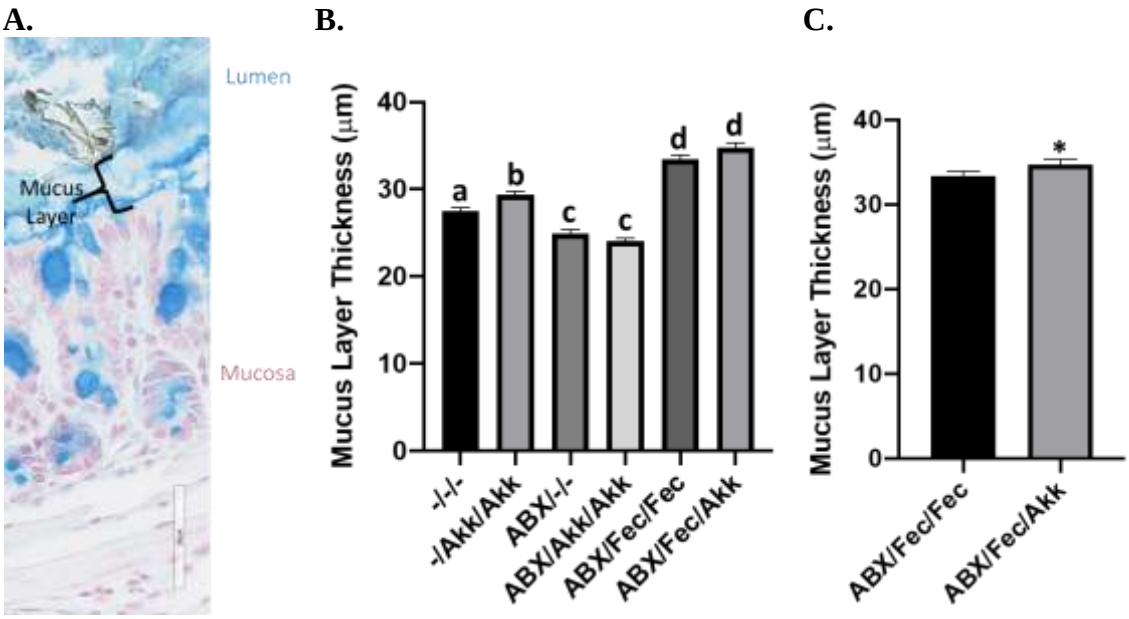

Figure IV.8 Average Mucus Layer Thickness in Distal Colon. A. Representative image of Carnoy's fixed, Alcian Blue/Nuclear Fast Red stained distal colon section with feces intact for mucus thickness measurements. Scale bar = 50 μm. B. Average mucus layer thickness of experimental groups (KW p<0.0001). n=480-598 measurements from 8-10 animals/group. Bars without a common letter differ significantly. C. Average mucus layer thickness of animals receiving fecal transplant with or without *Akkermansia muciniphila* treatment (MW p=0.0272, one-tailed). n=585, 480 measurements from 8-10 animals/group. Values are means ± SEM. * indicates p ≤ 0.05, ** indicates p ≤ 0.01, * indicates p ≤ 0.001, **** indicates p≤ 0.0001, and the absence of * indicates p-values >0.05. -, vehicle; ABX, antibiotics; Akk, *Akkermansia muciniphila*; Fec, fecal transplant.**

Percentage of Goblet Cells

The percentage of goblet cells per 100 nuclei was assessed in intact crypts in Carnoy's fixed, Alcian Blue/Nuclear Fast Red stained distal colon sections in 30 crypts per animal with 10 animals per group for a total of 300 crypts measured per group

(Figure IV.9A). Antibiotic treatment significantly decreased goblet cell percentage compared to animals treated with vehicle water regardless of *A. muciniphila* treatment (Figure IV.9B, KW p=0.0014, n=300 crypts measured per group). However, neither *A. muciniphila* treatment following antibiotics nor fecal transplant with or without *A. muciniphila* gavage significantly impacted goblet cell percentage compared to vehicle controls (Figure IV.9B).

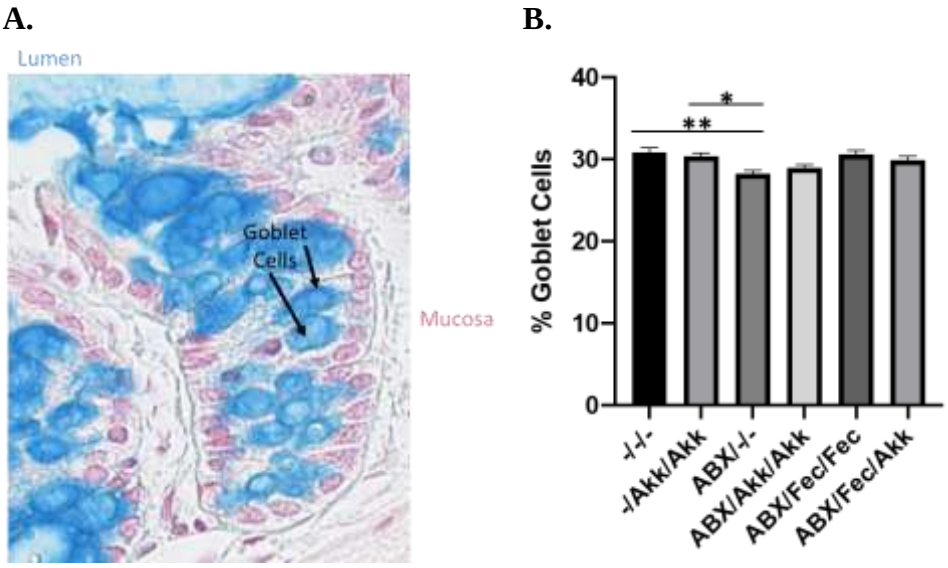

Figure IV.9 Percentage of Goblet Cells in Distal Colon. A. Representative image of Carnoy's fixed, Alcian Blue/Nuclear Fast Red stained distal colon section with feces intact. Goblet cells are indicated by black arrows. B. Percentage of goblet cells per 100 nuclei of experimental groups (KW p=0.0014). n=300 crypts measured/group. Values are means ± SEM. * indicates p ≤ 0.05, ** indicates p ≤ 0.01, * indicates p ≤ 0.001, **** indicates p≤ 0.0001, and the absence of * indicates p-values >0.05. -, vehicle; ABX, antibiotics; Akk, *Akkermansia muciniphila*; Fec, fecal transplant.**

Gene Expression

In order to assess the impact of antibiotics, *A. muciniphila*, and fecal transplant on tight junctions, relative gene expression of Claudin-2 (*Cldn2*), Occludin (*Ocln*), and Tight Junction Protein-1 or Zonula Occludens-1 (*ZO-1*) was quantified using rt-PCR.

When comparing all 6 experimental groups, *Cldn2* was significantly increased in groups that received fecal transplant, regardless of *A. muciniphila* treatment, as well as the group that receive *A. muciniphila* treatment following antibiotics compared to vehicle treated controls with or without *A. muciniphila* gavage (Figure IV.10A, ANOVA p=0.0002, n=7-10 animals/group). Relative *Ocln* expression is significantly increased in the group that only received *A. muciniphila* without antibiotic treatment compared to all other groups, except a trend toward increase compared to the fecal transplant alone group at p=0.0554 (Figure IV.10B, ANOVA p=0.0044, n=9-10 animals/group). *ZO-1* expression is increased in the group that received *A. muciniphila* following fecal transplant compared to groups that did not receive antibiotics regardless of *A. muciniphila* gavage and the group that received antibiotics alone (Figure IV.10C, ANOVA p=0.0003, n=8-10 animals/group). As a trend toward increase was observed in the group that received *A. muciniphila* after fecal transplant compared to fecal transplant alone, this difference was investigated in a post host analysis using student's t-test. This increase was significant at p=0.0500 (Figure IV.10M, n=10 animals/group).

As interesting microbial changes were observed with each individual treatment, relative expression of tight junction protein genes were compared between any animals treated with either antibiotics, *A. muciniphila*, or fecal transplant and animals that did not receive those respective treatments. *Cldn-2* expression was significantly increased in antibiotic treated animals (Figure IV.10D, t-test p=0.0003, n=14, 39 animals) and fecal transplant treated animals (Figure IV.10F, t-test p<0.0001, n=40, 20 animals), but not in *A. muciniphila* treated animals (Figure IV.10E, t-test p=0.8301, n=30, 29 animals)

compared to their respective vehicle treated controls. Conversely, a significant decrease in *Ocln* expression was measured in antibiotic treated animals (Figure IV.10G, t-test p=0.0044, n=20, 40 animals), a trend toward decrease occurred in animals that received fecal transplant (Figure IV.10I, t-test p=0.0592, n=20, 40 animals), and no significant difference was found in *A. muciniphila* gavaged animals (Figure IV.10H, t-test p=0.4275, n=20, 40 animals) compared to vehicle treated control animals. *ZO-1* expression was significantly increased in all animals receiving each of the treatments compared to all animals receiving their respective controls: antibiotics (Figure IV.10J, t-test p=0.0006, n=14, 40 animals), *A. muciniphila* (Figure IV.10K, t-test p=0.0042, n=27, 30 animals), and fecal transplant (Figure IV.10L, t-test p=0.0090, n=0.0090).

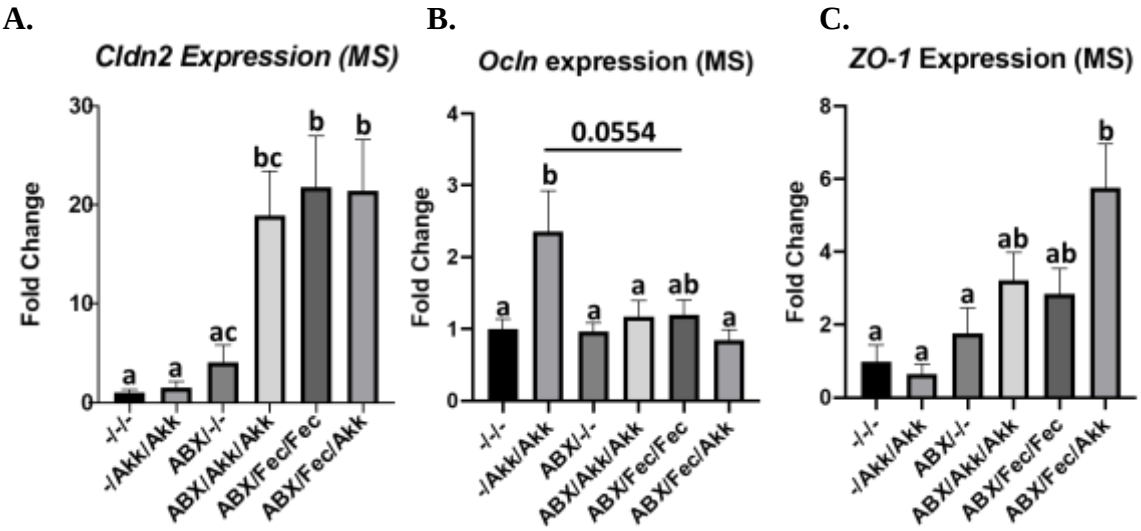

Figure IV.10 Relative Gene Expression of *Cldn2*, *Ocln*, and *Zo-1* in Colonic Mucosal Scrapings. Fold changes were calculated using the ddCT method. A. Relative *Cldn2* gene expression in experimental groups (ANOVA p=0.0002, n=7-10 animals/group). B. Relative *Ocln* gene expression in experimental groups (ANOVA p=0.0044, n= 9-10 animals/group). C. Relative *ZO-1* gene expression in experimental groups (ANOVA p=0.0003, n=8-10 animals/group). D. Relative *Cldn2* gene expression in antibiotic treated animals (t-test p=0.0003, n= 14, 39 animals). E. Relative *Cldn2* gene expression in *A. muciniphila* treated animals (t-test p=0.8301, n= 30, 29 animals). F. Relative *Cldn2* gene expression in fecal transplant treated animals (t-test p<0.0001, n= 40, 20 animals). G. Relative *Ocln* gene expression in antibiotic treated animals (t-test p=0.0044, n= 20, 40 animals). H. Relative *Ocln* gene expression in *A. muciniphila* treated animals (t-test p=0.4275, n= 20, 40 animals). I. Relative *Ocln* gene expression in fecal transplant treated animals (t-test p=0.0592, n= 20, 40 animals). J. Relative *ZO-1* gene expression in antibiotic treated animals (t-test p=0.0006, n= 14, 40 animals). K. Relative *ZO-1* gene expression in *A. muciniphila* treated animals (t-test p=0.0042, n= 27, 30 animals). L. Relative *ZO-1* gene expression in fecal transplant treated animals (t-test p=0.0090, n= 40, 20 animals). M. Relative *ZO-1* gene expression in the ABX/Fec/Akk group vs. the ABX/Fec/Fec group (t-test p= 0.0500, n= 10, 10 animals). Genes run in triplicate. Values are means ± SEM. Bars without a common letter differ significantly. * indicates p ≤ 0.05, ** indicates p ≤ 0.01, * indicates p ≤ 0.001, **** indicates p≤ 0.0001, and the absence of * indicates p-values >0.05. -, vehicle; ABX, antibiotics; Akk, *Akkermansia muciniphila*; Fec, fecal transplant; MS, mucosal scraping. No ABX consists of groups -/-/- and -/Akk/Akk, while ABX consists of ABX/-/-, ABX/Akk/Akk, ABX/Fec/Fec, and ABX/Fec/Akk Groups. No Akk consists of groups -/-/-, ABX/-/-, and ABX/Fec/Fec, while Akk consists of -/Akk/Akk, ABX/Akk/Akk, and ABX/Fec/Akk groups. No Fec consists of groups -/-/-, -/Akk/Akk, ABX/-/-, and ABX/Akk/Akk, while Fec consists of ABX/Fec/Fec and ABX/Fec/Akk groups.**

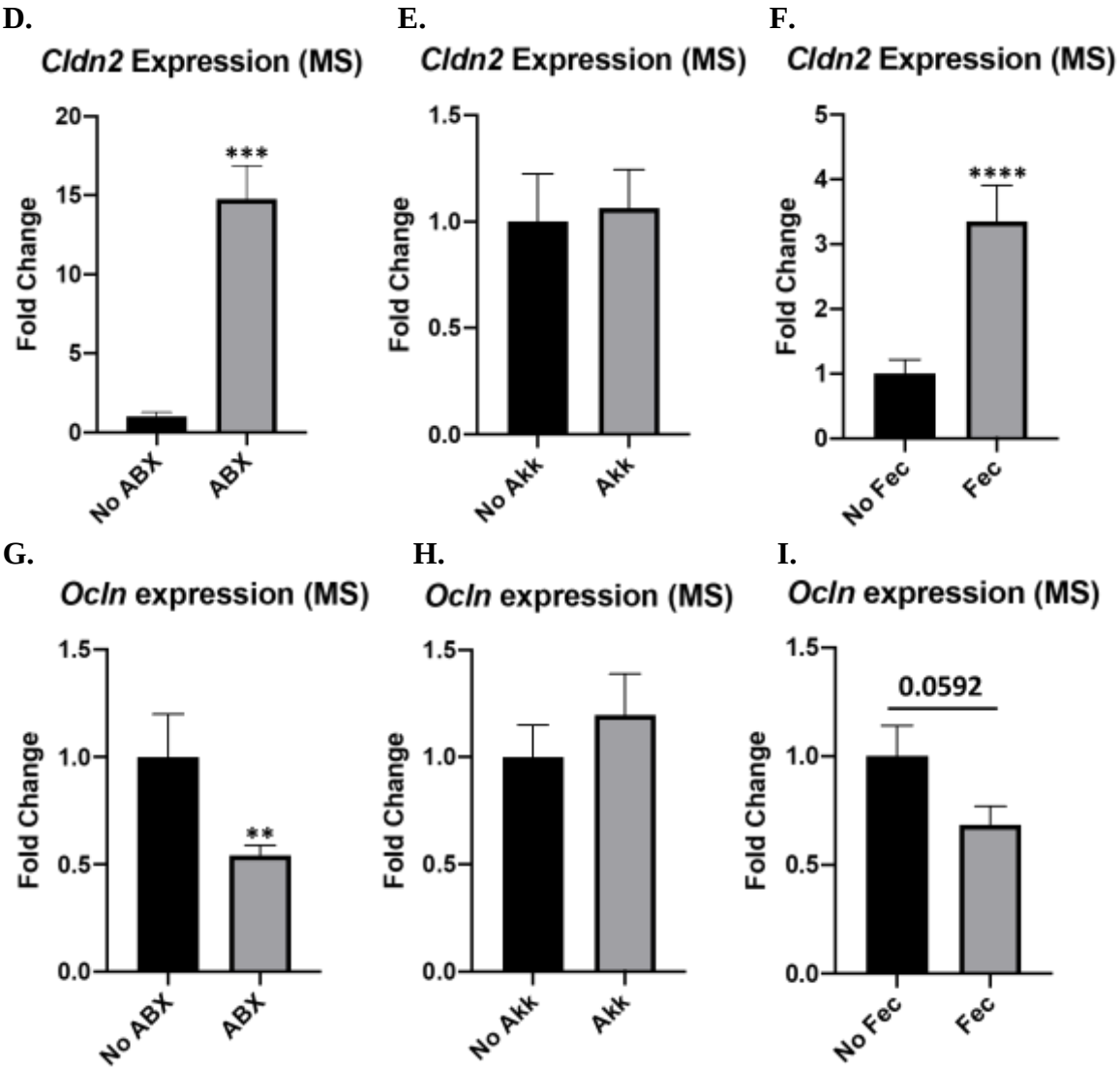

Figure IV.10 Continued.

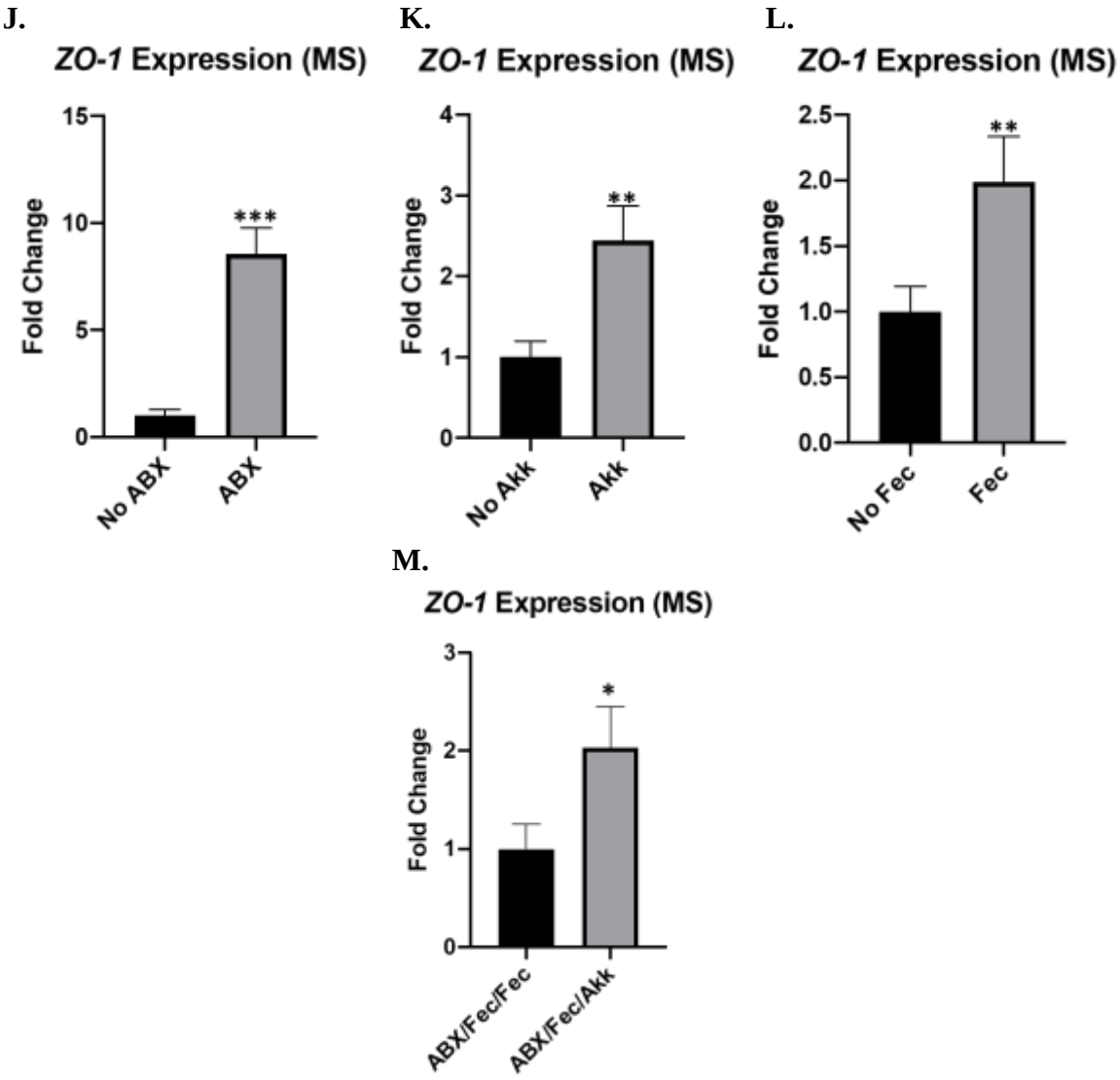

Figure IV.10 Continued.

The inflammatory profile of colon mucosal scrapings was also tested using rt-PCR to determine relative gene expression of Interleukin-6 (*Il-6*), Interleukin-22 (*Il-22*), and Lipocalin 2 (*Lcn2*). Relative gene expression of *Il-22* was significantly increased ($p<0.05$) or tended to increase ($0.05<p<0.1$) in the group that received *A. muciniphila* gavage alone, compared to all other treatment groups (Figure IV.11B, ANOVA $p=0.0140$, n=5-10 animals/group), however no significant differences were observed

between any other treatment groups. No differences were observed between experimental groups in either *Il-6* (Figure IV.11A, ANOVA p=0.1463, n=7-10 animals/group) or *Lcn2* (Figure IV.11C, ANOVA p=0.2386, n=9-10 animals/group). As interesting microbial changes were observed with each individual treatment, relative expression of tight junction protein genes were compared between any animals treated with either antibiotics, *A. muciniphila*, or fecal transplant and animals that did not receive those respective treatments. Similarly, when comparing animals that received individual treatments to their respective vehicle controls, no differences were observed in *Il-6* in antibiotic treated animals (Figure IV.11D, MW p=0.2870, n=13, 33 animals), *A. muciniphila* treated animals (Figure IV.11E, MW p=0.1206, n=22, 23 animals), or fecal transplant recipients (Figure IV.11F, MW p=0.2306, n=28, 17 animals). A lack of statistical difference was also observed in some of the same comparisons of *Il-22*: antibiotic treated animals (Figure IV.11G, t-test p=0.2971, n=20, 40 animals) or fecal transplant treated animals (Figure IV.11I, t-test p=0.3714, n=40, 20 animals) compared to their respective vehicle controls. However, relative *Il-22* expression was significantly increased in *A. muciniphila* gavaged animals compared to animals that received vehicle gavage (Figure IV.11H, t-test p=0.0135, n=30, 30 animals). Also, as a trend toward increase was observed in the group that received *A. muciniphila* after fecal transplant compared to fecal transplant alone, this difference was investigated in a post host analysis using student's t-test. This increase was significant at p=0.0439 (Figure IV.11J, n=8, 7 animals). Furthermore, *Lcn2* relative gene expression was significantly increased in animals that received antibiotics compared to animals that did not (Figure IV.11K, t-

test p=0.0095, n=15, 34 animals). Conversely, *Lcn2* expression was significantly decreased in animals that received *A. muciniphila* gavage compared to those that did not (Figure IV.11L, t-test p=0.0464, n=29, 27 animals). A trend toward increase was observed in *Lcn2* expression in fecal transplant recipients compared to animals that did not receive transplant (Figure IV.11M, t-test p=0.0913, n=30, 16 animals).

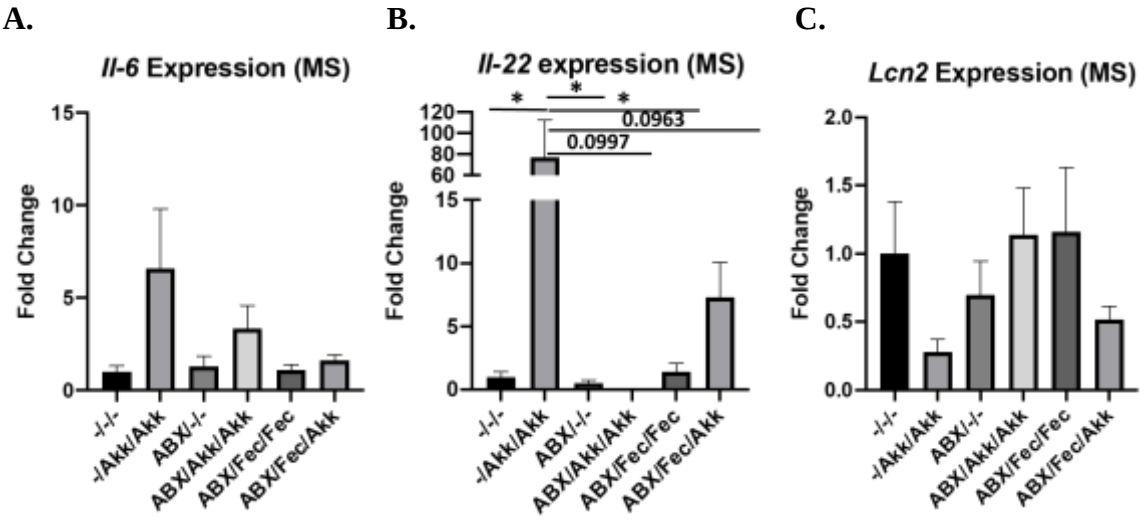

Figure IV.11 Relative Gene Expression of *Il-6, Il-22,* and *Lcn2* in Colonic Mucosal Scrapings. Fold changes were calculated using the ddCT method. A. Relative *Il-6* gene expression in experimental groups (ANOVA p=0.1463, n=7-10 animals/group). B. Relative *Il-22* gene expression in experimental groups (ANOVA p=0.0.140, n=5-10 animals/group). C. Relative *Lcn2* gene expression in experimental groups (ANOVA p=0.2386, n=9-10 animals/group). D. Relative *Il-6* gene expression in antibiotic treated animals (MW p=0.2870, n=13, 33 animals). E. Relative *Il-6* gene expression in *A. muciniphila* treated animals (MW p=0.1206, n=22, 23 animals). F. Relative *Il-6* gene expression in fecal transplant treated animals (MW p=0.2306, n=28, 17 animals). G. Relative *Il-22* gene expression in antibiotic treated animals (t-test p=0.2971, n=20, 40 animals). H. Relative *Il-22* gene expression in *A. muciniphila* treated animals (t-test p=0.0135, n=30, 30 animals). I. Relative *Il-22* gene expression in fecal transplant treated animals (t-test p=0.3714, n=40, 20 animals). J. Relative *Il-22* gene expression in the ABX/Fec/Akk group vs. the ABX/Fec/Fec group (t-test p= 0.0439, n=8, 7 animals). K. Relative *Lcn2* gene expression in antibiotic treated animals (t-test p=0.0095, n=15, 34 animals). L. Relative *Lcn2* gene expression in *A. muciniphila* treated animals (t-test p=0.0464, n=29, 27 animals). M. Relative *Lcn2* gene expression in fecal transplant treated animals (t-test p=0.0913, n=30, 16 animals). Genes run in triplicate. Values are means ± SEM. Bars without a common letter differ significantly. * indicates p ≤ 0.05, ** indicates p ≤ 0.01, * indicates p ≤ 0.001, **** indicates p≤ 0.0001, and the absence of * indicates p-values >0.05. -, vehicle; ABX, antibiotics; Akk, *Akkermansia muciniphila*; Fec, fecal transplant; MS, mucosal scraping. No ABX consists of groups -/-/- and -/Akk/Akk, while ABX consists of ABX/-/-, ABX/Akk/Akk, ABX/Fec/Fec, and ABX/Fec/Akk Groups. No Akk consists of groups -/-/-, ABX/-/-, and ABX/Fec/Fec, while Akk consists of -/Akk/Akk, ABX/Akk/Akk, and ABX/Fec/Akk groups. No Fec consists of groups -/-/-, -/Akk/Akk, ABX/-/-, and ABX/Akk/Akk, while Fec consists of ABX/Fec/Fec and ABX/Fec/Akk groups.**

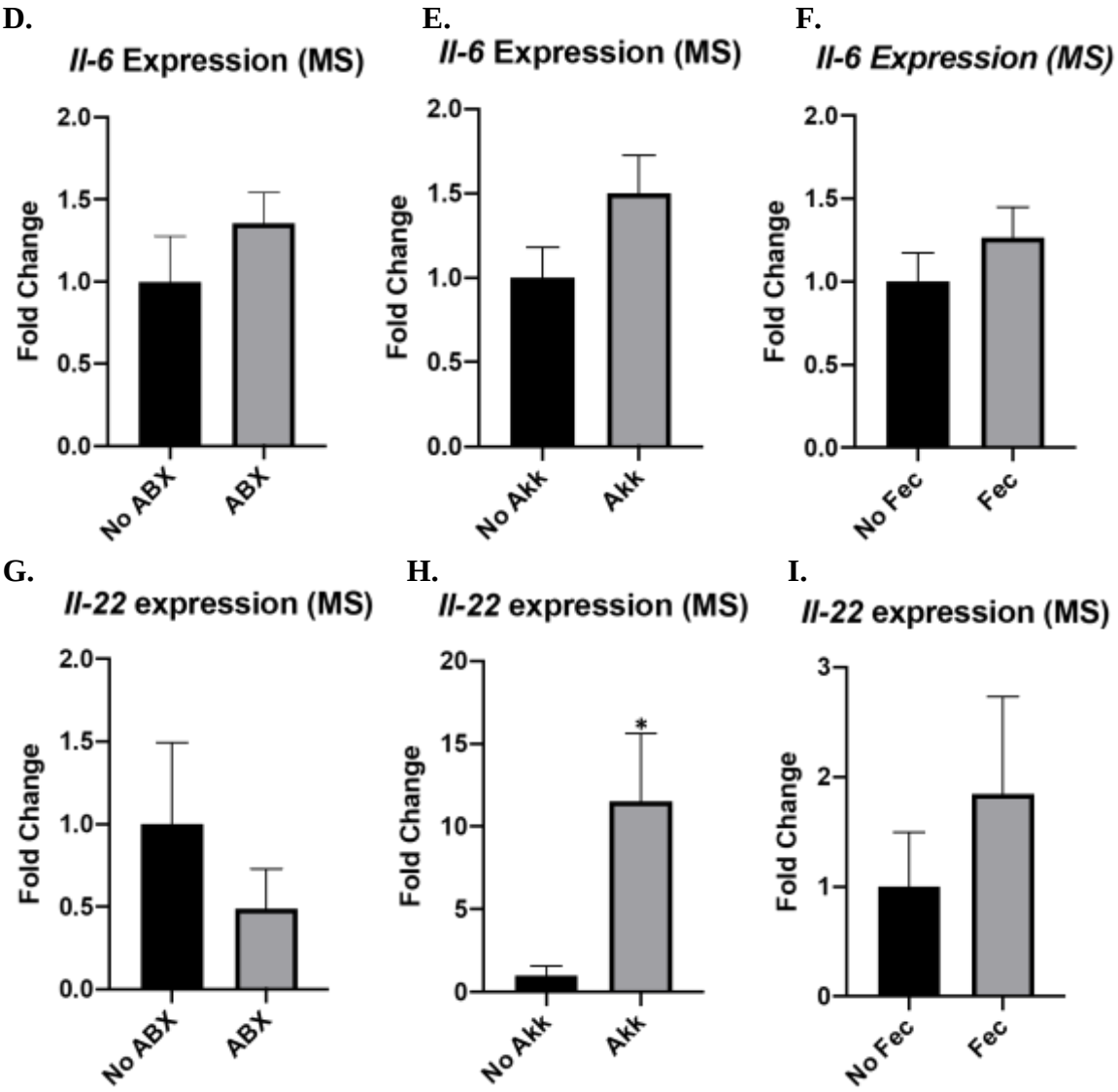

Figure IV.11 Continued.

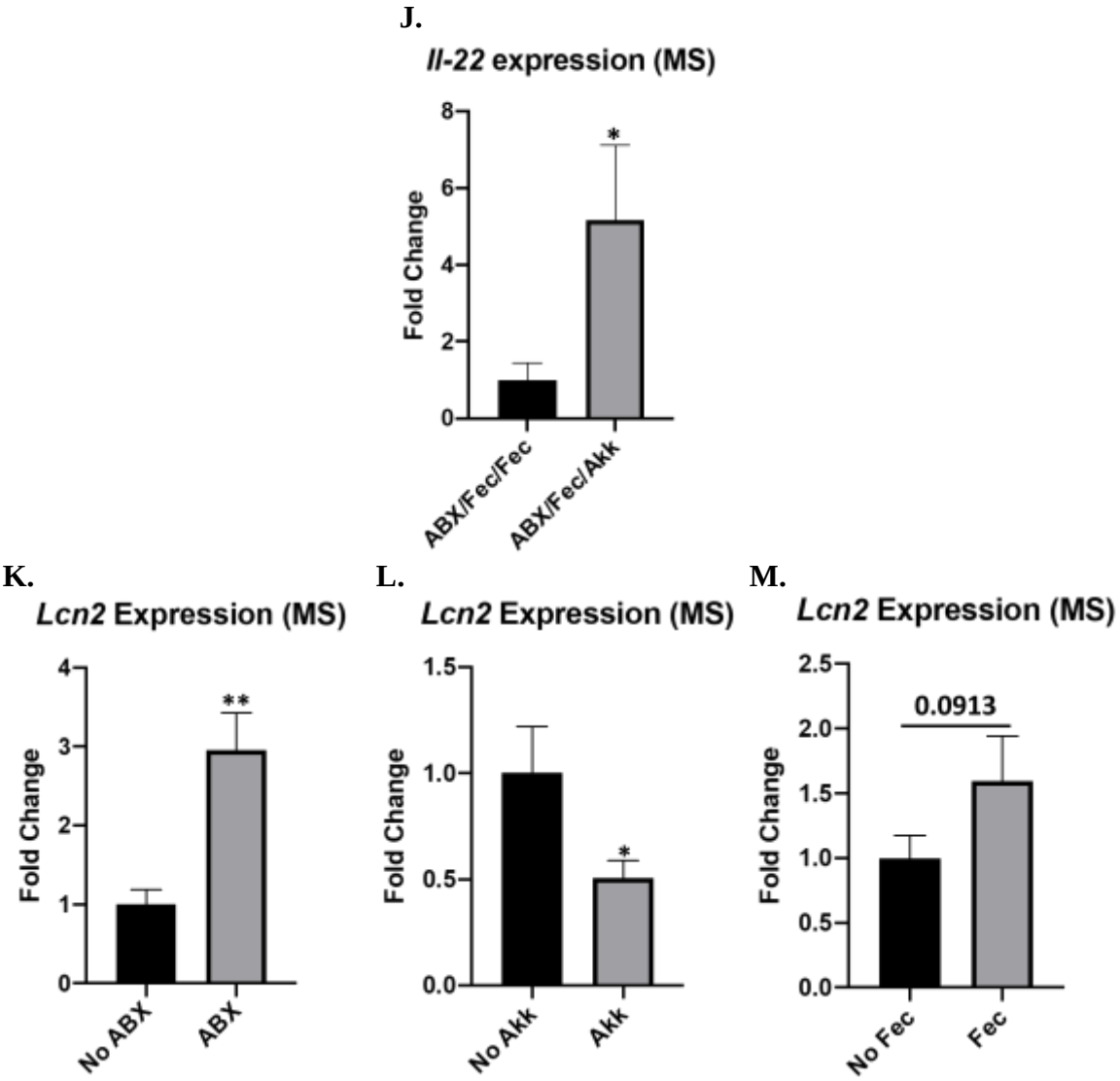

Figure IV.11 Continued.

Finally, to assess another aspect of gut barrier integrity, mucin production, rt-PCR was used to quantify the relative gene expression of Mucin-1 (*Muc1*), Mucin-2 (*Muc2*), and the ratio of *Muc1/Muc2*. No significant differences were found between the relative expressions of *Muc1* (Figure IV.12A, ANOVA p=0.4148, n=9-10 animals/group) or *Muc2* (Figure IV.12B, ANOVA p=0.3042, n=6-7 animals/group)

when comparing all 6 experimental groups. However, several trends were observed when comparing the *Muc1/Muc2* relative gene expression ratio (Figure IV.12C, ANOVA p=0.0506, n=7-10 animals/group); animals that received *A. muciniphila* after antibiotic treatment displayed an increased trend in *Muc1/Muc2* ratio compared to those that received *A. muciniphila* alone (Tukey's p=0.0500) or fecal transplant without *A. muciniphila* (Tukey's p=0.0663).

As interesting microbial changes were observed with each individual treatment, relative expression of tight junction protein genes were compared between any animals treated with either antibiotics, *A. muciniphila*, or fecal transplant and animals that did not receive those respective treatments. When comparing all animals that received each individual treatment compared to all animals that received their respective controls, no significant differences in *Muc1* relative gene expression were quantified with antibiotic treatment (Figure IV.12D, MW p=0.6689, n=20, 40 animals), *A. muciniphila* treatment (Figure IV.12E, Mw p=0.3615, n=29, 28 animals), or fecal transplant (Figure IV.12F, MW p=0.6444, n=38, 19 animals) compared to their own vehicle treated control animals. Antibiotic treatment significantly reduced *Muc2* expression compared to vehicle treated mice (Figure IV.12G, t-test p=0.0253, n=20, 40 animals/group), while neither *A. muciniphila* (Figure IV.12H, t-test p=0.1569, n=27, 29 animals) or fecal transplant (Figure IV.12I, t-test p=0.1378, n=40, 20 animals) significantly impacted relative *Muc2* gene expression compared to their respective controls. Investigation of the *Muc1/Muc2* relative gene expression ratio within all animals that received each treatment compared to all animals that did not revealed no significant difference in

antibiotic treated animals (Figure IV.12J, MW $p=0.3119$, $n=11$, 21 animals), a significant decrease in *A. muciniphila* treated colons (Figure IV.12K, MW $p=0.0326$, $n=28$, 17 animals), and a significant increase in fecal transplant recipients (Figure IV.12L, MW $p<0.0001$, $n=17$, 18 animals).

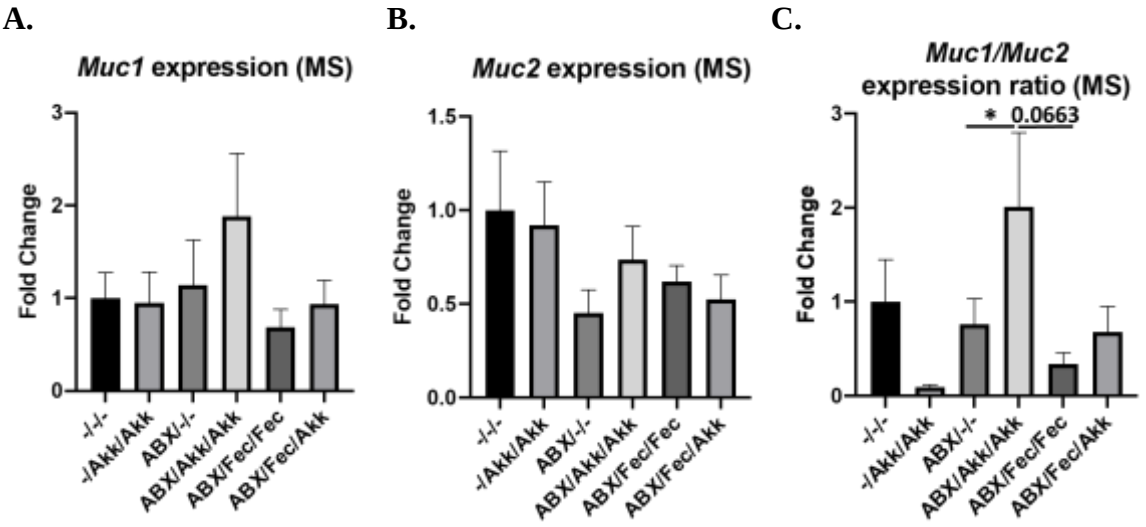

Figure IV.12 Relative Gene Expression of *Muc-1*, *Muc-2*, and the *Muc-1/Muc-2* ratio in Colonic Mucosal Scrapings. Fold changes were calculated using the ddCT method. A. Relative *Muc-1* gene expression in experimental groups (ANOVA p=0.4148, n=9-10 animals/group). B. Relative *Muc-2* gene expression in experimental groups (ANOVA p=0.3042, n=6-7 animals/group). C. The relative *Muc-1/Muc-2* gene expression ratio in experimental groups (ANOVA p=0.0506, n=7-10 animals/group). D. Relative *Muc-1* gene expression in antibiotic treated animals (MW p=0.6689, n=20, 40 animals). E. Relative *Muc-1* gene expression in *A. muciniphila* treated animals (MW p=0.3615, n=29, 28 animals). F. Relative *Muc-1* gene expression in fecal transplant treated animals (MW p=0.6444, n=38, 19 animals). G. Relative *Muc-2* gene expression in antibiotic treated animals (t-test p=0.0253, n=20, 40 animals). H. Relative *Muc-2* gene expression in *A. muciniphila* treated animals (t-test p=0.1569, n=27, 29 animals). I. Relative *Muc-2* gene expression in fecal transplant treated animals (t-test p=0.1378, n=40, 20 animals). J. The relative *Muc-1/Muc-2* gene expression ratio in antibiotic treated animals (MW p=0.3119, n=11, 21 animals). K. The relative *Muc-1/Muc-2* gene expression ratio in *A. muciniphila* treated animals (MW p=0.0326, n=28, 17 animals). L. The relative *Muc-1/Muc-2* gene expression ratio in fecal transplant treated animals (MW p<0.0001, n=17, 18 animals). Genes run in triplicate. Values are means ± SEM. Bars without a common letter differ significantly. * indicates p ≤ 0.05, ** indicates p ≤ 0.01, * indicates p ≤ 0.001, **** indicates p≤ 0.0001, and the absence of * indicates p-values >0.05. -, vehicle; ABX, antibiotics; Akk, *Akkermansia muciniphila*; Fec, fecal transplant; MS, mucosal scraping. No ABX consists of groups -/-/- and -/Akk/Akk, while ABX consists of ABX/-/-, ABX/Akk/Akk, ABX/Fec/Fec, and ABX/Fec/Akk Groups. No Akk consists of groups -/-/-, ABX/-/-, and ABX/Fec/Fec, while Akk consists of -/Akk/Akk, ABX/Akk/Akk, and ABX/Fec/Akk groups. No Fec consists of groups -/-/-, -/Akk/Akk, ABX/-/-, and ABX/Akk/Akk, while Fec consists of ABX/Fec/Fec and ABX/Fec/Akk groups.**

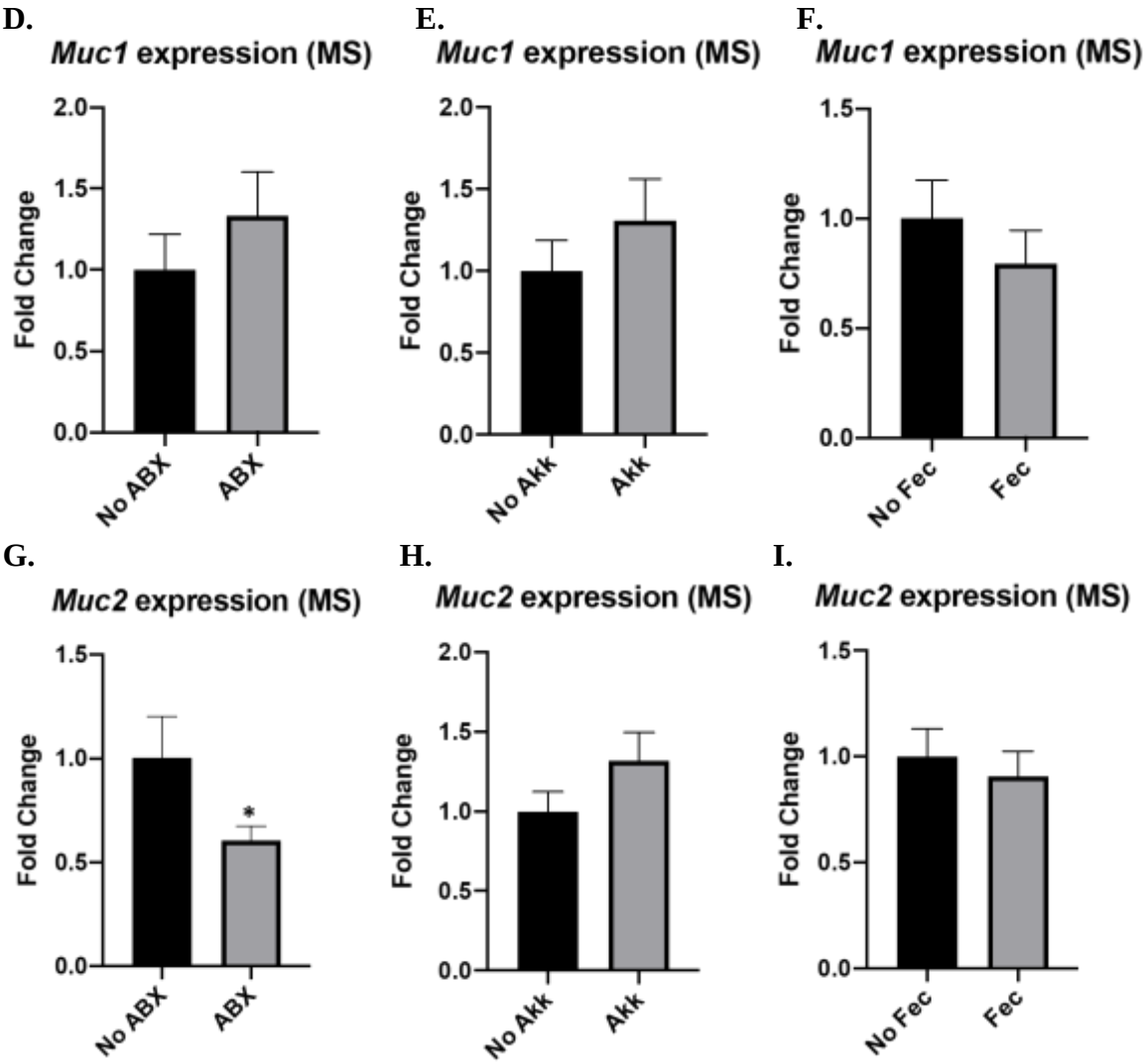

Figure IV.12 Continued.

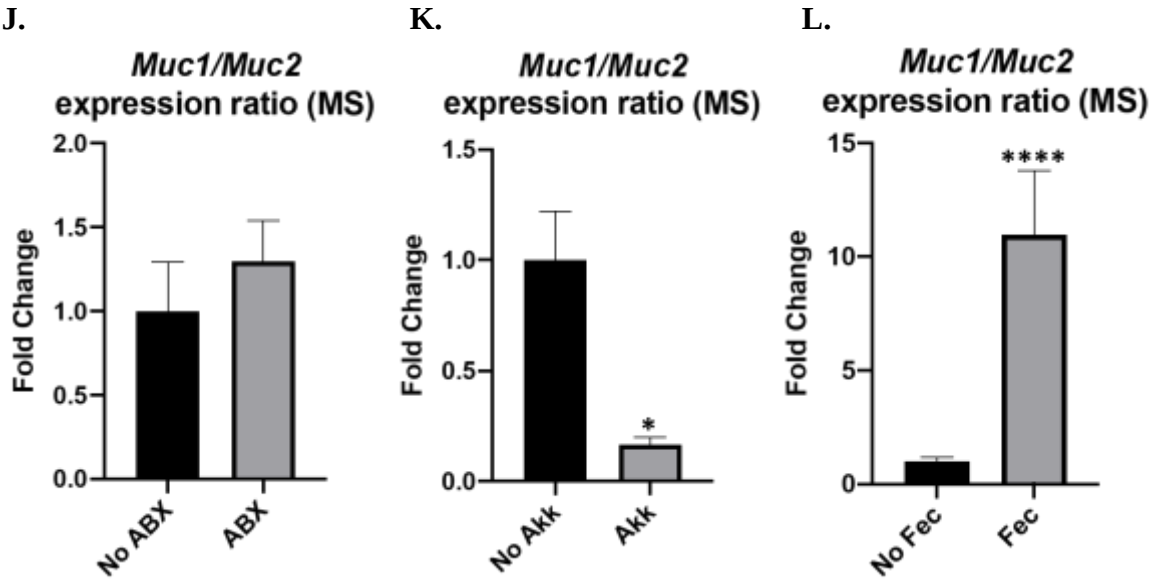

Figure IV.12 Continued.

Short Chain Fatty Acids

Concentrations of six SCFAs (acetic, butyric, isobutyric, isovaleric, propionic, and valeric acids) were quantified in feces using GC-MS. The averages of the sums of these concentrations are compared in Figure IV.12A. Antibiotic treatment with or without *A. muciniphila* treatment significantly reduced total SCFA concentration compared to *A. muciniphila* treatment alone or fecal transplant regardless of *A. muciniphila* gavage, but this reduction was not significant compared to vehicle treated control animals (Figure IV.13A, KW $p<0.0001$, n=8-10 animals/group). Acetic acid was significantly increased in animals that received fecal transplant alone compared to those that received vehicle alone, antibiotics alone, or antibiotics followed by *A. muciniphila* (Figure IV.13B, ANOVA $p=0.0005$, n=8-10 animals/group). Butyric acid was significantly reduced in the group that received only antibiotics compared to all other groups except for the group treated with antibiotics followed by *A. muciniphila* (Figure

IV.13C, ANOVA $p<0.0001$, n=8-10 animals/group). Significant differences were not noted between any groups in the concentrations of isobutyric (ANOVA $p=0.4940$, n=8-10 animals/group) or isovaleric (ANOVA $p=0.9176$, n=8-10 animals/group) acids (Figure IV.13D and E). Both propionic (Figure IV.13F, ANOVA $p<0.0001$, n=8-10 animals/group) and valeric (Figure IV.13G, ANOVA $p<0.0001$, n=8-10 animals/group) acids were significantly reduced in animals that received antibiotics with or without *A. muciniphila* compared to any group that did not receive antibiotics or fecal transplant, regardless of *A. muciniphila* treatment.

As a trend toward the increase of the concentration of several SCFAs was observed in the group treated with *A. muciniphila* following fecal transplant compared to the group that received fecal transplant alone, these concentrations were investigated in post hoc analyses. However, none of these increases were significant, including in an average of the sum of all SCFAs (data not shown, t-tests $p=0.3458$-0.8989, n=7-10 animals/group).

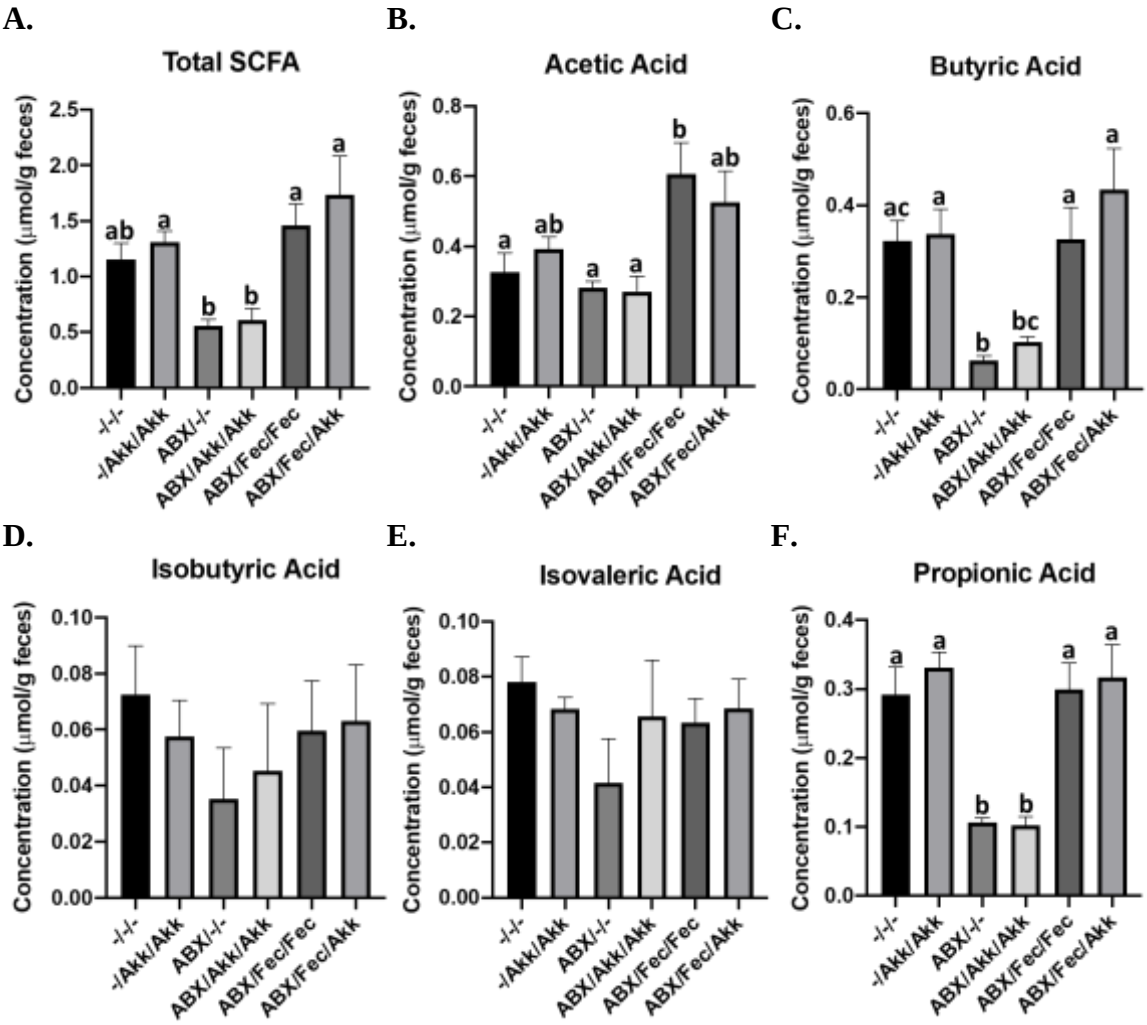

Figure IV.13 Concentrations of Short Chain Fatty Acids (SCFA) Termination in Micromoles per Gram of Feces. A. Average concentrations of total SCFA (KW p<0.0001). B. Average concentrations of acetic acid (ANOVA p=0.0005). C. Average concentrations of butyric acid (ANOVA p<0.0001). D. Average concentrations of isobutyric acid (ANOVA p=0.4940). E. Average concentrations of isovaleric acid (ANOVA p=0.9176). F. Average concentrations of propionic acid (ANOVA p<0.0001). G. Average concentrations of valeric acid (ANOVA p<0.0001). Each concentration was normalized to fecal sample weight and the d7-butyric acid spiked internal standard. n=8-10 animals/group. Means +/- SEM. Bars without a common letter differ significantly. -, vehicle; ABX, antibiotics; Akk, *Akkermansia muciniphila*; Fec, fecal transplant.

G.

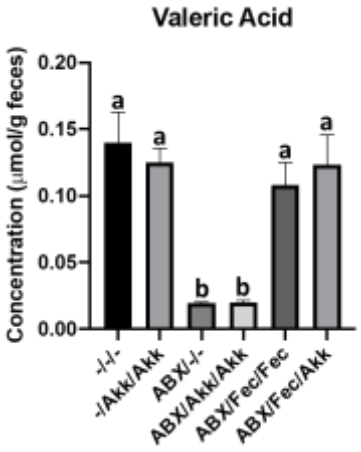

Figure IV.13 Continued.

Putative AhR Ligands Identified from Untargeted Metabolites Analysis

The metabolomic profile of feces collected for two days prior to termination was analyzed using LC-MS. Initial analysis focused on putative AhR ligands derived from aromatic amino acids, and 5 such metabolites were identified with reasonable certainty, including D-(+)-Tryptophan, 4-indolecarbaldehyde, 5-aminovaleric acid, indole-3-acetic acid, and indole-3-lactic acid. Both D-(+)-Tryptophan and 4-indolecarbaldehyde were significantly increased in animals treated with antibiotics alone and those that received fecal transplant followed by *A. muciniphila* compared to mice that only received vehicle (Figure IV.14A-B, ANOVA p=0.0020 and 0.0045, n=8-10 animals/group). 5-aminovaleric acid was increased in animals that receive antibiotics alone compared to vehicle treated controls and animals that received fecal transplant alone, however p-values for these comparisons are 0.0592 and 0.055, respectively (Figure IV.14C, ANOVA p=0.0117, n=7-10 animals/group). Similarly, indole-3-acetic acid was increased in antibiotic treated animals compared to vehicle treated controls, but the p-

value for this comparison was 0.058 in post hoc analysis and ANOVA p=0.0692 (Figure IV.14D, n=8-10 animals/group). No significant differences were observed between any groups in the relative intensities of indole-3-lactic acid (Figure IV.14E, ANOVA p=0.2160, n=9-10 animals/group).

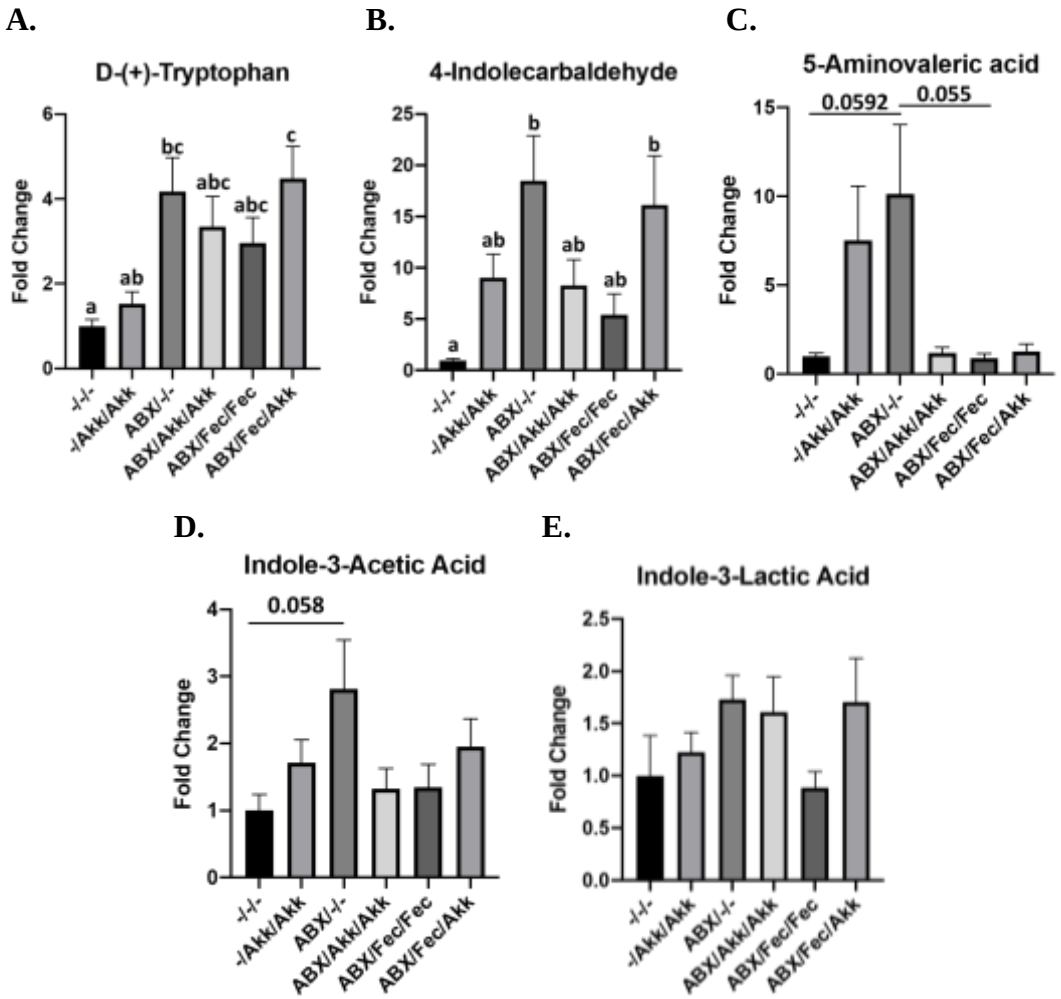

Figure IV.14 Relative Peak Intensities of Putative AhR Ligands in Feces at Termination. A. Relative intensities of D-(+)-Tryptophan (ANOVA p=0.0020). B. Relative intensities of 4-Indolecarbaldehyde (ANOVA p=0.0045). C. Relative intensities of 5-Aminovaleric acid (ANOVA p=0.0117). D. Relative intensities of Indole-3-acetic acid (ANOVA p=0.0692). E. Relative intensities of Indole-3-lactic acid (ANOVA p=0.2160). n=7-10 animals/group. Means +/- SEM. Bars without a common letter differ significantly. -, vehicle; ABX, antibiotics; Akk, *Akkermansia muciniphila*; Fec, fecal transplant.

As a trend toward the increase of the concentration of several metabolites was observed in the group treated with *A. muciniphila* following fecal transplant compared to the group that received fecal transplant alone, these concentrations were investigated in post hoc analyses. A trend toward increase of D-(+)-Tryptophan (Figure IV.15A, one-tailed t-test p=0.0664, n=10 animals/group) and indole-3-acetic acid (Figure IV.15D, one-tailed t-test p=0.0907, n=10 animals/group) was found in fecal transplanted animals that received *A. muciniphila* compared to those that did not. This increase was statistically significant in two of the 5 metabolites, 4-indolecarbaldehyde (Figure IV.15B, one-tailed t-test p=0.0327) and indole-3-lactic acid (Figure IV.15E, one-tailed t-test p=0.0487, n=9-10 animals/group), but not in 5-aminovaleric acid (Figure IV.15C, one-tailed t-test p=0.2200, n=8-9 animals/group).

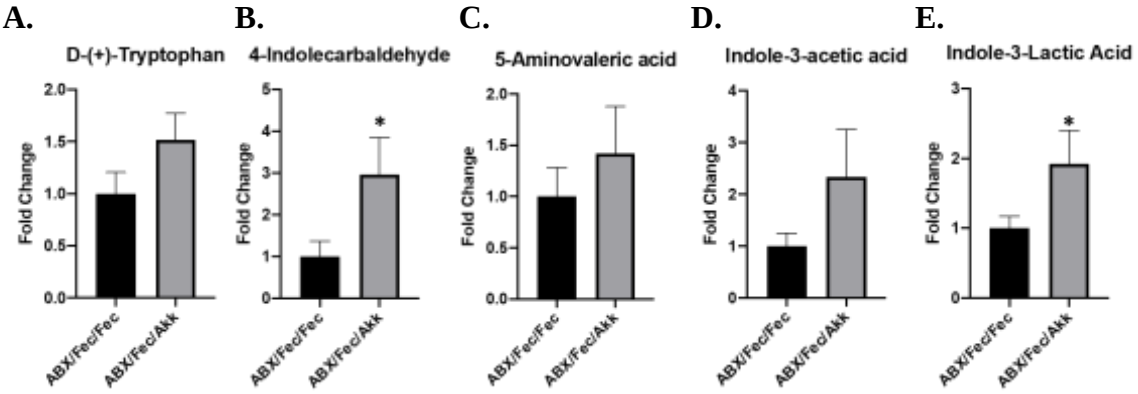

Figure IV.15 Relative Peak Intensities of Putative AhR Ligands in Feces at Termination in Fecal Transplant Groups with and without *Akkermansia muciniphila*. A. Relative intensities of D-(+)-Tryptophan (one-tailed t-test p=0.0664). B. Relative intensities of 4-Indolecarbaldehyde (one-tailed t-test p=0.0327). C. Relative intensities of 5-Aminovaleric acid (one-tailed t-test p=0.2200). D. Relative intensities of Indole-3-acetic acid (one-tailed t-test p=0.0907). E. Relative intensities of Indole-3-lactic acid (one-tailed t-test p=0.0487). n=8-10 animals/group. Means +/- SEM. Bars without a common letter differ significantly. * indicates p ≤ 0.05, ** indicates p ≤ 0.01, * indicates p ≤ 0.001, **** indicates p≤ 0.0001, and the absence of * indicates p-values >0.05. -, vehicle; ABX, antibiotics; Akk, *Akkermansia muciniphila*; Fec, fecal transplant.**

Discussion

The purpose of this research was to investigate the ability of *A. muciniphila* to rescue gut permeability, negative metabolite profiles, and pro-inflammatory changes associated with the dysbiotic gut microbial profile of $Ahr^{\Delta IEC}$ mice depleted in *A. muciniphila*. This hypothesis was tested by first depleting the gut microbiome overall and *Akkermansia* specifically in wild type animals as confirmed by qPCR analysis. Total bacterial depletion was similar to the results published in the studies from the Jobin group from which the antibiotic treatment protocols were adapted.[195,196] Feces depleted in *A. muciniphila* from $Ahr^{\Delta IEC}$ females were then transplanted into these controls once per week for three weeks before *A. muciniphila* gavage was subsequently administered once per week for three weeks.

Effects of an Increased Relative Abundance of Akkermansia following Antibiotic Treatment

Though antibiotic treatment alone reduced alpha diversity as expected,[208] the relative abundance of the phylum Verrucomicrobia was markedly increased at termination in animals that received antibiotics alone or *A. muciniphila* gavage following antibiotic treatment compared to animals that did not receive antibiotics or those that received fecal transplant. This unexpected result could be explained by a depletion in *Akkermansia* following antibiotic treatment, rather than a complete purge, as evidenced by qPCR analysis of this genus in the feces of mice on the sixth day of antibiotic treatment. Though *A. muciniphila* is generally associated with an improvement in gut microbial diversity,[209] reports exist of a bloom in *Akkermansia* spp. following antibiotic

exposure.[188] Due to the semi-quantitative nature of 16S rRNA sequencing data, it is possible that this marked increase in relative abundance is due to a decrease of other bacterial species rather than a bloom of *Akkermansia*. Therefore, a more thorough examination of the gut microbiome should be conducted in this study to confirm the microbial profiles posited by the 16S rRNA data. This could include investigating additional time points to determine when *Akkermansia* bloom occurs following antibiotic cessation, deeper sequencing techniques such as shotgun sequencing, or specific confirmation of *A. muciniphila* abundance data using more specific primers in qPCR.

Despite this unexpected result, this marked increase in the relative abundance of *Akkermansia* following antibiotic treatment, regardless of *A. muciniphila* gavage, allowed us to investigate the effects of an increase of *Akkermansia* in this model. Both of these treatment groups displayed improved gut barrier integrity compared to the fecal transplant groups, as measured by the concentration of FITC-labeled Dextran in the serum at termination. In concordance with this improvement in gut barrier integrity, an increase in *ZO-1* expression was observed in animals that received antibiotic treatment compared to those that did not receive antibiotics. Additionally, there was an increase of several putative AhR ligand MDAs in the group that received antibiotics alone compared to the vehicle alone group, including D-(+)-Tryptophan, 4-Indolecarbaldehyde, 5-Aminovaleric acid ($p=0.0592$), and Indole-3-Acetic acid ($p=0.0580$). This increase in putative AhR ligand MDAs and the corresponding increase in *ZO-1* expression could potentially be due to the increased relative abundance of the genus *Akkermansia* in the

antibiotic treated groups, regardless of *A. muciniphila* gavage. As AhR activation has been linked with the preservation of *ZO-1* expression via NOTCH-1 signaling in IECs following intestinal damage,[210] and dietary tryptophan supplementation has been shown to increase *ZO-1* expression in pig intestines,[211] a potential mechanism for improved gut barrier integrity in antibiotic treated groups could be due to the associated bloom of *Akkermansia*, increased MDAs in feces, and increased *ZO-1* expression compared to animals that did not receive antibiotics.

Interestingly, the concentrations of SCFAs butyric acid, propionic acid, and valeric acids and the total SCFA concentration were significantly reduced in antibiotic treated animals compared to either vehicle treated controls or fecal transplant recipients. Despite the increase in the relative abundance of *Akkermansia* in these groups, this is likely due to the decrease in alpha diversity in these groups. This is supported by the restoration of such diversity in fecal transplant recipients. It is possible that decreased *Muc2* and increased *Cldn2* expression in any antibiotic treated animals compared to animals that did not receive antibiotics could be due to the depletion of SCFAs as these compounds are known to regulate gut barrier integrity through mucin production and tight junction protein expression, irrespective of *A. muciniphila* gavage.[212,213] Furthermore, this decrease in SCFA could explain the observed decrease in mucus layer thickness that was observed in the antibiotic treated groups regardless of *A. muciniphila* gavage. Additionally, this decrease may be exacerbated by the increased relative abundance of *Akkermansia*, which is associated with the excessive and potentially harmful degradation of mucus under certain conditions.[214] The effects of increased

relative abundance of *Akkermansia* following antibiotic treatment is summarized in Figure IV.16A.

Effects Fecal Transplant

In another major finding, fecal transplant was successful, with both fecal transplanted groups, regardless of *A. muciniphila* gavage, clustering near each other and the donor 16S rRNA profile in the Bray-Curtis dissimilarity-based analysis of beta diversity. As hypothesized, fecal transplant, regardless of *A. muciniphila* gavage, made the gut more permeable, increased *Cldn-2* and decreased *Ocln* ($p=0.0592$) relative gene expression, and increased the *Muc1/Muc2* gene expression ratio compared to animals that did not receive fecal transplant. Due to the lack of increase in relative abundance in the group that received *A. muciniphila* gavage following fecal transplant, these results could be expected. However, interestingly, fecal transplant restored alpha diversity comparable to vehicle treated control animals versus the significantly lower alpha diversity found with antibiotic treatment alone. This restoration of alpha diversity likely resulted in the restoration of total SCFA concentration, as well as the specific concentrations of butyric, propionic, and valeric acids, which were restored to concentrations similar to that of the vehicle treated controls versus the significant reduction of these SCFAs in the antibiotic treated groups. It is unclear which microbes could be contributing to these changes, and additional deep sequencing and/or analysis of the genus level 16S rRNA microbiome data should be investigated to reconcile these findings. For example, many other species of gut bacteria are associated with SCFA production, including *Lactobacillus* and *Enterococcus* strains, *Roseburia* spp., and

Faecalibacterium prausnitzii.[215,216] The effects of fecal transplant from *Ahr*$^{\Delta IEC}$ mice into wild type animals are summarized in Figure IV.16B.

Effects of Akkermansia muciniphila Gavage following Fecal Transplant

Unexpectedly, gavage of *A. muciniphila* did not increase the relative abundance of the genus *Akkermansia* in any group relative to their respective control group. This resistance to colonization has been previously reported in both humans and mice with several probiotic strains, including *A. muciniphila*.[217,218] While is has been suggested that this resistance is predicated on the indigenous microbiome,[218] the mechanisms for this remain unknown, possibly due to competition with other bacteria for physical space or nutrients, quantity or timing of dose, or some other mechanism. However, the lack of increase in the relative abundance of *Akkermansia* was particularly unusual as several expected, beneficial effects associated with *A. muciniphila* were observed in the fecal transplant group that received *A. muciniphila* gavage compared to the group that received fecal transplant alone, including increased mucus layer thickness, increased relative *ZO-1* and *Il-22* expression, and increased AhR ligands produced from aromatic amino acids, including D-(+)-Tryptophan (one-tailed p=0.0664), 4-Indolecarbaldehyde, Indole-3-acetic acid (one-tailed p=0.0907), and Indole-3-Lactic acid. The increase in AhR ligands may at least partially explain the significant increases in *Il-22* expression and mucus layer thickness in this same comparison as metabolites derived from aromatic amino acids have been previously shown to activate AhR in ILC3s, resulting in increased IL-22 production by these cells, activation of STAT3 in IECs, and increased mucin production by IECs.[219–222]

One plausible explanation for the observed beneficial effects of *A. muciniphila* gavage without persistent colonization could be due to products of this species rather than colonization itself. Evidence suggests that the beneficial effects of *A. muciniphila* are not only associated with colonization by the bacteria itself, but by administration of the pasteurized bacteria, a membrane protein (Amuc_1100), or extracellular vesicles derived from the bacteria.[197,217,223] These findings support the hypothesis that administration of *A. muciniphila* without persistent colonization and therefore no increase in relative abundance could still have beneficial effects for the host. This is a promising finding as the culture and delivery of the strictly anaerobic *A. muciniphila* for therapeutic purposes is challenging. Conversely, an increase in gut permeability as measured by FITC-labeled Dextran in the serum of fecal transplant recipients and $Ahr^{\Delta IEC}$ donors was measured compared to vehicle treated wild type controls, but this increase was not rescued by *A. muciniphila* gavage. This was unexpected as *A. muciniphila* administration has been demonstrated to improve gut barrier integrity in Western diet and colitis-induced models of loss of gut barrier integrity.[224,225] However, three weeks of gavage or the lack of increase in relative abundance may not have been sufficient to improve permeability in our fecal transplant model that is likely less inflammatory compared to Western diet feeding or DSS-induced colitis. The effects of *A. muciniphila* gavage following fecal transplant is summarized in Figure IV.16C.

Additional Findings

Despite these unexpected findings in the relative abundances of *Akkermansia* in our model, interesting effects of antibiotic treatment, transplant of feces depleted of

Akkermansia, or *A. muciniphila* gavage were still observed. To further investigate if *A. muciniphila* gavage impacted any aspects of barrier integrity or inflammation, mucus layer thickness and mucin expression as well as expression of inflammatory genes and production of anti-inflammatory metabolites were measured. Mucus layer thickness was increased in fecal transplant recipients compared to all other groups regardless of *A. muciniphila* gavage. The mechanisms for this are unclear, but could be investigated by more closely examining additional changes in the gut microbial profile of fecal transplant groups compared to groups that did not receive antibiotics, as microbial species other than *A. muciniphila* are implicated in the stimulation of mucin production including *Bacteroides thetaiotaomicron* and *Faecalibacterium prausnitzii*,.[65] The ability of *A. muciniphila* administration to stimulate mucin production has been reported in the literature,[188,226,227] and, as expected, *A. muciniphila* gavage did increase inner mucus layer thickness in mice that did not receive antibiotics and in fecal transplant recipients compared to their respective control groups. *A. muciniphila* has also been shown to increase goblet cells in the intestines.[226,227] Though antibiotic treatment alone slightly reduced the percentage of goblet cells compared to groups that did not receive antibiotics, no other significant differences were observed. One plausible explanation is that mice were not gavaged with *A. muciniphila* for long enough to observe changes in cell differentiation and/or distribution in our model.

As the mucus layer is a major regulator of intestinal barrier integrity, the expression of two primary intestinal mucins was also probed in an effort to better understand changes in gut permeability. Few significant changes were observed in either

Muc1 or *Muc2* expression, though overall, antibiotic treatment did significantly decrease *Muc2* expression compared to any animal that did not receive antibiotics. As *Muc2* deficient mice have dysbiotic gut microbiomes compared to controls,[228] it is unclear if this relative reduction in *Muc2* expression is a cause or consequence of the altered microbial profiles in animals that received antibiotics. It has been previously reported that *Muc1* expression is increased in CRC samples from humans, and that a high *Muc1/Muc2* ratio indicated poor prognosis in those CRC patients.[229] When comparing the *Muc1/Muc2* expression ratio in the present study, fecal transplant significantly increased this ratio compared to vehicle treated controls, and *A. muciniphila* treatment did significantly reduce this ratio compared to animals that did not receive *A. muciniphila*. Furthermore, in support of the premise that *A. muciniphila* administration may not be beneficial in all contexts such as cases of lower alpha diversity, *A. muciniphila* gavage after antibiotic treatment tended to increase the relative *Muc1/Muc2* expression ratio compared to *A. muciniphila* gavage without antibiotic treatment or fecal transplant alone.

In an attempt to better characterize the differences observed in gut permeability, tight junction protein gene expression was measured as these complexes are another major factor in intestinal barrier integrity. Tight junctions are complex structures that include occludin, zonula-occludens, and claudin proteins.[4] As anticipated due to previously published studies,[223] *A. muciniphila* gavage in animals that did not receive antibiotics did increase *Ocln* expression compared to vehicle alone controls, suggesting that in some contexts, *A. muciniphila* can induce beneficial tight junction changes.

Furthermore, *A. muciniphila* gavage following fecal transplant did increase *ZO-1* expression, indicating that *A. muciniphila* may benefit some aspects of gut barrier integrity even in dysbiosis. While expression of *Ocln*, *ZO-1*, and most *Cldns* typically increases as gut barrier integrity increases, claudin-2 is specifically implicated in leaky gut and increases in IBD.[230] Relative *Cldn2* expression was increased in fecal transplant recipients, and *A. muciniphila* treatment after fecal transplant did not decrease this expression compared to fecal transplant alone. *A. muciniphila* gavage did not decrease *Cldn2* expression in animals not treated with antibiotics compared to their relative control group. This suggests that *A. muciniphila* gavage may not improve *Cldn2* expression. Interestingly, *A. muciniphila* gavage following antibiotic treatment significantly increased *Cldn2* expression compared to groups that did not receive antibiotics and had a trend toward increase in those that received antibiotics alone. This suggests that the overall microbial profile, in this case lower microbial diversity, can impact how *A. muciniphila* treatment effects tight junction protein expression in the host, which could have implications for CRC patients that have both decreased microbial diversity and an increase in relative abundance of *Akkermansia*.[190]

We also hypothesized that *A. muciniphila* would reduce inflammation in the colon and induce *IL-22* expression through the increased production of AhR ligands.[219–222] Even though it appears that gavaging *Akkermansia* did not result in colonization of the microbe, doing so in the absence of antibiotic treatment resulted in a significant increase in the relative gene expression of anti-inflammatory *Il-22* compared to vehicle treated control animals, or those that received antibiotics or fecal transplant alone.

Furthermore, increased *Il-22* expression was most prevalent in the group that received *A. muciniphila* gavage alone, even resulting in a trend toward increase compared to the groups that were gavaged with *A. muciniphila* following antibiotic treatment (p=0.0997). Furthermore, A. muciniphila gavage following fecal transplant significantly increased *Il-22* expression compared to fecal transplant alone. These results suggest that *A. muciniphila* gavage is more proficient at stimulating *Il-22* production in a gut microenvironment with a higher alpha diversity compared to one with fewer relative species of bacteria compared to the antibiotic treated groups. Conversely, no significant differences were observed in pro-inflammatory *IL-6* expression in our model. *IL-6* expression was relatively low, possibly due to the lack of strong inflammatory pressures on the large intestine 6 weeks after antibiotic treatment. Conversely, lipocalin-2, a more global measure of gut inflammation that is highly expressed in IBD[231] was significantly increased by antibiotic treatment and significantly reduced by *A. muciniphila* gavage compared to their respective vehicle treated animals. This may indicate that increased anti-inflammatory *Il-22* expression correlated with *A. muciniphila* gavage modulates host inflammation as measured by the significant reduction of a more global indicator such as lipocalin-2, compared to animals that received vehicle gavage.

Though *A. muciniphila* has been associated with reduced body weight in animal and human studies,[188] no significant difference in average body weight was observed between treatment groups at any time point in our study. While this could be due to the lack of persistent colonization of *Akkermansia* in our mice, this difference may also be diet related. The studies reported in the literature included obese human subjects or

animals on some combination of a high fat/high sucrose diet.[188,209] It is possible that the beneficial effects of *A. muciniphila* on body weight are more pronounced in cases where energy is in excess compared to normal weight, low fat diet fed animals as in our study. As body weight did not change significantly throughout the course of this study, findings can be viewed independently of body weight.

Conclusions

Findings of this chapter are summarized in Figure IV.16. This study is the first to show that transplant of dysbiotic feces from animals lacking AhR in IECs into wild type animals is sufficient to induce negative changes in gut barrier integrity due to decreased *Ocln* expression, increased *Cldn2* expression, and an increased *Muc1/Muc2* expression ratio, despite a restoration of SCFA and mucus layer thickness. Furthermore, *A. muciniphila* gavage did rescue some changes caused by this fecal transplant without persistent colonization, including increased mucus layer thickness, *Il-22* and *ZO-1* expression, and putative AhR ligand MDAs compared to fecal transplant alone. Finally, the blooming of *Akkermansia* in antibiotic treated groups correlated with increased barrier function, possibly due to an increase in putative AhR ligand MDAs and *ZO-1* expression. However, these changes may not be entirely beneficial as a decrease in SCFA concentration and increased relative abundance of *Akkermansia* likely contributed to a decrease in mucus layer thickness. Clearly, *A. muciniphila* plays a complex role in gut health and appears to be context dependent. However, the mechanisms by which *Ahr*$^{\Delta IEC}$ female mice fed a low fat diet consistently lose *A. muciniphila* are unclear and beyond the scope of this study. Future experiments should investigate potential

mechanisms for this shift as well as the rescue of negative gut permeability, metabolome, and inflammatory changes associated with the loss of AhR in IECs by other probiotic species.

A.

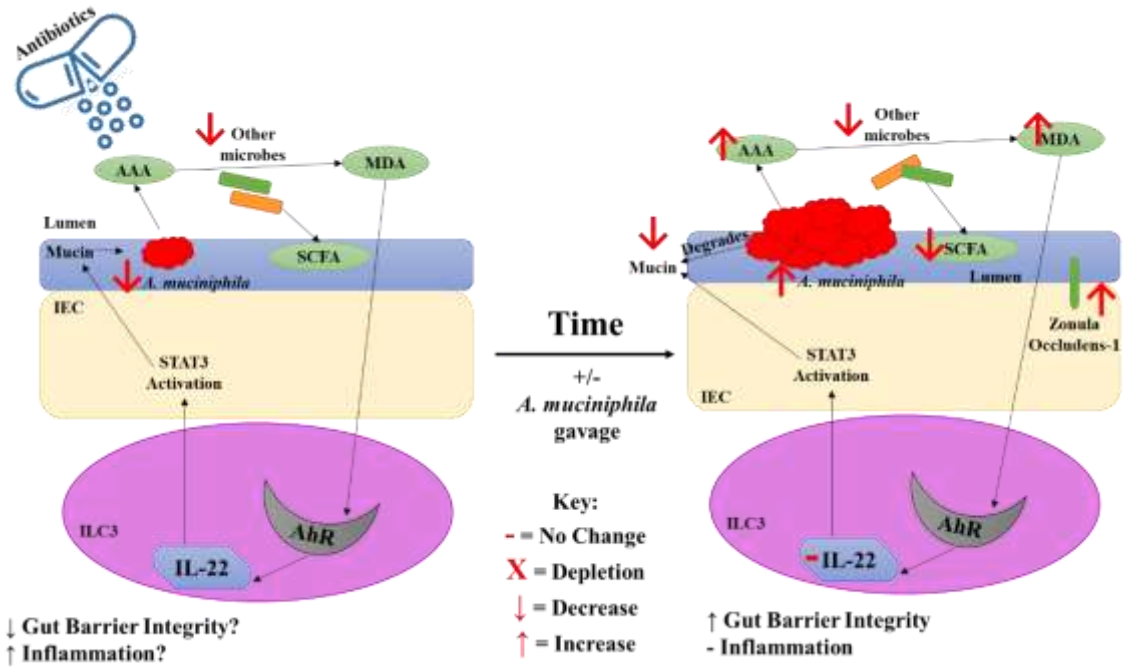

Figure IV.16 Effects of Antibiotic Treatment, Fecal Transplant from *Ahr*$^{\Delta IEC}$, and *Akkermansia muciniphila* in Wild-Type Mice on Gut Barrier Integrity, the Metabolome, and Colonic Inflammation. A. Effects of antibiotic treatment regardless of *A. muciniphila* gavage compared to other treatment groups. B. Overall effects of fecal transplant from *Ahr*$^{\Delta IEC}$ compared to other treatment groups. C. Effects of *A. muciniphila* gavage following fecal transplant from *Ahr*$^{\Delta IEC}$ compared to fecal transplant alone. AAA, Aromatic Amino Acids; AhR, Aryl Hydrocarbon Receptor; *Ahr*$^{\Delta IEC}$, Aryl Hydrocarbon Receptor Intestinal Epithelial Cell Specific Knock-Out; IEC, Intestinal Epithelial Cell; IL-22, Interleukin-22; ILC3, Innate Lymphoid Cells Type 3; MDA, Microbial Metabolites Derived from Aromatic Amino Acids; SCFA, Short Chain Fatty Acids.

B.

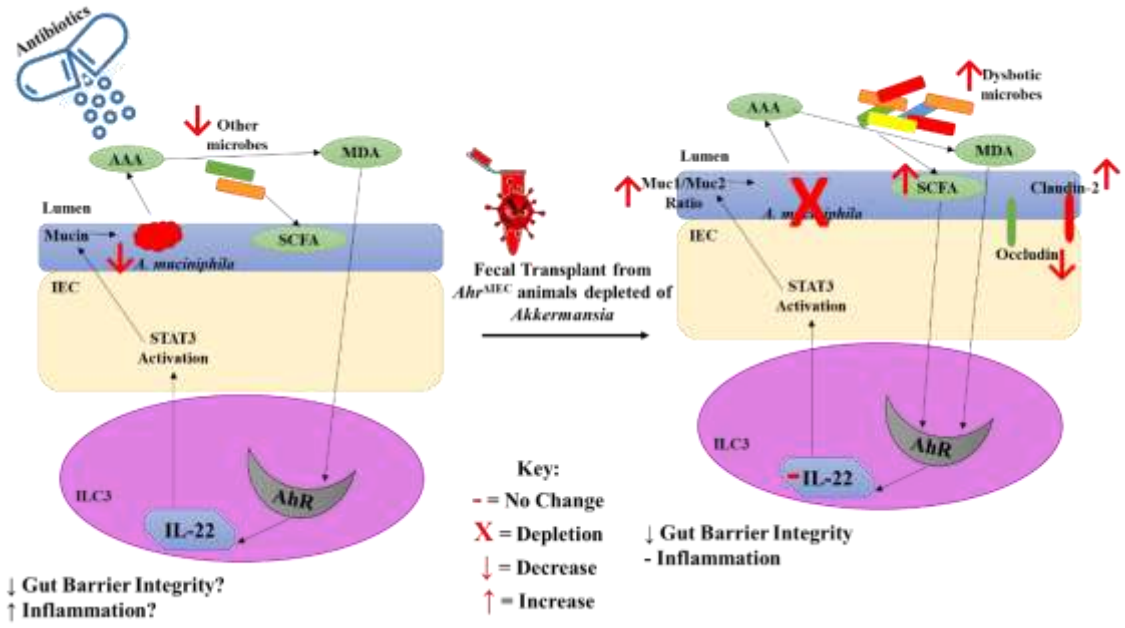

C.

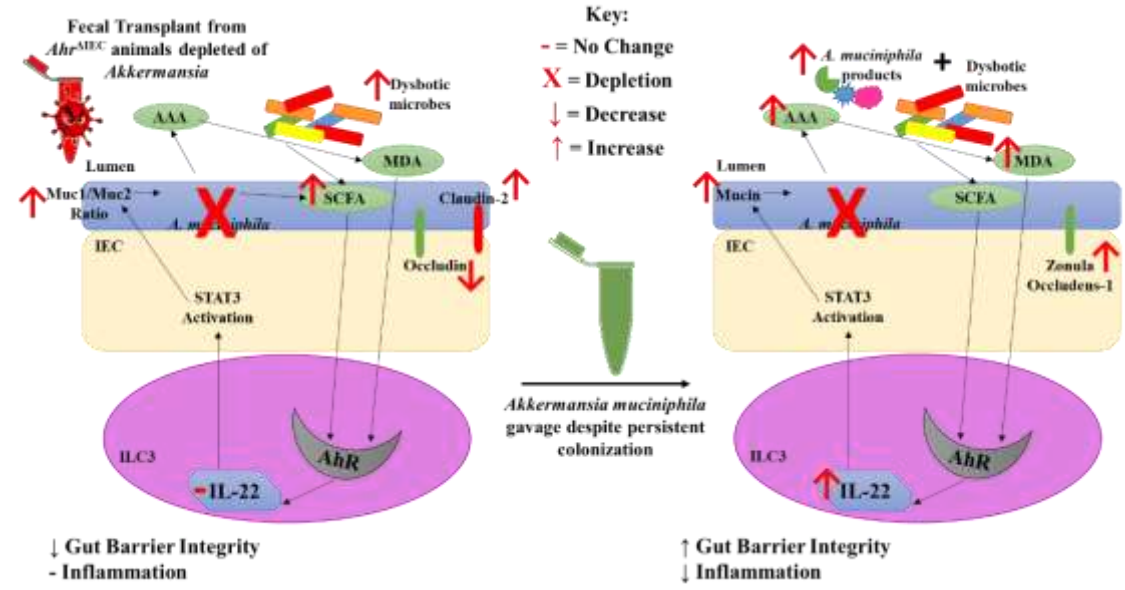

Figure IV.16 Continued.

CHAPTER V

CONCLUSIONS

The Duality of Nuclear Receptors in Colon Health

Context, Ligand, and Timing Dependent

It is widely accepted that the outcomes of nuclear receptor signaling are highly dependent upon several factors, including cell and tissue type, ligand activity, timing of activation, and environmental context. This is true for ERs, including ERβ that is generally considered beneficial in the prevention of cancer, but recent evidence suggests that idea is too simplistic.[232] Additionally, AhR activation has been implicated in tumor promotion and appears to be highly ligand and tissue dependent.[233]

The Role of the Gut Microbiome

The gut microbiome and host nuclear receptor signaling clearly interact to impact each other through various metabolites produced by each.[234] Though there has been an explosion of research regarding the human microbiome in recent years, many questions remain unanswered. Therefore, work such as that presented in this dissertation is vital to understanding the role of the gut microbiome and its metabolites in the context of host nuclear receptor signaling to drive the development of methods to prevent, slow, and treat intestinal diseases including IBDs and CRC.

Significance

Novel Findings

Several novel and important findings are presented in this dissertation. Chapter 2 includes results that are the first to show that BPA can negatively impact amino acid

metabolism by the gut microbiota in a way that has been associated with IBD. Additionally, this is the first evidence that the inhibition of recovery following DSS-induced colitis could be mediated through ERs as ICI blocks the reduction of non-transformed mouse colonocytes when co-treated with BPA versus BPA treatment alone. In the case of AhR, Chapter 3 demonstrates for the first time that the content of saturated fat in the diet, even if fed only during the peri-initiation period, as well as lack of AhR activity in IECs, are implicated in an increase in the multiplicity of and nuclear β-catenin in colon masses. Finally, Chapter 4 includes evidence that a dysbiotic fecal transplant from a genetically modified animal, in this case $Ahr^{\Delta IEC}$, can exacerbate gut permeability and inflammation in the colon, and that the administration of a specific bacterial species, *Akkermansia muciniphila*, can improve some measures of gut permeability and inflammation following fecal transplant. Additionally, the bloom of the genus *Akkermansia* in antibiotic treated groups that did not receive fecal transplant, though unexpected, does support the hypothesized ability of *Akkermansia muciniphila* to improve gut barrier integrity, degrade mucin, and produce putative AhR ligands derived from aromatic amino acids.

Relevance

IBD incidence is highest in industrialized nations and is increasing in developing countries, suggesting that as the world becomes more industrialized, alterations in environmental exposures influence the development of IBD.[235] Increasing IBD incidence is a concerning trend as treatment is lifelong and often requires surgery and because colitis is a risk factor for developing CRC.[6,7,10] Worldwide, CRC is the third leading

cancer diagnosis and the fourth leading cause of cancer mortality.[18] Though CRC incidence and mortality rates are declining overall in the USA, these same rates are increasing in those 20 to 49 years of age, a concerning trend as routine screening is not recommended for this age group.[16,236,237] Prevention is an important method for addressing this trend, and understanding the mechanisms of IBD and CRC development are vital to preventing these conditions.

As the mechanisms are discovered by which NRs including ERs and AhR modulate physiology to impact disease development, these receptors become increasingly interesting as targets for drug treatment of those diseases. In fact, several drugs have already been designed that target ERs and are primarily used to treat breast cancers, including tamoxifen and other antiestrogens.[238] However, both ER subtypes, ERα and ERß are currently being investigated as novel preventative or therapeutic targets in other cancers, including CRC.[239–241] Additionally, several new classes of AhR modulators have been developed that could provide therapeutic benefits for AhR related diseases.[242] Studies such as those described here help to elucidate the role of specific NRs in modulating host physiology, the gut microbiome and metabolome, and therefore preventing IBDs and CRC, furthering the ability to target them at various stages of disease development.

Furthermore, the human microbiome has been linked with many diseases, such as obesity, IBD, infectious diseases, and cancers.[243] Though particular alterations of the gut microbiome has been implicated in IBDs and CRC, such as an increase in pathogens or decreased microbial diversity, the effects of specific species remain to be fully

determined.[243] The manipulation of the gut microbiome through diet, antibiotics, or transplantation provides a method to improve the gut metabolome to prevent gastrointestinal diseases.[243] The elucidation of the mechanisms by which the gut microbiome, metabolome, and host physiology interact is vital to determining recommendations to beneficially alter the microbiome to improve health outcomes.

Future Directions

The impact of host nuclear receptor signaling including ERs and AhR on host gut health is clear. Therefore, future research should investigate host colon ER signaling and gut microbial changes associated with low dose exposures to BPA as well as methods to mediate these impacts, as BPA exposure is ubiquitous and unlikely to disappear. AhR's role in intestinal epithelial cells should continue to be probed in the context of a diet high in saturated fat for a longer duration. Furthermore, additional research is needed to elucidate how the loss of AhR in IECs results in a dysbiotic gut microbial profile and how such dysbioses can be rescued through the administration of single probiotic strains or combinations of probiotics and/or prebiotics.

REFERENCES

1. Azzouz LL, Sharma S. *Physiology, Large Intestine*. StatPearls Publishing; 2018.
2. Canny GO, McCormick BA. Bacteria in the intestine, helpful residents or enemies from within? *Infect Immun*. 2008;76(8):3360-3373. doi:10.1128/IAI.00187-08
3. Vancamelbeke M, Vermeire S. The intestinal barrier: a fundamental role in health and disease. *Expert Rev Gastroenterol Hepatol*. 2017;11(9):821-834. doi:10.1080/17474124.2017.1343143
4. Kayama H, Okumura R, Takeda K. Interaction between the Microbiota, Epithelia, and Immune Cells in the Intestine. *Annu Rev Immunol*. 2020;38:23-48. doi:10.1146/annurev-immunol-070119-115104
5. Frolkis A, Dieleman LA, Barkema HW, et al. Environment and the inflammatory bowel diseases. *Can J Gastroenterol*. 2013;27(3):e18-24.
6. Legaki E, Gazouli M. Influence of environmental factors in the development of inflammatory bowel diseases. *World J Gastrointest Pharmacol Ther*. 2016;7(1):112. doi:10.4292/wjgpt.v7.i1.112
7. Martin T, Chan S, Hart A. Environmental factors in the relapse and recurrence of inflammatory bowel disease: A review of the literature. *Dig Dis Sci*. 2015;60(5):1396-1405. doi:10.1007/s10620-014-3437-3
8. Jin J. Inflammatory bowel disease. *JAMA - J Am Med Assoc*. 2014;311(19):2034. doi:10.1001/jama.2014.1664
9. Ananthakrishnan AN, Kaplan GG, Ng SC. Changing Global Epidemiology of Inflammatory Bowel Diseases: Sustaining Health Care Delivery Into the 21st

Century. *Clin Gastroenterol Hepatol*. 2020;18(6):1252-1260. doi:10.1016/j.cgh.2020.01.028

10. Molodecky N, Kaplan G. Environmental risk factors for inflammatory bowel disease. *Gastroenterol Hepatol (N Y)*. 2010;6(5):339-346. doi:10.1007/s10620-014-3350-9
11. Loftus E, MacIntosh D, Fardy J, et al. Clinical epidemiology of inflammatory bowel disease: incidence, prevalence, and environmental influences. *Gastroenterology*. 2004;126(6):1504-1517. doi:10.1053/j.gastro.2004.01.063
12. Khalili H, Higuchi LM, Ananthakrishnan AN, et al. Hormone therapy increases risk of ulcerative colitis but not Crohn's disease. *Gastroenterology*. 2012;143(5):1199-1206. doi:10.1053/j.gastro.2012.07.096
13. Cornish JA, Tan E, Simillis C, Clark SK, Teare J, Tekkis PP. The Risk of Oral Contraceptives in the Etiology of Inflammatory Bowel Disease: A Meta-Analysis. *Am J Gastroenterol*. 2008;103(9):2394-2400. doi:10.1111/j.1572-0241.2008.02064.x
14. Cutolo M, Capellino S, Sullia A, et al. Estrogens and Autoimmune Diseases. *Ann N Y Acad Sci*. 2006;1089(1):538-547. doi:10.1196/annals.1386.043
15. Zelinkova Z, Woude CJ van der. Gender and Inflammatory Bowel Disease. *J Clin Cell Immunol*. 2014;05(04). doi:10.4172/2155-9899.1000245
16. Siegel RL, Miller KD, Fedewa SA, et al. Colorectal cancer statistics, 2017. *CA Cancer J Clin*. 2017;67(3):177-193. doi:10.3322/caac.21395
17. Rustgi AK. The genetics of hereditary colon cancer. *Genes Dev*.

2007;21(20):2525-2538. doi:10.1101/gad.1593107

18. Brenner H, Kloor M, Pox CP. Colorectal cancer. *Lancet*. 2014;383(9927):1490-1502. doi:10.1016/S0140-6736(13)61649-9

19. Terzi J, Grivennikov S, Karin E, Karin M. Inflammation and Colon Cancer. *YGAST*. 138:2101-2114.e5. doi:10.1053/j.gastro.2010.01.058

20. Munteanu I, Mastalier B. Genetics of colorectal cancer. *J Med Life*. 2014;7(4):507-511. doi:10.1016/b978-0-12-091075-5.50016-0

21. Song M, Chan AT, Sun J. Influence of the Gut Microbiome, Diet, and Environment on Risk of Colorectal Cancer. *Gastroenterology*. 2020;158(2):322-340. doi:10.1053/j.gastro.2019.06.048

22. S. Ranhotra H. Gut Microbiota and Host Nuclear Receptors Signalling. *Nucl Recept Res*. 2017;4. doi:10.11131/2017/101316

23. Robinson-Rechavi M, Escriva Garcia H, Laudet V. The nuclear receptor superfamily. *J Cell Sci*. 2003;116(Pt 4):585-586. doi:10.1242/JCS.00247

24. Levin ER, Hammes SR. Nuclear receptors outside the nucleus: extranuclear signalling by steroid receptors. *Nat Rev Mol Cell Biol*. 2016;17(12):783-797. doi:10.1038/nrm.2016.122

25. Beischlag T V, Luis Morales J, Hollingshead BD, Perdew GH. The aryl hydrocarbon receptor complex and the control of gene expression. *Crit Rev Eukaryot Gene Expr*. 2008;18(3):207-250.

26. Cui J, Shen Y, Li R. Estrogen synthesis and signaling pathways during aging: From periphery to brain. *Trends Mol Med*. 2013;19(3):197-209.

doi:10.1016/j.molmed.2012.12.007

27. Santen RJ, Simpson E. History of Estrogen: Its Purification, Structure, Synthesis, Biologic Actions, and Clinical Implications. *Endocrinology*. 2019;160(3):605-625. doi:10.1210/en.2018-00529

28. Kuiper GGJM, Enmark E, Pelto-Huikko M, Nilsson S, Gustafsson JÅ. Cloning of a novel estrogen receptor expressed in rat prostate and ovary. *Proc Natl Acad Sci U S A*. 1996;93(12):5925-5930. doi:10.1073/pnas.93.12.5925

29. Heldring N, Pike A, Andersson S, et al. Estrogen receptors: How do they signal and what are their targets. *Physiol Rev*. 2007;87(3):905-931. doi:10.1152/physrev.00026.2006

30. Yaşar P, Ayaz G, User SD, Güpür G, Muyan M. Molecular mechanism of estrogen-estrogen receptor signaling. *Reprod Med Biol*. 2017;16(1):4-20. doi:10.1002/rmb2.12006

31. Williams C, DiLeo A, Niv Y, Gustafsson J-Å. Estrogen receptor beta as target for colorectal cancer prevention. *Cancer Lett*. 2016;372(1):48-56. doi:10.1016/j.canlet.2015.12.009

32. Straub RH. The Complex Role of Estrogens in Inflammation. *Endocr Rev*. 2007;28(5):521-574. doi:10.1210/er.2007-0001

33. Koehler KF, Helguero LA, Haldosén LA, Warner M, Gustafsson JÅ. Reflections on the discovery and significance of estrogen receptor β. *Endocr Rev*. 2005;26(3):465-478. doi:10.1210/er.2004-0027

34. Principi M, Barone M, Pricci M, et al. Ulcerative colitis: from inflammation to

cancer. Do estrogen receptors have a role? *World J Gastroenterol*. 2014;20(33):11496-11504. doi:10.3748/wjg.v20.i33.11496

35. Antoni L, Nuding S, Wehkamp J, Stange EF. Intestinal barrier in inflammatory bowel disease. *World J Gastroenterol*. 2014;20(5):1165-1179. doi:10.3748/wjg.v20.i5.1165

36. Braniste V, Leveque M, Buisson-Brenac C, Bueno L, Fioramonti J, Houdeau E. Oestradiol decreases colonic permeability through oestrogen receptor β-mediated up-regulation of occludin and junctional adhesion molecule-A in epithelial cells. *J Physiol*. 2009;587(13):3317-3328. doi:10.1113/jphysiol.2009.169300

37. Caiazza F, Ryan EJ, Doherty G, Winter DC, Sheahan K. Estrogen receptors and their implications in colorectal carcinogenesis. *Front Oncol*. 2015;5:19. doi:10.3389/fonc.2015.00019

38. Armstrong C, Billimek A, Allred K, Sturino J, Weeks B, Allred C. A novel shift in estrogen receptor expression occurs as estradiol suppresses inflammation-associated colon tumor formation. *Endocr Relat Cancer*. 2013;20(4):515-525. doi:10.1530/ERC-12-0308

39. Stevens EA, Mezrich JD, Bradfield CA. The aryl hydrocarbon receptor: a perspective on potential roles in the immune system. *Immunology*. 2009;127(3):299-311. doi:10.1111/j.1365-2567.2009.03054.x

40. Poland A, Glover E, Kende AS, Decamp M, Giandomenico CM. 3,4,3′,4′-tetrachloro azoxybenzene and azobenzene: Potent inducers of aryl hydrocarbon hydroxylase. *Science (80-).* 1976;194(4265):627-630.

doi:10.1126/science.136041

41. Busbee PB, Rouse M, Nagarkatti M, Nagarkatti PS. Use of natural AhR ligands as potential therapeutic modalities against inflammatory disorders. *Nutr Rev*. 2013;71(6):353-369. doi:10.1111/nure.12024

42. Xie G, Raufman J-P. Role of the Aryl Hydrocarbon Receptor in Colon Neoplasia. *Cancers (Basel)*. 2015;7(3):1436-1446. doi:10.3390/cancers7030847

43. Poland A, Palen D, Glover E. Analysis of the four alleles of the murine aryl hydrocarbon receptor. *Mol Pharmacol*. 1994;46(5).

44. Kerley-Hamilton JS, Trask HW, Ridley CJA, et al. Obesity is mediated by differential aryl hydrocarbon receptor signaling in mice fed a western diet. *Environ Health Perspect*. 2012;120(9):1252-1259. doi:10.1289/ehp.1205003

45. Takamura T, Harama D, Matsuoka S, et al. Activation of the aryl hydrocarbon receptor pathway may ameliorate dextran sodium sulfate-induced colitis in mice. *Immunol Cell Biol*. 2010;88(6):685-689. doi:10.1038/icb.2010.35

46. Benson JM, Shepherd DM. Aryl hydrocarbon receptor activation by TCDD reduces inflammation associated with Crohn's disease. *Toxicol Sci*. 2011;120(1):68-78. doi:10.1093/toxsci/kfq360

47. Díaz-Díaz CJ, Ronnekleiv-Kelly SM, Nukaya M, et al. The Aryl Hydrocarbon Receptor is a Repressor of Inflammation-associated Colorectal Tumorigenesis in Mouse. *Ann Surg*. 2016;264(3):429-436. doi:10.1097/SLA.0000000000001874

48. Kawajiri K, Kobayashi Y, Ohtake F, et al. Aryl hydrocarbon receptor suppresses intestinal carcinogenesis in ApcMin/+ mice with natural ligands. *Proc Natl Acad*

Sci. 2009;106(32):13481-13486. doi:10.1073/pnas.0902132106

49. Islam J, Sato S, Watanabe K, et al. Dietary tryptophan alleviates dextran sodium sulfate-induced colitis through aryl hydrocarbon receptor in mice. *J Nutr Biochem*. 2017;42:43-50. doi:10.1016/j.jnutbio.2016.12.019

50. Donaldson GP, Lee SM, Mazmanian SK. Gut biogeography of the bacterial microbiota. *Nat Rev Microbiol*. 2015;14(1):20-32. doi:10.1038/nrmicro3552

51. Jandhyala SM, Talukdar R, Subramanyam C, Vuyyuru H, Sasikala M, Reddy DN. Role of the normal gut microbiota. *World J Gastroenterol*. 2015;21(29):8836-8847. doi:10.3748/wjg.v21.i29.8787

52. Ríos-Covián D, Ruas-Madiedo P, Margolles A, Gueimonde M, De los Reyes-Gavilán CG, Salazar N. Intestinal short chain fatty acids and their link with diet and human health. *Front Microbiol*. 2016;7(FEB):185. doi:10.3389/fmicb.2016.00185

53. He L, Prodhan MAI, Yuan F, et al. Simultaneous quantification of straight-chain and branched-chain short chain fatty acids by gas chromatography mass spectrometry. *J Chromatogr B Anal Technol Biomed Life Sci*. 2018;1092:359-367. doi:10.1016/j.jchromb.2018.06.028

54. Han Q, Phillips RS, Li J. Editorial: Aromatic amino acid metabolism. *Front Mol Biosci*. 2019;6(APR). doi:10.3389/fmolb.2019.00022

55. Parthasarathy A, Cross PJ, Dobson RCJ, Adams LE, Savka MA, Hudson AO. A Three-Ring circus: Metabolism of the three proteogenic aromatic amino acids and their role in the health of plants and animals. *Front Mol Biosci*. 2018;5(APR):29.

doi:10.3389/fmolb.2018.00029

56. Dehhaghi M, Kazemi Shariat Panahi H, Guillemin GJ. Microorganisms, Tryptophan Metabolism, and Kynurenine Pathway: A Complex Interconnected Loop Influencing Human Health Status. *Int J Tryptophan Res*. 2019;12. doi:10.1177/1178646919852996

57. Agus A, Planchais J, Sokol H. Gut Microbiota Regulation of Tryptophan Metabolism in Health and Disease. *Cell Host Microbe*. 2018;23(6):716-724. doi:10.1016/j.chom.2018.05.003

58. Costedio MM, Hyman N, Mawe GM. Serotonin and its role in colonic function and in gastrointestinal disorders. *Dis Colon Rectum*. 2007;50(3):376-388. doi:10.1007/s10350-006-0763-3

59. Yoshii K, Hosomi K, Sawane K, Kunisawa J. Metabolism of dietary and microbial vitamin b family in the regulation of host immunity. *Front Nutr*. 2019;6:48. doi:10.3389/fnut.2019.00048

60. Corrêa TAF, Rogero MM, Hassimotto NMA, Lajolo FM. The Two-Way Polyphenols-Microbiota Interactions and Their Effects on Obesity and Related Metabolic Diseases. *Front Nutr*. 2019;6:188. doi:10.3389/fnut.2019.00188

61. Koppel N, Rekdal VM, Balskus EP. Chemical transformation of xenobiotics by the human gut microbiota. *Science (80-)*. 2017;356(6344):1246-1257. doi:10.1126/science.aag2770

62. Pellock SJ, Redinbo MR. Glucuronides in the gut: Sugar-driven symbioses between microbe and host. *J Biol Chem*. 2017;292(21):8569-8576.

doi:10.1074/jbc.R116.767434

63. Megaraj V, Ding X, Fang C, Kovalchuk N, Zhu Y, Zhang QY. Role of hepatic and intestinal P450 enzymes in the metabolic activation of the colon carcinogen azoxymethane in mice. *Chem Res Toxicol*. 2014;27(4):656-662. doi:10.1021/tx4004769

64. Ansaldo E, Slayden LC, Ching KL, et al. Akkermansia muciniphila induces intestinal adaptive immune responses during homeostasis. *Science (80-).* 2019;364(6446):1179-1184. doi:10.1126/science.aaw7479

65. Alam A, Neish A. Role of gut microbiota in intestinal wound healing and barrier function. *Tissue Barriers*. 2018;6(3). doi:10.1080/21688370.2018.1539595

66. Hasan N, Yang H. Factors affecting the composition of the gut microbiota, and its modulation. *PeerJ*. 2019;2019(8). doi:10.7717/peerj.7502

67. Rothschild D, Weissbrod O, Barkan E, et al. Environment dominates over host genetics in shaping human gut microbiota. *Nature*. 2018;555(7695):210-215. doi:10.1038/nature25973

68. Conlon MA, Bird AR. The impact of diet and lifestyle on gut microbiota and human health. *Nutrients*. 2014;7(1):17-44. doi:10.3390/nu7010017

69. Nicholson JK, Holmes E, Kinross J, et al. Host-gut microbiota metabolic interactions. *Science*. 2012;336(6086):1262-1267. doi:10.1126/science.1223813

70. Rooks MG, Garrett WS. Gut microbiota, metabolites and host immunity. *Nat Rev Immunol*. 2016;16(6):341-352. doi:10.1038/nri.2016.42

71. Wong SH, Yu J. Gut microbiota in colorectal cancer: mechanisms of action and

clinical applications. *Nat Rev Gastroenterol Hepatol*. 2019;16(11):690-704. doi:10.1038/s41575-019-0209-8

72. Scott AJ, Alexander JL, Merrifield CA, et al. International Cancer Microbiome Consortium consensus statement on the role of the human microbiome in carcinogenesis. *Gut*. 2019;68(9):1624-1632. doi:10.1136/gutjnl-2019-318556

73. Garrett WS. The gut microbiota and colon cancer. *Science (80-).* 2019;364(6446):1133-1135. doi:10.1126/science.aaw2367

74. Zuo T, Ng SC. The Gut Microbiota in the Pathogenesis and Therapeutics of Inflammatory bowel disease. *Front Microbiol*. 2018;9(SEP):2247. doi:10.3389/fmicb.2018.02247

75. Eckburg PB, Bik EM, Bernstein CN, et al. Microbiology: Diversity of the human intestinal microbial flora. *Science (80-).* 2005;308(5728):1635-1638. doi:10.1126/science.1110591

76. Michałowicz J. Bisphenol A - Sources, toxicity and biotransformation. *Environ Toxicol Pharmacol*. 2014;37(2):738-758. doi:10.1016/j.etap.2014.02.003

77. Geens T, Aerts D, Berthot C, et al. A review of dietary and non-dietary exposure to bisphenol-A. *Food Chem Toxicol*. 2012;50(10):3725-3740. doi:10.1016/j.fct.2012.07.059

78. Vandenberg L, Hauser R, Marcus M, Olea N, Welshons W. Human exposure to bisphenol A (BPA). *Reprod Toxicol*. 2007;24(2):139-177. doi:10.1016/j.reprotox.2007.07.010

79. Calafat A, Ye X, Wong L, Reidy J, Needham L. Exposure of the U.S. population

to bisphenol A and 4-tertiary-octylphenol: 2003–2004. *Environ Health Perspect*. 2007;116(1):39-44. doi:10.1289/ehp.10753

80. Konieczna A, Rutkowska A, Rachoń D. Health risk of exposure to bisphenol A (BPA). *Rocz Panstw Zakl Hig*. 2015;66(1):5-11.

81. United States Environmental Protection Agency, Office of Research and Development IRISD. *Bisphenol A; CASRN 80-05-7.*; 1988.

82. Braniste V, Jouault A, Gaultier E, et al. Impact of oral bisphenol A at reference doses on intestinal barrier function and sex differences after perinatal exposure in rats. *Proc Natl Acad Sci*. 2010;107(1):448-453. doi:10.1073/pnas.0907697107

83. Willhite C, Ball G, McLellan C. Derivation of a bisphenol a oral reference dose (RfD) and drinking-water equivalent concentration. *J Toxicol Environ Heal Part B*. 2008;11(2):69-146. doi:10.1080/10937400701724303

84. Vandenberg L, Colborn T, Hayes T, et al. Hormones and endocrine-disrupting chemicals: Low-dose effects and nonmonotonic dose responses. *Endocr Rev*. 2012;33(3):378-455. doi:10.1210/er.2011-1050

85. Acconcia F, Pallottini V, Marino M. Molecular mechanisms of action of BPA. *Dose Response*. 2015;13(4).

86. Weige C, Allred K, Allred C. Estradiol alters cell growth in nonmalignant colonocytes and reduces the formation of preneoplastic lesions in the colon. *Cancer Res*. 2009;69(23):9118-9124. doi:10.1158/0008-5472.CAN-09-2348

87. Brinkmeyer-Langford C, Rodrigues A, Kochan K, et al. Consequences of perinatal bisphenol A exposure in a mouse model of multiple sclerosis.

Autoimmunity. 2014;47(1):57-66. doi:10.3109/08916934.2013.832220

88. Lai K, Chung Y, Li R, Wan H, Wong CK. Bisphenol A alters gut microbiome: Comparative metagenomics analysis. *Environ Pollut*. 2016;218:923-930. doi:10.1016/j.envpol.2016.08.039

89. Le Gall G, Noor S, Ridgway K, et al. Metabolomics of fecal extracts detects altered metabolic activity of gut microbiota in ulcerative colitis and irritable bowel syndrome. *J Proteome Res*. 2011;10(9):4208-4218. doi:10.1021/pr2003598

90. Coates M, Mahoney C, Linden D, et al. Molecular defects in mucosal serotonin content and decreased serotonin reuptake transporter in ulcerative colitis and irritable bowel syndrome. *Gastroenterology*. 2004;126(7):1657-1664. doi:10.1053/j.gastro.2004.03.013

91. Roy A, Gaylo A, Cao W, Saubermann L, Lawrence B. Neither direct nor developmental exposure to bisphenol A alters the severity of experimental inflammatory colitis in mice. *J Immunotoxicol*. 2013;10(4):334-340. doi:10.3109/1547691X.2012.747231

92. Armstrong C, Allred K, Weeks B, Chapkin R, Allred C. Estradiol has differential effects on acute colonic inflammation in the presence and absence of estrogen receptor β expression. *Dig Dis Sci*. 2017;62(8):1977-1984. doi:10.1007/s10620-017-4631-x

93. Verdú E, Deng Y, Bercik P, Collins S. Modulatory effects of estrogen in two murine models of experimental colitis. *Am J Physiol - Gastrointest Liver Physiol*. 2002;283(1):G27-G36. doi:10.1152/ajpgi.00460.2001

94. Cook L, Hillhouse A, Myles M, et al. The role of estrogen signaling in a mouse model of inflammatory bowel disease: A Helicobacter hepaticus model. *PLoS One*. 2014;9(4):e94209. doi:10.1371/journal.pone.0094209

95. Singh N, Gurav A, Sivaprakasam S, et al. Activation of Gpr109a, receptor for niacin and the commensal metabolite butyrate, suppresses colonic inflammation and carcinogenesis. *Immunity*. 2014;40(1):128-139. doi:10.1016/j.immuni.2013.12.007

96. Murthy S, Cooper H, Shim H, Shah R, Ibrahim S, Sedergran D. Treatment of dextran sulfate sodium-induced murine colitis by intracolonic cyclosporin. *Dig Dis Sci*. 1993;38(9):1722-1734. doi:10.1007/BF01303184

97. Sridharan G, Choi K, Klemashevich C, et al. Prediction and quantification of bioactive microbiota metabolites in the mouse gut. *Nat Commun*. 2014;5:5492. doi:10.1038/ncomms6492

98. Whitfield-Cargile C, Cohen N, Chapkin R, et al. The microbiota-derived metabolite indole decreases mucosal inflammation and injury in a murine model of NSAID enteropathy. *Gut Microbes*. 2016;7(3):246-261. doi:10.1080/19490976.2016.1156827

99. Ju YH, Carlson KE, Sun J, et al. Estrogenic effects of extracts from cabbage, fermented cabbage, and acidified brussels sprouts on growth and gene expression of estrogen-dependent human breast cancer (MCF-7) cells. *J Agric Food Chem*. 2000;48(10):4628-4634. doi:10.1021/jf000164z

100. Conover W, Iman R. Rank transformations as a bridge between parametric and

nonparametric statistics. *Am Stat*. 1981;35(3):124. doi:10.2307/2683975

101. Yan Y, Kolachala V, Dalmasso G, et al. Temporal and spatial analysis of clinical and molecular parameters in dextran sodium sulfate induced colitis. Bereswill S, ed. *PLoS One*. 2009;4(6):6073. doi:10.1371/journal.pone.0006073

102. Alex P, Zachos N, Nguyen T, et al. Distinct cytokine patterns identified from multiplex profiles of murine DSS and TNBS-induced colitis. *Inflamm Bowel Dis*. 2009;15(3):341-352. doi:10.1002/ibd.20753

103. Egger B, Bajaj-Elliott M, MacDonald T, Inglin R, Eysselein V, Büchler M. Characterisation of acute murine dextran sodium sulphate colitis: Cytokine profile and dose dependency. *Digestion*. 2000;62(4):240-248. doi:10.1159/000007822

104. Kim J, Shajib S, Manocha M, Khan W. Investigating intestinal inflammation in DSS-induced model of IBD. *J Vis Exp*. 2012;60:3678. doi:10.3791/3678

105. Yang Y, Hong Y, Oh S, et al. Bisphenol A exposure is associated with oxidative stress and inflammation in postmenopausal women. *Environ Res*. 2009;109(6):797-801. doi:10.1016/j.envres.2009.04.014

106. Savastano S, Tarantino G, D'Esposito V, et al. Bisphenol-A plasma levels are related to inflammatory markers, visceral obesity and insulin-resistance: A cross-sectional study on adult male population. *J Transl Med*. 2015;13:169. doi:10.1186/s12967-015-0532-y

107. Valentino R, D'Esposito V, Passaretti F, et al. Bisphenol-A impairs insulin action and up-regulates inflammatory pathways in human subcutaneous adipocytes and 3T3-L1 cells. Nadal A, ed. *PLoS One*. 2013;8(12):82099.

doi:10.1371/journal.pone.0082099

108. Yang M, Chen M, Wang J, et al. Bisphenol A promotes adiposity and inflammation in a nonmonotonic dose-response way in 5-week-old male and female C57BL/6J mice fed a low-calorie diet. *Endocrinology*. 2016;157(6):2333-2345. doi:10.1210/en.2015-1926

109. Roy A, Bauer S, Lawrence B. Developmental exposure to bisphenol A modulates innate but not adaptive immune responses to influenza A virus infection. *PLoS One*. 2012;7(6):38448. doi:10.1371/journal.pone.0038448

110. Waldner MJ, Neurath MF. Chemically induced mouse models of colitis. In: *Current Protocols in Pharmacology*. Vol 46. Hoboken, NJ, USA: John Wiley & Sons, Inc.; 2009:5.55.1-5.55.15. doi:10.1002/0471141755.ph0555s46

111. Chassaing B, Aitken J, Malleshappa M, Vijay-Kumar M. Dextran sulfate sodium (DSS)-induced colitis in mice. *Curr Protoc Immunol*. 2014;104:15.25.1-15.25.14. doi:10.1002/0471142735.im1525s104

112. Ikejima K, Enomoto N, Iimuro Y, et al. Estrogen increases sensitivity of hepatic Kupffer cells to endotoxin. *Am J Physiol*. 1998;274(4 Pt 1):G669-76.

113. Enomoto N, Yamashina S, Schemmer P, et al. Estriol sensitizes rat Kupffer cells via gut-derived endotoxin. *Am J Physiol*. 1999;277(3 Pt 1):G671-7.

114. Gkouskou K, Deligianni C, Tsatsanis C, Eliopoulos A. The gut microbiota in mouse models of inflammatory bowel disease. *Front Cell Infect Microbiol*. 2014;4:28. doi:10.3389/fcimb.2014.00028

115. Liu Y, Mei C, Liu H, et al. Modulation of cytokine expression in human

macrophages by endocrine-disrupting chemical bisphenol-A. *Biochem Biophys Res Commun*. 2014;451(4):592-598. doi:10.1016/J.BBRC.2014.08.031

116. Dambacher J, Beigel F, Seiderer J, et al. Interleukin 31 mediates MAP kinase and STAT1/3 activation in intestinal epithelial cells and its expression is upregulated in inflammatory bowel disease. *Gut*. 2007;56(9):1257-1265. doi:10.1136/gut.2006.118679

117. Heller F, Florian P, Bojarski C, et al. Interleukin-13 is the key effector Th2 cytokine in ulcerative colitis that affects epithelial tight junctions, apoptosis, and cell restitution. *Gastroenterology*. 2005;129:550-564. doi:10.1053/j.gastro.2005.05.002

118. Alkim C, Alkim H, Koksal A, Boga S, Sen I. Angiogenesis in inflammatory bowel disease. *Int J Inflam*. 2015;2015:970890. doi:10.1155/2015/970890

119. Chernoguz A, Crawford K, Vandersall A, et al. Pretreatment with anti-VEGF therapy may exacerbate inflammation in experimental acute colitis. *J Pediatr Surg*. 2012;47(2):347-354. doi:10.1016/j.jpedsurg.2011.11.028

120. Javurek A, Spollen W, Johnson S, et al. Effects of exposure to bisphenol A and ethinyl estradiol on the gut microbiota of parents and their offspring in a rodent model. *Gut Microbes*. 2016;7(6):471-485. doi:10.1080/19490976.2016.1234657

121. Bansal T, Alaniz R, Wood T, Jayaraman A. The bacterial signal indole increases epithelial-cell tight-junction resistance and attenuates indicators of inflammation. *Proc Natl Acad Sci*. 2010;107(1):228-233. doi:10.1073/pnas.0906112107

122. Nikolaus S, Schulte B, Al-Massad N, et al. Increased tryptophan metabolism is

associated With activity of inflammatory bowel diseases. *Gastroenterology*. 2017;153(6):1504-1516. doi:10.1053/j.gastro.2017.08.028

123. Zelante T, Iannitti R, Cunha C, et al. Tryptophan catabolites from microbiota engage aryl hydrocarbon receptor and balance mucosal reactivity via interleukin-22. *Immunity*. 2013;39(2):372-385. doi:10.1016/j.immuni.2013.08.003

124. Ghia J, Li N, Wang H, et al. Serotonin has a key role in pathogenesis of experimental colitis. *Gastroenterology*. 2009;137(5):1649-1660. doi:10.1053/j.gastro.2009.08.041

125. Ciorba M. Indoleamine 2,3 dioxygenase in intestinal disease. *Curr Opin Gastroenterol*. 2013;29(2):146-152. doi:10.1097/MOG.0b013e32835c9cb3

126. Spiller R. Recent advances in understanding the role of serotonin in gastrointestinal motility in functional bowel disorders: Alterations in 5-HT signalling and metabolism in human disease. *Neurogastroenterol Motil*. 2007;19(s2):25-31. doi:10.1111/j.1365-2982.2007.00965.x

127. Krishnan S, Ding Y, Saedi N, et al. Gut microbiota-derived tryptophan metabolites modulate inflammatory response in hepatocytes and macrophages. *Cell Rep*. 2018;23(4):1099-1111. doi:10.1016/j.celrep.2018.03.109

128. Xing J, Sun J, Sun J, et al. Protective effect of shikimic acid on acetic acid induced colitis in rats. *J Med Plants Res*. 2012;6(10):2011-2018. doi:10.5897/JMPR11.1748

129. Yoo G. *Influence of estradiol and phytoestrogens on colitis and colon cancer* [dissertation]. College Station, TX: Texas A&M University; 2015. Available

electronically from http://hdl.handle.net/1969.1/156457.

130. Jalal N, Surendranath AR, Pathak JL, Yu S, Chung CY. Bisphenol A (BPA) the mighty and the mutagenic. *Toxicol Reports*. 2018;5:76-84. doi:10.1016/j.toxrep.2017.12.013

131. Hill CE, Myers JP, Vandenberg LN. Nonmonotonic dose–Response curves occur in dose ranges that are relevant to regulatory decision-making. *Dose-Response*. 2018;16(3). doi:10.1177/1559325818798282

132. Gerona R, vom Saal FS, Hunt PA. BPA: have flawed analytical techniques compromised risk assessments? *Lancet Diabetes Endocrinol*. 2020;8(1):11-13. doi:10.1016/S2213-8587(19)30381-X

133. American Cancer Society. Key Statistics for Colorectal Cancer. https://www.cancer.org/cancer/colon-rectal-cancer/about/key-statistics.html. Published 2019. Accessed July 4, 2019.

134. Xie J. P. G. R. Role of the Aryl Hydrocarbon Receptor in Colon Neoplasia. *Cancers (Basel)*. 2015;7(3):1436-1446. doi:10.3390/cancers7030847

135. Marmol I, Sanchez-de-Diego C, Dieste AP, Cerrada E, Yoldi MJR. Colorectal Carcinoma: A General Overview and Future Perspectives in Colorectal Cancer. *Int J Mol Sci*. 2017;18(1):197. doi:http://dx.doi.org/10.3390/ijms18010197

136. Wargovich MJ, Brown VR, Morris J. Aberrant crypt foci: The case for inclusion as a biomarker for colon cancer. *Cancers (Basel)*. 2010;2(3):1705-1716. doi:10.3390/cancers2031705

137. Ruiz RB, Hernandez PS. Diet and cancer: Risk factors and epidemiological

evidence. *Maturitas*. 2014;77(3):202-208. doi:10.1016/J.MATURITAS.2013.11.010

138. Anand P, Kunnumakkara AB, Kunnumakara AB, et al. Cancer is a preventable disease that requires major lifestyle changes. *Pharm Res*. 2008;25(9):2097-2116. doi:10.1007/s11095-008-9661-9

139. DeClercq V, McMurray DN, Chapkin RS. Obesity promotes colonic stem cell expansion during cancer initiation. *Cancer Lett*. 2015;369(2):336-343. doi:10.1016/j.canlet.2015.10.001

140. Padidar S, Farquharson AJ, Williams LM, Kearney R, Arthur JR, Drew JE. High-fat diet alters gene expression in the liver and colon: links to increased development of aberrant crypt foci. *Dig Dis Sci*. 2012;57(7):1866-1874. doi:10.1007/s10620-012-2092-9

141. Kim E, Davidson LA, Zoh RS, et al. Homeostatic responses of colonic LGR5+ stem cells following acute in vivo exposure to a genotoxic carcinogen. *Carcinogenesis*. 2015;37(2):206-214. doi:10.1093/carcin/bgv250

142. Beyaz S, Mana MD, Roper J, et al. High-fat diet enhances stemness and tumorigenicity of intestinal progenitors. *Nature*. 2016;531(7592):53-58. doi:10.1038/nature17173

143. Penrose HM, Heller S, Cable C, et al. High-fat diet induced leptin and Wnt expression: RNA-sequencing and pathway analysis of mouse colonic tissue and tumors. *Carcinogenesis*. 2017;38(3):302-311. doi:10.1093/carcin/bgx001

144. Iain AM, Andrew DP, Gary HP. Aryl hydrocarbon receptor ligands in cancer:

friend and foe. *Nat Rev Cancer*. 2014;14(12):801-814. doi:10.1038/nrc3846

145. Ikuta T, Kurosumi M, Yatsuoka T, Nishimura Y. Tissue distribution of aryl hydrocarbon receptor in the intestine: Implication of putative roles in tumor suppression. *Exp Cell Res*. 2016;343(2):126-134. doi:10.1016/j.yexcr.2016.03.012

146. Kerley-hamilton JS, Trask HW, Ridley CJA, Dufour E, Ringelberg CS. Obesity Is Mediated by Differential Aryl Hydrocarbon Receptor Signaling in Mice Fed a Western Diet. 2012;1252(9):1252-1259. doi:10.1093/toxsci/kfs155

147. Metidji A, Omenetti S, Crotta S, et al. The Environmental Sensor AHR Protects from Inflammatory Damage by Maintaining Intestinal Stem Cell Homeostasis and Barrier Integrity. *Immunity*. August 2018. doi:10.1016/j.immuni.2018.07.010

148. Peng TL, Chen J, Mao W, et al. Potential therapeutic significance of increased expression of aryl hydrocarbon receptor in human gastric cancer. *World J Gastroenterol*. 2009;15(14):1719-1729. doi:10.3748/wjg.15.1719

149. Andersson P, McGuire J, Rubio C, et al. A constitutively active dioxin/aryl hydrocarbon receptor induces stomach tumors. *Proc Natl Acad Sci U S A*. 2002;99(15):9990-9995. doi:10.1073/pnas.152706299

150. Wang Q, Yang K, Han B, et al. Aryl hydrocarbon receptor inhibits inflammation in DSS-induced colitis via the MK2/p-MK2/TTP pathway. *Int J Mol Med*. 2017;41(2):868-876. doi:10.3892/ijmm.2017.3262

151. Biljes D, Hammerschmidt-kamper C, Merches K, Esser C. The Aryl Hydrocarbon Receptor In T Cells Contributes To Sustaining Oral Tolerance Against Ovalbumin In A Mouse Model. *EXCLI J*. 2017;16:291-301.

152. Walisser JA, Glover E, Pande K, Liss AL, Bradfield CA. Aryl hydrocarbon receptor-dependent liver development and hepatotoxicity are mediated by different cell types. *Pnas*. 2005;102(49):17858-17863. doi:10.1073/pnas.0504757102

153. The Jackson Laboratory. 006203 - STOCK Ahr/J. https://www.jax.org/strain/006203. Accessed October 17, 2017.

154. Walisser JA, Glover E, Pande K, Liss AL, Bradfield CA. Aryl hydrocarbon receptor-dependent liver development and hepatotoxicity are mediated by different cell types. *Proc Natl Acad Sci*. 2005;102(49):17858-17863. doi:10.1073/pnas.0504757102

155. Fan Y-Y, Davidson LA, Chapkin RS. Murine Colonic Organoid Culture System and Downstream Assay Applications. *Methods Mol Biol*. August 2016. doi:10.1007/7651_2016_8

156. Kim E, Davidson LA, Zoh RS, et al. Rapidly cycling Lgr5+stem cells are exquisitely sensitive to extrinsic dietary factors that modulate colon cancer risk. *Cell Death Dis*. 2016;7(11):e2460. doi:10.1038/cddis.2016.269

157. Fan YY, Monk JM, Hou TY, et al. Characterization of an arachidonic acid-deficient (Fads1 knockout) mouse model. *J Lipid Res*. 2012;53(7):1287-1295. doi:10.1194/jlr.M024216

158. Harrill JA, Hukkanen RR, Lawson M, et al. Knockout of the aryl hydrocarbon receptor results in distinct hepatic and renal phenotypes in rats and mice. *Toxicol Appl Pharmacol*. 2013;272(2):503-518. doi:10.1016/j.taap.2013.06.024

159. Kawajiri K, Fujii-Kuriyama Y. The aryl hydrocarbon receptor: a multifunctional chemical sensor for host defense and homeostatic maintenance. *Exp Anim*. 2017;66(2):75-89. doi:10.1538/expanim.16-0092

160. Velázquez KT, Enos RT, Carson MS, et al. Weight loss following diet-induced obesity does not alter colon tumorigenesis in the AOM mouse model. *Am J Physiol Liver Physiol*. 2016;311(4):G699-G712. doi:10.1152/ajpgi.00207.2016

161. Tuominen I, Al-Rabadi L, Stavrakis D, Karagiannides I, Pothoulakis C, Bugni JM. Diet-Induced Obesity Promotes Colon Tumor Development in Azoxymethane-Treated Mice. Sun J, ed. *PLoS One*. 2013;8(4):e60939. doi:10.1371/journal.pone.0060939

162. Díaz-Díaz CJ, Ronnekleiv-Kelly SM, Nukaya M, et al. The Aryl Hydrocarbon Receptor is a Repressor of Inflammation-associated Colorectal Tumorigenesis in Mouse. *Ann Surg*. 2016;264(3):429-436. doi:10.1097/SLA.0000000000001874

163. Saha S, Shaik M, Johnston G, et al. Tumor size predicts long-term survival in colon cancer: an analysis of the National Cancer Data Base. *Am J Surg*. 2015;209(3):570-574. doi:10.1016/j.amjsurg.2014.12.008

164. Sellin JH, Umar S, Xiao J, Morris AP. Increased beta-catenin expression and nuclear translocation accompany cellular hyperproliferation in vivo. *Cancer Res*. 2001;61(7):2899-2906.

165. Clevers H, Nusse R. Wnt/β-Catenin Signaling and Disease. *Cell*. 2012;149(6):1192-1205. doi:10.1016/J.CELL.2012.05.012

166. Zhang D, Fei F, Li S, et al. The role of β-catenin in the initiation and metastasis of

TA2 mice spontaneous breast cancer. *J Cancer*. 2017;8(11):2114-2123. doi:10.7150/jca.19723

167. De P, Carlson JH, Wu H, et al. Wnt-beta-catenin pathway signals metastasis-associated tumor cell phenotypes in triple negative breast cancers. *Oncotarget*. 2016;7(28):43124-43149. doi:10.18632/oncotarget.8988

168. Yang C-M, Ji S, Li Y, Fu L-Y, Jiang T, Meng F-D. β-Catenin promotes cell proliferation, migration, and invasion but induces apoptosis in renal cell carcinoma. *Onco Targets Ther*. 2017;10:711-724. doi:10.2147/OTT.S117933

169. Damsky WE, Curley DP, Santhanakrishnan M, et al. β-Catenin Signaling Controls Metastasis in Braf-Activated Pten-Deficient Melanomas. *Cancer Cell*. 2011;20(6):741-754. doi:10.1016/j.ccr.2011.10.030

170. Chen J, Huang X-F. High fat diet-induced obesity increases the formation of colon polyps induced by azoxymethane in mice. *Ann Transl Med*. 2015;3(6):79. doi:10.3978/j.issn.2305-5839.2015.03.46

171. Sikalidis AK, Fitch MD, Fleming SE. Diet induced obesity increases the risk of colonic tumorigenesis in mice. *Pathol Oncol Res*. 2013;19(4):657-666. doi:10.1007/s12253-013-9626-0

172. Day SD, Enos RT, McClellan JL, Steiner JL, Velázquez KT, Murphy EA. Linking inflammation to tumorigenesis in a mouse model of high-fat-diet-enhanced colon cancer. *Cytokine*. 2013;64(1):454-462. doi:10.1016/j.cyto.2013.04.031

173. Yang Y, Smith DL, Keating KD, Allison DB, Nagy TR. Variations in body

weight, food intake and body composition after long-term high-fat diet feeding in C57BL/6J mice. *Obesity*. 2014;22(10):2147-2155. doi:10.1002/oby.20811

174. Karunanithi S, Levi L, DeVecchio J, et al. RBP4-STRA6 Pathway Drives Cancer Stem Cell Maintenance and Mediates High-Fat Diet-Induced Colon Carcinogenesis. *Stem cell reports*. 2017;9(2):438-450. doi:10.1016/j.stemcr.2017.06.002

175. Doerner SK, Reis ES, Leung ES, et al. High-fat diet-induced complement activation 1 mediates intestinal inflammation and neoplasia, independent of obesity 2 3. 2016. doi:10.1158/1541-7786.MCR-16-0153

176. Zhang C, Zhang M, Pang X, Zhao Y, Wang L, Zhao L. Structural resilience of the gut microbiota in adult mice under high-fat dietary perturbations. *ISME J*. 2012;6(10). doi:10.1038/ismej.2012.27

177. Carmody RN, Gerber GK, Luevano JM, et al. Diet dominates host genotype in shaping the murine gut microbiota. *Cell Host Microbe*. 2015;17(1):72-84. doi:10.1016/j.chom.2014.11.010

178. Gao R, Gao Z, Huang L, Qin H. Gut microbiota and colorectal cancer. *Eur J Clin Microbiol Infect Dis*. 2017;36(5):757-769. doi:10.1007/s10096-016-2881-8

179. Gagnière J, Raisch J, Veziant J, et al. Gut microbiota imbalance and colorectal cancer. *World J Gastroenterol*. 2016;22(2):501-518. doi:10.3748/wjg.v22.i2.501

180. Lundberg R, Toft MF, August B, Hansen AK, Hansen CHF. Antibiotic-treated versus germ-free rodents for microbiota transplantation studies. *Gut Microbes*. 2016;7(1):68-74. doi:10.1080/19490976.2015.1127463

181. Staley C, Kaiser T, Beura LK, et al. Stable engraftment of human microbiota into mice with a single oral gavage following antibiotic conditioning. *Microbiome*. 2017;5(1):87. doi:10.1186/s40168-017-0306-2

182. Wong SH, Zhao L, Zhang X, et al. Gavage of Fecal Samples From Patients With Colorectal Cancer Promotes Intestinal Carcinogenesis in Germ-Free and Conventional Mice. *Gastroenterology*. 2017;153(6):1621-1633.e6. doi:10.1053/J.GASTRO.2017.08.022

183. Lamas B, Richard ML, Leducq V, et al. CARD9 impacts colitis by altering gut microbiota metabolism of tryptophan into aryl hydrocarbon receptor ligands. *Nat Med*. 2016;22(6):598-605. doi:10.1038/nm.4102

184. Murray IA, Nichols RG, Zhang L, Patterson AD, Perdew GH. Expression of the aryl hydrocarbon receptor contributes to the establishment of intestinal microbial community structure in mice. *Sci Rep*. 2016;6(1):33969. doi:10.1038/srep33969

185. Garcia-Villatoro EL, DeLuca JAA, Callaway ES, et al. Effects of high-fat diet and intestinal aryl hydrocarbon receptor deletion on colon carcinogenesis. *Am J Physiol - Gastrointest Liver Physiol*. 2020;318(3):G451-G463. doi:10.1152/ajpgi.00268.2019

186. Menon R, Garcia-Villatoro EL, Callaway ES, et al. Effect of Aryl Hydrocarbon Receptor Deletion and High Fat Diet on Fecal Microbiome and Inflammation. 2020:Submitted for Publication.

187. Derrien M, Vaughan EE, Plugge CM, de Vos WM. Akkermansia municiphila gen. nov., sp. nov., a human intestinal mucin-degrading bacterium. *Int J Syst Evol*

Microbiol. 2004;54(5):1469-1476. doi:10.1099/ijs.0.02873-0

188. Derrien M, Belzer C, de Vos WM. Akkermansia muciniphila and its role in regulating host functions. *Microb Pathog*. 2017;106:171-181. doi:10.1016/j.micpath.2016.02.005

189. Dingemanse C, Belzer C, Van Hijum SAFT, et al. Akkermansia muciniphila and Helicobacter typhlonius modulate intestinal tumor development in mice. *Carcinogenesis*. 2015;36(11):1388-1396. doi:10.1093/carcin/bgv120

190. Weir TL, Manter DK, Sheflin AM, Barnett BA, Heuberger AL, Ryan EP. Stool Microbiome and Metabolome Differences between Colorectal Cancer Patients and Healthy Adults. White BA, ed. *PLoS One*. 2013;8(8):e70803. doi:10.1371/journal.pone.0070803

191. Shin NR, Lee JC, Lee HY, et al. An increase in the Akkermansia spp. population induced by metformin treatment improves glucose homeostasis in diet-induced obese mice. *Gut*. 2014;63(5):727-735. doi:10.1136/gutjnl-2012-303839

192. Everard A, Belzer C, Geurts L, et al. Cross-talk between Akkermansia muciniphila and intestinal epithelium controls diet-induced obesity. *Proc Natl Acad Sci U S A*. 2013;110(22):9066-9071. doi:10.1073/pnas.1219451110

193. Gulhane M, Murray L, Lourie R, et al. High Fat Diets Induce Colonic Epithelial Cell Stress and Inflammation that is Reversed by IL-22. *Sci Rep*. 2016;6. doi:10.1038/srep28990

194. Kanehisa M, Goto S. *KEGG: Kyoto Encyclopedia of Genes and Genomes*. Vol 28.; 2000.

195. Sun X, Threadgill D, Jobin C. Campylobacter jejuni induces colitis through activation of mammalian target of rapamycin signaling. *Gastroenterology*. 2012;142(1):86. doi:10.1053/j.gastro.2011.09.042

196. Thomas RM, Gharaibeh RZ, Gauthier J, et al. Intestinal microbiota enhances pancreatic carcinogenesis in preclinical models. *Carcinogenesis*. 2018;39(8):1068-1078. doi:10.1093/carcin/bgy073

197. Plovier H, Everard A, Druart C, et al. A purified membrane protein from Akkermansia muciniphila or the pasteurized bacterium improves metabolism in obese and diabetic mice. *Nat Med*. 2017;23(1):107-113. doi:10.1038/nm.4236

198. Hasegawa Y, Mark Welch JL, Rossetti BJ, Borisy GG. Preservation of three-dimensional spatial structure in the gut microbiome. Mantis NJ, ed. *PLoS One*. 2017;12(11):e0188257. doi:10.1371/journal.pone.0188257

199. Kamphuis JBJ, Mercier-Bonin M, Eutamène H, Theodorou V. Mucus organisation is shaped by colonic content; A new view. *Sci Rep*. 2017;7(1):1-13. doi:10.1038/s41598-017-08938-3

200. Zhang LC, Wang Y, Tong LC, et al. Berberine alleviates dextran sodium sulfate-induced colitis by improving intestinal barrier function and reducing inflammation and oxidative stress. *Exp Ther Med*. 2017;13(6):3374-3382. doi:10.3892/etm.2017.4402

201. Gupta J, delBarcoBarrantes I, Igea A, et al. Dual Function of p38α MAPK in Colon Cancer: Suppression of Colitis-Associated Tumor Initiation but Requirement for Cancer Cell Survival. *Cancer Cell*. 2014;25(4):484-500.

doi:10.1016/j.ccr.2014.02.019

202. Demehri FR, Frykman PK, Cheng Z, et al. Altered fecal short chain fatty acid composition in children with a history of Hirschsprung-associated enterocolitis. In: *Journal of Pediatric Surgery*. Vol 51. W.B. Saunders; 2016:81-86. doi:10.1016/j.jpedsurg.2015.10.012

203. Lei M, Menon R, Manteiga S, et al. Environmental Chemical Diethylhexyl Phthalate Alters Intestinal Microbiota Community Structure and Metabolite Profile in Mice. *mSystems*. 2019;4(6).

204. Segata N, Izard J, Waldron L, et al. Metagenomic biomarker discovery and explanation. *Genome Biol*. 2011;12(6). doi:10.1186/gb-2011-12-6-r60

205. Kozich JJ, Westcott SL, Baxter NT, Highlander SK, Schloss PD. Development of a dual-index sequencing strategy and curation pipeline for analyzing amplicon sequence data on the miseq illumina sequencing platform. *Appl Environ Microbiol*. 2013;79(17):5112-5120. doi:10.1128/AEM.01043-13

206. Geerlings S, Kostopoulos I, de Vos W, Belzer C. Akkermansia muciniphila in the Human Gastrointestinal Tract: When, Where, and How? *Microorganisms*. 2018;6(3):75. doi:10.3390/microorganisms6030075

207. Belzer C, De Vos WM. Microbes insidefrom diversity to function: The case of Akkermansia. *ISME J*. 2012;6(8):1449-1458. doi:10.1038/ismej.2012.6

208. Burdet C, Nguyen TT, Duval X, et al. Impact of antibiotic gut exposure on the temporal changes in microbiome diversity. *Antimicrob Agents Chemother*. 2019;63(10). doi:10.1128/AAC.00820-19

209. Xu Y, Wang N, Tan HY, Li S, Zhang C, Feng Y. Function of Akkermansia muciniphila in Obesity: Interactions With Lipid Metabolism, Immune Response and Gut Systems. *Front Microbiol*. 2020;11:219. doi:10.3389/fmicb.2020.00219

210. Liu Z, Li L, Chen W, et al. Aryl hydrocarbon receptor activation maintained the intestinal epithelial barrier function through Notch1 dependent signaling pathway. *Int J Mol Med*. 2018;41(3):1560-1572. doi:10.3892/ijmm.2017.3341

211. Liu W, Mi S, Ruan Z, et al. Dietary Tryptophan Enhanced the Expression of Tight Junction Protein ZO-1 in Intestine. *J Food Sci*. 2017;82(2):562-567. doi:10.1111/1750-3841.13603

212. Zheng L, Kelly CJ, Battista KD, et al. Microbial-Derived Butyrate Promotes Epithelial Barrier Function through IL-10 Receptor–Dependent Repression of Claudin-2. *J Immunol*. 2017;199(8):2976-2984. doi:10.4049/jimmunol.1700105

213. Burger-van Paassen N, Vincent A, Puiman PJ, et al. The regulation of intestinal mucin MUC2 expression by short-chain fatty acids: Implications for epithelial protection. *Biochem J*. 2009;420(2):211-219. doi:10.1042/BJ20082222

214. Desai MS, Seekatz AM, Koropatkin NM, et al. A Dietary Fiber-Deprived Gut Microbiota Degrades the Colonic Mucus Barrier and Enhances Pathogen Susceptibility. *Cell*. 2016;167(5):1339-1353.e21. doi:10.1016/j.cell.2016.10.043

215. Nagpal R, Wang S, Ahmadi S, et al. Human-origin probiotic cocktail increases short-chain fatty acid production via modulation of mice and human gut microbiome. *Sci Rep*. 2018;8(1):1-15. doi:10.1038/s41598-018-30114-4

216. Den Besten G, Van Eunen K, Groen AK, Venema K, Reijngoud DJ, Bakker BM.

The role of short-chain fatty acids in the interplay between diet, gut microbiota, and host energy metabolism. *J Lipid Res*. 2013;54(9):2325-2340. doi:10.1194/jlr.R036012

217. van der Lugt B, van Beek AA, Aalvink S, et al. Akkermansia muciniphila ameliorates the age-related decline in colonic mucus thickness and attenuates immune activation in accelerated aging Ercc1−/Δ7 mice. *Immun Ageing*. 2019;16(1):6. doi:10.1186/s12979-019-0145-z

218. Zmora N, Zilberman-Schapira G, Suez J, et al. Personalized Gut Mucosal Colonization Resistance to Empiric Probiotics Is Associated with Unique Host and Microbiome Features. *Cell*. 2018;174(6):1388-1405.e21. doi:10.1016/j.cell.2018.08.041

219. Sovran B, Loonen LMP, Lu P, et al. IL-22-STAT3 Pathway Plays a Key Role in the Maintenance of Ileal Homeostasis in Mice Lacking Secreted Mucus Barrier. 2015. doi:10.1097/MIB.0000000000000319

220. Monteleone I, Rizzo A, Sarra M, et al. Aryl hydrocarbon receptor-induced signals up-regulate IL-22 production and inhibit inflammation in the gastrointestinal tract. *Gastroenterology*. 2011;141(1):237-248.e1. doi:10.1053/j.gastro.2011.04.007

221. Turner J-E, Stockinger B, Helmby H. IL-22 Mediates Goblet Cell Hyperplasia and Worm Expulsion in Intestinal Helminth Infection. Wynn TA, ed. *PLoS Pathog*. 2013;9(10):e1003698. doi:10.1371/journal.ppat.1003698

222. Sugimoto K, Ogawa A, Mizoguchi E, et al. IL-22 ameliorates intestinal inflammation in a mouse model of ulcerative colitis. *J Clin Invest*.

2008;118(2):534-544. doi:10.1172/JCI33194

223. Ashrafian F, Shahriary A, Behrouzi A, et al. Akkermansia muciniphila-Derived Extracellular Vesicles as a Mucosal Delivery Vector for Amelioration of Obesity in Mice. *Front Microbiol*. 2019;10. doi:10.3389/fmicb.2019.02155

224. Bian X, Wu W, Yang L, et al. Administration of Akkermansia muciniphila Ameliorates Dextran Sulfate Sodium-Induced Ulcerative Colitis in Mice. *Front Microbiol*. 2019;10:2259. doi:10.3389/fmicb.2019.02259

225. Li J, Lin S, Vanhoutte PM, Woo CW, Xu A. Akkermansia muciniphila protects against atherosclerosis by preventing metabolic endotoxemia-induced inflammation in Apoe-/- Mice. *Circulation*. 2016;133(24):2434-2446. doi:10.1161/CIRCULATIONAHA.115.019645

226. Shin J, Noh J-R, Chang D-H, et al. Elucidation of Akkermansia muciniphila Probiotic Traits Driven by Mucin Depletion. *Front Microbiol*. 2019;10(MAY):1137. doi:10.3389/fmicb.2019.01137

227. Zhu L, Lu X, Liu L, Voglmeir J, Zhong X, Yu Q. Akkermansia muciniphila protects intestinal mucosa from damage caused by S. pullorum by initiating proliferation of intestinal epithelium. *Vet Res*. 2020;51(1):34. doi:10.1186/s13567-020-00755-3

228. Wu M, Wu Y, Li J, Bao Y, Guo Y, Yang W. The dynamic changes of gut microbiota in muc2 deficient mice. *Int J Mol Sci*. 2018;19(9). doi:10.3390/ijms19092809

229. Kasprzak A, Siodla E, Andrzejewska M, et al. Differential expression of mucin 1

and mucin 2 in colorectal cancer. *World J Gastroenterol*. 2018;24(36):4164-4177. doi:10.3748/wjg.v24.i36.4164

230. Luettig J, Rosenthal R, Barmeyer C, Schulzke JD. Claudin-2 as a mediator of leaky gut barrier during intestinal inflammation. *Tissue Barriers*. 2015;3(1). doi:10.4161/21688370.2014.977176

231. Moschen AR, Adolph TE, Gerner RR, Wieser V, Tilg H. Lipocalin-2: A Master Mediator of Intestinal and Metabolic Inflammation. *Trends Endocrinol Metab*. 2017;28(5):388-397. doi:10.1016/j.tem.2017.01.003

232. Guillette TC, Jackson TW, Belcher SM. Duality of estrogen receptor β action in cancer progression. *Curr Opin Pharmacol*. 2018;41:66-73. doi:10.1016/j.coph.2018.05.001

233. Murray IA, Patterson AD, Perdew GH. Aryl hydrocarbon receptor ligands in cancer: Friend and foe. *Nat Rev Cancer*. 2014;14(12):801-814. doi:10.1038/nrc3846

234. Duszka K, Wahli W. Enteric microbiota–gut–brain axis from the perspective of nuclear receptors. *Int J Mol Sci*. 2018;19(8). doi:10.3390/ijms19082210

235. Molodecky NA, Soon IS, Rabi DM, et al. Increasing Incidence and Prevalence of the Inflammatory Bowel Diseases With Time, Based on Systematic Review. *Gastroenterology*. 2012;142(1):46-54.e42. doi:10.1053/J.GASTRO.2011.10.001

236. Arnold M, Sierra MS, Laversanne M, Soerjomataram I, Jemal A, Bray F. Global patterns and trends in colorectal cancer incidence and mortality. *Gut*. 2017;66(4):683-691. doi:10.1136/gutjnl-2015-310912

237. Siegel RL, Miller KD, Jemal A. Colorectal Cancer Mortality Rates in Adults Aged 20 to 54 Years in the United States, 1970-2014. *JAMA*. 2017;318(6):572. doi:10.1001/jama.2017.7630

238. May FE. Novel drugs that target the estrogen-related receptor alpha: their therapeutic potential in breast cancer. *Cancer Manag Res*. 2014;6:225-252. doi:10.2147/CMAR.S35024

239. Gallo D, De Stefano I, Grazia Prisco M, Scambia G, Ferrandina G. Estrogen receptor beta in cancer: an attractive target for therapy. *Curr Pharm Des*. 2012;18(19):2734-2757.

240. Sareddy GR, Vadlamudi RK. Cancer therapy using natural ligands that target estrogen receptor beta. *Chin J Nat Med*. 2015;13(11):801-807. doi:10.1016/S1875-5364(15)30083-2

241. Shanle EK, Xu W. Selectively targeting estrogen receptors for cancer treatment. *Adv Drug Deliv Rev*. 2010;62(13):1265-1276. doi:10.1016/j.addr.2010.08.001

242. Safe S, Lee S-O, Jin U-H. Role of the aryl hydrocarbon receptor in carcinogenesis and potential as a drug target. *Toxicol Sci*. 2013;135(1):1-16. doi:10.1093/toxsci/kft128

243. Wang B, Yao M, Lv L, Ling Z, Li L. The Human Microbiota in Health and Disease. *Engineering*. 2017;3(1):71-82. doi:10.1016/J.ENG.2017.01.008

APPENDIX A

COMPOSITIONS OF EXPERIMENTAL DIETS

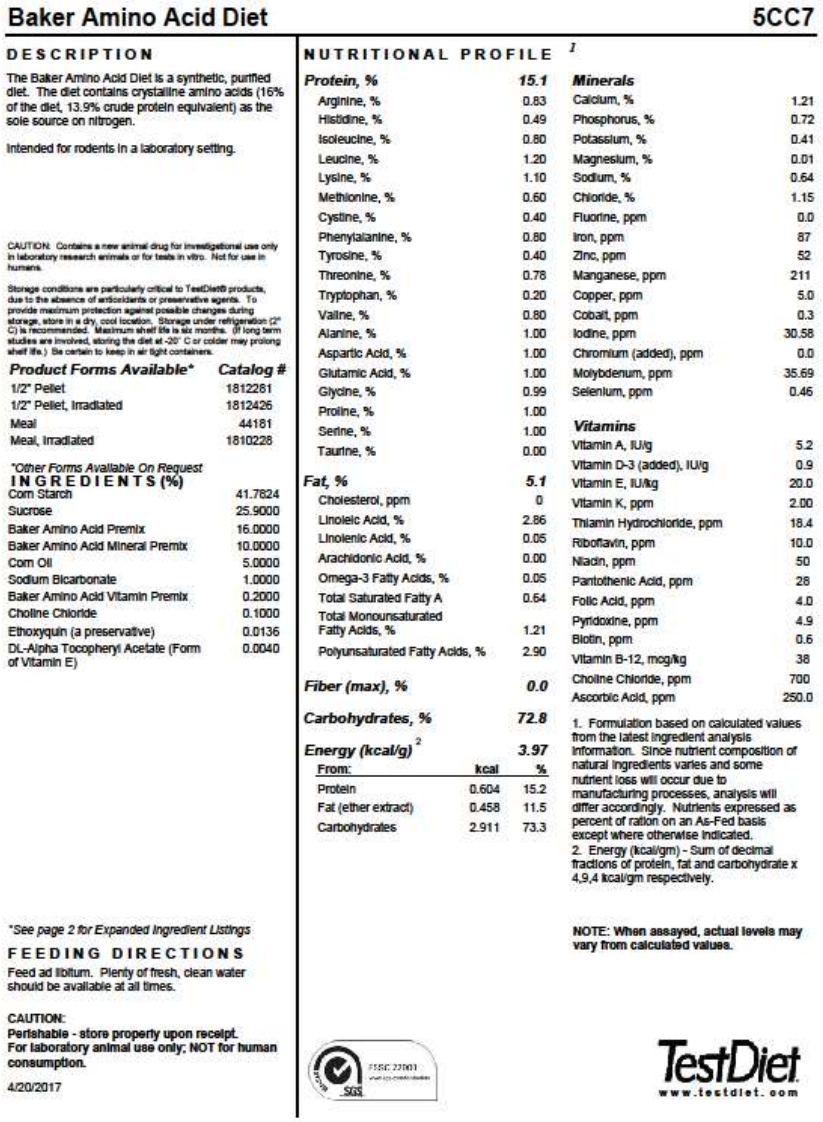

Baker Amino Acid Diet 5CC7

DESCRIPTION

The Baker Amino Acid Diet is a synthetic, purified diet. The diet contains crystalline amino acids (16% of the diet, 13.9% crude protein equivalent) as the sole source on nitrogen.

Intended for rodents in a laboratory setting.

CAUTION: Contains a new animal drug for investigational use only in laboratory research animals or for tests in vitro. Not for use in humans.

Storage conditions are particularly critical to TestDiet® products, due to the absence of antioxidants or preservative agents. To provide maximum protection against possible changes during storage, store in a dry, cool location. Storage under refrigeration (2° C) is recommended. Maximum shelf life is six months. (If long term studies are involved, storing the diet at -20° C or colder may prolong shelf life.) Be certain to keep in air tight containers.

*Product Forms Available**	*Catalog #*
1/2" Pellet	1812261
1/2" Pellet, Irradiated	1812426
Meal	44181
Meal, Irradiated	1810228

**Other Forms Available On Request*

INGREDIENTS (%)

Corn Starch	41.7824
Sucrose	25.9000
Baker Amino Acid Premix	16.0000
Baker Amino Acid Mineral Premix	10.0000
Corn Oil	5.0000
Sodium Bicarbonate	1.0000
Baker Amino Acid Vitamin Premix	0.2000
Choline Chloride	0.1000
Ethoxyquin (a preservative)	0.0136
DL-Alpha Tocopheryl Acetate (Form of Vitamin E)	0.0040

**See page 2 for Expanded Ingredient Listings*

FEEDING DIRECTIONS

Feed ad libitum. Plenty of fresh, clean water should be available at all times.

CAUTION:
Perishable - store properly upon receipt. For laboratory animal use only; NOT for human consumption.

4/20/2017

NUTRITIONAL PROFILE [1]

Protein, %	***15.1***
Arginine, %	0.83
Histidine, %	0.49
Isoleucine, %	0.80
Leucine, %	1.20
Lysine, %	1.10
Methionine, %	0.60
Cystine, %	0.40
Phenylalanine, %	0.80
Tyrosine, %	0.40
Threonine, %	0.78
Tryptophan, %	0.20
Valine, %	0.80
Alanine, %	1.00
Aspartic Acid, %	1.00
Glutamic Acid, %	1.00
Glycine, %	0.99
Proline, %	1.00
Serine, %	1.00
Taurine, %	0.00
Fat, %	***5.1***
Cholesterol, ppm	0
Linoleic Acid, %	2.86
Linolenic Acid, %	0.05
Arachidonic Acid, %	0.00
Omega-3 Fatty Acids, %	0.05
Total Saturated Fatty A	0.64
Total Monounsaturated Fatty Acids, %	1.21
Polyunsaturated Fatty Acids, %	2.90
Fiber (max), %	***0.0***
Carbohydrates, %	***72.8***
Energy (kcal/g) [2]	***3.97***

From:	kcal	%
Protein	0.604	15.2
Fat (ether extract)	0.458	11.5
Carbohydrates	2.911	73.3

Minerals	
Calcium, %	1.21
Phosphorus, %	0.72
Potassium, %	0.41
Magnesium, %	0.01
Sodium, %	0.64
Chloride, %	1.15
Fluorine, ppm	0.0
Iron, ppm	87
Zinc, ppm	52
Manganese, ppm	211
Copper, ppm	5.0
Cobalt, ppm	0.3
Iodine, ppm	30.58
Chromium (added), ppm	0.0
Molybdenum, ppm	35.69
Selenium, ppm	0.46
Vitamins	
Vitamin A, IU/g	5.2
Vitamin D-3 (added), IU/g	0.9
Vitamin E, IU/kg	20.0
Vitamin K, ppm	2.00
Thiamin Hydrochloride, ppm	18.4
Riboflavin, ppm	10.0
Niacin, ppm	50
Pantothenic Acid, ppm	28
Folic Acid, ppm	4.0
Pyridoxine, ppm	4.9
Biotin, ppm	0.6
Vitamin B-12, mcg/kg	38
Choline Chloride, ppm	700
Ascorbic Acid, ppm	250.0

1. Formulation based on calculated values from the latest ingredient analysis information. Since nutrient composition of natural ingredients varies and some nutrient loss will occur due to manufacturing processes, analysis will differ accordingly. Nutrients expressed as percent of ration on an As-Fed basis except where otherwise indicated.
2. Energy (kcal/gm) - Sum of decimal fractions of protein, fat and carbohydrate x 4,9,4 kcal/gm respectively.

NOTE: When assayed, actual levels may vary from calculated values.

FSSC 22000 SGS

TestDiet www.testdiet.com

Figure A.V.1 Composition of Baker Amino Acid Diet used in *in vivo* Experiment Presented in Chapter II.

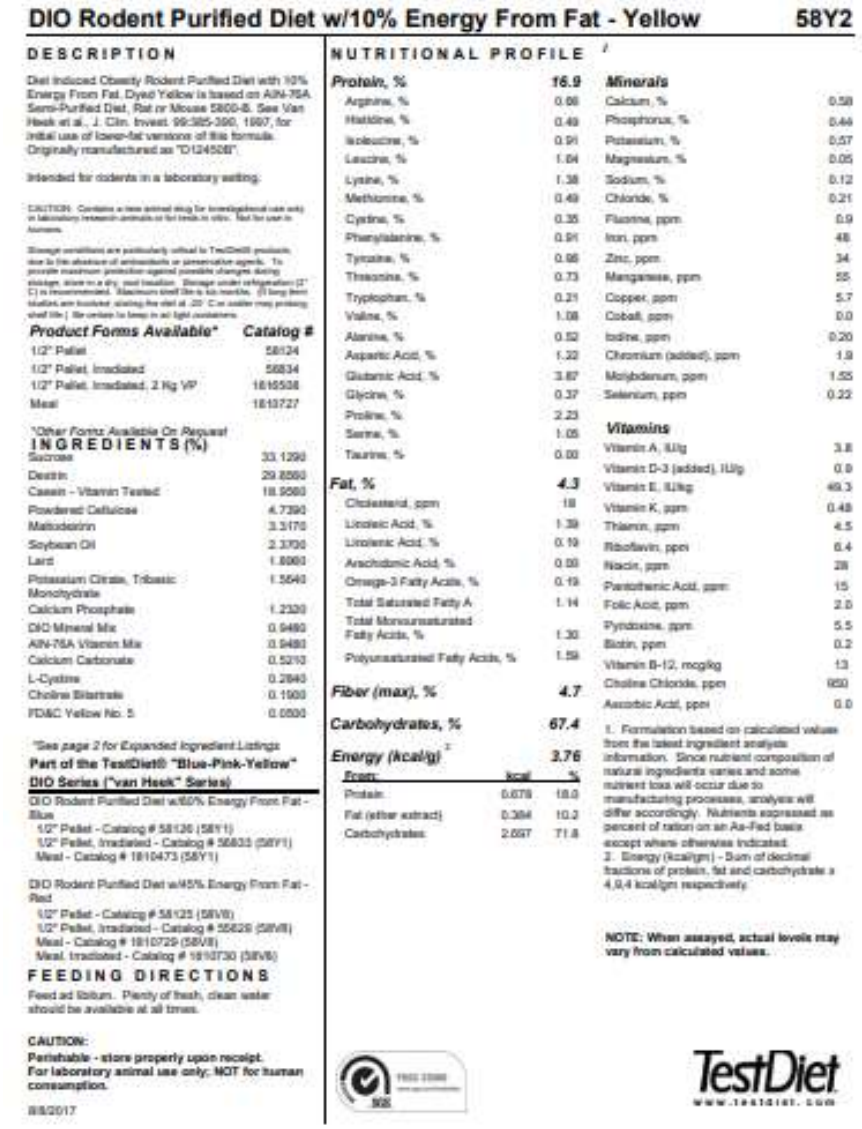

DIO Rodent Purified Diet w/10% Energy From Fat - Yellow 58Y2

DESCRIPTION

Diet Induced Obesity Rodent Purified Diet with 10% Energy From Fat. Dyed Yellow is based on AIN-76A Semi-Purified Diet, Rat or Mouse 5800-B. See Van Heek et al., J. Clin. Invest. 99:385-390, 1997, for initial use of lower-fat versions of this formula. Originally manufactured as "D12450B".

Intended for rodents in a laboratory setting.

CAUTION: Contains a new animal drug for investigational use only in laboratory research animals or for tests in vitro. Not for use in humans.

Storage conditions are particularly critical to TestDiet® products due to the absence of antioxidants or preservative agents. To provide maximum protection against possible changes during storage, store in a dry, cool location. Storage under refrigeration (2° C) is recommended. Maximum shelf life is six months. (If long term studies are involved, storing the diet at -20° C or colder may prolong shelf life.) Be certain to keep in air tight containers.

Product Forms Available*	Catalog #
1/2" Pellet	58124
1/2" Pellet, Irradiated	56834
1/2" Pellet, Irradiated, 2 Rg VP	1810538
Meal	1810727

*Other Forms Available On Request

INGREDIENTS (%)

Sucrose	33.1290
Dextrin	29.8560
Casein - Vitamin Tested	18.5580
Powdered Cellulose	4.7390
Maltodextrin	3.3170
Soybean Oil	2.3700
Lard	1.8960
Potassium Citrate, Tribasic Monohydrate	1.5640
Calcium Phosphate	1.2320
DIO Mineral Mix	0.9480
AIN-76A Vitamin Mix	0.9480
Calcium Carbonate	0.5210
L-Cystine	0.2840
Choline Bitartrate	0.1900
FD&C Yellow No. 5	0.0500

See page 2 for Expanded Ingredient Listings

Part of the TestDiet® "Blue-Pink-Yellow" DIO Series ("van Heek" Series)

DIO Rodent Purified Diet w/60% Energy From Fat - Blue
- 1/2" Pellet - Catalog # 58126 (58Y1)
- 1/2" Pellet, Irradiated - Catalog # 56833 (58Y1)
- Meal - Catalog # 1810473 (58Y1)

DIO Rodent Purified Diet w/45% Energy From Fat - Red
- 1/2" Pellet - Catalog # 58125 (58V8)
- 1/2" Pellet, Irradiated - Catalog # 56828 (58V8)
- Meal - Catalog # 1810729 (58V8)
- Meal, Irradiated - Catalog # 1810730 (58V8)

FEEDING DIRECTIONS

Feed ad libitum. Plenty of fresh, clean water should be available at all times.

CAUTION:
Perishable - store properly upon receipt.
For laboratory animal use only; NOT for human consumption.

8/8/2017

NUTRITIONAL PROFILE [1]

Protein, %	**16.9**
Arginine, %	0.66
Histidine, %	0.49
Isoleucine, %	0.91
Leucine, %	1.64
Lysine, %	1.38
Methionine, %	0.49
Cystine, %	0.35
Phenylalanine, %	0.91
Tyrosine, %	0.66
Threonine, %	0.73
Tryptophan, %	0.21
Valine, %	1.08
Alanine, %	0.52
Aspartic Acid, %	1.22
Glutamic Acid, %	3.87
Glycine, %	0.37
Proline, %	2.23
Serine, %	1.05
Taurine, %	0.00
Fat, %	**4.3**
Cholesterol, ppm	18
Linoleic Acid, %	1.39
Linolenic Acid, %	0.19
Arachidonic Acid, %	0.00
Omega-3 Fatty Acids, %	0.19
Total Saturated Fatty A	1.14
Total Monounsaturated Fatty Acids, %	1.30
Polyunsaturated Fatty Acids, %	1.59
Fiber (max), %	**4.7**
Carbohydrates, %	**67.4**
Energy (kcal/g) [2]	**3.76**

From:	kcal	%
Protein	0.678	18.0
Fat (ether extract)	0.384	10.2
Carbohydrates	2.697	71.8

Minerals	
Calcium, %	0.58
Phosphorus, %	0.44
Potassium, %	0.57
Magnesium, %	0.05
Sodium, %	0.12
Chloride, %	0.21
Fluorine, ppm	0.9
Iron, ppm	48
Zinc, ppm	34
Manganese, ppm	55
Copper, ppm	5.7
Cobalt, ppm	0.0
Iodine, ppm	0.20
Chromium (added), ppm	1.9
Molybdenum, ppm	1.55
Selenium, ppm	0.22

Vitamins	
Vitamin A, IU/g	3.8
Vitamin D-3 (added), IU/g	0.9
Vitamin E, IU/kg	49.3
Vitamin K, ppm	0.48
Thiamin, ppm	4.5
Riboflavin, ppm	6.4
Niacin, ppm	28
Pantothenic Acid, ppm	15
Folic Acid, ppm	2.0
Pyridoxine, ppm	5.5
Biotin, ppm	0.2
Vitamin B-12, mcg/kg	13
Choline Chloride, ppm	950
Ascorbic Acid, ppm	0.0

1. Formulation based on calculated values from the latest ingredient analysis information. Since nutrient composition of natural ingredients varies and some nutrient loss will occur due to manufacturing processes, analysis will differ accordingly. Nutrients expressed as percent of ration on an As-Fed basis except where otherwise indicated.
2. Energy (kcal/gm) - Sum of decimal fractions of protein, fat and carbohydrate x 4,9,4 kcal/gm respectively.

NOTE: When assayed, actual levels may vary from calculated values.

TestDiet
www.testdiet.com

DIO Rodent Purified Diet w/10% Energy From Fat - Yellow 58Y2

EXPANDED INGREDIENT LIST

AIN-76A Vitamin Mix	Sucrose, DL-Alpha Tocopheryl Acetate (Form of Vitamin E), Nicotinic Acid, Vitamin A Palmitate, Calcium Pantothenate, Pyridoxine Hydrochloride, Riboflavin, Thiamine Hydrochloride, Cholecalciferol, Folic Acid, Vitamin B12, Menadione Sodium Bisulfite (source of vitamin K), Biotin
DIO Mineral Mix	Sucrose, Sodium Chloride, Magnesium Sulfate, Magnesium Oxide, Ferric Citrate, Manganese Carbonate, Zinc Carbonate, Chromium Potassium Sulfate, Cupric Carbonate, Ammonium Molybdate, Sodium Fluoride, Sodium Selenite, Potassium Iodate

Figure A.V.2 Composition of Low Fat Diet (LFD) and Irradiated LFD used in *in vivo* Experiment Presented in Chapter III and Chapter IV, Respectively.

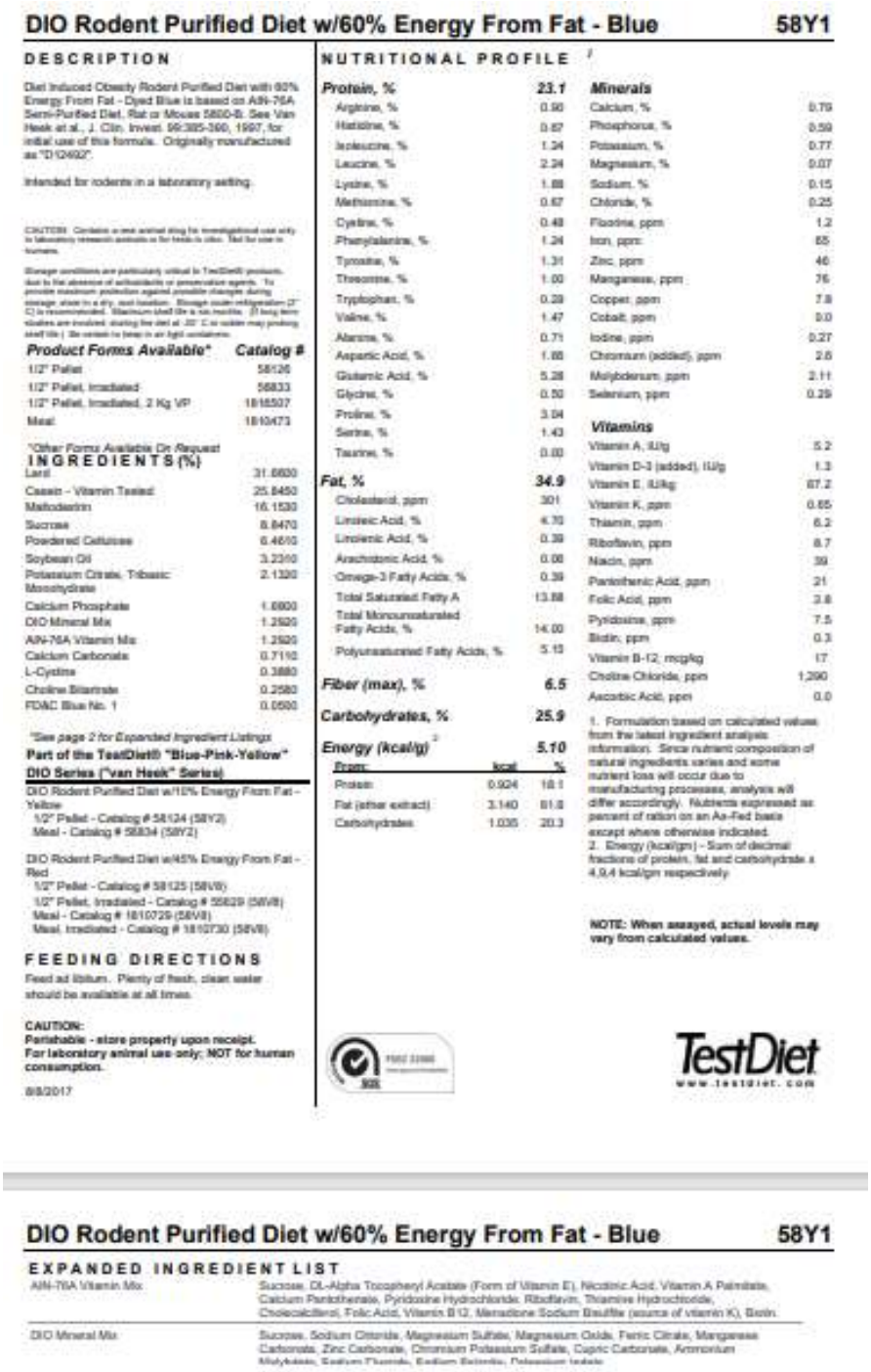

DIO Rodent Purified Diet w/60% Energy From Fat - Blue 58Y1

DESCRIPTION

Diet Induced Obesity Rodent Purified Diet with 60% Energy From Fat - Dyed Blue is based on AIN-76A Semi-Purified Diet, Rat or Mouse 5800-B. See Van Heek et al., J. Clin. Invest. 99:385-390, 1997, for initial use of this formula. Originally manufactured as "D12492".

Intended for rodents in a laboratory setting.

CAUTION: Contains a vital animal drug for investigational use only in laboratory research animals or for feeds in vitro. Not for use in humans.

Storage conditions are particularly critical in TestDiet® products, due to the absence of antioxidants or preservative agents. To provide maximum protection against possible changes during storage, store in a dry, cool location. Storage cooler refrigeration (2° C) is recommended. Maximum shelf life is six months. (If long term studies are involved, storing the diet at -20° C or colder may prolong shelf life.) Be certain to keep in air tight containers.

Product Forms Available*	Catalog #
1/2" Pellet	58126
1/2" Pellet, Irradiated	58833
1/2" Pellet, Irradiated, 2 Kg VP	1816507
Meal	1810473

*Other Forms Available On Request

INGREDIENTS (%)

Lard	31.6600
Casein - Vitamin Tested	25.8450
Maltodextrin	16.1530
Sucrose	8.8470
Powdered Cellulose	6.4610
Soybean Oil	3.2310
Potassium Citrate, Tribasic Monohydrate	2.1320
Calcium Phosphate	1.6800
DIO Mineral Mix	1.2920
AIN-76A Vitamin Mix	1.2920
Calcium Carbonate	0.7110
L-Cystine	0.3880
Choline Bitartrate	0.2580
FD&C Blue No. 1	0.0500

See page 2 for Expanded Ingredient Listings

Part of the TestDiet® "Blue-Pink-Yellow" DIO Series ("van Heek" Series)

DIO Rodent Purified Diet w/10% Energy From Fat - Yellow
- 1/2" Pellet - Catalog # 58124 (58Y2)
- Meal - Catalog # 58834 (58Y2)

DIO Rodent Purified Diet w/45% Energy From Fat - Red
- 1/2" Pellet - Catalog # 58125 (58W8)
- 1/2" Pellet, Irradiated - Catalog # 58829 (58W8)
- Meal - Catalog # 1810729 (58W8)
- Meal, Irradiated - Catalog # 1810730 (58W8)

FEEDING DIRECTIONS

Feed ad libitum. Plenty of fresh, clean water should be available at all times.

CAUTION:
Perishable - store properly upon receipt.
For laboratory animal use only; NOT for human consumption.

8/8/2017

NUTRITIONAL PROFILE [1]

Protein, %	**23.1**
Arginine, %	0.98
Histidine, %	0.67
Isoleucine, %	1.24
Leucine, %	2.24
Lysine, %	1.88
Methionine, %	0.67
Cystine, %	0.48
Phenylalanine, %	1.24
Tyrosine, %	1.31
Threonine, %	1.00
Tryptophan, %	0.29
Valine, %	1.47
Alanine, %	0.71
Aspartic Acid, %	1.88
Glutamic Acid, %	5.28
Glycine, %	0.59
Proline, %	3.04
Serine, %	1.43
Taurine, %	0.00
Fat, %	**34.9**
Cholesterol, ppm	301
Linoleic Acid, %	4.70
Linolenic Acid, %	0.39
Arachidonic Acid, %	0.08
Omega-3 Fatty Acids, %	0.39
Total Saturated Fatty A	13.88
Total Monounsaturated Fatty Acids, %	14.00
Polyunsaturated Fatty Acids, %	5.13
Fiber (max), %	**6.5**
Carbohydrates, %	**25.9**
Energy (kcal/g) [2]	**5.10**

Proximates	kcal	%
Protein	0.924	18.1
Fat (ether extract)	3.140	61.6
Carbohydrates	1.035	20.3

Minerals	
Calcium, %	0.79
Phosphorus, %	0.59
Potassium, %	0.77
Magnesium, %	0.07
Sodium, %	0.15
Chloride, %	0.25
Fluorine, ppm	1.2
Iron, ppm:	65
Zinc, ppm	46
Manganese, ppm	76
Copper, ppm	7.8
Cobalt, ppm	0.0
Iodine, ppm	0.27
Chromium (added), ppm	2.6
Molybdenum, ppm	2.11
Selenium, ppm	0.29

Vitamins	
Vitamin A, IU/g	5.2
Vitamin D-3 (added), IU/g	1.3
Vitamin E, IU/kg	67.2
Vitamin K, ppm	0.65
Thiamin, ppm	6.2
Riboflavin, ppm	6.7
Niacin, ppm	39
Pantothenic Acid, ppm	21
Folic Acid, ppm	2.8
Pyridoxine, ppm	7.5
Biotin, ppm	0.3
Vitamin B-12, mcg/kg	17
Choline Chloride, ppm	1,290
Ascorbic Acid, ppm	0.0

1. Formulation based on calculated values from the latest ingredient analysis information. Since nutrient composition of natural ingredients varies and some nutrient loss will occur due to manufacturing processes, analysis will differ accordingly. Nutrients expressed as percent of ration on an As-Fed basis except where otherwise indicated.
2. Energy (kcal/gm) - Sum of decimal fractions of protein, fat and carbohydrate x 4,9,4 kcal/gm respectively.

NOTE: When assayed, actual levels may vary from calculated values.

TestDiet
www.testdiet.com

DIO Rodent Purified Diet w/60% Energy From Fat - Blue 58Y1

EXPANDED INGREDIENT LIST

AIN-76A Vitamin Mix	Sucrose, DL-Alpha Tocopheryl Acetate (Form of Vitamin E), Nicotinic Acid, Vitamin A Palmitate, Calcium Pantothenate, Pyridoxine Hydrochloride, Riboflavin, Thiamine Hydrochloride, Cholecalciferol, Folic Acid, Vitamin B12, Menadione Sodium Bisulfite (source of vitamin K), Biotin
DIO Mineral Mix	Sucrose, Sodium Chloride, Magnesium Sulfate, Magnesium Oxide, Ferric Citrate, Manganese Carbonate, Zinc Carbonate, Chromium Potassium Sulfate, Cupric Carbonate, Ammonium [illegible]

Figure A.V.3 Composition of High Fat Diet (HFD) used in *in vivo* Experiment Presented in Chapter III.

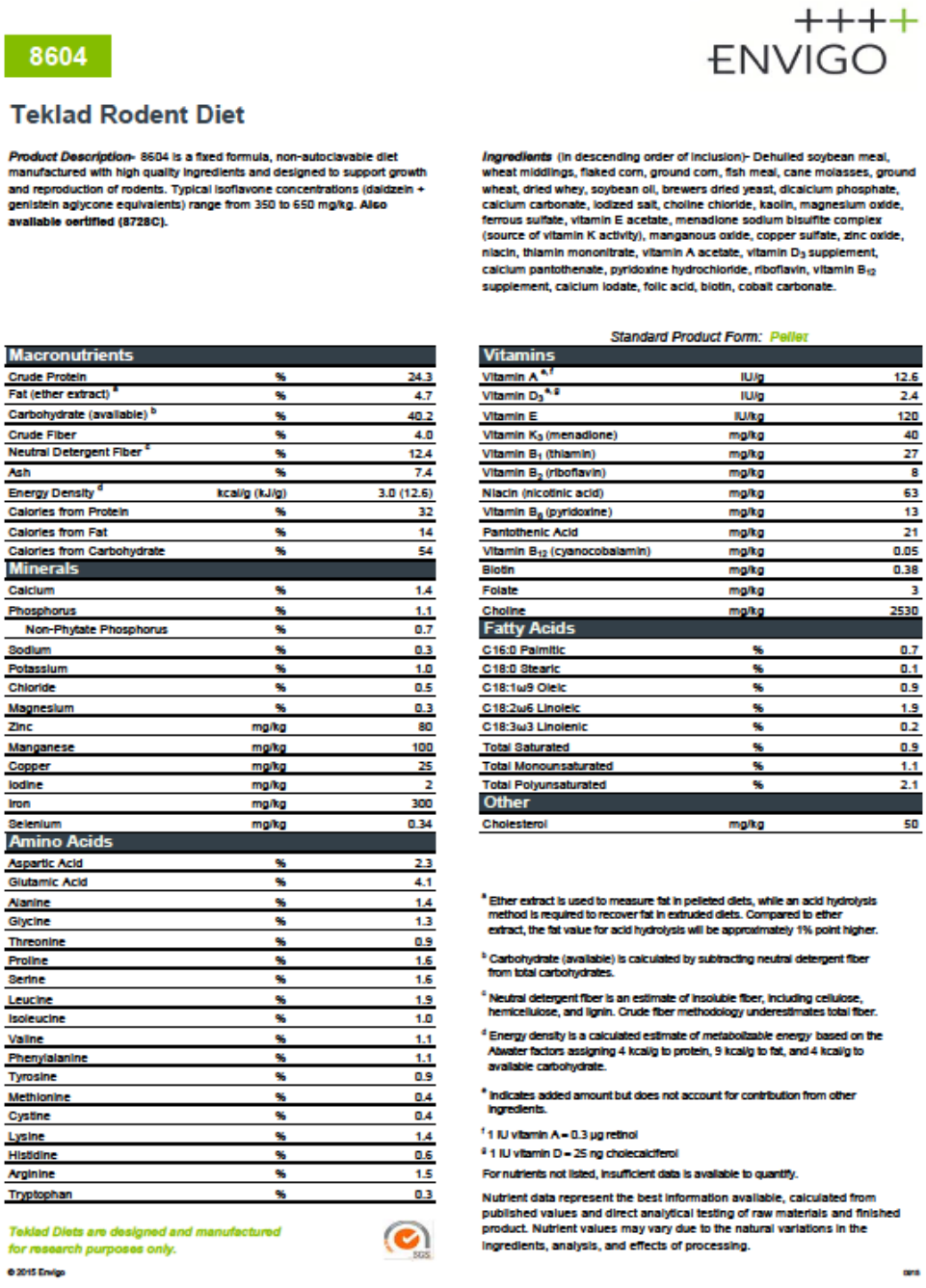

8604

ENVIGO

Teklad Rodent Diet

Product Description- 8604 is a fixed formula, non-autoclavable diet manufactured with high quality ingredients and designed to support growth and reproduction of rodents. Typical isoflavone concentrations (daidzein + genistein aglycone equivalents) range from 350 to 650 mg/kg. **Also available certified (8728C).**

Ingredients (in descending order of inclusion)- Dehulled soybean meal, wheat middlings, flaked corn, ground corn, fish meal, cane molasses, ground wheat, dried whey, soybean oil, brewers dried yeast, dicalcium phosphate, calcium carbonate, iodized salt, choline chloride, kaolin, magnesium oxide, ferrous sulfate, vitamin E acetate, menadione sodium bisulfite complex (source of vitamin K activity), manganous oxide, copper sulfate, zinc oxide, niacin, thiamin mononitrate, vitamin A acetate, vitamin D_3 supplement, calcium pantothenate, pyridoxine hydrochloride, riboflavin, vitamin B_{12} supplement, calcium iodate, folic acid, biotin, cobalt carbonate.

Standard Product Form: Pellet

Macronutrients		
Crude Protein	%	24.3
Fat (ether extract) [a]	%	4.7
Carbohydrate (available) [b]	%	40.2
Crude Fiber	%	4.0
Neutral Detergent Fiber [c]	%	12.4
Ash	%	7.4
Energy Density [d]	kcal/g (kJ/g)	3.0 (12.6)
Calories from Protein	%	32
Calories from Fat	%	14
Calories from Carbohydrate	%	54
Minerals		
Calcium	%	1.4
Phosphorus	%	1.1
Non-Phytate Phosphorus	%	0.7
Sodium	%	0.3
Potassium	%	1.0
Chloride	%	0.5
Magnesium	%	0.3
Zinc	mg/kg	80
Manganese	mg/kg	100
Copper	mg/kg	25
Iodine	mg/kg	2
Iron	mg/kg	300
Selenium	mg/kg	0.34
Amino Acids		
Aspartic Acid	%	2.3
Glutamic Acid	%	4.1
Alanine	%	1.4
Glycine	%	1.3
Threonine	%	0.9
Proline	%	1.6
Serine	%	1.6
Leucine	%	1.9
Isoleucine	%	1.0
Valine	%	1.1
Phenylalanine	%	1.1
Tyrosine	%	0.9
Methionine	%	0.4
Cystine	%	0.4
Lysine	%	1.4
Histidine	%	0.6
Arginine	%	1.5
Tryptophan	%	0.3

Vitamins		
Vitamin A [e,f]	IU/g	12.6
Vitamin D_3 [e,g]	IU/g	2.4
Vitamin E	IU/kg	120
Vitamin K_3 (menadione)	mg/kg	40
Vitamin B_1 (thiamin)	mg/kg	27
Vitamin B_2 (riboflavin)	mg/kg	8
Niacin (nicotinic acid)	mg/kg	63
Vitamin B_6 (pyridoxine)	mg/kg	13
Pantothenic Acid	mg/kg	21
Vitamin B_{12} (cyanocobalamin)	mg/kg	0.05
Biotin	mg/kg	0.38
Folate	mg/kg	3
Choline	mg/kg	2530
Fatty Acids		
C16:0 Palmitic	%	0.7
C18:0 Stearic	%	0.1
C18:1ω9 Oleic	%	0.9
C18:2ω6 Linoleic	%	1.9
C18:3ω3 Linolenic	%	0.2
Total Saturated	%	0.9
Total Monounsaturated	%	1.1
Total Polyunsaturated	%	2.1
Other		
Cholesterol	mg/kg	50

[a] Ether extract is used to measure fat in pelleted diets, while an acid hydrolysis method is required to recover fat in extruded diets. Compared to ether extract, the fat value for acid hydrolysis will be approximately 1% point higher.

[b] Carbohydrate (available) is calculated by subtracting neutral detergent fiber from total carbohydrates.

[c] Neutral detergent fiber is an estimate of insoluble fiber, including cellulose, hemicellulose, and lignin. Crude fiber methodology underestimates total fiber.

[d] Energy density is a calculated estimate of metabolizable energy based on the Atwater factors assigning 4 kcal/g to protein, 9 kcal/g to fat, and 4 kcal/g to available carbohydrate.

[e] Indicates added amount but does not account for contribution from other ingredients.

[f] 1 IU vitamin A = 0.3 µg retinol

[g] 1 IU vitamin D = 25 ng cholecalciferol

For nutrients not listed, insufficient data is available to quantify.

Nutrient data represent the best information available, calculated from published values and direct analytical testing of raw materials and finished product. Nutrient values may vary due to the natural variations in the ingredients, analysis, and effects of processing.

Teklad Diets are designed and manufactured for research purposes only.

Teklad Diets • Madison WI • envigo.com • tekladinfo@envigo.com • (800) 483-5523

Figure A.V.4 Composition of Chow Diet used in *in vivo* Experiments.

APPENDIX B

PROTOCOLS

BPA Gavage

Dose: 50 ug/kg body weight/day of BPA in corn oil
Limit gavage amount to no more than 10 mL/kg body weight/day
Dissolve BPA in EtOH and add to corn oil fresh before EACH gavage!

Example:
25 g mouse = 0.025 kg mouse

$$\frac{50\ ug\ BPA}{1\ kg\ mouse} = \frac{x\ ug\ BPA}{0.025\ kg\ mouse}$$

X = 1.25 ug BPA for 25 g mouse

Max corn oil:

$$\frac{10\ mL\ corn\ oil}{1\ kg\ mouse} = \frac{x\ mL\ corn\ oil}{0.025\ kg\ mouse}$$

X = 0.25 mL corn oil
Maximum of 0.25 mL corn oil can be gavaged in 25 g mouse.
Therefore, calculated the BPA dose for 25 g mouse in only 0.20 mL of corn oil.

BPA concentration in corn oil:

$$\frac{1.25\ ug\ BPA}{0.200\ mL\ corn\ oil} = \frac{x\ ug\ BPA}{1\ mL\ corn\ oil}$$

X = 6.25 ug BPA/1 mL corn oil

For reasonably measurable volumes:

$$\frac{0.00625\ mg\ BPA}{1\ mL\ corn\ oil} = \frac{1\ mg\ BPA}{x\ mL\ corn\ oil}$$

X = 1 mg BPA/160 mL corn oil

BPA must first be dissolved in ethanol. Dissolve 1 mg BPA in 16 uL of 100% ethanol. Vortex at room temperature to mix.

$$\frac{16\ uL\ EtOH\ with\ BPA}{160\ mL\ corn\ oil} = \frac{x\ uL\ EtOH\ with\ BPA}{10\ mL\ corn\ oil}$$

X = 1 uL EtOH with BPA in 10 mL corn oil
Add 1 uL EtOH with BPA to 10 mL corn oil and vortex again. Make fresh before each gavage.

Final concentration of EtOH in corn oil = 0.01%
Vehicle gavage: 0.01% EtOH in corn oil

Fecal Collection

Materials:
Animal List (for labeling and notes)
1 clean, empty microisolator cage/animal (ordered from clean cage in LARR several days in advance)
Label tape
Marker
1 labeled cryovial/animal
Thermos with LN2

1.) Order individual clean cages from clean cage staff several days in advance. Need one tiny mouse cage and microisolator lid for each animal. Be sure to specify nothing else needed in cage (empty – no bedding, nestlet, grid, food, or water) and all cages should be on a rack that fits all of them (not stacked).
2.) Label cryotubes several days in advance with animal number, date collected, initials, animal group or cohort, and fecal collection number. Be sure labels are clear as others will likely complete analysis of samples.
3.) The afternoon before fecal collection, label cages with lab tape with animal number and home cage number. Place all numbers from a single home cage on one fecal collection cage. Skip the corresponding number of cages for the rest of the mice in that home cage. Continue until all cages labeled.
4.) The morning of fecal collection (early), remove animals from home cage one at a time and place in corresponding empty fecal collection cages. Use a new pair of gloves for each home cage.
5.) After all animals are placed in fecal collection cages, identify each animal and move label tape to appropriate fecal collection cage.
6.) Allow animals time to defecate, and then begin to collect feces in appropriately labeled cryotube. Collect at least 5 pellets. Use one pair of gloves per cage – pay attention to cage number on label tape.
AVOID TOUCHING FECES WITH HANDS AS MUCH AS POSSIBLE. USE TUBE OR LID TO SCOOP FECES UP.
7.) If animals haven't given enough pellets, gently scruff animals and rub their abdomens. If animals still haven't defecated, animals can be gently wrapped in paper towels to keep them active.
DO NOT WRAP TIGHTLY IN PAPER TOWELS.
8.) Record any abnormalities noted in feces, animals, etc. on animal list. This includes number of pellets collected for each animal if less than 5.
9.) Once five pellets collected in tube, tightly close and place tube in container containing liquid nitrogen.
10.) After feces collected, place animal back in home cage, remove label tape from dirty cage and return all cages to dirty cage on rack. Animals should be returned to home cage as soon as possible; avoid keeping animals in fecal collection cages for more than a couple of hours.

Note: You can collect feces from all animals from one home cage wearing the same pair of gloves, then return all animals to that single home cage before replacing gloves and moving on to next cage.

11.) Store cryovials at -80 until ready to analyze.

Cytokine Multiplex Analysis

Adapted from Ji-Hye Yoo, Dr. Clinton Allred's Lab

Millipore MCYTOMAG-70K-9
Thermo T-PER® TissueProtein Extraction Reagent Cat. 78510
Bio-Rad DC Protein Assay Reagents Package Kit Cat. 5000116

1. Snap frozen colon tissues

2. Homogenize tissues ON ICE in 1 mL Tissue Protein Extraction Reagent (for ½ of whole colon).

3. Centrifuge at 10,000g for 5 min

4. Aliquot 100 µl supernatant and store in -80°C

5. Total protein content was assessed using the *DC* Protein Assay (Bio-Rad); follow kit protocol

6. All samples (on ice) were diluted with TPER to 4 or 8 mg/ml. (Can use 2 mg/mL)

7. Prepare all necessary reagents from Milliplex Kit.

8. Add 400 µl wash buffer/well and Shake for 10 min

9. Vortex Beads for 1 min and transfer beads to an e-tube. **NOTE: Be sure to vortex all beads well before adding!**

- Each bead is 50X. Dilute in assay buffer. Follow kit protocol.
- Eg) 17 µl each bead/ 850 µl assay buffer-> 9 types of beads, mix 17 µl each beads and 697 µl assay buffer

10. 25 µl diluted sample was added per well of a 96-well plate.

11. Add 25 µl of the magnetic beads mixture provided in the kit.

12. The plate was sealed, covered by Foil and agitated on a plate shaker overnight at 4°C.

13. 96-well plate was placed on a hand-held magnet and the contents of the wells removed.

14. Wash twice

a) Hold the plate on a hand-hold magnet for 1 min
b) Remove the contents
c) Add 200 µl of Wash buffer/well
d) Shake the plate for 30 sec
e) Repeat the steps

15. Remove wash buffer and Add 25 µl of detection antibodies to each well

16. Incubate at room temperature for 1 hr with agitation.

17. NO WASH Add 25 µl of Streptavidin-Phycoerythrin

18. Incubated at room temperature for 30 min with agitation.

19. Wash twice.

20. Add 150 µl Luminex Sheath Fluid to resuspend the magnetic beads

21. Shake the plate for 5 min

22. Run on a Luminex 200.

Charcoal-Dextran Stripped Fetal Bovine Serum

For 1 Liter FBS

1. Set serum bottle in 4° 2-3 days prior to treatment
2. Autoclave centrifuge bottles day before needed. These bottles should only be used for charcoal use afterwards
3. Have one water bath set at 37°C
4. Set another water bath for between 56-59°C with water level high enough to meet serum level
5. On day of treatment warm serum bottle in 37° bath and store protected from light. Keep lights off in culture room and hood (lights in main lab are ok).
6. Centrifuge a 50 ml portion of Charcoal-Dextran (CD) @ 1,925 rpm for 5 min
7. Using aseptic technique, decant saline and discard. Add 25 ml serum to CD and mix carefully with pipet until homogenous. It is easiest to mix some then pipet it into the serum bottle and pipet out another 25 ml and so on.
8. Once all the CD is in the serum bottle cap the bottle tightly and parafilm seal the cap. Mix well by shaking and place bottle in 56-59°C bath. Set a timer for 6 minutes and one for 45 min.
   Total incubation time is 45 min, assuming 15 minutes for the serum to reach 56°C plus 30 min for incubation at 56°C. The temperature must remain at or above 56°C for at least 30 minutes.
9. After 6 minutes mix serum well by inverting the bottle and swirling several times.
   Place serum back in bath and continue to mix every 6 minutes until the 45 min is up.
10. Using aseptic technique mix and transfer to centrifuge bottles (2-6 bottles) adjusting so the volume will be equal in each pair of bottles. Cap bottles and centrifuge at 4°C for 30 min at 3,600 rpm. (If you want to CD strip the serum 2 times go back to step 7 at this time and repeat from there).
11. Decant serum gently, avoid transferring CD lines, and transfer to a second set of centrifuge bottles. (Alternatively, transfer serum to an autoclaved bottle and rinse centrifuge bottles with water and ethanol, shake out excess ethanol). Transfer serum to bottles in equal amounts and centrifuge at 4°C for 30 min at 4,400 rpm.
12. Label 50 ml tubes with CDFBS and the date.
13. Combine all serum into an autoclaved bottle and then filter through a 0.22μm filter using a vacuum filter.
14. Aliquot into 50 ml tubes.
15. Store at -20°C. Serum is stable for up to 2 years at -20°C.
16. To disinfect centrifuge bottles used for CD rinse any remaining CD out and then soak in ethanol overnight and wash as normal.

ß-Catenin and EdU Co-Stain

Adapted from Eunjoo Kim of Dr. Robert Chapkin's Lab

Antibody and reagents:

Mouse monoclonal ß-Catenin antibody (BD Transduction, 610154, dilution 1:500)
Donkey anti-Mouse Alexa Fluor 647 (Life Technologies, A-31571, dilution 1:200)
Click-It Plus EdU Alexa Fluor 488 Imagine Kit (Invitrogen, C10637)
ProLong Gold AntiFade + DAPI (Life Tech, P36931)

Solutions (All filtered):

Day 1:

10mM sodium citrate (Sigma, S4641)
Ethanol (KOPEC, V1001) 100%, 95%, 70%, and Xylene (Fisher, X2P-1GAL)
dH2O (Gibco, 15230-170) (Nanopure fine, but filter it)
TBST buffer (1x TBS with 0.1% Tween-20 (Sigma, P9416))
10X TBS: 24.2 g Tris base ($C_4H_{11}NO_3$) (JT Baker, 4109-01) + 80 g sodium chloride (NaCl) (Sigma, S3014)/1 L dH_2O. Adjust pH to 7.6, store at 4 degrees.
Donkey serum (Millipore, S30-100mL)
0.05 M Tris-HCl buffer
6.057 g Tris-HCl (JT Baker 4103-04)/1 L dH2O. Adjust pH to 7.6, store at 4 degrees.
2% BSA in Tris-HCl buffer
2g BSA (Sigma, A7030) + 100 mL 0.05 Tris-HCl buffer (pH 7.6)
1x PBS
3% Bovine Serum Albumin (BSA) in PBS, IgG Free (Sigma, A7030)
1.2 g BSA/38.8 mL PBS 1x, shake/vortex well
0.5% Triton X-100 (Sigma, 9002-93) in PBS
225 uL Triton X-100/45 mL PBS 1x

Other Materials:

Slide Holders
PAP Pen
Metal Pot
Dark moisture chamber
Coverslip
Nail Polish

1st day

Procedure:

___ Prepare 1.2 L of 10 mM sodium citrate, pH 6.0 (3.52 g sodium citrate trisodium ($C_6H_5Na_3O_7 \cdot 2H_20$) in 850 ml H_2O, adjust pH to 6.0 and then take final volume of 1.2 L). Preheat on hot plate by bringing to a boil at the level 10 on Thermolyne heat plate and once boiling, switch to level 5.9. **We want to make sure the solution is NOT bubbling at all once the tissues go in**

Deparaffinization/Rehydration

___ ___ ___ Xylene 3X 5 min
___ Circle with PAP pen if needed **Make a thick circle and dry out completely**
(Notes from LD: Since you need to apply PAP pen to a dry slide, you need to do this

immediately after the xylene step, once the slide is dry. Once the tissue has been rehydrated in water, you don't want to let it dry out or you could produce staining artifacts.)
NOTE: Do not allow slides to dry at any time during this procedure.
___ ___ ___ 100% ethanol 3X 4 min
___ ___ ___ 95% ethanol 3X 4 min
___ ___ 70% ethanol 2 x 4 min
___ ___ ___ dH_2O 3X 3 min
Antigen Unmasking:
___ 20 min in sub-boiling citrate in metal pot.
___ Cool metal pot for 20 min in tub of tap water.

ß-Catenin labeling

___ ___ dH_20 2x 5 min
___ ___ Wash slides in TBST 2X 5 min
___ Blocking sol'n 40 min at RT: 5% donkey serum in TBST (47.5 mL TBST with 2.5 mL donkey serum in coplin jar; filter in #1 Whatman paper)
___ Prepare primary antibody: Anti ß-catenin (50 µL each)
1:500 in 2% BSA in 0.05 M Tris-HCl buffer (pH 7.6)
Per 3 sections: 3 mg BSA and 150 µL Tris-HCL
Per 3 sections: 0.3 µL ß-catenin AB + 149.7 µL 2% BSA in 0.05 M Tris-HCl=150 µL
___ ___ Wash slides in 0.05 M Tris-HCl Buffer (pH 7.6) 2X5 min
___ Tap serum off
___ Put slides in the immune stain moisture chamber and add primary antibody
___ Incubate overnight at 4°C in a humidified chamber

Note: The solution beads up (on some steps) into a little ball. You have to really drag it with a pipet tip to cover the tissue. And you need to look very closely to make sure the outer edge is covered with solution to avoid artifact during imaging.

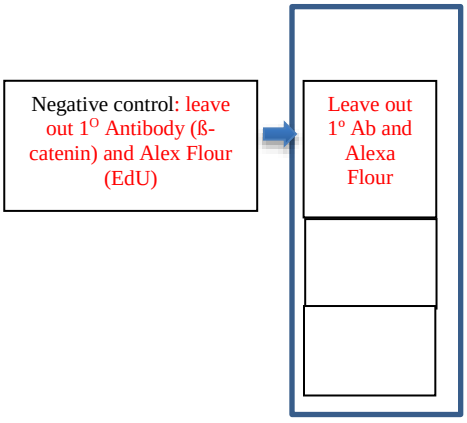

2nd day

___ ___ ___ Wash in 0.05 M Tris-HCl buffer (pH7.6) 3X5 min
___ Prepare 2° antibody (LT donkey anti-mouse IgG – Alexa Fluor 647)

1:200 in 2% BSA in 0.05 M Tris-HCl buffer (pH 7.6) for 1 hr at RT.
Per 3 sections, 0.75 µl 2° Ab + 149.25 µl 2% BSA in 0.05 M Tris-HCl = 150 µl
___ ___ ___ Wash slides in 0.05 M Tris-HCl buffer (pH 7.6) 3X5 min
___ ___ ___ Wash slides in dH2O 3X5 min

Edu assay for proliferating cells

___ 3% BSA in PBS, wash (dip 3-4 times)
___ 0.5% Triton X-100 in PBS, 20 min
___ Prep Click-It Reaction Cocktail, Table. Add reagents in order. Store in the dark and use within 15 minutes. (Note: don't use until indicated below!)

	Per 10 sections	Per __ sections
10X Rxn buffer (D)	44 µl	
Water	396 µl	
CuSO4 (E)	10 µl	
Alexa Fluor (B) (leave out)	1.2 µl	
10X Rxn buffer additive (F)	5 µl	
Water	45 µl	
Total	500µl	

For negative control, omit Alexa.
___ 3% BSA in PBS, wash (dip 3-4 times)
___ Add 50 µl Click-It reaction cocktail to each sample, incubate 30 min RT, in the DARK box
___ Tap off slide, 3% BSA in PBS wash (dip 2-3 times)
___ PBS, 1 x 30sec

Coverslip with ProLong AntiFade + DAPI.

___ Coverslip using ProLong Gold Antifade. Tap off most liquid, apply a drop of Prolong below each section and coverslip. Let cure at RT in the dark overnight. Seal with nail polish for longer lasting imaging. Image using Cy5 (647) and FITC (488) filters. (Not Texas Red or TRITC)

Antibiotic Cocktail

Provided by Dr. Christian Jobin's Lab, University of Florida

For 1L solution (1X)
Streptomycin - 2g/L
Bacitracin - 1g/L
Gentamycin 0.5g/L
Ciprofloxacin 0.125g/L
** Note: Antibiotics are light sensitive.

First dissolved Streptomycin completely, followed by gentamycin. The strep and gentamycin dissolved completely. Then added the cipro- which turned the solution cloudy and lastly added the bacitracin (which has a slight yellowish tint) turned the

solution yellow tint (did not fully dissolved). Tiny particles will float around. Stir for at least 3-4 hours, or overnight with concentrated solution, wrapped in aluminum foil to protect from light.
If having 4 cages or less, make 1X solution in ACS provided water. Making more concentrated solutions will decrease the solubility, but is still effective. If doing so, make sure to completely mix/shake bottle to ensure that when diluting the appropriate amount of antibiotics will be administered.
Prepared a 2.5X solution (2L) and diluted to final concentration of 1X with ACS provided water (from water bottles).
Exposed mice to antibiotic water in Red water bottles (provided by ACS) to protect antibiotics from light. After 3-4 days fresh antibiotic water needs to be added. After day 7, regular water is added for 24 hours recovery, the following day, mice were gavaged with bacteria of interest.

Fecal Transplant

Required Materials:

- Donor Mice for feces
- Sterile, empty fecal collection cages: 1/donor mouse
- Autoclaved forceps
- Anaerobic Jar
- Anaerobic BHI media
- Aliquoted in sterile test tube with butyl rubber stopper to collect feces.
- Additional volume required to prepare fecal slurry in anaerobic chamber.
- Gas Pack
- Anaerobic Chamber with scale, sterile inoculating loops, sterile test tubes with butyl rubber stoppers and caps, etc. to prepare slurry.
- Syringes
- Gavage needles
- Mice receiving transplant

Aliquot Anaerobic BHI Media:
Aliquot enough anaerobic BHI media into sterile test tube with butyl rubber stopper in anaerobic chamber to sufficiently cover desired number of fecal pellets. Example: About 5 fecal pellets should be sufficiently covered in 1 mL of anaerobic BHI.
Fecal Collection:
Bring aliquoted BHI to animal facility in anaerobic jar.
Place donor mice into individual, sterile, empty cages and allow them to defecate.
As soon as the required number of pellets have been left in cage, collect feces from donors into anaerobic BHI or media (based on vehicle or other groups used). Use autoclaved forceps to collect feces. Avoid collecting fecal pellets that are exposed to urine.
Quickly place collected pellets into tube containing anaerobic BHI.

Quickly return capped tube to anaerobic jar, and quickly add gas pack to minimize oxygen exposure.
LIMIT OPENING OF JAR AND TUBE AND CLOSE BOTH TIGHTLY AS SOON AS FECAL PELLETS ARE IN ANAEROBIC BHI. If BHI turned pink, it has been exposed to oxygen. Try again, performing collection more quickly.

Slurry Feces:

Return anaerobic jar with tube containing feces to anaerobic chamber. Inside anaerobic chamber, weigh appropriate amount of feces and add to the appropriate volume of anaerobic BHI in a new, sterile test tube with butyl rubber stopper. Slurry with sterile inoculating loop until feces is well mixed in BHI.

# Animals Receiving Transplant	Weight of Feces	Volume Anaerobic BHI
6	0.2 g	1 mL

Place tube of slurried feces back in anaerobic jar, and return to animal facility.

Gavage Fecal Slurry:

Gavage 150 uL of slurried feces per animal receiving fecal transplant. **Fecal slurry will be thick and difficult to gavage. Allow tube to settle before drawing up gavage dose from top of liquid to avoid clogging gavage needle.**

Vehicle Gavage:

Aliquot required volume of anaerobic BHI for vehicle gavage group. Gavage 150 uL anaerobic BHI per animal.

Carnoy Fixation of Colon Tissue

60 mL Ethanol, absolute (VWR 64-17-5)
10 mL Acetic acid, glacial (VWR 64-19-7)
30 mL Chloroform (EMD Millipore 67-66-3)
All mixing, fixation, transferring, etc. must be done in the chemical fume hood, and all waste must be disposed as hazardous waste.
Make fresh.
Fix 1 cm proximal or distal colon pieces (in cassettes) with intact feces 2 h on ice
Carefully pour off Carnoy's, discard into waste bottle in hood
Add 100% EtOH. Immediately change to fresh 100% EtOH and allow to sit for 20min
Fresh 100% EtOH, allow to sit for 20 min
Store cassettes immersed in fresh 100% ethanol at 4°C. Take to histology for further processing

FITC-Dextran Gavage and Gut Permeability Assessment

Provided by Yang-Yi Fan, Dr. Robert Chapkin's Lab

Materials:

FITC-dextran (Sigma, #FD4)
Prepare 80 mg/ml FITC-dextran in sterile 1x PBS. (*Can be prepared ahead of time, store at 4°C, prevent from light) (1g in 12. 5 mL)*

Procedure:
Fast mice **overnight**[3,4] prior to gavage FITC-dextran (keep water). (*Use 1 extra mouse without FITC-dextran as background control*)
Gavage FITC-dextran to each mouse (**600 mg/kg, BW**). (eg: 7.5 µL of 80 mg/mL stock /g BW) A gap of 10~15 minutes (*depends on how fast the sample collection at termination*) between each mouse is recommended for FITC-dextran oral gavage.
After 4 hours, collect the blood using a 1 ml syringe with 25 G needle by cardiac puncture, then kill the mice by cervical dislocation. At least 300~400 ul of blood are needed in order to get enough serum for the next step.
Let the blood clot for 30-45 min at RT. Spin at 12,000 g for 4 min at RT.
Transfer the serum to a new pre-labelled tube. Aliquot to 2 tubes (120 µL and the remaining). Keep at 4°C.
Once all samples are collected, dilute the 120 µL samples tubes with equal volume of PBS. (Store the other set of tubes at -80°C for other assay)
Add 100 ul of diluted serum to a 96-well microplate in duplicate.
Determine the serum concentration of FITC in a Fluorometer with an excitation 485 nm and emission 528 nm (20 nm band width) using as standard serially diluted FITC-dextran* (0, 125, 250, 500, 1000, 2000, 4000, 8000 ng/ml). *Serum from mice not administrated with FITC-dextran is used to determine the background*.
*FITC-dextran serial dilution from the stock [80 mg/mL]:
100x dilute stock in PBS => [800,000 ng/mL] S0
100x dilute S0 in PBS => [8,000 ng/mL] S1
2 fold serial dilute from S1 to S7 => [4000, 2000, 1000, 500, 250, 125 ng/mL]
Reference:
PMID: 27912750 (1), 28234358 (2), 28587416 (3), 24684847 (4).

Alcian Blue-Nuclear Fast Red Stain

Adapted from Abcam ab245876 Alcian Blue PAS Stain Kit & Amy Ferrell

Reagents:
Xylene
100%, 95%, 70% Ethanol
dH20
50 mL 3% Acetic Acid (from Abcam kit ab245876)
50 mL Alcian Blue pH 2.5 (from Abcam kit ab245876)
50 mL Nuclear Fast Red Stain
- 5 g Aluminum Sulfate (Sigma, 368458)
- 0.1 g Nuclear Fast Red (Sigma, N8002)
- 100 mL dH20

*Dissolve aluminum sulfate in water. Add NFR and slowly heat to boil and cool. Filter before use.
Permount

Procedure:

NOTE: Filter all reagents before use. Do not allow slides to dry at any time during this procedure.

Deparaffinization/Rehydration:

___ ___ ___ Xylene 3 X 5 min
___ ___ ___ 100% ethanol 3 X 4 min
___ ___ ___ 95% ethanol 3 X 4 min
___ ___ 70% ethanol 2 X 4 min
___ ___ ___ dH_2O 3 X 3 min

Stain:

___ Acetic Acid Solution (3%) 2 min
___ Tap off excess Acetic Acid Solution (3%)
___ Alcian Blue (pH 2.5) 30 min
___ Rinse in running dH_2O 2 min
___ ___ dH_2O 2 X 2 min
___ Nuclear Fast Red Stain 10 min
___ Rinse in running dH_2O 2 min
___ ___ dH_2O 2 X 2 min

Dehydration/Clearing:

___ ___ 70% ethanol 2 X 4 min
___ ___ ___ 95% ethanol 3 X 4 min
___ ___ ___ 100% ethanol 3 X 4 min
___ ___ Xylene 2 X 2 min

Mounting:

___ Coverslip using Permount. Tap off most liquid, dry slide with Kim wipe, apply a drop of Permount below each section and coverslip. Let cure at RT overnight. Seal with nail polish the next morning for longer lasting imaging.